Oxygen-enriched biomass combustion studies and an analysis of the development of the carbon capture and storage industry in the UK

Samuel Colin Pickard

Submitted in accordance with the requirements for the degree of Doctor of Philosophy as part of the Integrated PhD/MSc in Low Carbon Technologies

University of Leeds

School of Process, Environmental and Materials Engineering

Doctoral Training Centre in Low Carbon Technologies

December 2013

The candidate confirms that the work submitted is his/her own, except where work which has formed part of jointly authored publications has been included. The contribution of the candidate and the other authors to this work has been explicitly indicated below. The candidate confirms that appropriate credit has been given within the thesis where reference has been made to the work of others.

Work in some of the following chapters is closely related to that published in academic journals, the full bibliographic details of which may be found in the 'Publications' section. In each of the jointly authored publications the candidate was the lead author and responsible for the data collection and evaluation. The coauthors in each of the publications were responsible for supervisory support. Chapter 4 is largely based on published work (*Energy & Fuels* [2013] **27**(5), 2818–2826) while some of the results discussed have also been published, as in Chapter 6 (*Energy Procedia* [2013] **37**, 6062–6069) and Chapter 7 (*Energy Procedia* [2013] **37**, 7613–7621).

Samuel C. Pickard

Acknowledgements

The work in this thesis was carried out thanks to funding from the Engineering and Physical Sciences Research Council via the Low Carbon Technologies Doctoral Training Centre (DTC) - which provided a student stipend, support for conferences and meetings - and with Seedcorn funding from the University of Teesside thanks to Richard Lord. Without this support it is highly unlikely the work would have been possible and so I am exceptionally grateful to the funders.

Although putting to pen to paper in writing a thesis is a fairly individual affair, carrying out the research and living through a PhD has, for me, very much been a time of collaboration and interdependence. In reflection of that there are a host of people who I wish to thank who have supported and helped me in ways big and small over the last four years.

First, to my supervisors - Bill Nimmo, Mohamed Pourkashanian and Tim Foxon - I owe an enormous debt of gratitude for teaching, guiding and stretching me over the course of the PhD. Their wonderful blend of experience and inquisitiveness has helped to shape my research and understanding of the subject and how it fits in to the wider energy landscape. Academically I also extend many thanks to Sheraz Daood, for being so helpful whenever asked, and to Derek Ingham for his timely proofreading. I am also very grateful to Matthew Billson for his support and advice during my placement with DECC.

In actually carrying out the research I have also been very fortunate to work with a range of superb staff at Leeds. Bob Harris deserves a special mention for his unwavering support, wealth of experience and good chat that made gruelling experimental days fly by. Similarly, Adrian Cunliffe, Simon Lloyd, Stuart Micklethwaite, Sara Dona and Leilani Darvell have all provided invaluable help with experimental facilities and the odd requests that come with naive students.

Hailing from the Low Carbon Technologies Doctoral Training Centre, I have been privileged to be so fantastically supported and directly thank Paul Williams as its director. Within the DTC, life would undoubtedly been harder without the fantastic can-do attitude of David (DI) Haynes and Rachael Brown. Having nurtured us in the first-cohort through the four years I am deeply grateful to James McKay, not least for providing support for doing things differently.

The strength and joy of university life is the people you meet along the way and the

exchange of ideas and cultures. In being part of the DTC and ETII I could not have wanted for a better group of colleagues, coworkers and friends. From walking with the PowerHikingDudes - Janos, Sandy and Ray - to the frequent coffees and exploration of all things cultural - Clare, Jo and Rici - my time in Leeds has been thoroughly enriched by those around me. Closest, in proximity and state of mind, are (in no particular order) Tom, Hannah, Gilli, Gemma, Jayne and Zarashpe and my wonderful flatmates Joel, Pip and Shem, thanks to whom I've spent so much of the last four years smiling.

Ultimately, I would not be in this position without the support of my family over the decades of education I've been privileged to be able to undertake. Particular thanks go to Mum who I thank for always supporting me and, from a young age, pushing me to make my own decisions. I am truly grateful.

Executive Summary

Biomass combustion with carbon capture and storage (Bio-CCS) has been identified as a key contributing technology to long-term carbon emissions reductions in many global and UK scenarios, but the development and implementation of this technology would require significant technical and non-technical barriers to be overcome. This thesis describes research undertaken to address these barriers, to contribute to the role that Bio-CCS could play in reducing carbon emissions for the UK electricity sector.

Technical studies investigate the characteristics of coal and biomass combustion in atmospheres relevant to CCS at bench-scale and in a 20 kW furnace. Analysis of bench-scale results, using a modified Coats-Redfern procedure, suggests oxygen-enrichment increases reactivity during the breakdown of cellulosic material and char oxidation. At 20 kW scale, experiments that investigate biomass blending ratio and extent of oxidant staging conclude that, compared to air-firing of coal, cofiring in oxygen-enriched, oxidant-staged conditions results in enhanced combustion, reduced NO emissions and a flue gas richer in CO_2. Cofiring of coal with 15% biomass is also carried out in partial-oxyfuel combustion atmospheres. The results suggest no major technical issues, showing biomass cofiring and oxygen-enrichment counter reductions in reactivity due to higher CO_2 concentrations. However, further tests show that dedicated firing of biomass in such conditions would likely require modifications to the combustion set up.

The development of an industry depends on more than its level of technological readiness. Modelled as a technical innovation system, development of Bio-CCS is gauged from the results of an expert survey on the wider UK CCS industry and analysis of relevant publications. Findings show that, as well as biomass sustainability criteria and a need to reward negative emission processes, the development of Bio-CCS is dependent on the wider CCS industry in the UK which, driven by uncertainties, has suffered due to a lack of market creation and entrepreneurship.

Publications

Academic output:

Pickard, S., Daood, S.S., Pourkashanian, M. and Nimmo, W. [2013], 'Robust Extension of the Coats–Redfern Technique: Reviewing Rapid and Realiable Reactivity Analysis of Complex Fuels Decomposing in Inert and Oxidizing Thermogravimetric Analysis Atmospheres', *Energy & Fuels* **27**(5), 2818–2826.

Pickard, S., Daood, S.S., Nimmo, W., Lord, R., and Pourkashanian, M. [2013], 'Bio-CCS: Co-firing of Established Greenfield and Novel, Brownfield Biomass Resources under Air, Oxygen-enriched Air and Oxy-fuel Conditions', *Energy Procedia* **37**, 6062–6069.

Pickard, S. and Foxon, T.J. [2013], 'The State of Development of the UK CCS Industry: An Expert Questionnaire and Systems-based Approach', *Energy Procedia* **37**, 7613–7621.

Contributions to wider literature:

APGTF [2011], 'Cleaner Fossil Power Generation in the 21st Century - Maintaining a Leading Role', Technical Report, August 2011, Advanced Power Generation Technology Forum.

DECC [2012], 'CCS Roadmap: Supporting development of Carbon Capture and Storage in the UK'

DECC, Carbon Trust, ECOFYS [Unpublished] 'CCS Technological Innovation Needs Assessment', Technical Report.

Nomenclature

Symbol	Units	Description
Latin characters:		
A	s^{-1}	Arrhenius equation pre-exponential (frequency) factor (here expressed as first order)
AI	$kg\,GJ^{-1}$	Alkali index
BSR	none	Burner stoichiometric ratio. Analogous to λ_{pz}
BBR	none	Biomass blending ratio on a thermal basis
c	varies	Intercept value for linear regression
C_P	$J\,kg^{-1}\,K^{-1}$	Specific heat capacity
d ($\bar{d}$)	μm	Particle diameter (average)
DTG_{max}	$mg\,K^{-1}$	Maximum rate of mass loss observed from the derivative of the thermogram
ΔE	$J\,g^{-1}$	Energy released to water during bomb calorimetry
E_A	$J\,mol^{-1}$	Arrhenius equation activation energy
Err	varies	Calculated error value associated with given measurement
$f(\alpha)$	none	Reaction dependence on extent of reaction
$g(\alpha)$	none	Integral of $f(\alpha)$
k	s^{-1}	Arrhenius equation rate constant (here expressed as first order)
l	varies	Slope value for linear regression
LOI	%	Loss on ignition
m_1 / M	g	Mass of component 1/ Total mass
n	none	Order of reaction
$n_{i,1}$/ N_1	$L\,min^{-1}$	Volumetric flow of component 'i' in stream 1 / total volumetric flow of stream 1
P	bar	Pressure
$p(\zeta)$	none	The temperature integral used in extracting kinetic data from TGA
r^2	none	Square of the Pearson product moment coefficient for linear regression
R	$J\,mol^{-1}\,K^{-1}$	Universal gas constant
$R_{b/a}$	none	Base to acid ratio
S_i	none	Fuel reactivity in TGA experiments relative to base case
t	s	Time
T	K or °C	Temperature
T_{bo}	K	Temperature at which fuel burn out is complete
T_{ig}	K	Temperature at which fuel volatiles ignite
T_m	K	Temperature at maximum rate of reaction
x_i	%	Volumetric fraction of component 'i'
X	varies	Example of measured variable in error calcuations
XS	%	Percentage of excess oxygen delivered to furnace relative to stoichiometric ratio
Y_d	none	Fraction of particles with diameter greater than d
z	none	Rosin-Rammler spread parameter
Z	none	Random number used in generating data 'noise'

Nomenclature (cont.)

Symbol	Units	Description
Greek characters:		
α	none	Extent of reaction defined by normalising reacting mass to initial and final masses
β	$\mathrm{K\,min^{-1}}$ or $\mathrm{K\,s^{-1}}$	Heating ramp rate used in TGA
Γ	none	Target function for minimisation in the Vyazovkin Method for kinetic analysis
λ	none	Primary zone ratio of oxidant to fuel expressed as function of the stoichiometric ratio. Analogous to BSR
ρ	$\mathrm{kg\,m^{-3}}$	Density
ζ	none	Defined as $\zeta = E_A/RT$
θ	none	Number of reactions occurring in TGA decomposition
τ	none	Number of points used in width of either-side smoothing parameter
Subscripts:		
0		intial, start of reaction
f		final, end of reaction
i		time-step
j, k		Denote different experimental heating rate in Vyazovkin Method for kinetic analysis
q		Total number of experiments in Vyazovkin Method for kinetic analysis
t		at time t
tc		mass fraction of total combustibles in fuel
uc		mass fraction of unburned combustibles in ash

List of Abbreviations

Abbreviation	Description
APGTF	Advanced Power Generation Technology Forum
Bio-CCS	Biomass combustion and carbon capture and storage
COP	Conference of Parties
CCC	The Climate Change Committee
CCS	Carbon capture and storage
CR	Coats-Redfern
CRTF	Cost-Reduction Task Force
DECC	UK Department for Energy and Climate Change
Demo1	The first UK CCS demonstration programme
DSC	Differential scanning calorimeter
DTG	Derivative thermogram (first derivative of mass-loss with respect to temperature)
EDX	Energy-dispersive X-ray
EFR	Entrained flow reactor
EMR	Electricity Market Reform
En-Air	Oxygen-enriched air
En-Oxy	Oxyfuel combustion atmosphere with 30% O_2
FTIR	Fourier-Transform Infra-Red spectrometry
FF	Fossil fuels
GHG	Greenhouse gas(es)
IEA	International Energy Agency
IPCC	Intergovernmental Panel on Climate Change
IS	Innovation system
MC	Miscanthus
NGO	Non-governmental organisation
OCCS	Office of Carbon Capture and Storage within DECC
OEC	Oxygen-enriched combustion
OFA	Over-fired air
Oxy	Oxyfuel combustion atmosphere with 21% O_2
PCC	Post-combustion capture
RCG	Reed canary grass
RF	Radiative forcing
SEM	Scanning electron microscope
SM	Shea meal
SRC	Short-rotation coppiced willow
SRES	Emission trajectories defined by the IPCC Special Report on Emissions Series
TINA	Technology innovation needs assessment
TIS	Technical innovation system
TGA	Thermogravimetric analysis
TRL	Technology readiness level
UN	United Nations
UNEP	United Nations Environmental Programme
UNFCCC	United Nations Framework Convention on Climate Change
WC	Williamson coal
XRF	X-ray fluorescence

Contents

List of Figures

List of Tables

Chapter 1

Introduction and Background

1.1 Introduction to the thesis

Biomass combustion with carbon capture and storage (Bio-CCS) has been identified as a key contributing technology to long-term carbon emissions reductions in many global and UK scenarios, but the development and implementation of this technology would require significant technical and non-technical barriers to be overcome. This thesis describes research undertaken to address these barriers, to contribute to the role that Bio-CCS could play in reducing carbon emissions for the UK electricity sector.

In focussing on the technical barriers to Bio-CCS, the focus of a large part of this thesis is on testing to better understand the combustion of biomass in the novel combustion regimes that CCS may require. This is first carried out at small scale in order to investigate the change in reactivity of the combustion mixture that may be expected in a Bio-CCS setting. These results are then used to inform testing in a larger experimental facility that provides a more realistic appraisal of how Bio-CCS applications may react and allows the implementation of combustion techniques traditionally employed to reduce the emission of other pollutants from combustion processes.

In addressing the implementation of CCS and Bio-CCS in the UK, it is recognised that a wide range of influences have the potential to impact on the development of a UK CCS industry. To understand how these influencing factors interact and affect the development of CCS, the developing industry was modelled as technical innovation system (TIS). The results from a survey of experts and an analysis of relevant government, industry and

academic literature are used to provide a rich account of the TIS and to highlight its strengths and potential barriers to further development.

1.2 Historical climate change

The Earth's climate is changing. Although the complex interplay of countless factors render the climate a truly dynamic system, several indicative measurements strongly suggest that the climate is changing faster than has ever been the case. Figure 1.1 shows observed increases in land and sea surface temperatures over the last century that mirror increases in other climatic indicators such as ocean acidification, sea levels and the likelihood of extreme weather events. The models used to produce Figure 1.1 use data for a range of climate-forcing phenomena as inputs that then predict their effect on the climate. Although over the period since before the start of the industrial revolution (c.1750) and today there have undoubtedly been natural variations in the climate system, Figure 1.1 shows how the measured change in the Earth's surface temperature at various points around the globe cannot be explained by natural phenomenon alone. These increases may, to a non-specialist, appear unremarkable; however, the scale of the system they operate in is such that the minute changes will have consequences for all life on Earth.

1.3 Drivers of climate change

The changing climate is largely anthropogenic in nature and has been caused mainly by increasing atmospheric concentrations of greenhouse gases (GHGs). Since the industrial revolution an ever-increasing amount of energy has been required globally as nations develop. To power this growth humanity has almost invariably turned to fossil fuels (FFs) as a cheap and plentiful source of energy. However, liberating this energy by the process of combustion produces carbon dioxide (CO_2) and other GHGs which are emitted to the atmosphere. Figure 1.2 shows the increase in the consumption of energy, the associated emissions of CO_2 and the measured atmospheric concentrations of CO_2 over the last half of the 20th century. Figure 1.3 shows within the long-lived GHGs CO_2 has had the greatest effect on the climate over the last 250 years and that the effects of GHGs and CO_2 are the best understood and accordingly the impacts of these are viewed as being some of the surest estimates. Despite continued lobbying from fossil fuel companies, the

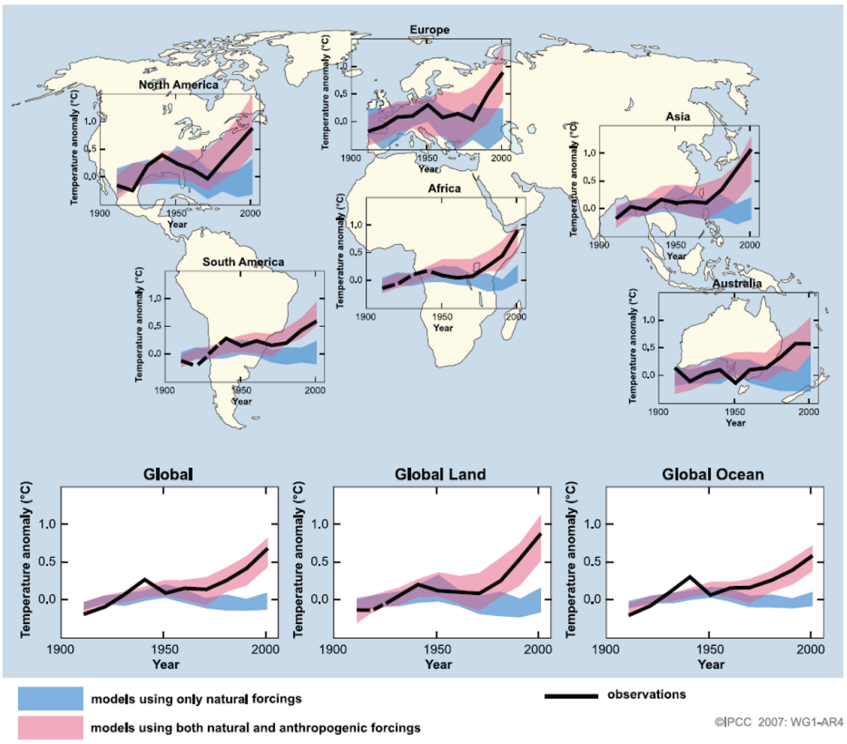

Figure 1.1: Climate modelling showing that natural phenomena alone are unable to explain the increase in temperatures witnessed since the start of the industrial revolution [Hegerl et al., 2007]

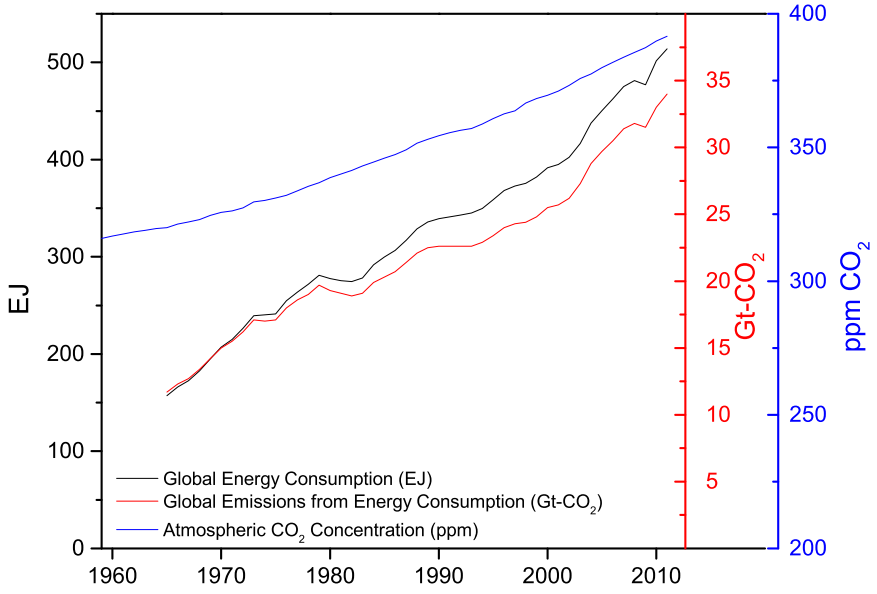

Figure 1.2: Atmospheric CO_2 concentrations measured at Mauna Loa, Hawaii across the period 1958 - 2013 [Tans and Keeling, 2013] plotted alongside energy consumption and CO_2 emissions 1965-2012 [BP, 2013]

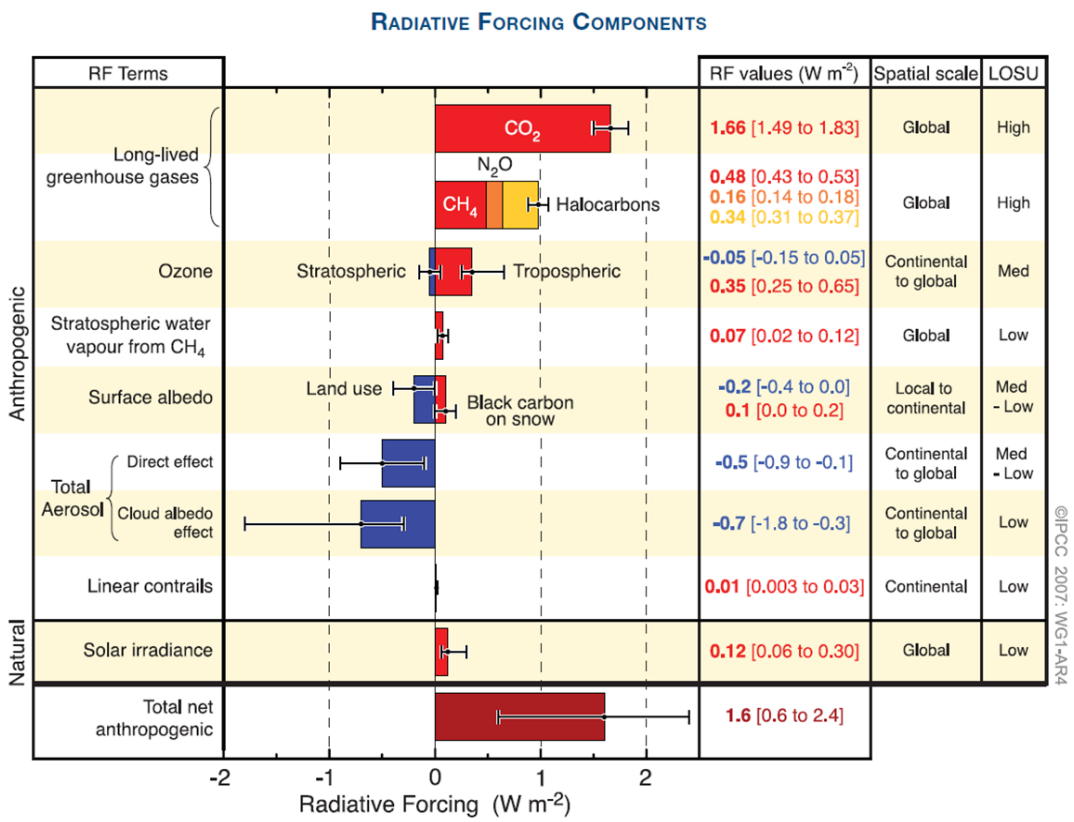

Figure 1.3: Radiative Forcing (RF) values of climate changing phenomena [Forster et al., 2007]. Positive RF values indicate the phenomena causes the Earth to absorb more radiation than it emits back to space at the top of the atmosphere.

ongoing publication of the Fifth Assessment Report by the Intergovernmental Panel on Climate Change (IPCC) confirms the scientific community and most governments are now overwhelmingly convinced that the emissions of anthropogenic GHGs are a significant contributor to changes to the Earth's climate.

1.4 Future projections of climate change

Future modelling projections suggest a continued overall warming of the climate. Having successfully modelled historical climate change, the models used to establish that it cannot be argued away as a natural phenomenon are then employed in attempt to understand what the climate of the future may look like. However, unlike the predictions in Figure 1.1, data for future climate-forcing phenomena is open to significant variability as predicting the distant future is full of uncertainties. Thus, rather than attempting to model what the world in 2100 will look like, climate scientists instead make use of a series of theoretical pathways (SRES) defined by the Intergovernmental Panel on Climate Change (IPCC). The scenarios "*are grouped into four scenario families (A1, A2, B1 and B2) that*

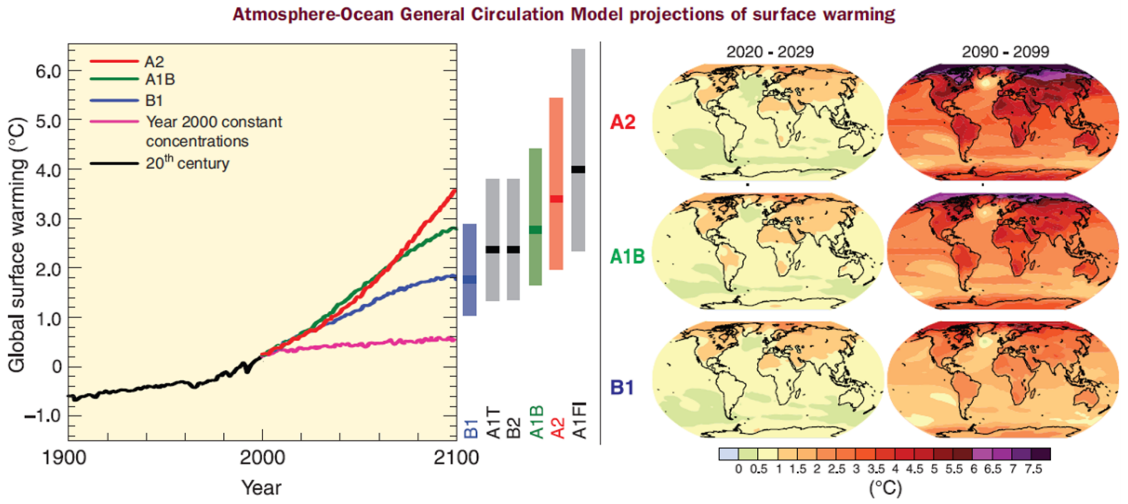

Figure 1.4: Temperature projections for various emissions scenarios [Bernstein et al., 2007]

explore alternative development pathways, covering a wide range of demographic, economic and technological driving forces and resulting GHG emissions" and "*[t]ogether they describe divergent futures that encompass a significant portion of the underlying uncertainties in the main driving forces.*" [IPCC WG III, 2000] Using the emissions profiles in these theoretical pathways as inputs to global climate models (GCMs) produces a range of results of how the climate may change by 2100. Figure 1.4 displays the range of changes in global average surface temperature which may be expected by 2100 using the GCMs with the SRES inputs. All scenarios suggest the average global temperature in 2100 will be 1 to 6 °C higher than in 2000 with most projections suggesting the increase will be in the range 2 to 3.5 °C. These projections also show that the temperature increases vary significantly across the World.

The changing climate could have devastating impacts for future generations and the environment they inhabit. This is especially true since projected increases in globally-averaged temperatures are only one factor of the changing climate and effects such as rising sea levels and increased frequency and severity of severe weather events like droughts and floods are also expected. In order to understand the effects these physical changes could lead to Figure 1.5 illustrates the severity of impacts on several tangible factors which may be expected if the global average temperatures are to rise. Recognising the gravity of the situation, the leaders of nations attending the 15th session of the Conference of Parties (COP 15) to the United Nations Framework Convention on Climate Change (UNFCCC) drafted and signed the Copenhagen Accord which states:

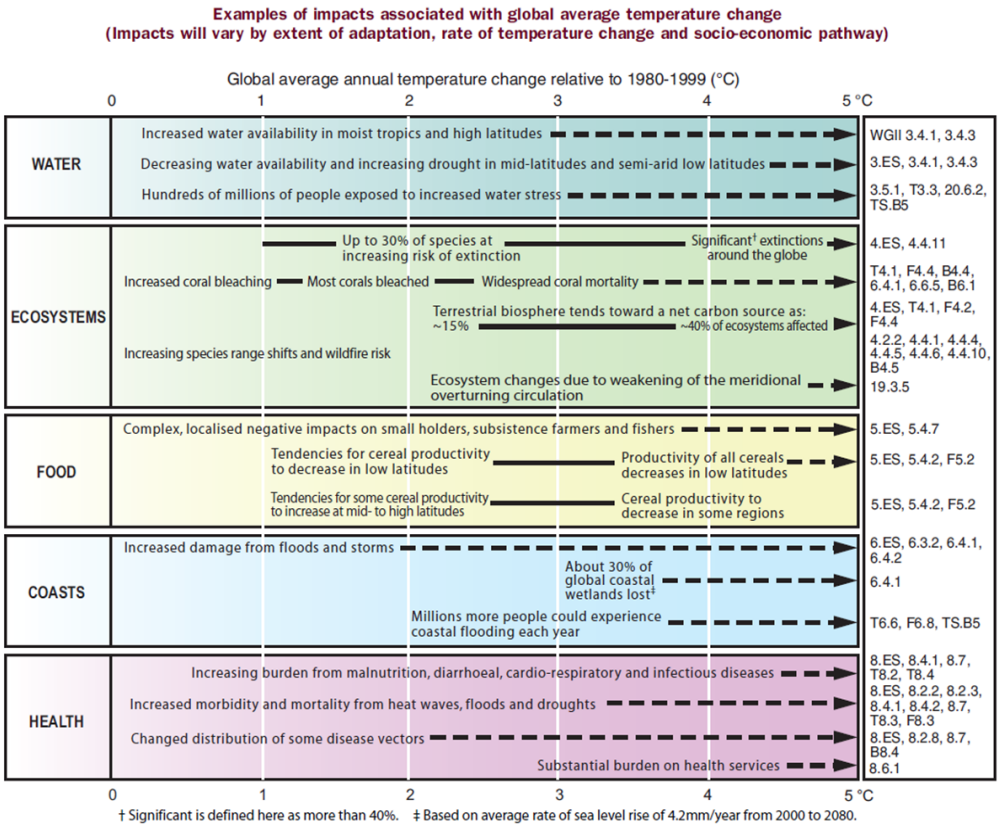

Figure 1.5: Impacts of increasing global surface temperature [Bernstein et al., 2007]

> "We underline that climate change is one of the greatest challenges of our time. We emphasise our strong political will to urgently combat climate change in accordance with the principle of common but differentiated responsibilities and respective capabilities. To achieve the ultimate objective of the Convention to stabilize greenhouse gas concentration in the atmosphere at a level that would prevent dangerous anthropogenic interference with the climate system, we shall, recognizing the scientific view that the increase in global temperature should be below 2 degrees Celsius, on the basis of equity and in the context of sustainable development, enhance our long-term cooperative action to combat climate change. We recognize the critical impacts of climate change and the potential impacts of response measures on countries particularly vulnerable to its adverse effects and stress the need to establish a comprehensive adaptation programme including international support." [COP15, 2009].

While the projections in Figure 1.4 illustrate that business as usual is not an option for adhering to the 2 °C limit, Figure 1.6 supports the scientific consensus that to have at least a 50% chance of limiting temperature rise to 2 °C by 2100 will require stabilising atmospheric GHG concentrations at around 450ppm.

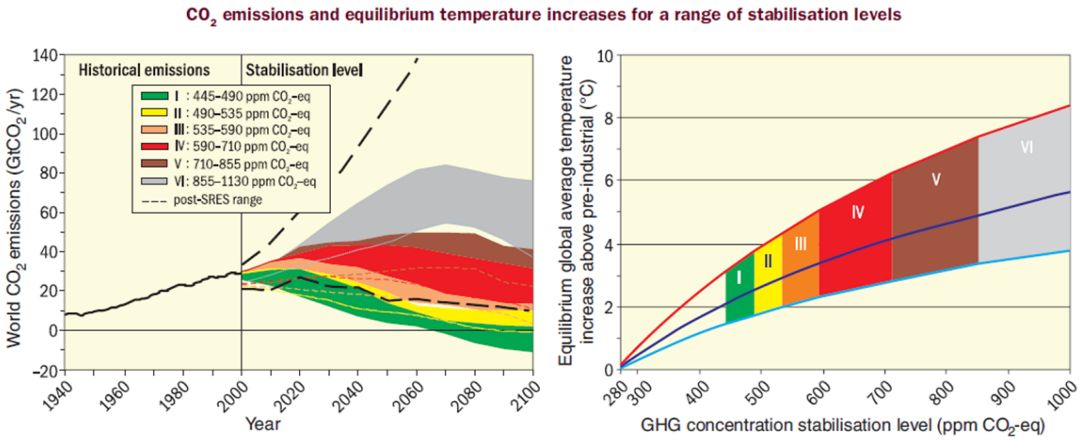

Figure 1.6: Emission trajectories for achieving various CO_2 stabilisation levels (left) and their relative increase in equilibrium global average temperature (right) [Bernstein et al., 2007]

1.5 Current GHG emission profiles

Current emissions of GHGs are largely due to the combustion of fuels for energy production and are unequally distributed around the World. Figure 1.7 shows that total GHG emissions by sector in 2009 were dominated by energy (responsible for 69.9% of all GHGs) and that the largest single sector responsible for GHG emissions is the provision of electricity and heat. Figure 1.8 shows GHG emissions are distributed in a highly unequal fashion with wealthy, developed nations almost invariably showing higher GHG emissions per capita than developing nations. In order to meet the 2 °C limit while noting the "*basis of equity*" in the Copenhagen Accord it is clear that dramatic reductions in GHG emissions must occur alongside increased provision of energy to developing countries.

1.6 Global and regional commitments to reducing emissions

It is possible to reduce emissions in line with the Copenhagen Accord and reducing emissions more quickly is both safer and cheaper. In 2006 the Stern Review analysed the economics of climate change and found that: *"The costs of stabilising the climate are significant but manageable; delay would be dangerous and much more costly"* [Stern et al., 2006]. Despite global summits on the issue having occurred for decades, and despite much pressure from progressive governments and NGOs, the World's largest emitters of GHGs, and in particular CO_2 continue to refuse to sign up to any international emission reduction targets which will achieve the 2 °C limit. To date, the closest the World has

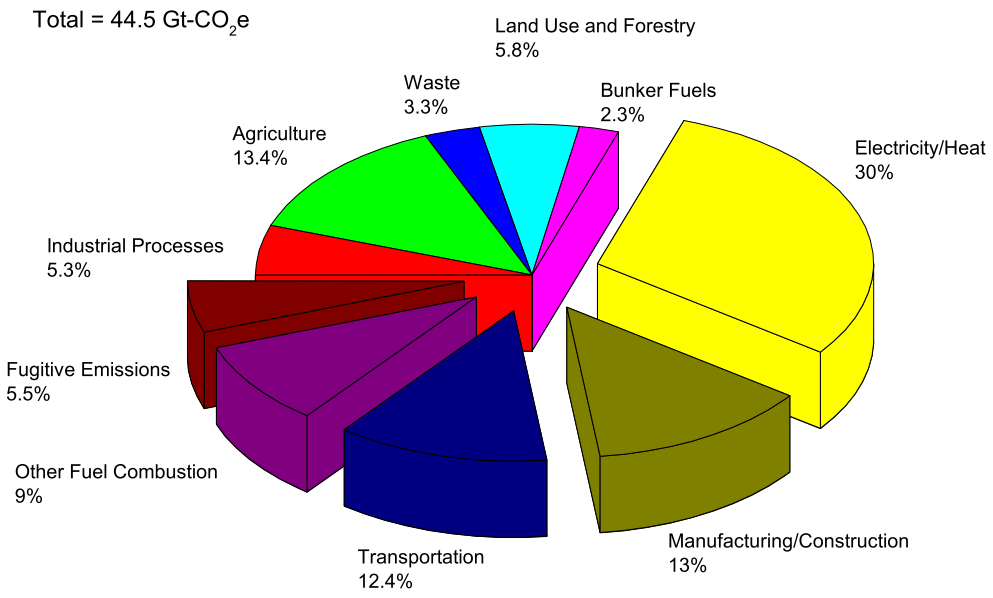

Figure 1.7: Global GHG emissions by sector in 2009 [WRI, 2013]. Exploded wedges are all categorised as sub-sections of energy

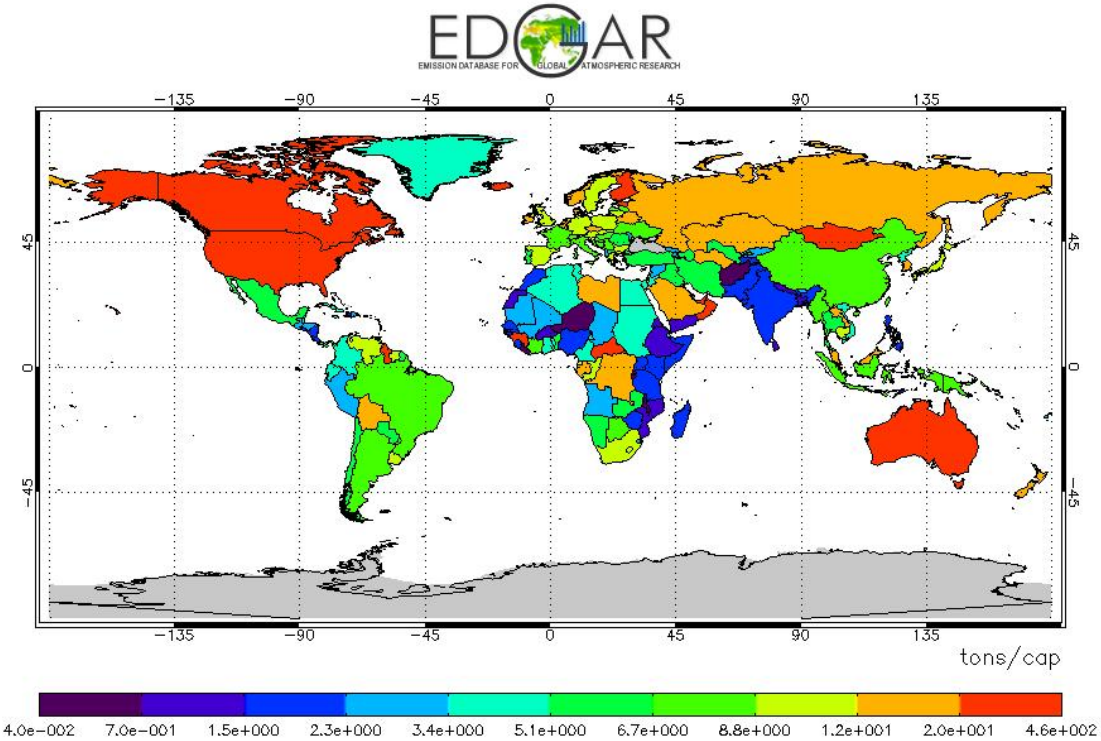

Figure 1.8: Global per capita GHG emissions in 2010 [EC-JRC, 2013]

come to an agreement was the Kyoto Protocol. The Protocol was signed in 1997, ratified in 2005 and committed 37 developed nations to limit their GHG emissions to those they emitted 1990 by 2012 [UN, 1998]. Most of the Annex I (developed) countries that signed the Protocol achieved their reductions, though the USA never ratified the Protocol and Canada withdrew from it in 2011. Although there remains no legally-binding arrangement, in 2010 76 developed nations voluntarily pledged to reduce their emissions at COP16 in Cancun, Mexico. At COP17 in Durban in 2011 a decision was made "*to deliver a new and universal greenhouse gas reduction protocol, legal instrument or other outcome with legal force by 2015 for the period beyond 2020*"[UNFCCC, 2012]. Having failed to achieve a global agreement to succeed the Kyoto Protocol, in Doha in 2012 all nations that signed and ratified the protocol with the exception of Russia, Japan and Canada, have agreed to continued reductions in their emissions by 2020. The amendment notes that the European Union is currently committed to a 20% reduction by 2020 but "*the European Union reiterates its conditional offer to move to a 30 per cent reduction by 2020 compared to 1990 levels, provided that other developed countries commit themselves to comparable emission reductions and developing countries contribute adequately according to their responsibilities and respective capabilities*" [UN, 2012]. A recent report by the United Nations Environment Programme (UNEP) "*provides a sobering assessment of the gulf between ambition and reality in respect to keeping a global average temperature rise this century under 2 degrees Celsius*" [UNEP, 2012] suggesting the need for global agreement and action on reducing emissions is increasingly important.

Among the developed nations the European Union has strongly supported emissions reductions both internationally and within Europe. To support its commitment to reductions by 20% by 2020 and 80-95% by 2050, the European Union has set out an emissions trajectory up to 2050 in its 2011 roadmap, which is shown in Figure 1.9. This requires significant extra effort over and above what current policies will achieve and indicates milestones of 40 % and 60 % reductions by 2030 and 2040 respectively [EC, 2011] and also suggests that GHG emissions from the power sector should be reduced by $> 50\%$ by 2030 and $> 90\%$ by 2050 (compared to 1990 levels).

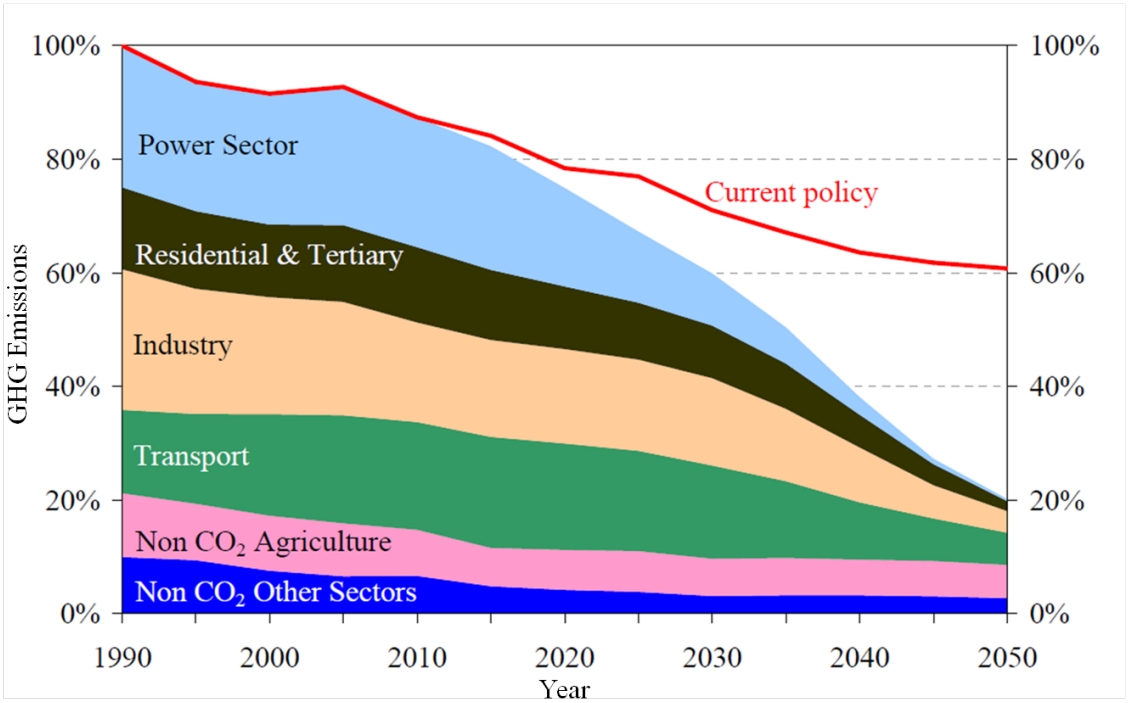

Figure 1.9: GHG Emissions reduction trajectory to 2050 for the European Union [EC, 2011]

1.7 UK GHG emissions targets

In 2008 the UK became the first nation to employ legally-binding emissions reductions targets. The 2008 UK Climate Change Act requires that by 2050 UK emissions of GHGs are 80% lower than 1990 levels and 34 % lower by 2020 [HMG, 2008]. Figure 1.10 shows the progress made so far. The Act also requires that the UK sets five-yearly carbon budgets which satisfy the downward emissions trajectory up until 2050. The fourth budget for the period 2023-2027 was set in 2011 and commits the UK to reduce emissions to 1950 Mt $CO_{2,e}$ over the five year period equating to a reduction of 50 % compared to 1990 levels as per the recommendations of the Climate Change Committee (CCC) [CCC, 2010, Huhne, 2011]. A recent report by the CCC found that the UK had met the reductions of the first carbon budget (23%), was on track to meet the reduction in the second budget (29%) but currently was not on track to make the 35% and 50% reductions in the third and fourth budgets [CCC, 2013]. The fifth carbon budget is due to be set in 2015 after the publication of the Fifth Assessment Report by the IPCC. Alongside the Climate Change Act, in 2009 the Renewable Energy Directive committed the UK to sourcing 15% of its energy demand from renewable sources by 2020.

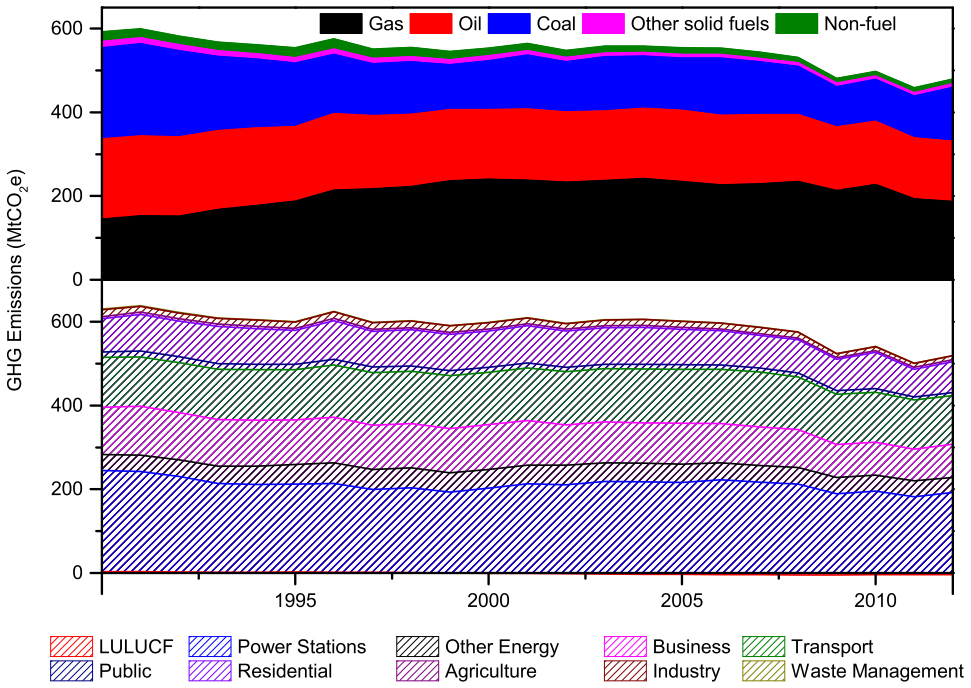

Figure 1.10: Sectors and fuels responsible for UK GHG emissions [DECC, 2013*b*]

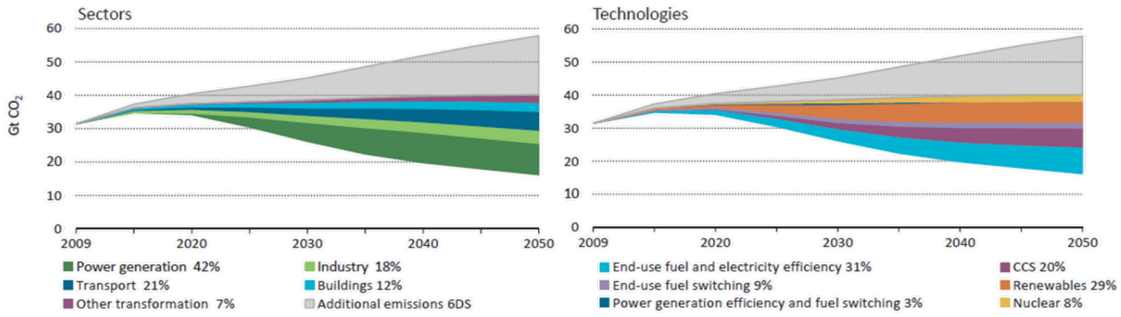

Figure 1.11: Sectoral (left) and technological (right) changes to achieve 2 °C limit in addition to effort specified in the 4 °C scenario [IEA, 2012]

1.8 Reducing GHG emissions from energy

Scenarios that achieve the 2 °C limit involve substantial reductions in emissions from energy consumption. The International Energy Agency's 450 and 2DS scenarios are target-driven to achieve the outcomes decried in the Copenhagen Accord [IEA, 2012]. In order to meet the targets, emissions from energy are required to half by 2050. To achieve these reductions Figure 1.11 highlight that significant changes are needed across many sectors, especially in power generation.

To achieve the 2050 targets substantial decarbonisation of energy consumption must occur with early decarbonisation of power generation a priority. Figure 1.10 shows that

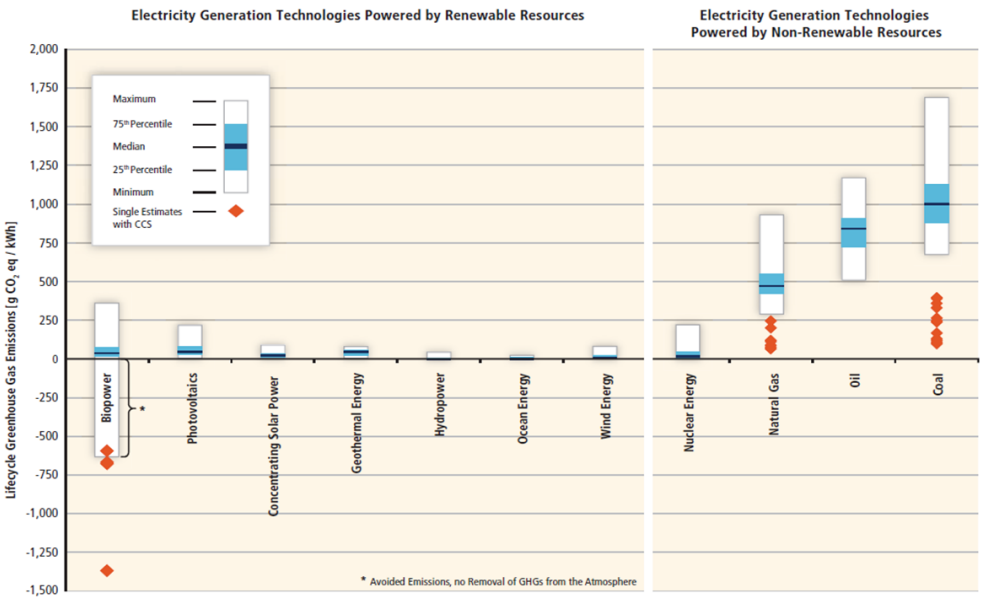

Figure 1.12: Life-cycle emissions of CO_2 from renewable and non-renewable electricity generation sources [Sathaye et al., 2011]

the global emissions profile is mirrored in the UK where energy generation from power plants accounts for 32.6 % of the total emissions with coal contributing 26.9 % to the total [DECC, 2013*b*]. Although it is clear the UK must reduce its GHG emissions from power generation, the pathway to a low-carbon future is less certain. As Figure 1.12 shows, a number of options for electricity generation exist. Figure 1.12 also shows that between and within technology options emissions of CO_2 vary considerably. In general, renewable technologies emit less than 5% of the life-cycle emissions of current median coal plant, though CCS is able to significantly reduce emissions from fossil fuel combustion and when combined with biopower is the only technology option able to effect net negative emissions of CO_2. However, analysis of life-cycle emissions is not the only factor in deciding energy futures as many other constraints such as cost, security of supply, public support and existing infrastructure must also be taken into account. For example, while the high GHG emissions of fossil-fuelled power stations may indicate the need to replace them with renewable technologies, the security of supply they afford through their flexible and dispatchable nature operation is likely to see them continue to operate for several decades at least.

In 2010 the 2050 Pathways Analysis was published as a tool to help policymakers, the energy industry and the public make informed choices of how to move to a low-carbon future [DECC, 2010]. The Pathways Analysis was conducted by producing six scenarios which each have a range of assumptions pertaining to the the UK's future. Among the findings,

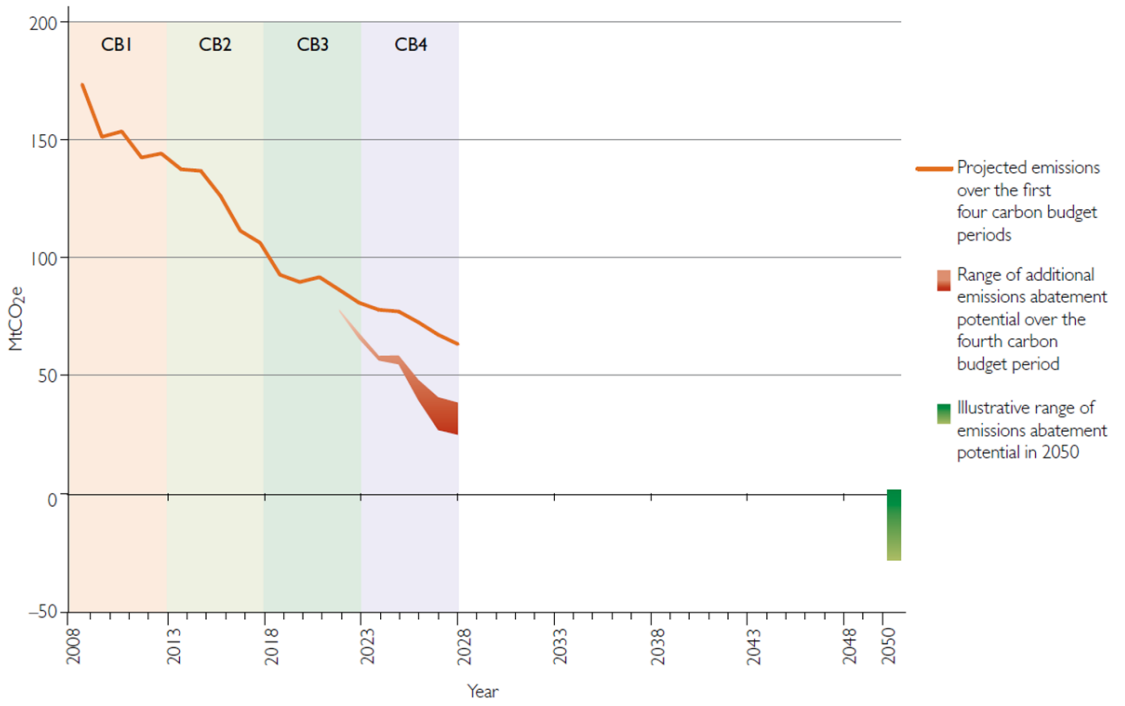

Figure 1.13: Projected decarbonisation of UK electricity over the carbon budgets (CB) 1-4 and target for 2050 [HMG, 2011]

DECC concluded that for the majority of scenarios considerable reductions in per capita energy consumption were required but that electricity consumption is likely to rise due to an increased population and due to the increasing electrification of transport and heating. However, in order to meet the carbon targets this increase in electrification can only occur if electricity is decarbonised. The report also notes that as well as nuclear and renewable technologies, fossil fuels are likely to continue to play a major role in energy supply but the extent of this is dependent on the development of carbon capture and storage (CCS), a process that allows mitigation of the emissions usually associated with FF combustion by storing them underground rather than releasing GHGs to atmosphere. Building on the scenarios offered by the 2050 Pathways work, the Government published the Carbon Plan and the Electricity Market Reform white paper [DECC, 2011, HMG, 2011]. Unlike the Pathways Analysis which was not prescriptive, these publications lay out how the UK is to move to meet it's 2050 targets and to "*address the twin challenges of tackling climate change and maintaining our energy security in a way that minimises costs and maximises benefits to our economy.*" [HMG, 2011]. In terms of power generation: "*By 2050, the three sources of UK electricity are likely to be renewables (in particular onshore and offshore wind farms); coal, biomass or gas-fired power stations fitted with CCS technology; and nuclear power.*" Although the actual amounts of each technology are uncertain and dependent on each

technology's price competitiveness, by 2030 an extra 40-70 GW of capacity is expected to be required both to replace existing generating plant which is set to close and to provide the extra capacity required by increasing demand. Figure 1.13 shows how reductions in emissions from electricity generation must occur up until the mid 2020s and the final limit required in 2050. Despite the requirement of early decarbonisation of the electricity sector the Government have continued to resist pressure to implement a 2030 decarbonisation target. The CCC advocate a carbon intensity target of 50 gCO_2 /kWh - an order of magnitude reduction compared to the 448 gCO_2 /kWh value in 2009 - as the cheapest way for the UK to ensure it satisfies its 2050 emissions reduction targets [CCC, 2010, 2012].

In this thesis the significant role of other important technologies and changes required to achieve the 2050 decarbonisation target are acknowledged, yet it is considered beyond the scope of this thesis to cover them in detail. In 2050 the way energy is supplied and consumed will be considerably different. As well as more efficient demand devices and more efficient supply technologies, renewable energy technologies are expected to make up the bulk of the UK's generating capacity in the future. However, the variability of renewables predicates they alone cannot be depended on to supply all of the UK's energy needs. Thus, although there is no place for any fossil or nuclear fuelled power in a truly sustainable world, the flexibility that fossil fuels offer and the base load capacity of nuclear fuel are seen as essential for ensuring the UK's energy security in the coming decades. Moreover, the availability and relatively cheap price of coal means that development of FF technologies in rapidly industrialising countries is almost inevitable. A pressing need to develop methods of producing electricity from coal that emit drastically fewer GHGs is therefore required to be market-ready as soon as possible, with some experts suggesting industrialised nations should be responsible for developing the technologies [Gibbins and Chalmers, 2008*b*]. The following sections describe three methods of reducing emissions from coal-fired power plant.

1.9 Substituting coal with biomass

Substituting sustainable biomass for fossil fuels could lead to considerable reductions in emissions from electricity generation. Replacing coal with less carbon-intensive fuels to supply energy for electricity generation is one method of reducing emissions of GHGs while still providing a flexible energy supply. Although biomass also produces GHGs when

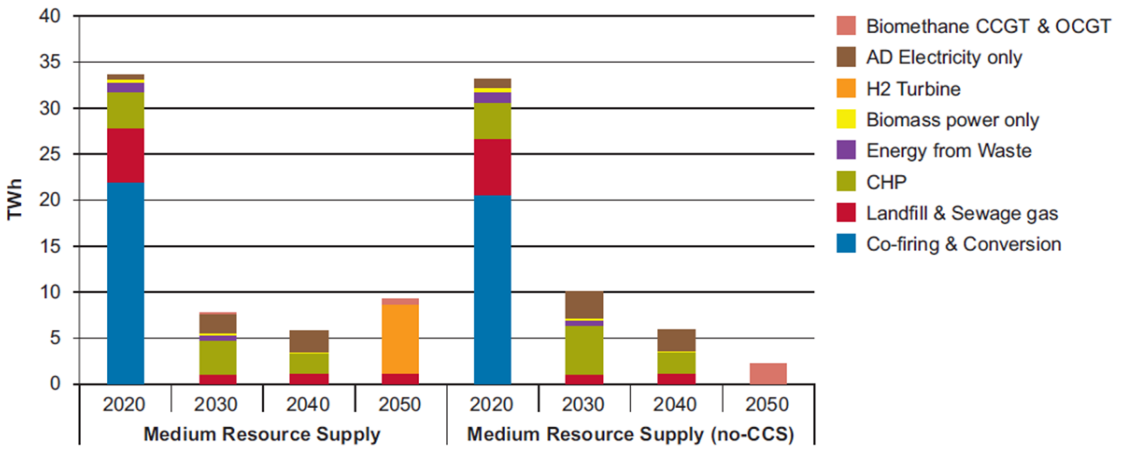

Figure 1.14: Projections of contribution of biomass to UK power sector [DfT et al., 2012]

it is burned, it is assumed that these emissions to the atmosphere are balanced against the GHGs the biomass absorbed from the atmosphere when it was growing. Thus, so long as emissions from transport and processing can be assumed to be negligible or accounted for elsewhere, the combustion of biomass is deemed to be carbon neutral. It is possible to substitute a fraction of the original fuel and cofire biomass alongside coal or to completely eradicate the use of coal in dedicated biomass combustion. The UK Bioenergy Strategy suggests that excluding biomass from the 2050 energy system causes an increase in the total energy systems cost of £44bn, though how much biomass can be used is highly dependent on the development of other technologies and the amount of biomass resource available [DfT et al., 2012]. In the nearer term, having been practised in industry in the UK since 2002, Figure 1.14 shows that for a medium estimate of resource-supply, increasing the amount of biomass that is cofired with coal or used to completely substitute coal is expected to increase as ageing fossil-fuel plants come to the end of their life [DfT et al., 2012, Drax Group Plc, 2010].

1.10 Carbon capture and storage (CCS)

Although unproven at scale, CCS is forecast to be responsible for significant reductions in GHG emissions from the power sector over the coming decades. Although there are many variants, the basic premise of CCS is to capture the GHGs produced by combustion of carbonaceous fuels and then store them in deep geological formations, hence preventing them entering the atmosphere and contributing to climate change. A simple schematic of the process is shown in Figure 1.15. In order to satisfy the 2 °C limit, the IEA Blue Map

scenario estimate 19 % of the emissions reductions by 2050 could be met by CCS and that without CCS the capital costs of reducing emissions from energy consumption could be up to 40% higher [IEA, 2010, 2012]. In the UK, the Carbon Plan suggests CCS could represent 10GW of capacity in the UK in 2030 and up to 40 GW by 2050 [HMG, 2011]. Most of the low-cost decarbonisation pathways include some fossil-fuelled power plant which would require CCS in operate by 2050. Excluding CCS from the future energy mix is forecast to increase the costs of the energy system in the UK by 2050 by £42bn. However, there are no operating CCS projects which can be considered as sufficiently similar to the type of project expected in the UK and as a result many questions regarding the technology remain. The CCS Roadmap sets out the UK Government's ambition for developing a UK CCS industry and is underpinned by the Commercialisation Competition that will provide £1bn in capital funding to projects that can demonstrate CCS at a scale that is meaningful for the UK power generation industry. This is complementary to the ongoing process of Electricity Market Reform (EMR) which aims to create an electricity market where all low-carbon options can compete with conventional electricity plant. EMR relevant to CCS is discussed in more detail in Chapter 7 though in brief it comprises a series of measures designed to promote investment in low carbon generation technologies required to decarbonise the UK power sector. The main aspects are an emissions performance standard that outlaws the construction of any new coal-fired power plant, contracts for difference that provide a degree of price certainty for power suppliers and a capacity market which flexible plant may bid for in order to ensure supply meets demand. Chapter 7 provides further detail on the development of a UK CCS industry.

1.11 Combining biomass firing and CCS (Bio-CCS) for negative emissions

The combination of biomass-firing and CCS is seen as a powerful combination to fight climate change that has the potential to actively reduce atmospheric concentration of GHGs. Using CCS technology to prevent GHGs from the combustion of biomass escaping to the atmosphere presents an opportunity for active removal of CO_2 from the atmosphere. This may be carried out either through cofiring biomass with coal or by firing biomass alone. For the biomass component of the fuel, this is a CO_2-negative process whereby CO_2 in the atmosphere is absorbed by plants during their growth stage and ultimately stored under-

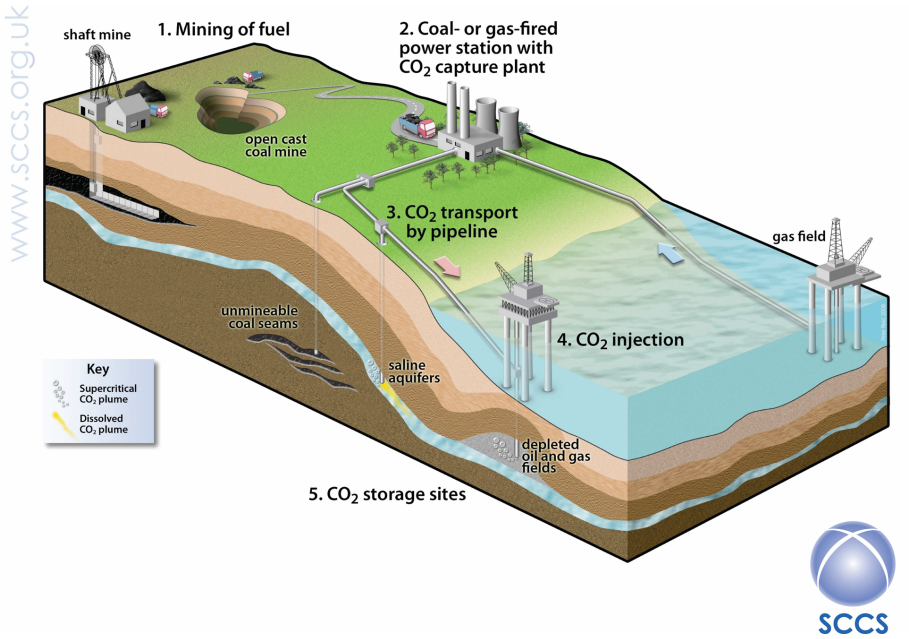

Figure 1.15: Simplified schematic diagram of CCS [SCCS, 2013]

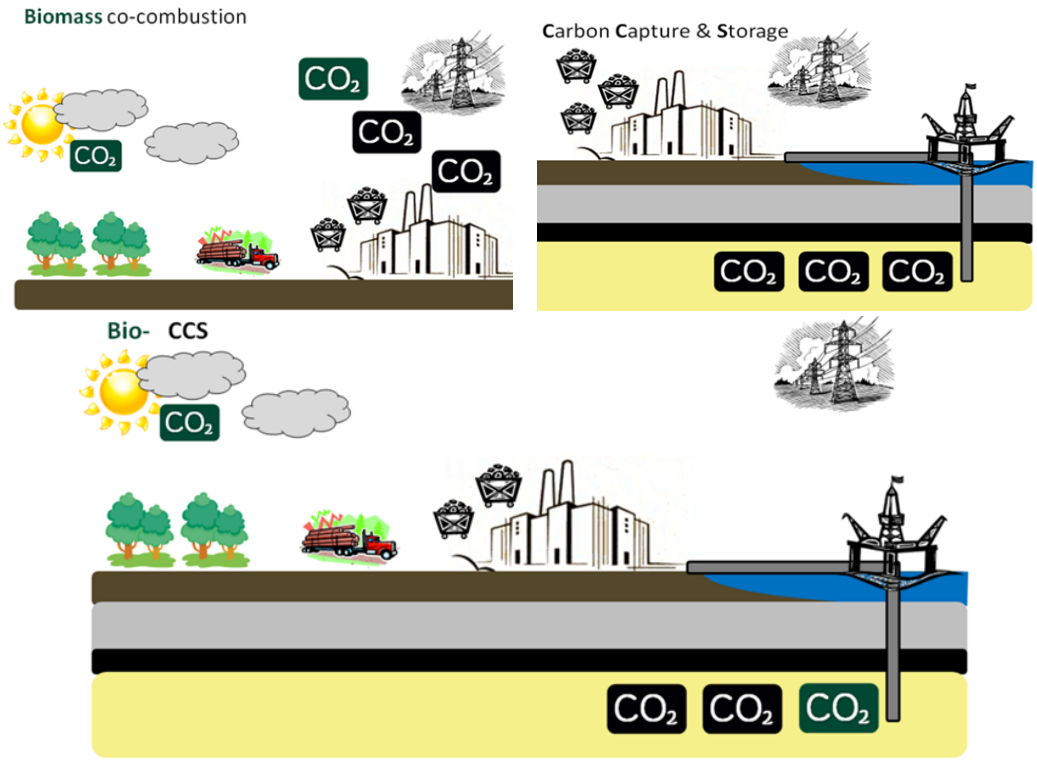

Figure 1.16: Simplified schematic of the methods for reducing GHG emissions from electricity generation from combustion plant

ground. One particular benefit of Bio-CCS (also commonly labelled BECCS) is its ability to "*mitigate emissions from any CO_2 emission source* [...including...] *the emissions that are the most difficult and expensive to cut back*" and its ability to "*mitigate emissions which have already occurred*" [Biorecro and GCCSi, 2010]. A recent report by the OECD [2011] suggests that: "*Achieving lower concentration targets (450 ppm) depends significantly on the use of BECCS.*" While by 2020 Bio-CCS is expected to make a small contribution (0.1–0.4 Gt CO_2 per year), by 2050 this is projected to increase to 2.2–12.4 $GtCO_2$ per year and continue increasing throughout the century [Sathaye et al., 2011]. At a European level, the European Technology Platform for Zero Emission Fossil Fuel Power Plants (ZEP) suggest that by 2050 up to 800 $MtCO_2$ could be extracted from the atmosphere by Bio-CCS annually [ZEP, 2012]. Interest in Bio-CCS in the UK is also strong, where as well as being responsible for the possibility of negative emissions from the electricity sector shown in Figure 1.13, the technology is mentioned in many Government publications [DECC, 2010, 2012*a*, HMG, 2011].

1.12 Technological hurdles for emerging low-carbon energy technologies

The development of Bio-CCS broadly relies on the development of CCS and also on dedicated research into the effects of biomass in CCS applications. Perhaps due to its more immediate need considerable research effort is dedicated to fossil-fuelled CCS around the world. However, although biomass can be substituted for fossil fuels in most scenarios there is a relative lack of research that is directly relevant to Bio-CCS. In 2011 the Advanced Power Generation Technology Forum published a research and development technology needs matrix covering the areas which needed focus in order to deliver a CCS system in the UK in line with achieving its emissions reduction targets [APGTF, 2011]. In this report and many published subsequently, Bio-CCS research is highlighted as a critical area for the UK. For example a recent expert review found that: *"Potential priorities for public sector innovation support* ... [include] ...*Retrofit coal, gas and biomass capture components, and their integration* ... [and] ...*In terms of UK-specific needs and the potential value of innovation, the biggest additional priority area would be issues specific to biomass firing or cofiring.*" [LCICG, 2012]

1.13 Technologies for CCS

The role of a power station in a CCS technology chain is to provide a CO_2 stream of high purity that can be transported and stored in deep geological formations while simultaneously generating affordable electricity. Although several ways to create such a stream exist, Figure 1.17 shows the three main options for CCS: post-combustion capture (PCC), pre-combustion capture and oxyfuel firing[1]. To date, none of these technologies have demonstrated an ability to outperform the others, with each technology operating within technological niches, thus suggesting all options should continue to be developed [IEA, 2012, Scott et al., 2012]. The addition of CCS to power plant reduces the overall efficiency of converting chemical energy in the fuel to electricity since the separation of a high-purity CO_2 stream requires a substantial amount of energy. In post- and pre-combustion capture this energy penalty is due to the selective removal of CO_2 from a nitrogen-rich mixture of the flue gas or syngas respectively. In oxyfuel combustion converting the flue gas to a high purity CO_2 stream is considerably simpler and is largely accomplished by removal of water and other conventional pollutants. However, in order to produce this CO_2-rich stream high-purity oxygen must be provided and changes to the combustion process must be understood. Currently the energy penalty for separating O_2 from air is comparable to the separation of CO_2 in post- and pre-combustion processes. Table 1.1 shows the current and desired efficiency targets for the three technology options. Although pre-combustion capture appears to offer the greatest efficiency opportunities, it is the least applicable to retrofitting. The IEA Energy Technologies Perspective report suggests that currently 470GW of coal-fired plant which has already been built would be suitable for retrofitting to reduce GHG emission in line with the 2 °C target [IEA, 2012]. Development of PCC and oxyfuel are necessary if this is to occur and in this thesis only PCC and oxyfuel firing are considered.

[1]The development of various combustion technologies has created a range of 'oxyfuel' environments. In this thesis, oxyfuel firing describes combustion where the fuel is burned in a mixture of oxygen and recycled flue gas (consisting of CO_2 and, depending on whether it is a wet or dry recycle, water too). In Chapter 6 a partial-oxyfuel atmosphere is investigated in which some of the nitrogen content of the combustion atmospheres is replaced with CO_2

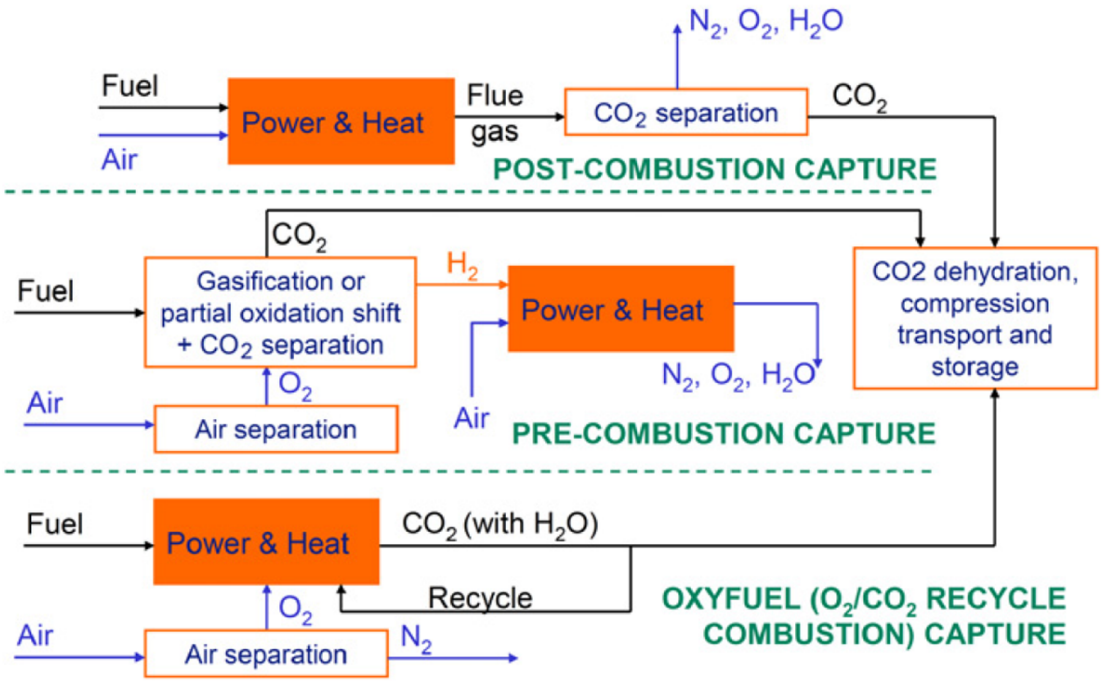

Figure 1.17: Schematic overview of the three main capture options for CCS [Gibbins and Chalmers, 2008*a*]

Table 1.1: Current and 2020 efficiency targets for CCS capture technologies [APGTF, 2011]

Technology	**Current**	**~ 2020**
Unabated coal plant	Efficiency (LCV) ~ 45%	Efficiency (LCV) ~ 50–55%
CCS coal - post-combustion capture	~ 12%point efficiency loss	~ 8%point efficiency loss
CCS coal - oxyfuel combustion	~ 10%point efficiency loss	~ 8%point efficiency loss
CCS coal - pre-combustion carbonisation	~ 7–9%point efficiency loss	~ 5–6%point efficiency loss
CCS gas - post-combustion capture	~ 8%point efficiency loss	~ 7%point efficiency loss
CCS gas - oxyfuel combustion	~ 11%point efficiency loss	~ 8%point efficiency loss

1.14 Non-technical barriers to implementation of new technologies

The success of Bio-CCS, and CCS in general, in combating climate change will be dependent on many factors outside of technology development. Although research to better understand how Bio-CCS technologies will perform is essential to developing a Bio-CCS industry, the level of Government intervention in the electricity market and provision of significant amounts of capital for demonstration highlights a wide range of factors which lie outside of the influence of the technology developer. These factors are also highly important to the successful development and deployment of CCS and Bio-CCS industries.

1.15 Biomass resources

Although biomass currently supplies approximately 10–15% of the global energy demand, mostly as a cooking and heating fuel in less developed countries, it's contribution to the UK energy sector is far smaller. While economic and operational issues contribute to fossil fuels being preferred, sourcing biomass resources is an issue for the UK. However, UK biomass consumption is forecast to increase. The 2050 Pathways Report indicates that currently an area about half the size of Wales is used to produce biomass for UK consumption but that this figure could rise by four-to-eight times by 2050, with half being domestically supplied and half imported [DECC, 2010].

The development of the biomass industry depends strongly on sustainable sourcing of biomass fuels. Since the sustainability of a biomass fuel is individual with the type of fuel, growing location, fuel processing techniques, method of transport and many other factors affecting the GHG emissions and wider sustainability criteria (including among others the impact on ecosystems, bio-diversity and land use change) the issue of biomass sustainability is considered outside of the scope of this thesis. Despite this, sustainability of feedstock is noted as a major external influence on the development of biomass and Bio-CCS industries.

One of the most contentious issues climate change mitigation has faced in recent years is the so called food versus fuel debate whereby argument exists that if it becomes more profitable to produce energy crops than food many farmers will switch, driving up food prices and contributing to famine in the poorest nations. One option to sidestep this

debate is to grow energy crops on land that is unsuitable for food crop production. In the UK the BioReGen (**Bio**mass **Re**mediation (Re)**Gen**eration) Life project focused on the growth of energy crops on brownfield sites. These sites were previously developed for non-agricultural use and are potentially contaminated or derelict thereby requiring remediation prior to reuse [Lord, 2011]. The project focused on the North East of England where it is estimated that over 20 000 ha of contaminated land exists [Tees Valley Joint Strategy Unit et al., 2006]. One aspect of the project was to produce biomass suitable as a fuel for power generation. Reed canary grass, miscanthus and short-rotation coppiced willow were grown in the study with the canary grass producing up to 10 oven-dried tonnes of material per hectare [Pratt and Lord, 2010].

Although the potential for reusing brownfield sites is appealing in that it doesn't impact on food production, to do so must not create extra pollution on account of contaminants present in the soil the crops are grown on. The BioReGen project investigated the uptake of various contaminants by the plants and combustion tests with a large combined heat and power unit. The combustion tests proved acceptable and the project suggested testing of the fuels by cofiring with coal to represent PF firing to further investigate combustion properties and suitability for use as a fuel [Pratt and Lord, 2010].

1.16 Other emissions

In addition to reducing GHG emissions, legislation continues to reduce the level of emissions of other by-products common in the power generation industry that are detrimental to humans and the environment. Any new technologies must also be able to satisfy the tightening limits, in particular on the emissions of sulphur dioxide (SO_2), nitrogen dioxide (NO_2) and dust (particulate matter). SO_2 is a major contributor to acidification via the formation of sulphate and sulphuric acid and is relatively resilient in the atmosphere so can be transported considerable distances polluting far from the source. NO_x is known to be an irritant and causes damage to respiratory organs as well as contributing to eutrophication, tropospheric ozone formation and acidification, forming nitric and nitrous acids. Dust covers a range of solid and liquid particles which can, depending on their size and composition, contribute to radiative forcing and create human health problems such as asthma, lung cancer and cardiovascular disease [DEFRA and ONS, 2012, UNECE, 2012]. In terms of the impact of these substances, Mekaroonreung and Johnson [2012] concluded

Table 1.2: Emission Limit Values in the EU Industrial Emissions Directive [EC, 2010*b*] based on 6% exit O_2 concentration

Pollutant	**ELV (mg/Nm^3)**
NO_2	200
SO_2	200
Dust	50

that the shadow price per ton of NO_2 and SO_2 from power generation cast on US society is \$409–1352 and \$201–343 respectively. Updating the 1999 Gothenburg Protocol, the 2010 Industrial Emissions Directive (IED) states that from 1st January 2016 any new large power plant (>300 MW_{th}) wishing to operate in the EU must conform to the emissions of the oxides of nitrogen and sulphur and dust particles shown in Table 1.2.

1.17 Focus and structure of the thesis

This thesis describes the progress achieved during the PhD section of the Integrated MSc-PhD course in Low Carbon Technologies and the research performed during the period 2011–2013 that contributes to the knowledge surrounding Bio-CCS technology and the potential for its development in a UK CCS industry. The sections above illustrate Bio-CCS could play an important role in combating climate change but that a lack of experience firing biomass for CCS applications means that a number of technical questions remain unanswered. Of particular importance is the development of knowledge relating to the combustion reactivity and subsequent emissions produced from Bio-CCS combustion. Complementary to increasing technological knowledge, a wider view of the industry is necessary in order to fully understand the impact Bio-CCS may be able to make in reducing GHG emissions in the UK and globally.

In this thesis the interdisciplinarity offers a rich account of research in the connected areas of combustion of biomass for carbon capture and storage applications and the potential for this technology to make an impact in the UK electricity market. These topics are related, yet research in these areas is normally carried out from different disciplinary viewpoints. Having set the context for the research in this chapter, rather than tortuously attempting to join disparate research areas, the thesis is then divided into two separate parts to reflect the multi-disciplinary nature of the work presented.

Part 1 of the thesis discusses the research that relates to the combustion process in Bio-CCS. Here, the term Bio-CCS is used interchangeably to represent both dedicated biomass firing and the cofiring of biomass with fossil fuels in CCS applications, since in both cases the biomass component of the fuel is able to achieve negative CO_2 emissions. Chapter 2 presents an overview of the relevant published literature and concludes by articulating specific research questions this part of thesis will aim to answer. Chapter 3 is the experimental methodology which introduces and develops experimental and analysis techniques that are employed in order to answer these research questions. Chapter 4 analyses the sensitivity of the Coats-Redfern method of kinetic analysis during its use with idealised data and demonstrates how the procedure may be optimised for the treatment of experimental data. Chapter 5 applies the optimised procedure to real data from bench-scale experiments in order to understand how the combustion of biomass in CCS applications may differ to conventional combustion processes. Chapter 6 presents and discusses the results obtained from the combustion of biomass fuels cofired with coal in a pilot-scale combustion rig which is operated under combustion atmospheres relevant to oxyfuel combustion and post-combustion capture for CCS. Here, the impact of enrichment of the oxygen and carbon dioxide content of the combustion atmosphere and variation of the amount of biomass blending on the combustion characteristics and process pollutants is investigated.

Part 2 forms the interdisciplinary section of this thesis and seeks to develop an understanding of the state of development of the Bio-CCS industry in the UK. During the initial stages of this section of the research it was recognised that the development of a Bio-CCS industry is largely dependent on the development of the wider technical innovation system that underpins the UK CCS industry. Thus, Chapter 7 presents an analysis of the UK CCS industry as a TIS. Along with this introduction to set the context, Chapter 7 includes a complete research picture in one concise chapter. Here, the relevant literature is presented, and methodologies used in the work are developed, before the results of an expert survey and in-depth industry analysis are presented to gauge development and highlight strengths and barriers to the growth of UK CCS.

In-depth discussion and conclusions from the results presented in the research chapters of the thesis are presented within the research chapters. The focus of Part 3 of the thesis is then to relate the results to the posed research questions and coherently draw the conclusions together to highlight the contribution of the thesis to the development of knowledge

in relation to the UK Bio-CCS industry. This final part also permits reflection on areas that are not included in this thesis and presents opportunities for future research in the studied areas.

Part I

Solid Fuel Combustion Studies

Chapter 2

Literature and Background Theory

2.1 Chapter overview

This chapter presents the relevant literature necessary to understand the need and methodologies for the research carried out in the subsequent chapters. It is useful to again emphasise that in this work both dedicated biomass firing and cofiring with coal for CCS, in particular for post-combustion capture and oxyfuel combustion, is considered. Although similarities between these technology options exist, the development of research in each of the areas varies between specific technologies. Thus, the common characteristics are first presented before more specialist areas are included. The chapter begins with an overview of carbonaceous fuels and their chemistry of combustion characteristics before illustrating application in common real world scenarios with coal-firing in air where typical pollutant control measures are also introduced. Enrichment of the combustion atmosphere with oxygen and carbon dioxide are considered for coal combustion before the combustion of biomass is discussed and the differences between coal and biomass combustion highlighted. An overview of methods of extracting reactivity data from bench-scale experiments is then presented to provide sufficient background for the development of a method conducted in Chapter 4. Drawing on the critical survey of the literature, and in line with the research goals in Section 1.17, research questions are then articulated for the combustion studies section of this thesis.

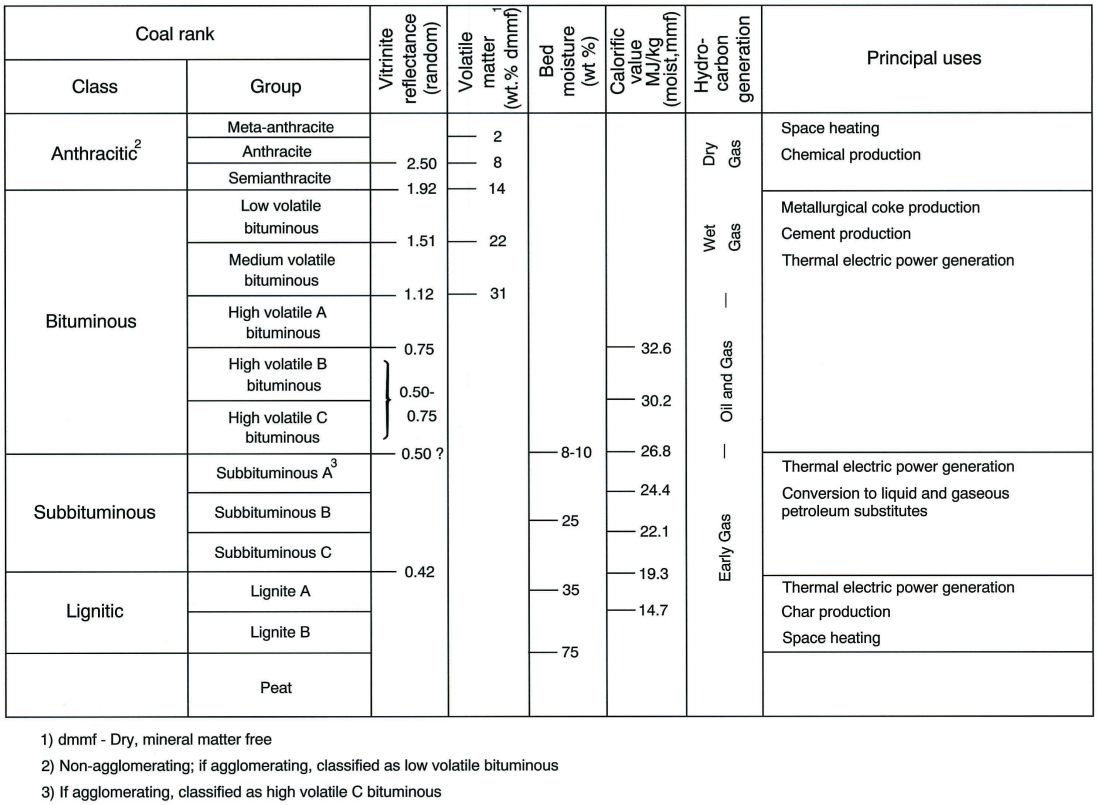

Figure 2.1: Coal rank chart [Smith et al., 1994]

2.2 Carbonaceous fuels

Coal and biomass, the foci of this thesis, are both categories of carbonaceous fuels which can be burned (oxidised) to produce energy. In this thesis 'biomass' refers to plant-based matter comprising of a mixture of cellulosic, hemicellulosic and lignin-based materials and does not include animal-derived biomass. Coal is a sedimentary rock that formed over millions of years from biomass which did not fully decay. The oldest coals began to form over 300 million years ago during the carboniferous period when biomass material was deposited into lake or swamp areas. A lack of access to air permitted only limited decay of the biomass and over time it was transformed into peat. Continued deposition of sediment above the peat compressed and elevated the temperature which caused more chemical changes such as the degradation of cellulose, conversion of lignin to humic materials and the subsequent conversion of these humic materials to coal. With the passage of time functional groups were removed from the main carbon chains and further condensation reactions occurred giving rise to increasing aromaticity and carbon content in older coals as they move up in rank from lignite to sub-bituminous to bituminous and finally to anthracites as shown in Figure 2.1 and discussed by Miller and Tillman [2008].

When these fuels are burned in oxygen, a significant amount of energy is released as heat. In power generation this heat is used to vapourise pressurised steam that then is forced through a turbine, expanding the steam and generating electricity.

Coal and biomass are broad classifications that include an enormous range of highly varied mixtures. Coal and biomass largely comprise of carbon (C), hydrogen (H) and oxygen (O) with smaller amounts of nitrogen (N) and, in coal particularly, sulphur (S) and chlorine (Cl). Both fuels also contain much smaller amounts of a wide range of inorganic components which may be organically bound or present as mineral matter. The major inorganic components found in carbonaceous fuels include silicon (Si), aluminum (Al), iron (Fe), mercury (Hg) and alkali metals such as sodium (Na) and potassium (K), and the alkaline earth metals calcium (Ca) and magnesium (Mg). The actual composition of a given coal or biomass covers an incredibly wide spectra of mixtures of these elements and the compounds they form including both complex organic molecules as well as a range of minerals including aluminosilicates, pyrites, and oxides among many others. As a result it has proved impossible to definitively classify these fuels' combustion characteristics and behaviour on the basis of their composition alone. However, a number of indicative measures are regularly used to group fuels and predict their likely behaviour, a famous example of such is the van Krevelen diagram, an example of which for biomass and coals is shown in Figure 2.2. This graph plots the ratio of hydrogen to carbon against the ratio of oxygen to carbon. Moving from the top-right to the bottom left of the van Krevelen diagram essentially represents coalification and then maturation of coal as the closer one moves to the origin the higher the energy density of the fuel. As well as the ultimate analysis of its composition, the proximate analysis of a fuel is also used to identify the proportion of the fuel that is moisture, volatile combustible matter, combustible material which remains bound to the particle (fixed carbon), and the amount of residual ash left after combustion has occurred. Other techniques such as petrography, vitrinite reflection and maceral analysis are also used to classify coals but are not useful for biomass analysis and are not used in this study.

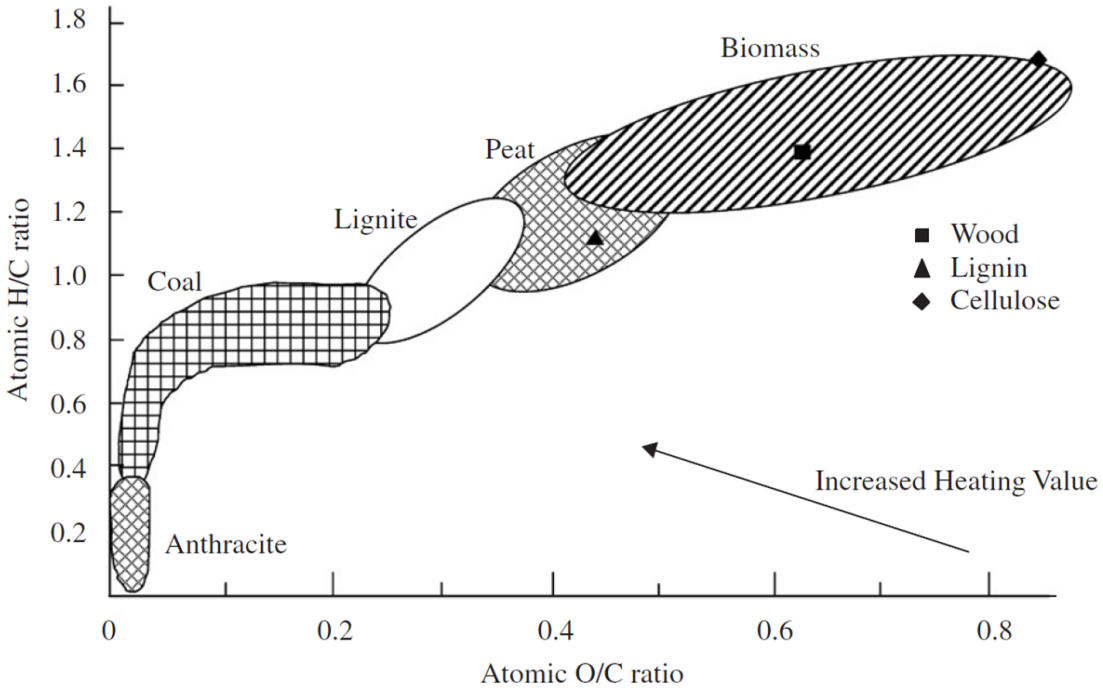

Figure 2.2: Van Krevelen diagram for biomass and coals [Prins et al., 2007]

2.3 Fundamentals of, and emissions from, the combustion of solid fuels

Combustion of carbonaceous fuels is understood principally based on the the macro components of the fuel and their reaction with oxygen. The combustion of fuels containing proportions of carbon (C_a), hydrogen (H_b) and oxygen (O_c) can broadly be understood by the following equation [Tillman, 1991]:

$$C_aH_bO_c + \left(a + \frac{b}{4} - \frac{c}{2}\right) O_2 \rightarrow aCO_2 + \frac{b}{2}H_2O + \text{heat} \tag{2.1}$$

The combustion process is often divided into four stages which occur at increasing temperatures in furnaces. The stages of combustion of a solid particle are widely acknowledged in the combustion community as drying, devolatilisation, combustion of volatiles and finally char combustion. A simplified schematic showing these stages is presented in Figure 2.3 while a more detailed overview of the processes occurring at each stage is presented in Figure 2.4. The drying stage begins around 100 °C during which surface and inherent moisture is vapourised and released from the particle causing it to shrink slightly. If intrinsic moisture in pore spaces is vapourised with no route of egress some particle fracturing may occur, particularly at the higher heating rates witnessed in commercial

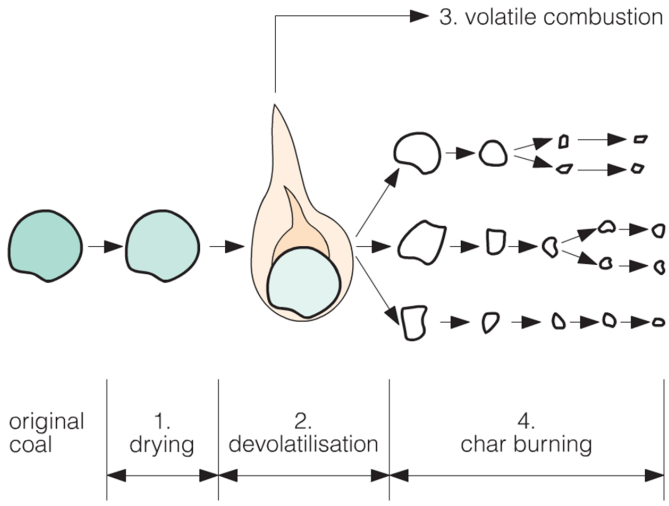

Figure 2.3: Schematic of the stages of the combustion process [Anthony and Preto, 1995, Carpenter et al., 2007]

pulverised fuel (PF) furnaces. As temperature continues to increase, devolatilisation then occurs with light, non-condensible and condensible, tar volatile fractions of the fuel being released from the particle. Most of these volatiles are then oxidised when they contact oxygen in the bulk combustion zone away from the particle. Finally, diffusion of oxygen from the bulk flow to the char then occurs and char-carbon is oxidised. Were this reaction to occur at relatively low temperatures it would be kinetically controlled, but at the temperatures in PF furnaces, which can typically reach 1500 °C, the diffusion of oxygen from the bulk gas through the boundary layer is the rate limiting step for the char oxidation which is itself the slowest of the combustion stages. Competition for oxygen at the particle tends to cause carbon on the char to be oxidised first to CO and then onto CO_2 once released from the particle into the bulk flow in a two-stage process [Carpenter et al., 2007, Tillman, 1991] .

2.3.1 Nitrogen combustion chemistry

The combustion of coal and biomass also involves production of nitrogen oxides via a variety of pathways but is dominated by the partial oxidation of fuel-bound nitrogen. Standard reporting for power stations is usually carried out according to emissions of total NO_x. However, approximately 95% of the total emissions of NO_x from combustion is NO though this is readily oxidised to NO_2 in the atmosphere. NO_2 and N_2O are also formed during combustion but these are less common due to a relative lack of oxygen in the furnace to produce NO_2 and due to rapid reduction of N_2O back to elemental nitrogen

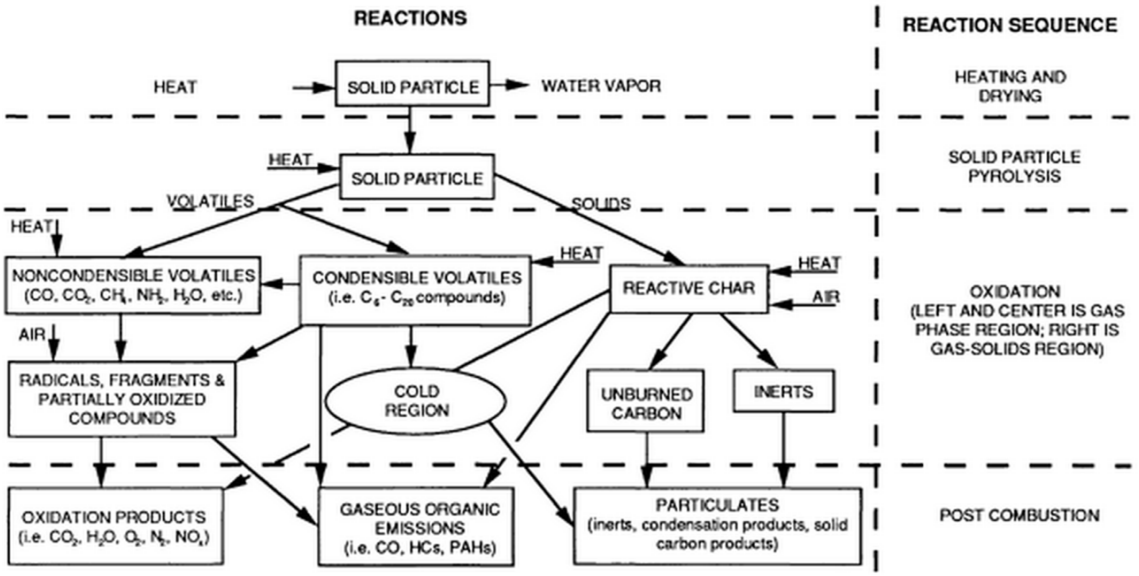

Figure 2.4: Schematic showing the stages and major reactions occurring during the combustion process [Tillman, 1991]

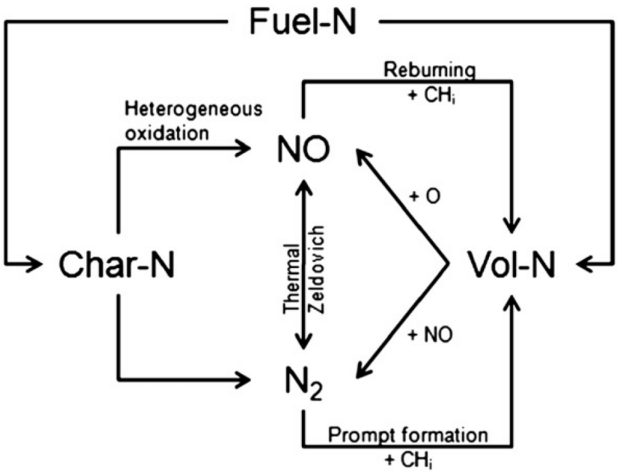

Figure 2.5: NO formation in combustion [Toftegaard et al., 2010]

by radicals in the furnace. Thus, the formation of NO is generally considered to be the most important stage in understanding the emissions of NO_x. Figure 2.5 illustrates that formation of NO during combustion is a complex coupling of three possible reactions classified as thermal, prompt and fuel routes with the potential of destruction of any NO formed. Toftegaard et al. [2010] conclude from the work of Glarborg [2003] that 80 % of NO is formed from fuel-bound nitrogen and the remainder is mainly formed via the thermal route, with prompt-NO seen as the least important of the mechanisms outside of nitrogen-lean fuels combusted in fuel-rich flames.

2.3.1.1 Thermal NO

Formation of NO by the thermal route occurs by the Zeldovich mechanism [Zeldovich, 1946] shown in Equation (2.2) and as noted by both Hill and Smoot [2000] and Glassman [1996]. Here, oxygen molecules dissociate into radicals that attack the nitrogen molecule producing NO and a nitrogen radical which can itself be oxidised to NO. Dissociation of oxygen incurs a substantial energy of activation; [Glarborg, 2003] suggests it is only possible above temperatures of 1800 K while [Nordstrand et al., 2008] suggests it does not become important until temperatures exceed 2200 K.

Thermal mechanism for NO formation

$$\begin{gathered}\text{Overall: } O_2 + N_2 \rightleftharpoons 2NO \\ \text{Stepwise: } O_2 \rightleftharpoons 2O \\ O + N_2 \rightleftharpoons NO + N \\ N + O_2 \rightleftharpoons NO + O\end{gathered} \tag{2.2}$$

The extended form of which includes the reaction:

$$N + OH \rightleftharpoons NO + H$$

2.3.1.2 Prompt NO

The prompt-NO formation pathway involves fuel-radicals reacting with elemental nitrogen near the flame to produce cyano compounds which are then oxidised liberating NO shown in Equation (2.3) as first suggested by Fenimore [1976] and noted in Hill and Smoot [2000] and Glassman [1996].

Prompt mechanism for NO formation

$$\begin{gathered}CH + N_2 \rightleftharpoons HCN + N \\ C_2 + N_2 \rightleftharpoons 2CN \\ N + OH \rightleftharpoons NO + H\end{gathered} \tag{2.3}$$

2.3.1.3 Fuel NO

Oxidation of nitrogen contained in both the volatile and char sections of the fuel is the most important NO formation mechanism in solid-fuel combustion. As Figure 2.5 shows, nitrogen can be bound into both the volatile or char fractions of the fuel. However, as Figure 2.6 shows the temperature at which char is formed strongly affects the propensity for nitrogen to be retained in the char (reducing for increasing temperature) and that for unstaged coal combustion NO is dominantly formed from the volatiles [Glarborg, 2003, Pershing and Wendt, 1979]. During devolatilisation,32.6 % nitrogen in the fuel forms cyanide and ammonia molecules which are then either oxidised to NO by the reactions shown in Equation (2.4) or reduced to N_2 depending on local conditions [De Soete, 1975, Hill and Smoot, 2000]. Char-bound nitrogen is directly oxidised by heterogenous reaction with oxygen diffusing to the particle surface, however this is readily reduced back to elemental nitrogen by further reactions with the char, soot or CO [Carpenter et al., 2007, Glarborg, 2003].

Mechanism for NO formation from fuel-bound N

$$\begin{aligned} \text{Fuel} &\rightarrow \text{HCN}/\text{NH}_3 + \text{char} + \ldots \\ \text{HCN}/\text{NH}_3 + \text{O}_2 &\rightarrow \text{NO} + \ldots \end{aligned} \tag{2.4}$$

2.3.1.4 NO recycling

Equation (2.5) shows that the NO formed can itself then be reduced to N_2 by other volatiles or recycled back to HCN through a heterogeous reaction with the char surface [Corlett et al., 1979, Hill and Smoot, 2000].

NO destruction mechanisms

$$\begin{aligned} \text{NO} + \text{HCN}/\text{NH}_3 &\rightarrow \text{N}_2 + \ldots \\ \text{NO} + \text{C}_x\text{H}_y &\rightarrow \text{HCN} + \ldots \end{aligned} \tag{2.5}$$

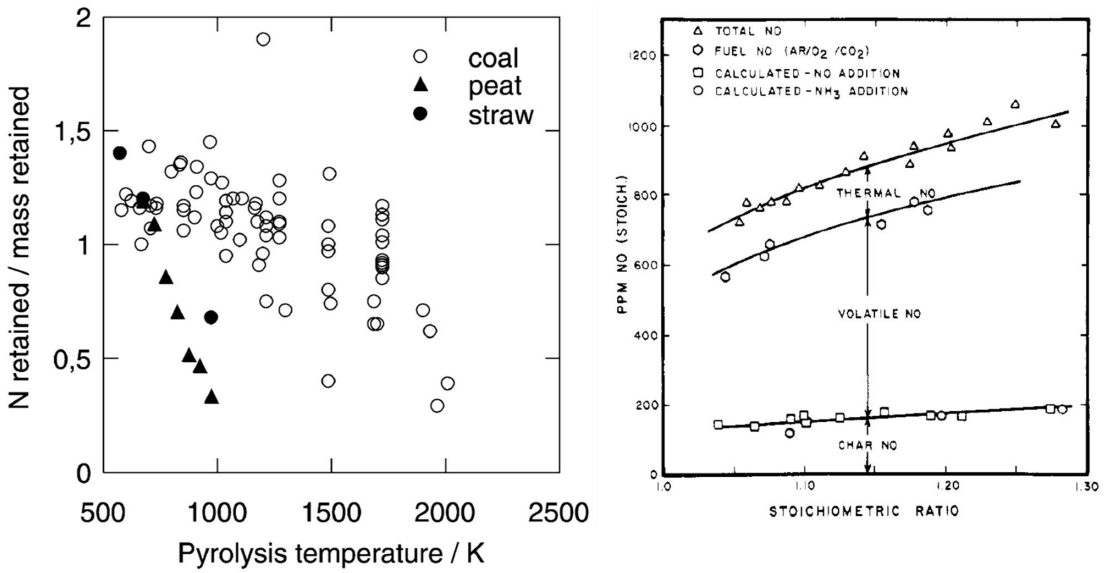

Figure 2.6: Variation in partitioning of nitrogen in fuels due to devolatilisation temperature (left) [Glarborg, 2003] and respective emissions from fuel partitions for unstaged pulverised coal combustion (right) [Pershing and Wendt, 1979]

2.3.2 Sulphur combustion chemistry

In coal combustion operating with excess oxidant, the majority of fuel-bound sulphur is oxidised to SO_2 with a small amount being further oxidised to either SO_3 or a sulphate ion retained in the ash. Sulphur may exist in coal in a variety of forms, though during combustion with excess oxygen most of these forms are oxidised to SO_2. Alkali and alkaline earth metals present in the fuel ash may capture some sulphur as sulphate ions and a small amount of sulphur is further oxidised in the furnace and emitted as SO_3 [Boardman and Smoot, 1993, Sarofim, 1987, Tillman, 2008].

2.3.3 Ash formation

Solid residue left after the combustion process can comprise a wide range of compounds which may cause detriment to the furnace and downstream equipment. Figure 2.7 shows that non-combustible materials present in the fuel can be one of three types. First, particularly common in biomasses and lower-rank coals, some alkali metals and alkaline earth metals can be found organically bonded within the coal molecule [McLennan et al., 2000]. During combustion, as the char oxidises these are vapourised and ejected from the coal particle, typically forming either submicron particles - through condensing and coalescing - or alternatively condensing on the surface of other larger ash particles. The other non-

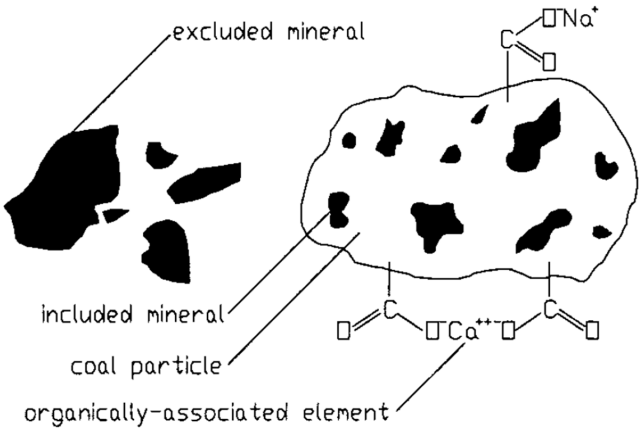

Figure 2.7: Ash components found in coal particles [McLennan et al., 2000]

combustible materials are generally labelled mineral matter and depending on whether this is found in the coal particle or is separated by the milling process, is labelled as included or excluded material. Mineral matter typically includes alumino-silicates, silicates, carbonates and disulphides with lesser amounts of sulphates, sulphides and oxides [McLennan et al., 2000]. Attempting to accurately describe the processes that occur during combustion is incredibly complex, since as Carpenter et al. [2007] note, mineral matter may undergo a wide range of changes including: "*coalescence, fragmentation, fusion, vaporisation and condensation that can occur sequentially or simultaneously.*" If ash components are in a molten state and impact the furnace walls or heat transfer equipment, the rapid cooling offered can cause the ash to condense and form a deposit on the surface. Deposition of ash in the form of slagging and fouling is problematic for combustion systems as the deposits form a barrier to heat transfer on key heat exchange surfaces. If left unremedied this can change the heat flux distribution through the furnace and cause an associated reduction in efficiency of the overall combustion system. Ash deposition is itself complex with: "*particle composition, particle size and shape, particle and surface temperatures, gas velocity, flow pattern and other factors* [able to] *influence the extent and nature of ash deposition*" [Babcock and Wilcox, 2005]. Detailed analysis of ash formation and deposition is therefore considered beyond the scope of this work. Instead use is made of several common indicators of the propensity of ashes to become deposited on the combustion equipment, either in the furnace or further along the pathway of combustion products.

2.3.3.1 Alkali index

In their experimental work, Miles et al. [1996] mention that the coal industry had developed the empirical alkali index (AI, $\mathrm{kg\,GJ^{-1}}$) shown in Equation (2.6) to predict whether fuels or blends of fuels were likely to cause deposition on heat transfer surfaces. The index compares the amount of alkali metals per unit of energy and the authors suggest that at values of 0.17 to $0.34\,\mathrm{kg\,GJ^{-1}}$ a slagging risk exists and that above $0.34\,\mathrm{kg\,GJ^{-1}}$ the fuel is virtually certain to slag and foul to an unmanageable degree.

$$AI = \frac{\mathrm{kg\,(K_2O + Na_2O)}}{\mathrm{GJ}} \tag{2.6}$$

2.3.3.2 Base-to-acid ratio

Another valuable predictor often used with biomasses, which was adopted from the coal industry, is the base-to-acid ratio ($R_{b/a}$) proposed by Salour et al. [1993] and shown in Equation (2.7). Here, a comparison between the mass fractions of basic and acidic oxides found in the ash is carried out. A value of approximately 0.7-0.8 indicates the minimum in ash melting temperature for coal ashes, though the minimum tends to occur at a lower value for biomass ashes [Bridgeman et al., 2007, Bryers, 1996, Jenkins et al., 1998]. Unlike the alkali index, the base-to-acid ratio implies that high alkali content can to some extent be mitigated by the presence of acidic ash components.

$$R_{b/a} = \frac{\mathrm{Fe_2O_3 + CaO + MgO + K_2O + Na_2O}}{\mathrm{SiO_2 + TiO_2 + Al_2O_3}} \tag{2.7}$$

2.3.3.3 Carbon in ash/ loss on ignition (LOI)

The amount of combustibles that remain in the ash offers an approximation of the efficiency of the combustion process. Although all of the combustibles in a fuel are able to burn, actual combustion conditions may inhibit the complete oxidation of all of the combustible material in the fuel. Any combustible material which passes through the furnace without being fully oxidised and releasing its energy is viewed as a loss in the overall efficiency of the process. The loss on ignition (LOI, %) of an ash sample heated in an oxidising atmosphere is used to compare the efficiency of combustion between experiments

Table 2.1: LOI requirements for reuse of fly ash in various nations [Dong, 2010]

Nation	LOI Limit (% Maximum)
Australia	3–6
Canada	3–10
China	5–15
EU (by type)	(A) 5; (B) 2–7; (C) 4–8
India	5
Japan	3–8
Russia	(Basic Ash) 3–5; (Acidic Ash) 2–25
South Africa	5
USA	6

and is defined by ASTM Standard D7348 [ASTM, 2008]. The calculation for LOI is shown in Equation (2.8).

$$LOI = \frac{\text{Mass of unburned fuel}}{\text{Mass of dry combustion ash sample}} \tag{2.8}$$

Ash is a substantial byproduct of the combustion process and in order to be used effectively in the production of construction materials the LOI value must be below certain values. Table 2.1 shows the limits for various nations.

2.4 Air-fired combustion of pulverised coal

Firing of PF in air is well-established technology for raising steam for power generation. A schematic of a modern PF generation plant is shown in Figure 2.8, which can be designed to accommodate a heat input of 900 MW [B&W, 2013]. Although almost all of the chemical energy in a fuel is liberated in the boiler, the global-average overall efficiency of converting this to electrical energy for PF boilers is about 30%. In the UK Drax is the most thermally efficient coal-fired power station and, following a recent turbine upgrade, operates with a thermal efficiency of just under 40% [Siemens, 2012]. Owing to their established use the performance of PF boilers has continued to improve through incremental innovations and dedicated research and development programmes. The main source of performance increase is now the development of materials able to withstand higher temperature steam cycles as higher steam temperatures promote an increased efficiency of the Carnot cycle. Modern supercritical boilers are able to operate steam cycles at considerably

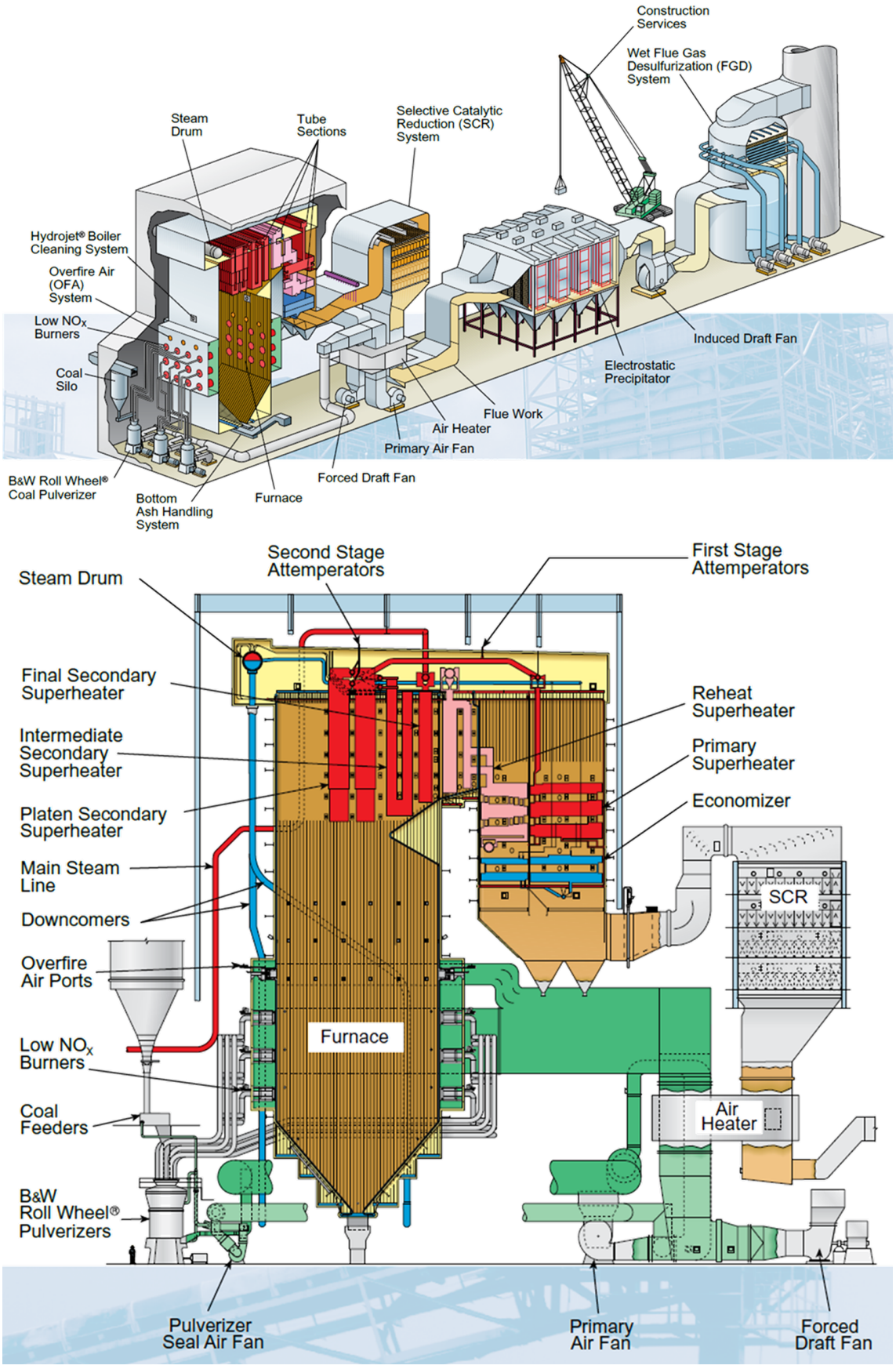

Figure 2.8: Schematic PF generation plant (above) with a detailed schematic of the boiler (below) [B&W, 2013]

higher temperatures than older plant and have efficiencies of approximately 45% (NCV basis). There is ambition to increase this to 50% with steam temperatures of 700 °C and above over the coming decades [APGTF, 2011].

2.4.1 Measures to reduce emissions of nitrogen oxides

In order to comply with increasingly tightening regulations on the emission of NO_x and other pollutants, various changes to the combustion system and the introduction of flue gas clean up technologies have been increasingly required. To comply with the European Industrial Emissions Directive (and its forerunner the Large Combustion Plant Directive) power plant operators have had to modify the combustion systems and flue gas cleaning operations in order to reduce the amount of NO their plant emit in the flue gas. Since NO is not present before combustion, measures to reduce emissions of NO can either be categorised as processes that prevent NO formation or processes that destroy or remove from the flue gas any NO produced. Stringent emission limits tend to predicate processes in both of these groups are employed together, since few, if any, techniques are able to reduce NO to permitted levels. Indeed, recent conclusions by a technical working group of the Environment Agency concluded that a mixture of primary measures to reduce NO creation and selective removal were to be considered the best available technology in the UK for achieving the IED limits [EA, 2011].

Flue gas clean up typically involves either destruction of NO by either reducing or oxidising it, or selective capture of NO by sorption mechanisms. Alternatively, reducing zones which destroy NO that has formed may be created in the furnace by selective injection of fuel or recycled flue gases. A reduction in the amount of NO produced can be brought about by other changes to the combustion process and can include techniques which operate by reducing the amount of nitrogen in the fuel, reducing the temperature in the furnace or reducing the availability of oxygen during the initial stages of combustion. Although this thesis focusses on processes which limit the production of NO during combustion, a brief overview of processes which remove or destroy NO remaining after combustion is also included.

Table 2.2: Ultimate analysis of solid fuels; dry, ash-free basis [Bridgeman et al., 2010]

Fuel Sample	**C (%)**	**H (%)**	**N (%)**	**S (%)**	**Cl (%)**	**O (%)**	**GCV (GJ kg^{-1})**
Pittsburgh 8	84.6	5.1	1.7	0.0	0.1	7.6	34.4
San Juan Basin	77.6	5.5	1.4	1.2	0.0	14.3	31.7
Willow	49.1	5.8	0.6	0.1	0.0	41.1	19.3
Miscanthus	43.5	5.7	0.3	0.1	0.1	38.9	17.6
Scrap Tires	85.9	8.0	0.4	1.0	0.1	2.3	40.0
Refuse Derived Fuel	51.3	7.5	0.8	0.2	0.6	29.7	23.1

2.4.1.1 Reduction in fuel-nitrogen

Using fuels with a lower nitrogen content can considerably reduce flue gas concentration of NO. As noted in Section 2.3.1, the majority of NO generated during PF combustion is via the fuel-NO route. Thus, measures to reduce the content of nitrogen in the fuels entering the combustion zone can directly affect the amount of NO produced. Table 2.2 highlights the range of nitrogen content in common fuels used in PF combustion with the biomasses (willow and miscanthus) displaying 2–6 times less nitrogen content than the coals (Pittsburg 8 and San Juan Basin). Indeed, energy crops generally are found to have nitrogen content of $<$1% [Jenkins et al., 1998, Vassilev et al., 2010] though some power station fuels have been shown to display N-content of up to 3.5% [Darvell et al., 2010]. However, when considering switching fuels the thermal input must be kept constant. Since biomass typically has a lower calorific value than coal, a higher mass of biomass will be required to achieve the same thermal output. In the comparison between coal and biomass above, accounting for the change in heating value, substituting coal for biomass could reduce the fuel-nitrogen entering the boiler by 30–65%. Direct comparisons are further complicated as biomasses tend to partition nitrogen to the volatiles more readily than coal [Glarborg, 2003] which could lead to higher NO emissions than may have occurred from char-bound nitrogen depending on the combustion conditions.

2.4.1.2 Methane de-NO$_x$

Thermal treatment of fuel to remove nitrogen before it enters the furnace is a developing technology option. One example of this approach was a project sponsored by the USA National Energy Technology Laboratories (NETL) which succeeded in significant reductions in NO$_x$ emissions by heating coal prior to combustion using natural gas in an oxygen lean

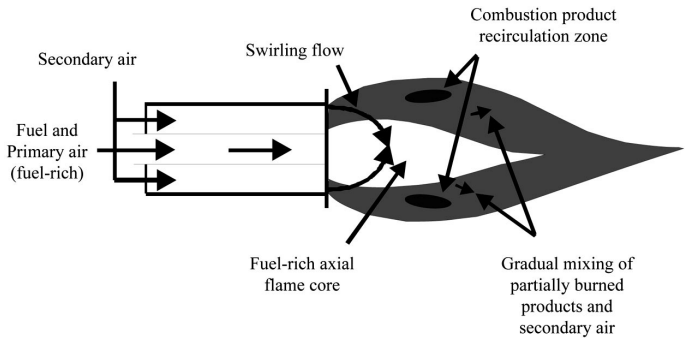

Figure 2.9: Schematic of a low-NO_x burner [Srivastava et al., 2005]

atmosphere. The process causes devolatilsation to occur in a reducing atmosphere which converts volatile-bound nitrogen to N_2 before the remaining fuel is passed to the furnace. The project was tested at 1 MW scale and found to be effective at reducing NO_x emissions by up to a half [Nester et al., 2003, Srivastava et al., 2005] but little further work has been reported.

2.4.1.3 Low NO_x burners

Low-NO_x burners (LNBs) are a well established technology able to deliver 40-80% reductions in NO_x emissions by regulating the stoichiometry and temperature profiles in the early stages of combustion in a way which reduces NO formation [Bedi, 2013, Sharp, 2013]. A schematic of a low-NO_x burner shown in Figure 2.9 illustrates the main focus of a LNB is to delay complete mixing of fuel and oxidant for as long as possible [Srivastava et al., 2005]. This is achieved by separating the combustion air and slowly mixing oxidant into a fuel-rich zone. Although Figure 2.9 displays the general principle for LNB operation, more advanced designs included extra annuli for staging the air into the burner and fuel concentrators to further delay mixing. This reduction in availability of oxidant prevents complete combustion of the fuel in the primary combustion zone which results in less energy being released and the temperature in the flame to be reduced thereby reducing the formation of thermal-NO. Simultaneously, this zone is reducing in nature and inhibits the formation of NO from nitrogen released during devolatilisation, instead favouring the pathway to N_2 as well as reducing the likelihood of prompt-NO formation. As the combustion air is mixed in combustion occurs in a staged fashion in several zones which tends to elongate the flame and can reduce the efficiency of combustion by increasing the amount of unburned carbon retained in the ash and emissions of CO. However, development over the last two decades has reduced losses in this area and the newest LNBs claim to have no

reduction on combustion efficiency [Bedi, 2013].

2.4.1.4 Oxidant staging

Staging combustion can also be carried out by injecting a portion of the combustion air into the furnace later in the combustion pathway. By removing a portion of the oxidant from the burner and injecting it as over-fired air (OFA), a further 10–25% reduction in NO emissions may be realised above that created by the use of LNBs through creating fuel-rich combustion near the burner and then adding oxidant to complete char burnout further into the furnace [Srivastava et al., 2005]. The amount of air that is injected as OFA tends to vary between 5–20% of the total in commercial applications. In a laboratory setting the results of the work of Ribeirete and Costa [2009] shown in Figure 2.10 found reduction in NO tends to increase with staging up to about 30% though substantial increases in CO emissions tend to occur when more than 20% of air is staged, which is line with findings by other researchers, for example [Daood et al., 2011]. In order to increase the amount of staging it is common to use fans to inject boosted over-fired air (BOFA) which increases mixing and combustion of char in the over-fired zone, thereby reducing carbon in ash and CO emissions [Costa and Azevedo, 2007]. An alternative technique to OFA is to inject high velocity air as rotating opposed fire air (ROFA) which disrupts the flame, and promotes thermal and component mixing during high temperature combustion by creating a swirling effect in the furnace [Srivastava et al., 2005]. Changes to the overall furnace operation such as reducing the overall excess air levels and operating burners out of service (BOOS) can also reduce the local oxidant concentration during the early stages of combustion.

2.4.1.5 Diluents

Reducing the local concentration of heat and oxygen can also be carried out by injecting a diluent into the combustion zone. Injection of cooled, recycled flue gas or steam into the primary combustion zone reduces the local oxidant concentration, acts as a medium to dilute the heat of combustion and also reduces the fuel residence time in the primary combustion zone. As well as limiting the formation of NO, any recycled NO in the flue gas is exposed to a reducing environment and may undergo reduction to N_2 during the second combustion process [EC, 2006, UNECE, 2012].

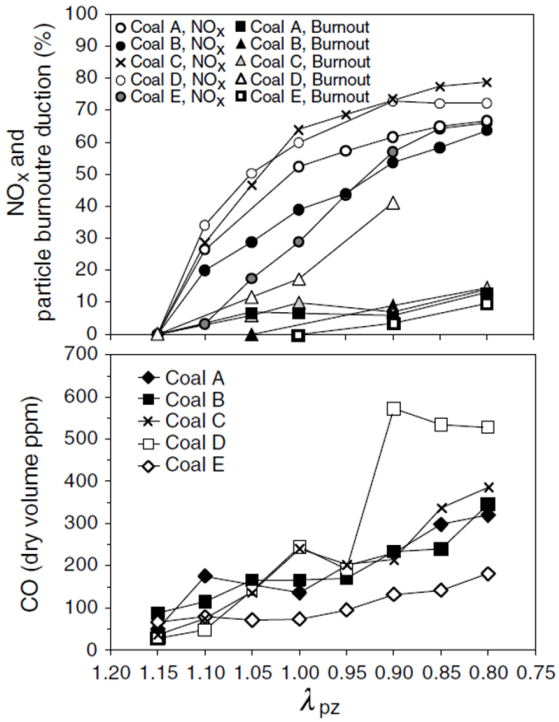

Figure 2.10: Effect varying the primary zone stoichiometric ratio (λ_{pz}) on NO_x emissions and carbon burnout (top) and CO emissions (bottom) [Ribeirete and Costa, 2009]

Table 2.3: Selected measures to reduce NO creation in PF boilers [Srivastava et al., 2005][a],[Nalbandian, 2009][b], [EC, 2006][c]

Technology	**NO_x removal efficiency (%)**	**Potential plant impacts**
Low NO_x Burners (LNB)	up to 50[a] 30–50[b]	elongates flame which may increase wall fouling and corrosion
Over-fired air (OFA)	additional 10–25 beyond LNB[a] 20–30[b]	may reduce fuel burnout, reducing efficiency and ash quality
Rotation Opposed Fire Air (ROFA)	45–60[a]	uses booster fan but improves burnout and temperature distribution
Oxygen-enhance combustion	50[a]	auxiliary power requirements $< 1\%$, increases carbon burnout
Preheat combustion system (methane de-NO_x)	42–67[a]	3–5% thermal input used for preheating of coal
Flue Gas Recirculation (FGR)	30 [c]	spacial issues for cooling and recycling large flue gas volumes

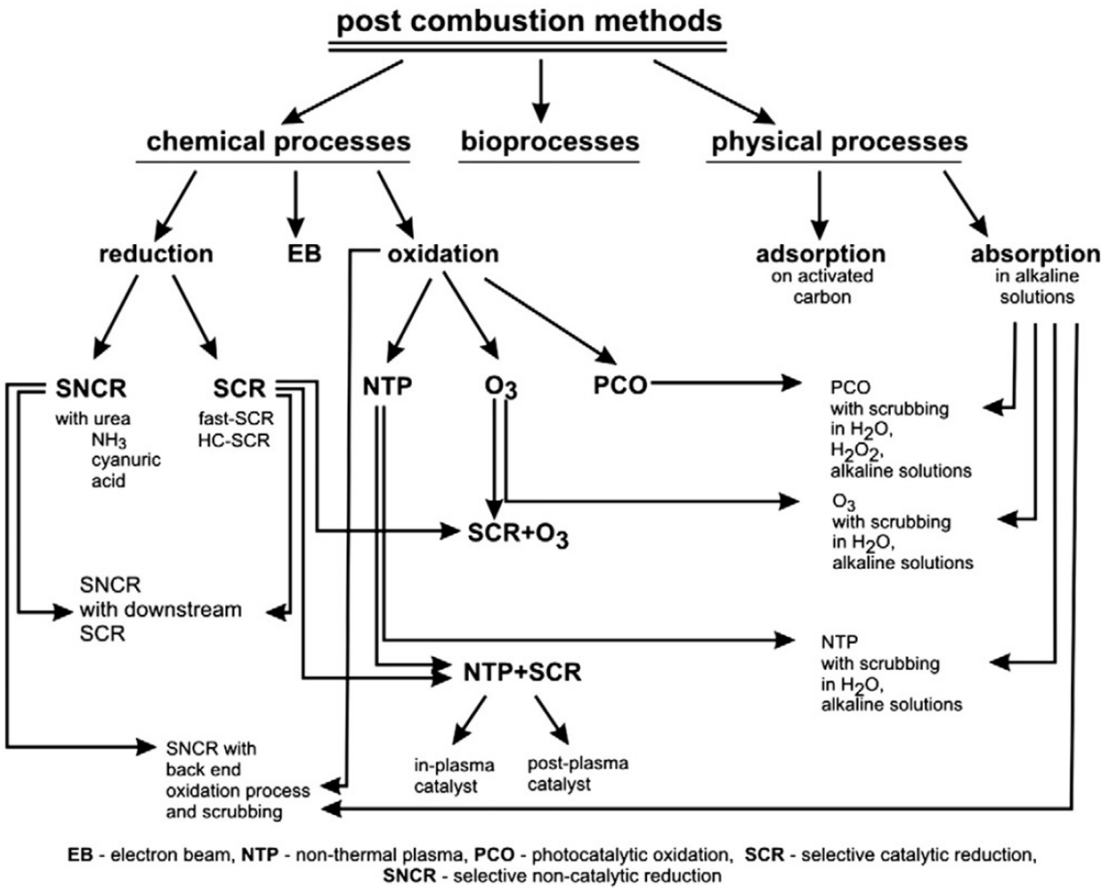

Figure 2.11: Overview of post-combustion techniques to remove NO from flue gas streams [Skalska et al., 2010]

2.4.1.6 Techniques for NO removal

As noted above, a detailed assessment of methods which destroy or selectively remove NO from the flue gas or by injection of another agent into the combustion system is considered beyond the scope of this thesis. However, for reference an overview of the wide range of post-combustion NO removal systems is presented in Figure 2.11 and Table 2.4 presents an overview of the effectiveness of the most commonly practised options at reducing NO emissions. Table 2.5 details a list of the large number of available techniques that remove SO_2 and NO_x from the flue gas concurrently.

2.4.2 Measures to reduce emissions of sulphur oxides

Reductions in SO_2 emissions can to some extent be achieved by modifications to the combustion process, though the majority of effort for reducing SO_2 is focussed on scrubbing SO_2 from the flue gas. Measures to reduce SO_2 formation during combustion are limited in comparison to the range of options available for reducing NO_x emissions since

Table 2.4: Selected measures to destroy or selectively remove NO from PF boilers [Srivastava et al., 2005][a],[Nalbandian, 2009][b]

Technology	NO_x removal efficiency (%)	Potential plant impacts
Reburning	39–67[a] 50–60[b]	may affect flame stability, combustion efficiency and CO emisssions
Selective non-catalytic reduction (SNCR)	30–66[a] 15–35[b]	may require multiple injection zones in temperature window
Selective catalytic reduction (SCR)	80–90+[a] 80–90[b]	catalyst deactivation requires maintenance, potential for increase in NH_3 emissions
Advanced gas reburning (AGR)	68–76[a]	ammonia slip or high-temperature injection needed
Fuel-lean gas reburning (FLGR)	30–45[a]	careful injection and controlled mixing of natural gas required
Amine-Enhanced fuel lean gas reburning (AEFLGR)	55–73[a]	nitrogen compound injected into reducing zone
Hybrid-selective reduction (HSR)	up to 95[a]	lower capital cost than SCR
In-duct SCR	85–90[a]	allows SCR on space-constrained units

Table 2.5: Selected measures to simultaneously remove NO and SO_2 from PF boilers [Srivastava et al., 2005]

Technology	SO_2 and NO_x removal efficiency (%)	Potential plant impacts
Electron-Beam	SO_2 >95 NO_x ≤90	Extensive by-product treatment and high energy requirement
ROFA/ ROTAMIX	SO_2 64–69 NO_x ≤80	Slagging, fouling and corrosion issues
SNOX	SO_2 >90 NO_x >90	Increased auxiliary power requirements and ammonia storage issues
SNRB	SO_2 80–90 NO_x ≤90	Bag filter reliability issues
Activated coke	SO_2 90–98 NO_x 60–80	Warm up time and reaction interdependence issues
Electrocatalytic Oxidation	SO_2 98–99 NO_x ≤90	3% auxiliary power requirement
NOXSO	SO_2 ≤98 NO_x 75–90	Desorption reactions add complexity
Copper Oxide	SO_2 ≤90 NO_x ≤90	High-temperature regeneration

almost all sulphur present in the fuel is fully oxidised to SO_2 in most combustion systems [UNECE, 2012]. Switching to lower-sulphur fuels is one route of reducing SO_2 emissions commensurate with the reduction of sulphur entering the furnace. Biomass fuels are a key option for such reduction because, as shown in Table 2.2, they tend to have substantially lower sulphur content than coals. Alternatively, SO_2 produced during combustion may be reacted with alkali metals or alkaline earth metals to produce sulphates as the reactions below show. Group I and II metals may be provided by the fuel itself, in which case sulphur is trapped in the ash, or in post-combustion clean-up systems known as flue gas desulphurisation (FGD). FGD is widely employed at most modern power stations and seen as necessary for meeting IED limits of 200 mg/Nm^3. The process for wet-FGD referred to by Toftegaard et al. [2010], which is able to remove 92–98% SO_2 from flue gas and is most common in coal-fired power stations, is shown in Equations (2.9) to (2.13). This FGD process produces gypsum ($CaSO_4 \cdot 2H_2O$) which is often sold for the manufacture of plaster board.

$$SO_2 + H_2O \rightleftharpoons HSO_3^- + H^+ \tag{2.9}$$

$$CaCO_3 + 2H^+ \rightleftharpoons Ca^{2+} + HCO_3^- + H^+ \tag{2.10}$$

$$Ca^{2+} + HCO_3^- + H^+ \rightleftharpoons Ca^{2+} + H_2O + CO_2 \tag{2.11}$$

$$HSO_3^- + {}^1\!/_2O_2 \rightarrow SO_4^{2-} + H^+ \tag{2.12}$$

$$SO_4^{2-} + Ca^{2+} + 2H_2O \rightleftharpoons CaSO_4 \cdot 2H_2O \tag{2.13}$$

2.4.3 Measures to reduce emissions of solid particulates

For the majority of modern PF combustion plants particulate matter produced during the combustion process is removed by the use of electrostatic precipitators (ESPs), though bag filters and cyclones may also be used. ESPs operate by forcing flue gas through channels created by earthed plates. In the centre of the channels are emitting electrodes which ionise the gas near them causing it to be attracted to the plates at the channel walls. As ionised gases moves toward the channel walls they collide with, and charge, ash particles that are then also attracted to the plates. The particles impact on and stick to the plates. Periodical rapping of the plates causes the collected particles to drop into hoppers that collect the ash [EC, 2006]. If this ash meets the criteria highlighted in Table 2.1 it can be

sold to the construction industry for use as an aggregate in concrete production. ESPs are highly efficient, removing $\geq$99.95% of particles larger than 5 μm and $\geq$98.3% of particles larger than 2 μm, resulting in emissions from new plants of $\leq$5–10 mg/Nm^3 [EC, 2006, UNECE, 2012].

2.5 Biomass combustion

Biomass combustion displays similarities to combustion of coal, though differences in composition and structure predicate treatment of biomass must be individual in nature. Although biomass is considerably different from coal as a fuel source, combustion of biomass is similar in many ways to coal combustion, particularly when used for electricity generation. However, the recent review of the subject by Williams et al. [2012] concludes that: "*The basic features of biomass combustion and resultant pollutant formation are understood but much of the detail is lacking ... The analogy with the processes occurring in coal combustion is not adequate.*" In particular, differences in the ultimate and proximate composition of biomass and significant differences in particle structure and morphology highlight areas where coal-derived knowledge must be modified if to be successfully applied to the combustion of biomass. Despite these differences, large-scale combustion of biomass for electricity generation is widely practised with biomass co-fired with coal as well as providing the sole energy input to boilers at many industrial sites in the UK and Europe. This has presented a situation where experimentally biomass combustion is understood well enough to be considered a mature technology while in academic, and especially modelling studies that rely on fundamental understanding, many gaps in knowledge remain. The wide range of biomasses available for combustion and the variety of combustion techniques have sustained academic and industrial research in this area. In this work the focus is on experimental combustion of PF and this is reflected by the following literature. However, where relevant, crossovers into modelling and alternative combustion technologies will be presented.

The fundamental stages of combustion and chemistry presented for all carbonaceous fuels in Section 2.3 are valid for the combustion of biomass. However, variation in the fuel can lead to changes in the importance of individual stages of the combustion process, which in turn affects the emissions of pollutants and practical combustion operations. Biomass covers a very wide variety of materials and the composition and results of proximate

Table 2.6: Proximate analysis of selected solid fuels; as received basis [McKendry, 2002][a], [Vassilev et al., 2010][b]

Fuel Sample	Moisture (%)	VM (%)	FC (%)	Ash (%)
Bituminous coal[a]	11	35	45	9
Bituminous coal[b]	3	29	53	15
Lignite[a]	34	29	31	6
Lignite[b]	11	33	26	31
Wood[a]	20	82	17	1
Wood[b]	8	78	15	0
Barley Straw[a]	30	46	18	6
Barley Straw[b]	12	67	16	5
Miscanthus [b]	11	72	14	3
Reed Canary Grass [b]	8	68	16	8
Willow [b]	10	74	14	1

analysis varies by species and within species according to tissue type, developmental stage, cell type, growing season and growing environment [Tanger et al., 2013]. As shown in Tables 2.2 and 2.6, biomass resources can vary considerably but tend to comprise of a higher moisture, volatile matter and oxygen content and lower content of fixed carbon, nitrogen, sulphur and heavy metals than coals. These trends tend to indicate that biomass of all types has a lower heating value than typical of coal, while also being less likely to emit NO_x and SO_2 emissions. However, the amount of chlorine and alkali and alkaline earth metals can be higher in biomasses which can cause slagging, fouling and corrosion issues in commercial boilers.

Lignocellulosic biomass largely consists of material that makes up the cell wall and can be divided by varying amounts into three main components: hemicellulose, cellulose and lignin. Hemicellulose represents the lightest of the molecules and includes a range of five- and six-carbon sugar molecules which form heterogenous branched chains. Cellulose is formed from a consistent polymer chain of D-glucose units. Lignin includes a complex mixture of branched phenolic molecules forming long polymers [Tanger et al., 2013]. Table 2.7 shows that like the ultimate and proximate analyses, the content of each of these three subcomponents varies between biomass resources. Such a variety in biomass resources makes ranking and grouping types difficult and to date no satisfactory method has been used to classify the range of reserves [Williams et al., 2012]. However, similar trends can emerge when investigating types of biomass and to this end virgin biomass is

Table 2.7: Lignin, hemi-cellulose and cellulose content of selected biomass samples [Robbins et al., 2012]

Fuel Sample	Cellulose (%)	Hemi-cellulose (%)	Lignin (%)	Ash (%)	Solubles (%)
Wheat Straw	34.9	22.5	21.3	9.4	11.9
Miscanthus	41.9	16.6	13.3	3.2	15.0
Switchgrass	46.1	32.2	12.3	4.7	ND
Reed Canary Grass	28.0	22.0	14.0	8.0	28.0
Hard Wood	43.3	21.8	24.4	0.5	ND
Soft Wood	40.4	31.1	28.0	0.5	ND

ND = Not determined, values presented as percentage dry weight

often grouped into woody biomasses, agricultural residues and grasses. Fuels for energy generation may be sourced from either of these groups [Vassilev et al., 2010].

Comparison of the combustion of biomass with that of coal is complex and often dependent on the biomass (and the coal) used for comparison. The following is a summary of the relevant differences between coal and biomass PF firing largely drawn from the findings of Williams et al. [2012]. Upon heating of biomass, typically more moisture needs to be driven off which can retard combustion. However, once the fuel has been dried, hemicellulose begins to decompose with the onset of devolatilisation occurring in the range 160–250 °C, several hundred degrees earlier than the onset seen in coal [Carpenter et al., 2007, Williams et al., 2012]. With typically twice the content of volatile matter of coals, biomasses release the majority of their calorific value during the oxidation of volatiles before proceeding to char combustion. NO_x formation is dominated by the fuel-NO pathway and, owing to the larger volatile content, control of NO_x-formation can be carried out by primary control methods such as LNBs and OFA [Hein and Bemtgen, 1998]. The low sulphur content of biomass tends to reduce SO_2 emissions while higher alkali and alkaline earth metals can contribute to an increased likelihood of corrosion and fouling. Dust emissions vary between biomasses and depend on the ash content of the fuel, the content of aerosol-forming metal compounds and a complex suite of reactions occurring in the furnace as detailed in Figure 2.12. In general, the lower carbon content and CV and higher amount of moisture and volatiles can cause ignition and burnout problems when combusted alone, particularly when larger, non-spherical fuel particles are used. However, once ignited biomass tends to burn at a faster rate than coal due to rapid volatile release

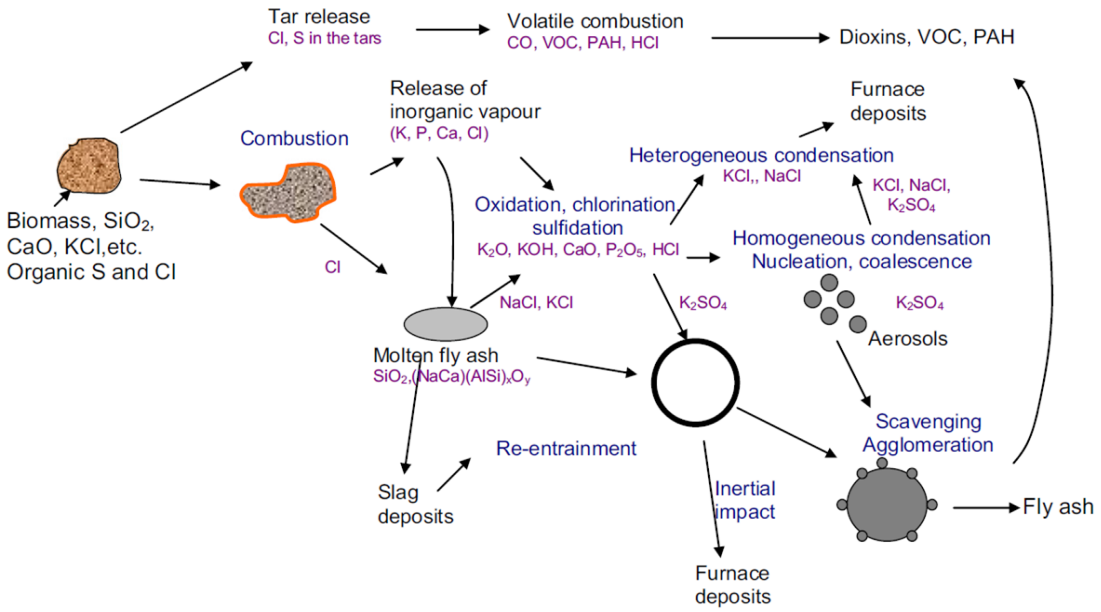

Figure 2.12: Formation pathways for aerosols, furnace deposits and solid pollutants for K, Cl and S compounds [Williams et al., 2012]

and increased porosity, reactive surface areas, presence of catalytic metals and intrinsic oxygen of biomass chars [Williams et al., 2012].

2.5.1 Cofiring with coal

Cofiring of biomass with coal has successfully been used for electricity generation for approximately two decades and is now a well-established technology option for large-scale PF combustion plant with over 150 operating plant worldwide [Al-Mansour and Zuwala, 2010, Hein and Bemtgen, 1998, Pedersen et al., 1996, Williams et al., 2012]. Continued interest in cofiring biomasses has occurred due to its ability to reduce net GHG emissions from PF plant which has led to a considerable amount of laboratory and pilot-scale research in the area. Sami et al. [2001] note the three main options that may be applied when cofiring is introduced: *a*) separate feed lines and separate burners for coal and biomass fuels; *b*) separate feed lines and a common burner; and *c*) common feed lines and a common burner with pre-mixed coal biomass blends. In this work, only the third option is considered relevant to experimental apparatus available. The following paragraphs detail relevant work reported in the literature for cofiring of PF burned in this way.

In the 1990s a large multi-partner European project investigated biomass cofiring in fluidised bed (FB) and PF combustion at scales ranging from laboratory furnace to industrial

power station, using a range of fuels and implementing a range of combustion techniques. Of the range of experiments carried out, PF firing of straw, wood, miscanthus and waste paper relate to the current work. In their summary review Hein and Bemtgen [1998] report on several non-combustion aspects, such as the need for separate milling procedures for biomasses. As a result of combustion tests, the authors note that the increased residence time flexibility in large boilers permitted substantially larger biomass particle sizes than could be accommodated at pilot scale. In the smaller-scale tests dimensions of 4–8mm diameter and 2–3cm length were required for miscanthus and straw while wood needed to be reduced to less than 1mm in size for satisfactory combustion. As a result of combustion testing the authors drew several conclusions: *a*) the high volatile content of biomass proved sufficient to maintain fuel ignition; *b*) biomass cofiring in PF boilers can reduce NO_x emissions through conventional methods; *c*) biomass fuels with lower nitrogen and sulphur contents reduce NO_x and SO_2 emissions relative to coal firing; and *d*) corrosion levels increased with increased Cl contained in the fuel, but that these levels and those for fouling were acceptable to plant operators.

Spliethoff and Hein [1998] used a 0.5 MW down-fired PF furnace to demonstrate cofiring of miscanthus, straw and sewage sludge with coal. Under unstaged conditions the relative nitrogen content of the fuel caused NO_x emissions to fall for increasing biomass blending ratios (BBR) of miscanthus and straw but to increase with increasing blending of the nitrogen-rich sewage sludge. Provided sufficient time was allowed for combustion of the relatively large (4mm) biomass particles, air staging was found to reduce NO_x emissions from 1400 mg/Nm^3 for unstaged combustion to 400–600 mg/Nm^3 for stoichiometric ratio (λ) of 0.9 and as low as 200–400 mg/Nm^3 for $\lambda = 0.6$–0.8 at 6% exit [O_2]. The work also demonstrated that reburning was effective at reducing NO_x emissions and that SO_2 emissions reduced due to a lower-sulphur fuel and due to Ca and Mg present in the biomasses retaining sulphur in the ash.

As a baseline for wider investigations Nimmo et al. [2010] showed that cofiring 15% shea meal and cotton stalks under 31% oxidant staging (λ = 0.8 for 16% excess O_2) at 20 kW scale was able to achieve NO_x emissions of 250 ppm and 190 ppm, respectively. Using the same experimental apparatus Munir et al. [2010] showed that variation in the blending ratio from 5–15% of these fuels could reduce NO_x emissions by up to 60% for λ = 0.9 and 70% for λ = 0.8 when compared to an unstaged coal baseline. In follow on work, Munir et al. [2011] investigated the effect on carbon burnout and NO_x emissions of

cofiring the fuels used previously as well as wood chips and sugar cane bagasse. Increasing residence time in the reducing zone was able to reduce NO_x emissions but at the cost of increasing LOI results. Blending of biomass was found favourable to the trade off which concluded $\lambda = 0.9$ represented the optimum extent of oxygen staging with OFA injected at port 3 in their apparatus. At these optimum conditions variation of BBR levels was found able to reduce NO_x emissions by $\sim$ 50-75% while suggesting that carbon burnout was maximised at BBR of 10% for all fuels except the wood chips which displayed reduced burnout compared to coal for all tests. The results reported that carbon burnout under staged conditions was lower than in unstaged conditions for all cases.

Hussain et al. [2013] fired cereal co-product (CCP) with Daw Mill coal at 100 kW under unstaged conditions mainly to investigate the deposition potential of the fuels on heat exchanger surfaces. The relatively high nitrogen content of the biomass (2.7%$_{ar}$) coupled with the reduction in calorific value of the fuel when switching from coal to biomass (from 21.4–16.3 MJ kg^{-1}) increased the amount of nitrogen entering the furnace by approximately a factor of three. Although the authors note that the actual changes are fuel-dependent, the results show a trend of slight increase in NO emissions as BBR increases though the results which suggest a decrease in conversion of fuel-N to NO_x with increasing BBR. SO_2 emissions were found to be relatively stable for increasing BBR until 80%$_{wt}$ CCP where SO_2 emissions reduced dramatically. The deposition flux when the pure fuels were fired was found to be higher than all of the cofiring tests except BBR = 20%$_{wt}$. From this maximum increasing BBR reduced the deposition flux for all other cofiring ratios. The deposition of potassium (K), S and phosphorus (P) increased with increasing BBR reflecting the higher content in the CCP and similarly Al deposits reduced during this trend as this was far richer in the coal ash. Deposition of Si remained relatively constant despite the amount of Si entering the furnace increasing with BBR. Using the same apparatus for firing miscanthus with Daw Mill coal, Khodier et al. [2012] found reductions in NO_x from 400–290 ppm, in SO_2 from 450–10 ppm and in HCl from 100–10 ppm when moving from coal to dedicated biomass firing. For NO_x and HCl this decrease was fairly linear as BBR increased. However, SO_2 emissions remained relatively stable for the coal and co-fired cases at approximately 300–450 ppm but fell sharply when the biomass was fired alone. For both sets of results, increasing BBR caused an increase in exit moisture concentrations.

In their work at 500 kW Bartolomé and Gil [2013] reported at BBR = 15%$_{th}$ emissions

of CO varied from increasing 30% compared to coal for cynara and decreasing by 15% for poplar. Emissions of SO_2 fell with increasing BBR. This effect was almost directly correlated to BBR for poplar with 15% effecting a 14% reduction in SO_2 emissions. The trend was broadly linear for cynara too though less pronounced with 15% effecting a 3.5% reduction in SO_2 emissions. For NO_x the effectiveness of the biomasses at reducing emissions was reversed with cynara reducing emissions by 20% while poplar only accounted for a 9% reduction at BBR = 15%. The authors suggest this could be due to fluid dynamic differences between the fuels and their firing regimes.

From their work with a 20 kW entrained flow reactor (EFR) cofiring several coals and biomasses, Kazagic and Smajevic [2009] conclude that fuel-N content alone cannot explain NO_x emissions. The work validates for biomass fuels that increasing furnace temperatures increases thermal-NO and reducing the available oxidant in the reactor reduces NO_x emissions through preventing oxidation of fuel-N. The results suggest that above temperatures of 1200–1300 °C temperature and oxidant staging had no effect on SO_2 emissions.

2.5.2 Dedicated biomass combustion

Dedicated combustion of pulverised biomass is less frequently reported in the literature compared to cofiring with coal. Instead, dedicated biomass combustion tends to be completed in FB or in grate boilers, typically operating at lower energy input than industrial PF boilers. For example, a review of biomass combustion experiments in Denmark in the decade to 2005 included PF cofiring up to 20% BBR, FB cofiring up to 50% BBR and only in grate firing was dedicated biomass firing conducted [Jappe Frandsen, 2005]. Even where reported, PF firing of biomass tends to be dominated by large-scale CFD modelling studies or, if experimental, the focus is on ash deposition on heat transfer surfaces with limited or no reporting of gas emissions. For example see the work of Wu et al. [2013], Bashir et al. [2012] or Tobiasen et al. [2007]. Both these types of studies tend to focus on large-scale ($>$1MW) units and as a result are less able to investigate a variety of combustion techniques such as for example variation in oxidant staging for NO_x control.

In the work of Spliethoff and Hein [1998] highlighted above the researchers also investigated dedicated biomass combustion. The focus of the work is cofiring and only limited dedicated results are reported. In summary, the work reports the following: *a*) cofiring of coal and biomass is synergistic with regard to achieving higher burnout; *b*) unstaged

emissions of NO_x are lower than emissions from cofiring but that oxidant staging to reduce λ to below 0.8 results in lower NO_x emissions from coal and co-fired fuels than for 100% straw; *c*) although not as effective at reducing emissions as for coal and cofiring applications, oxidant staging of miscanthus, straw and wood combustion with residence times of 2.5s in the reducing zone is able to substantially reduce NO_x emissions from 1400 mg/Nm^3 to a minimum of 300 mg/Nm^3 at a value of $\lambda = 0.65$–0.75; and *d*) increasing BBR reduces the conversion of fuel-sulphur to SO_2 from 80–100% for coal to 46% and 32% for dedicated firing of straw and pine, respectively.

The work of Ma et al. [2007] is focussed on CFD modelling of a 1MW PF boiler though in this work the authors allude to experimental results used to validate their predictions. The combustion test facility (CTF) is equipped with LNB and OFA and for wood-firing the authors report experimental NO_x emissions were 140ppm. Owing to the low sulphur content of the fuel (0.026 $\%_{ar}$) it is assumed SO_2 emissions are negligible. The lower CV of biomass (value not reported) is thought to be responsible for the reduction in furnace exit temperature compared to coal combustion at $\sim$ 1000 °C. In addition to this lower combustion temperature, consumption of NO_x-forming radicals by K released by the biomass is thought to further reduce NO_x emissions though the impact of this is reported to relatively unknown but thought to be small. The authors comment that the low ash content of biomass indicates a high LOI value is more acceptable in terms of combustion efficiency, though this may not be the case for reuse of the ash in the aggregates industry.

The work of Skrifvars et al. [2004] is concerned with investigating the deposition on heat exchanger surfaces during combustion of pulverised wood in a 80 MW_{th} down-fired boiler. In this work the authors investigated the effect on deposition of adding peat and elemental S to boiler. In both cases this caused emissions of SO_2 to increase, to a maximum of 105ppm for 5% peat and 0.1% elemental sulphur added. In addition to increasing SO_2 emissions and the sulphur content in the ash, the authors report an increase in HCl emissions and a decrease in Cl deposition.

Nordgren et al. [2013] also studied the deposition nature of biomasses fired as a PF. The authors note the relative dearth of publications relating to suspension firing of biomass (as opposed to bed or grate firing) and denote it as being due to the technique being relatively new. The work provides an in depth analysis of ash formation and deposition due to the cofiring of straw with wood and bark at a scale of 100–150 kW in a horizontally

fired LNB, staged with 40% of the combustion air being delivered by the tertiary stream. While the majority of the work focusses on detailed evaluation of changes in ash oxide deposition some combustion process measurements are reported. For the range of biomass blends the gas temperature in the furnace was measured in the range of 1100–1200 °C and exit O_2 concentrations of 3–4% were used (6% for straw/bark cofiring). Emissions of CO were found to be $<$120 mg/Nm^3. Emissions for the relatively S-rich straw (0.13%) were 155 mg/Nm^3 which corresponded to 44% of fuel-S being converted to SO_2. Blending of the straw with wood and bark reduced this conversion to 17–30% and 11–22%, respectively. The finer ash particles were found to be rich in K, Cl and S while the larger ash particles were found to also contain considerable amounts of Si and Ca. Through comparing experimental ash with modelled predictions the authors conclude that the fast heating rate and relatively short residence time (compared to other biomass combustion options) is largely responsible for non-equilibrium behaviour of the ashes produced.

Also noting a lack of research in the area, Lin et al. [2009] investigated the impact of air staging on emissions of NO_x and CO when firing wood (beech saw dust) and cofiring wood and straw in a 20 kW PF boiler. The authors report on parameters used to define an optimum location for OFA and extent of oxidant staging though conclude that precise optimisations for a given furnace are fuel dependent. Figure 2.13 shows a minimum in NO_x emissions in the range $\lambda = 0.75$–0.85 for an overall excess of 25% while Figure 2.14 shows that below values of approximately $\lambda = 0.9$ emissions of CO increase substantially. This is thought to reflect a loss in combustion efficiency as the residence time in the oxidising section is too short to allow complete combustion to occur. Temperatures in the 1.85 m furnace vary from around 1200–800 °C during wood combustion with the maximum typically found approximately 300 mm downstream of the burner throat. As the level of staging increased (decreasing λ) temperatures in the top of the furnace initially increased until $\lambda \approx 0.9$ after which temperatures began to gradually decrease with decreasing λ. As observed in coal combustion, increased staging tended to increase temperatures further down the furnace as combustion was delayed. When cofiring two biomasses the synergistic effect seen when cofiring biomass with coal was also observed with a reduction of conversion of fuel-N to NO_x compared to the individual fuels.

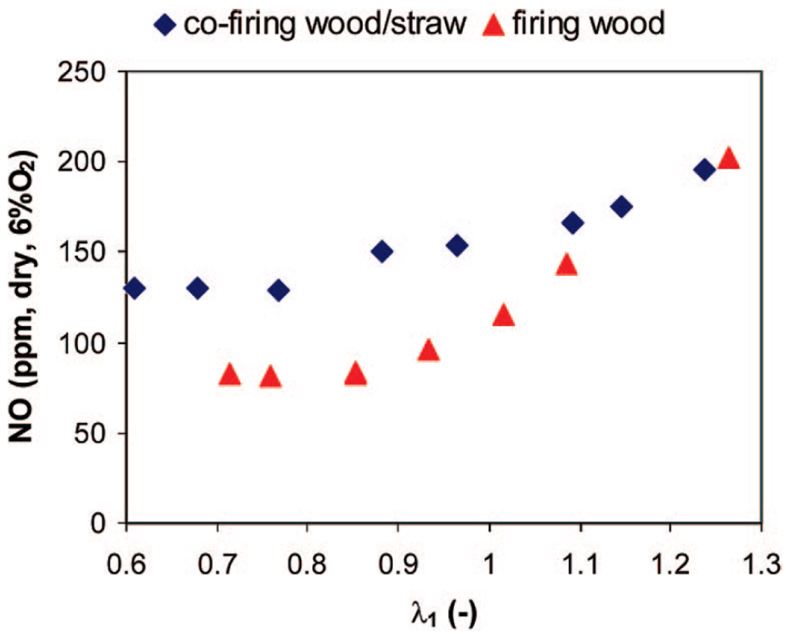

Figure 2.13: Variation in emissions of NO due to oxidant staging at 20 kW [Lin et al., 2009]

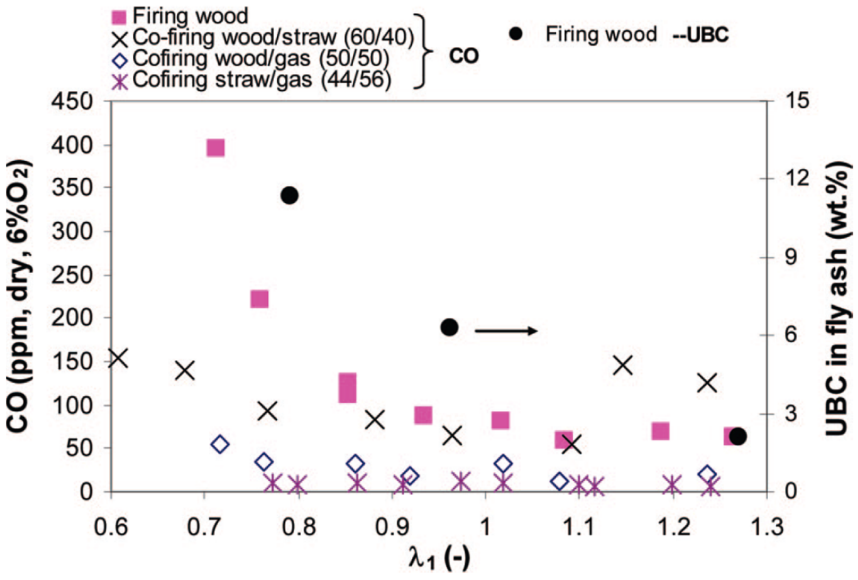

Figure 2.14: Variation in emissions of CO due to oxidant staging at 20 kW [Lin et al., 2009]

2.6 Oxygen-enriched air combustion (OEC)

Combustion of fuels in oxygen-enriched air aims to combine the best features of post-combustion capture and oxyfuel combustion for CCS [Smart and Riley, 2012]. The concept involves enriching the oxygen concentration of combustion air in order to increase the CO_2 concentration in the flue gas. While requiring a considerably smaller air separation unit than full oxyfuel firing the process benefits from increased CO_2 concentrations by increasing the efficiency of a PCC separation process, reducing the amount of medium required to separate the CO_2 and reducing the size of the PCC system, ultimately reducing cost and the efficiency penalty of PCC [Smart and Riley, 2012, Zanganeh and Shafeen, 2007]. OEC also offers potential benefits over oxyfuel combustion. By using air to form some of the combustion gas, many of the performance criteria for oxyfuel combustion may be relaxed. In particular the need for high-purity O_2 is negated and air leakage into the system is less of a concern. On a practical basis this means that the boiler can be operated at a negative pressure, removing the risk of exposing operators to combustion gases, and in retrofitting terms this allows conventional air-driven fuel handing systems to be used, considerably reducing the retrofit cost [Zanganeh and Shafeen, 2007]. The concept of OEC, originally implemented as a low-NO_x measure by Praxair in the USA [Thompson et al., 2004], drew interest in CCS-related work in Europe (since due to compression and recycling of flue gas, reductions of NO_x in the boiler is particularly important) and was investigated as part of the EU Enhanced Capture with Oxygen Scrubbing of CO_2 (ECO-Scrub) project which ran from 2007–2010 [Riley et al., 2013]. As a developing technology this technique has been investigated both in experimental and modelling studies. The focus of this work is on experimental research and literature reported for laboratory bench scale and pilot-scale in larger test facilities is discussed in this section.

2.6.1 Bench-scale tests

Although laboratory scale experiments cannot replicate the exact conditions experienced in industrial-scale furnaces, small-scale work is useful for quickly and economically evaluating larger scale practices. The work of Gil et al. [2012*b*] notes that too many differences exist between bench and industrial scale combustion for results obtained in a laboratory to be able to be directly scalable to industrial furnaces. However, Davini et al. [1996] showed that data extracted from bench-scale techniques such as thermogravimetric ana-

lysis (TGA) correlates with phenomena witnessed during larger-scale combustion. For this reason qualitative comparisons are valid and TGA is often used in initial industrial studies considering changing fuels, for example [Wang et al., 2011]. In light of this TGA is recognised as a useful analogue for full-scale combustion and has been widely adopted to assess trends in fuel reactivity in both air and OEC scenarios.

Table 2.8 presents a synthesis of a selection of the many TGA results presented for fuels combusted in OEC. While exact results tend to vary between fuels, the following trends towards increase rate of combustion are highlighted when [O_2] of the combustion atmosphere is increased and temperatures are greater than $\sim$250 °C:

- the temperature at which ignition of the volatiles (T_{ig}) occurs tends to reduce
- the temperature at which burn out of the char (T_{bo}) occurs tends to reduce
- the maximum combustion rate (DTG_{max}) tends to increase

The work of Murphy and Shaddix [2006] is complementary to the TGA results presented. In this work an EFR was used to investigate the effect on coal particle burning rates during combustion in a range of [O_2]. The work concludes that oxygen enrichment accelerates combustion due to increasing the char particle temperature which results in shorter burnout times and more intense combustion. Figure 2.15 shows that during the early stages of combustion (residence time $<$100 ms) increasing oxygen concentration can substantially increase the rate of char burnout and volatile release which together result in a shorter more intense flame.

Comprehensive analysis of particle combustion for four coals and sugar cane bagasse in a range of [O_2] conditions combusted in drop tube furnace (DTF) was carried out by Khatami et al. [2012]. The findings support those presented above for TGA and EFR with the authors noting: "*Increasing the oxygen mole fraction in N_2 , increased flame and char surface temperatures, and decreased burnout times; particles of all fuels burned more intensely with an increasing tendency of the volatiles to burn closer to the char surface.*"

2.6.2 Larger-scale tests

In the work by Thompson et al. [2004], the development of OEC as a low-NO_x technology involved testing coal combustion under a range of oxygen-enriched and oxidant-stage settings. In the initial stages of the project, researchers at the University of Arizona used a

Table 2.8: Synthesis of results of published literature reporting TGA of OEC

Reference	Fuels	Atmosphere	Heating Rate	Results
Liu et al. [2013]	bituminous coal, beet & switchgrass & BBR 20, 40, 60 and 80%$_{wt}$	N_2/O_2 blends at 21, 40, 60, 80 & 100%	40 K min^{-1}	Cofiring reduces T_{ig} & T_{bo}; increasing [O_2] reduces T_{ig} & T_{bo} more in coal than in biomass and blends; blends show non-linear trend implying fuel interactions
Chen et al. [2011]	micro-algae	N_2/O_2 blends at 20, 50, 60 and 80 % O_2	10, 20 & 40 K min^{-1}	T_{ig} & particularly T_{bo} reduce with increasing [O_2]; maximum rate loss increases with increasing [O_2]
Liu et al. [2010]	paper mill sludge	N_2/O_2 blends at 20, 40, 60 and 80 % O_2	10, 20 & 40 K min^{-1}	Increasing [O_2] accelerates onset and increases DTG$_{max}$ of combustion stages; increasing heating rate retards and increases DTG$_{max}$ of combustion stages
Yuzbasi and Selçuk [2011]	lignite & olive residue & 50:50 blend	Air & 30% O_2:70%N_2	40 K min^{-1}	elevated [O_2] shift combustion profiles to lower temperatures and increase the rate of weight loss
Luo et al. [2009]	biomass micro-fuel	N_2/O_2 blends at 20, 40, 60, 80 and 100% O_2	20 K min^{-1}	Increasing [O_2] reduces T_{ig} & particularly T_{bo}; Increasing [O_2] increases average and maximum mass loss rates; above [O_2] of 60% char combustion overlaps with volatile combustion
Lai et al. [2012]	mixed paper waste	N_2/O_2 blends at 20, 30, 40 and 50 % O_2	20 K min^{-1}	"with increasing [O_2] ignition became easier, a lower temperature was needed to reach maximum of the DTG curves, and the curves gradually shifted to a lower temperature range"
Haykiri-Acma et al. [2010]	Lignite & seed shells at BBR 5, 10 & 20%$_{wt}$	air & pure O_2	20 K min^{-1}	"As a whole, usage of oxygen enhanced the burning reactivity for all the samples at any temperature. Moreover, it is reported that as oxygen concentration increases, the maximum rates of combustion shifts to lower temperatures, and the burnout duration shortens"
Haykiri-Acma et al. [2013]	Lignite, olive milling residue & rice husks at BBR 5, 10 & 20%$_{wt}$	air & pure O_2	20 K min^{-1}	"when the combustion tests were carried out using pure oxygen instead of dry air, the rates of the mass losses augmented seriously . . . the temperatures at these rates were lower than the corresponding temperatures in the case of dry air . . . lignite under oxygen changed in such away that the broad burning region that observed using dry air transformed into a very narrow sharp peak with at least five-fold increase in the intensity"
Yüzbaşı and Selçuk [2012]	coal, petcoke & lignite blends	Air & 30% O_2:70%N_2	unknown	"at elevated oxygen levels, volatile matter and char burning steps are separated, weight loss rates increase, and characteristic temperatures decrease"

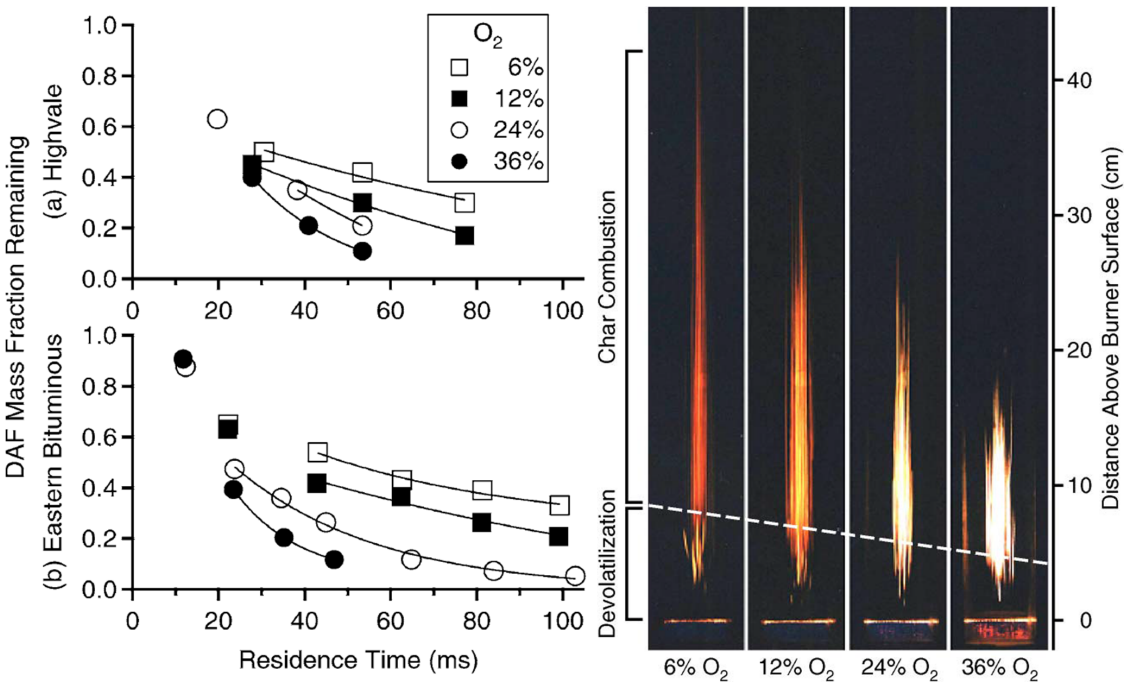

Figure 2.15: The effect of OEC on char burnout (left) and flame for coal particles burning in an EFR [Murphy and Shaddix, 2006]

17 kW down-fired combustor to experiment with two coals being fired in residence times of approximately 2 s. Due to commercial sensitivity, little data is available regarding the specifics of the findings. However, Figure 2.16 presents the effects on NO_x emissions from one of the coals being fired in combustion atmospheres of air and of 25% O_2 at a variety of levels of staging. Though the extent of staging cannot be read from the graph, the results show that although in unstaged conditions NO_x emissions are greater in OEC, under staged combustion NO_x emissions from OEC are lower than air-staged combustion. The OEC with oxidant staging was then successfully shown to reduce NO_x emissions at 44 MW scale and ultimately marketed as a low-NO_x technology by Praxair [2004].

In the ECO-Scrub report an attempt was made to validate a NO_x combustion model tailored to oxygen-enriched combustion. The model aimed to investigate the interaction between turbulence and chemistry in order to explain the change in priority of NO formation routes (from mainly fuel-NO in an air-fired baseline to thermal-NO formation in O_2-enriched conditions). However, when compared to experimental measurements of coal combustion the model predicted NO_x emissions of 578ppm. This was considerably higher than the measured value of 306ppm, suggesting a need for continued experimental work to expand understanding and validate continuing development in advanced computer modelling. The relevant experimental findings of ECO-Scrub programme, expanded and presented in the academic literature by Daood et al. [2011], Nimmo et al. [2010] and

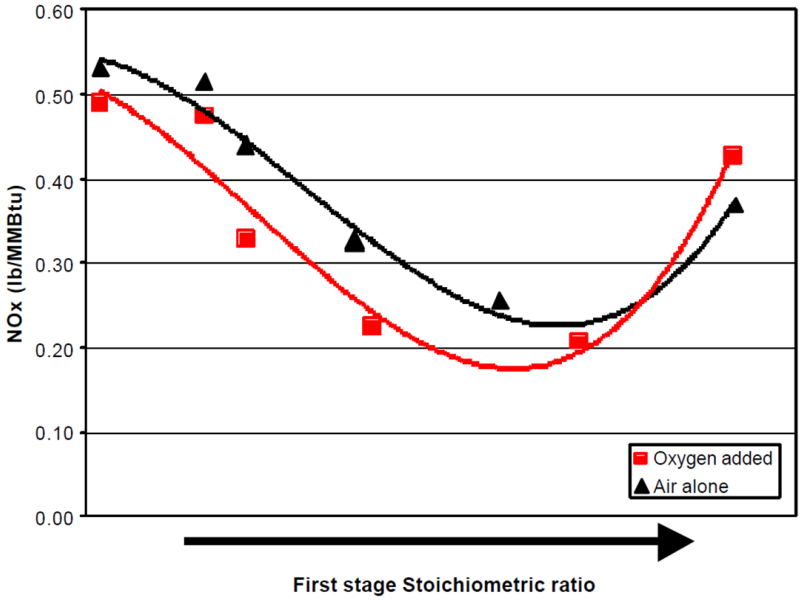

Figure 2.16: Effect of variation in λ on emissions of NO_x for air firing and OEC of coal [Thompson et al., 2004]

Smart and Riley [2012] are detailed below.

Daood et al. [2011] used a 20 kW down-fired PF combustor to investigate the effect of OEC on NO emissions and combustion efficiency. The study focussed parametrically on varying the extent of oxidant staging ($\lambda = 1.16$–0.7) while employing various levels of O_2-enrichment (ranging from 21–100% in the secondary and OFA flows). The work confirms the findings of Thompson et al. [2004] that under staged conditions OEC can reduce NO emissions while simultaneously increasing combustion efficiency, measured as carbon burnout in the ash tracer method. At high levels of oxidant staging of $\lambda = 0.8$ and 0.7 a broadly linear reduction in NO emissions was observed. Increasing $[O_2]$ in the secondary stream as NO emissions were found to reduce from 325–450ppm to 250–325ppm and from 350–550 to 350–375 for $\lambda = 0.8$ and 0.7, respectively, for a range of OFA enrichment levels. However, at $\lambda = 0.9$ the results shown in Figure 2.17 were found. At $\lambda = 0.9$ (22% staging) a peak in NO_x emissions was observed when O_2 in the secondary air was enriched to $[O_2] = 70\%$ with overall $[O_2]$ ranging from 26.4–30.4%. A wide range of reasons for this peak, which wasn't observed for the high extent of staging, was analysed by the authors, though highlighting the precise reasons for this peak is complex. The work concludes that the swirl number of the flame is relatively constant across the range of enrichment levels, though the swirl intensity and associated degree of mixing may be reduced with decreasing secondary oxidant mass flows. OEC was found to operate at higher temperatures near the burner than air-fired both under staged conditions with

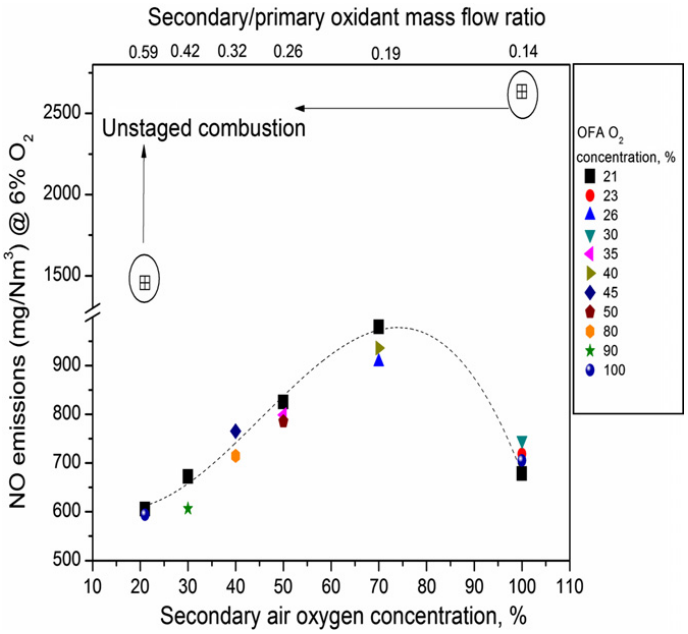

Figure 2.17: Effect on emissions of NO due to increasing O_2-enrichment in secondary and OFA streams for $\lambda = 0.9$ for coal-fired combustion [Daood et al., 2011]

temperatures increasing by $\sim 150\,^{\circ}$C for $\lambda = 0.9$–0.8 and by $\sim 100\,^{\circ}$C for $\lambda = 0.7$. As $[O_2]$ of the secondary flow increased temperatures near the burner were seen to increase. The increase in temperature stabilised at various levels of $[O_2]$ in the secondary stream: at $\lambda = 0.9$ temperatures rose to $\sim$1450 °C by 70% secondary $[O_2]$ before levelling off; for $\lambda = 0.8$ a similar temperature was attained at 60–70% secondary $[O_2]$; while at $\lambda = 0.7$ maximum temperatures of $\sim$1350 °C were reached when secondary $[O_2]$ was increased passed 30%. The authors suggest increased temperatures near the burner may lead to an increase in thermal-NO formation while also increasing the release of volatile N species. An increased residence time in the reducing zone could lead to more fuel-N being ultimately reduced to N_2. However, too great a degree of oxidant staging may lead to reductions in burner temperatures causing more N being retained in the char and subsequently released in the oxidising region with a higher propensity to form NO.

Nimmo et al. [2010] report on similar work to that later reported by [Daood et al., 2011] though in the earlier work an investigation into the effect of cofiring under OEC is also presented. The authors fired hard Russian coal under oxygen enriched conditions with the cotton stalk and shea meal reported in air-staged firing by [Munir et al., 2010]. The work observes variation in NO emissions due to changes in the extent of enrichment of secondary and OFA $[O_2]$ is dependent on the fuel(s) being fired and that trends at one level of oxidant staging are not necessarily representative for a range of levels of oxidant staging. This is highlighted by Figure 2.18 which shows the changes in NO due to changing

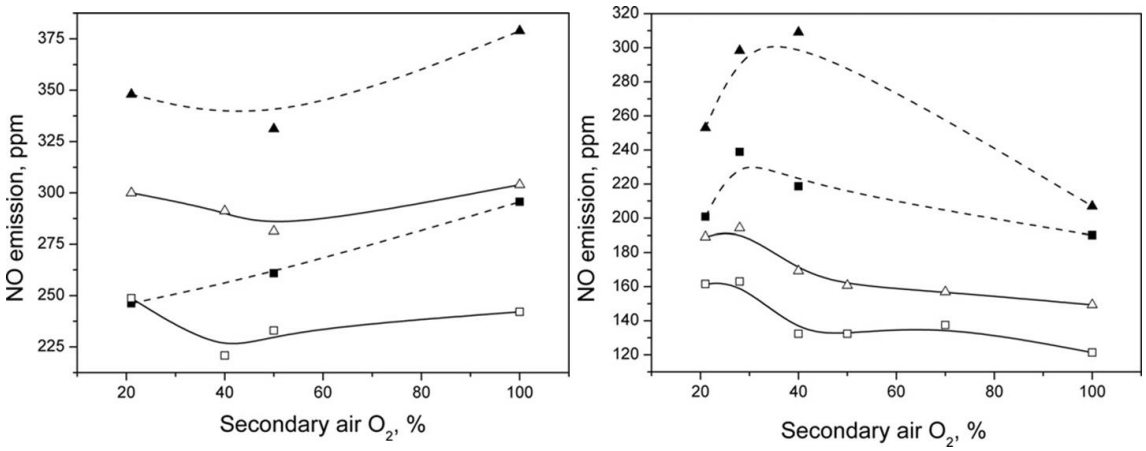

Figure 2.18: Effect on emissions of NO due to increasing O_2-enrichment in secondary and OFA streams for $\lambda = 0.9$ (left) and $\lambda = 0.8$ (right) for coal cofired with 15% biomass. Key: solid shapes - shea meal; hollow shapes - cotton stalk; triangles - 21% [O_2] OFA; squares - 100% [O_2] OFA [Nimmo et al., 2010]

levels of secondary and OFA enrichment at both $\lambda = 0.9$ and 0.8. Combustion efficiency, measured as carbon burnout, was observed to increase when cofiring compared to coal firing in both air and OEC with the cotton stalk enhancing burnout slightly more than the shea meal. Burnout also increased with O_2 enrichment with the effect largest for enrichment in the secondary stream. In summary, despite variations between fuels, the results show significant reductions in NO emissions under staged, OEC of cofired fuels and demonstrate increased carbon burnout under OEC compared to air firing of coal.

Smart and Riley [2012] reported on OEC of coal at 0.5 MW scale in a LNB with [O_2] varied between 19–27% with CO_2 added to simulate dry recycled flue gas. The work does not discuss emissions but investigates the effect of [O_2] on radiative heat transfer (RHF), convective heat transfer (CHF) and combustion efficiency (measured as carbon in ash (CIA)). Dissimilar to the work above where flue gas [O_2] was allowed to vary, for the majority of the cases the authors vary the [O_2] entering the burner while maintaining exit [O_2] at 3% hence reducing the excess O_2 with increasing [O_2]. The results show an increase in RHF with increasing [O_2] both near the burner and extending up to 2.5m downstream. Increasing [O_2] in the secondary stream was found to increase RHF over increasing [O_2] in the tertiary stream. A reverse trend was found for CHF as mass flow rate of gas was reduced with increasing [O_2]. Increasing [O_2] was found to reduce CIA though this effect was amplified when flue gas exit [O_2] was increased (reductions from 6.5–4.5% and 7–4% for fixed and unfixed flue gas [O_2], respectively). The results suggested approximately 23% [O_2] would be required to best match the heat exchange profile of an air based system but that in terms of increasing [CO_2] in the flue gas while reducing the

amount of O_2 required from an ASU an $[O_2]$ of 27% was selected as the optimum case for this work.

2.7 Oxyfuel combustion with exhaust gas recirculation

This section presents a critical review of relevant research in oxyfuel combustion, particularly focussing on combustion characteristics and emissions when firing pulverised coal under a variety of combustion conditions[1]. The first suggestion of oxyfuel technology to produce a CO_2-rich flue gas was presented over three decades ago in an attempt to produce a stream suitable for enhanced oil recovery in the USA [Abraham et al., 1982] (in [Scheffknecht et al., 2011, Smart, O'Nions and Riley, 2010]). Since then, and particularly due to the development of CCS over the last decade, oxyfuel combustion has received much attention in academic and industrial literature. The continuing interest in the technology has created an enormous number of publications, summarised in part by at least five review publications [Davidson and Santos, 2010, Fujimori and Yamada, 2013, Scheffknecht et al., 2011, Toftegaard et al., 2010, Wall et al., 2009]. Use is made of these reviews to provide a sufficient background of the research areas in oxyfuel technology[2] before focussing more specifically on publications relevant to the current work. First, the physical and chemical changes oxyfuel combustion brings compared to air-firing is briefly introduced. This is followed by an overview of work on emissions of the oxides of nitrogen and sulphur before a review of the research of oxyfuel combustion of biomass is presented.

Unlike post- and pre-combustion capture which remove the CO_2 from the bulk gas, an idealised oxyfuel process creates the conditions for combustion to produce only CO_2 and water by removal of N_2 before combustion occurs. For the majority of cases of pulverised fuel firing studied to date, in order to avoid excessive combustion temperatures, 60–80% of flue gas is recycled into the combustor and mixed with pure O_2 for combustion [Toftegaard et al., 2010]. The flue gas from the process is substantially higher in CO_2 with water forming the major other constituent. Through removing water and performing gas traditional clean up practices a stream ready for compression and ultimately injection into

[1] In this thesis, as noted in Section 1.13, 'oxyfuel' processes are considered those which burn fuel in a mixture of pure O_2 and recycled exhaust gas.

[2] while necessary for development of a holistic view of oxyfuel technology, a wide range of research including for example the effects of burner design, mercury and SO_3 emissions, recycle location and oxygen purity are not included in this work

Table 2.9: Typical composition of main gases present before and after combustion in air and oxyfuel systems [Makino, 2005]

Location	O_2 ($\%_{wb}$)	N_2 ($\%_{wb}$)	CO_2 ($\%_{wb}$)	H_2O ($\%_{wb}$)
Windbox - Air	21	79	0	small
Windbox - Oxyfuel	21–30	0–10	40–50	10–20
Flue gas - Air	3–4	70–75	12–14	10–15
Flue gas - Oxyfuel	3–4	0–10	60–70	20–25

a storage site is produced. A schematic of the process is shown in Figure 2.19 while typical gas compositions found before and after combustion in air and oxyfuel firing are shown in Table 2.9.

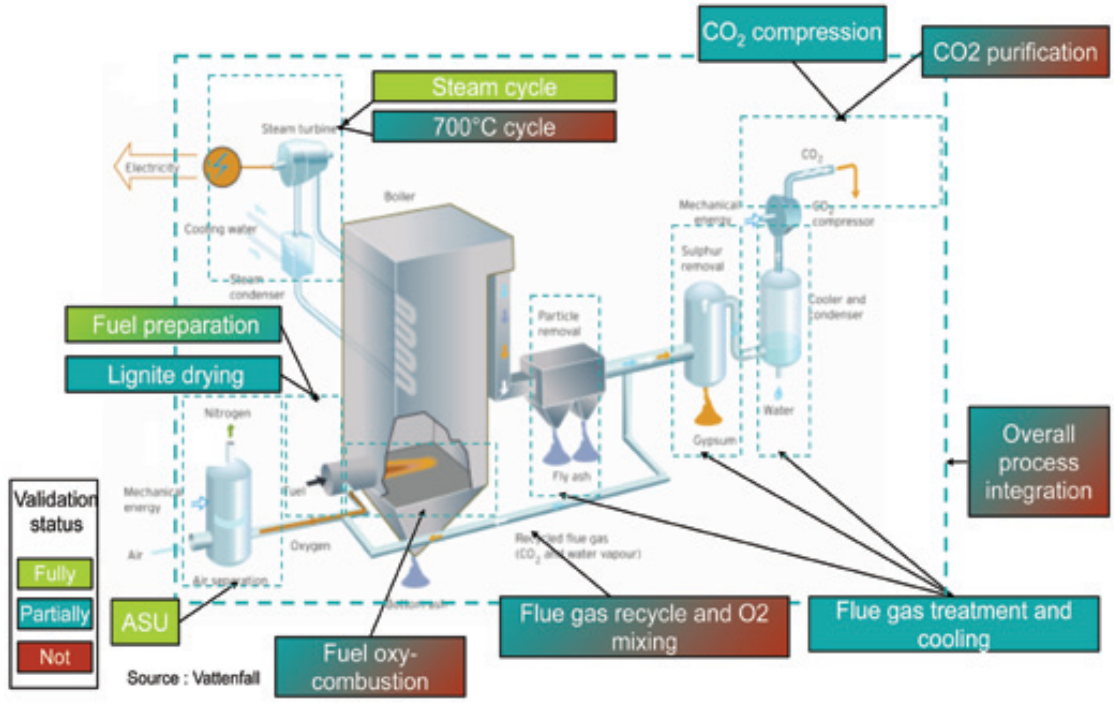

Figure 2.19: Schematic diagram of the oxyfuel combustion process, showing technology validation status in the late 2000s [APGTF, 2009]

2.7.1 Ignition, burnout & heat transfer

As noted in Section 1.13, due to the long lifetime of conventional PF power plant, retrofitting oxyfuel technology to traditional air-fired combustors could be a potential route for capturing CO_2 from existing plant over the coming decades. However, in order to preserve the optimised characteristics of the plant achieved under air-fired conditions, any retrofitted combustor should attempt to match the thermal output in the radiative and convective sections of the installed air-fired boiler. However, the replacement of N_2 in air with CO_2

and water vapour creates issues with thermal matching since physical differences exists between these gases, in particular their densities, specific heat capacities, diffusivities and radiative heat transfer coefficients [Wall et al., 2009].

Variation in the physical properties of the main combustion gases is presented in Table 2.10. Tappe and Krautz [2009] suggest the increased viscosity of CO_2 compared to N_2 may hinder the diffusion of volatiles and combustion products from the surface of fuel particles and similarly diffusion of O_2 to the particle during char oxidation. Radiation is the main mechanism for transfer of heat in conventional furnaces and the effect on heat transfer is complex due to the higher density and specific heat capacity of oxyfuel mixtures. On the one hand for a given amount of fuel a similar volume of gas of higher specific heat capacity water would reduce the adiabatic flame temperature, reducing radiative heat flux. However, water, CO_2, CO, SO_2, soot, and particles of char and ash are all considered responsible for radiative heat transfer [Toftegaard et al., 2010]. Thus, for a given temperature increasing the gas concentration of particularly CO_2 and water (and to some extent SO_2) will increase the radiative heat flux from the gas compared to air-firing. In order to take account of changes in the physical properties of the gases involved in oxyfuel combustion, changes to the composition of the combustion atmosphere are required. This is typically carried out by adjusting the amount of flue gas that is recycled to the combustor to dilute the O_2 and affecting the balance of increasing radiative heat transfer and diluting flame temperature. This in turn affects the temperature and mass flowing through the later furnace sections and thus the rate of convective heat transfer. Since many factors govern the thermal output of a boiler, balancing oxyfuel thermal output with that of air-firing during retrofitting necessitates trade offs which effect physical and chemical changes within the furnace. Figure 2.20 shows increasing radiative heat flux is at the expensive of convective heat flux. In practice the precise level of recycled flue gas and oxygen content required to balance the thermal output with air-firing varies depending on the temperature of the recycled gases and the fuel used. However, Smart, O'Nions and Riley [2010] suggest that recycle ratio of 72–74% is air-equivalent and that slightly lower recycle ratios could be used for new-build oxyfuel units corresponding to the higher [O_2] shown in Table 2.9. In short, the temperature - and therefore reaction kinetics - during oxyfuel combustion differ to those seen in air-fired combustion.

Significant changes to the combustion atmosphere promotes the importance of two reactions which are largely ignored during air-fired combustion: direct gasification of carbon

Table 2.10: Physical properties at 1400 K of main gases present before and after combustion in air and oxyfuel systems [Khare et al., 2008]

Property	H_2O	O_2	N_2	CO_2
Density ($kg\,m^{-3}$)	0.157	0.278	0.244	0.383
Thermal conductivity ($W\,m^{-1}\,K$)	1.363e–01	8.721e–02	8.184e–02	9.719e–02
Specific heat capacity at const. pressure (kJ/kmolK)	45.67	36.08	34.18	57.83
Dynamic viscosity ($kg\,m^{-1}\,s$)	5.018e–05	5.811e–05	4.877e–05	5.023e–05

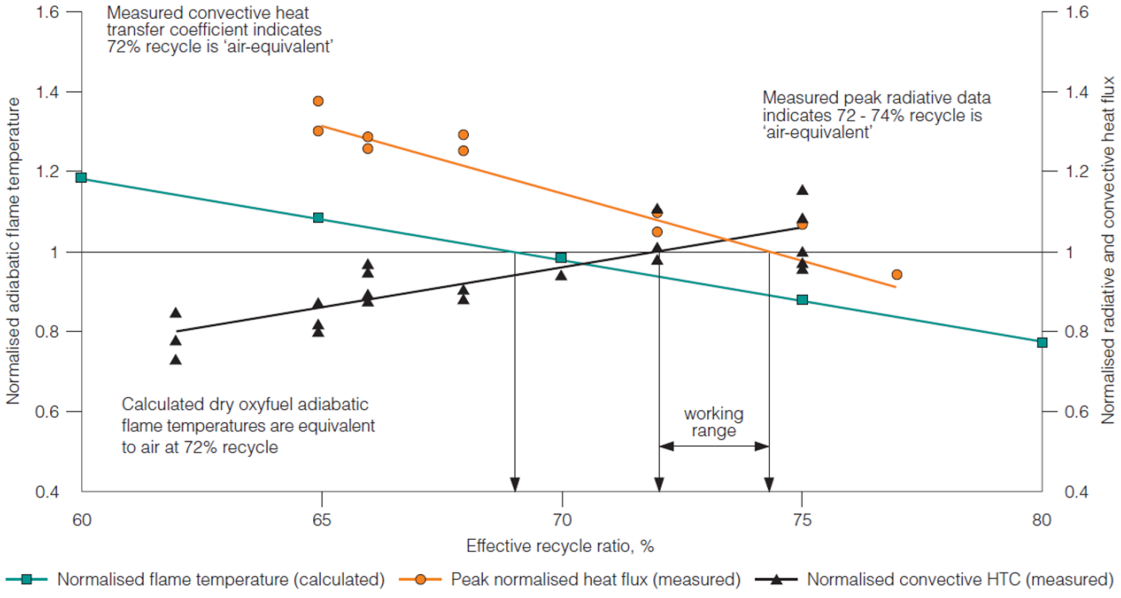

Figure 2.20: The effect of flue gas recycle ratio on flame temperature, peak radiative heat flux and convective heat transfer coefficient (HTC) redrawn by Davidson and Santos [2010] from the work of Smart, O'Nions and Riley [2010]

by CO_2 (the Boudouard reaction Equation (2.14)) and gasification of carbon by water (Equation (2.15)) [Toftegaard et al., 2010].

The Boudouard reaction

$$C + CO_2 \rightleftharpoons 2\,CO \tag{2.14}$$

Gasification by water

$$C + H_2O \rightleftharpoons CO + H_2 \tag{2.15}$$

Substitution of N_2 in air-fired combustion with recycled flue gas containing CO_2 and increased amounts of water has several effects on the initial stages of combustion. In the

review by Davidson and Santos [2010] the authors highlight results for a variety of scales that observe at similar [O_2] ignition is delayed in a CO_2-rich environment. Molina and Shaddix [2007] studied the effect of increasing [O_2] from 21–30% on ignition and devolatilisation of pulverised coal particles with CO_2 and water as diluents in a laminar EFR. The work observes delayed ignition in CO_2 atmospheres due to the increased specific heat capacity and accelerated ignition in higher [O_2] due to increasing mixture reactivity. In later work, Shaddix and Molina [2009] used higher resolution imaging and higher temperatures to further study the phenomenon. In the later work the authors confirm CO_2 delays ignition and suggest as well as increased specific heat capacity, the ability of CO_2 to reduce the radical pool required during ignition may be responsible. The diffusivity of volatiles and O_2 in CO_2 is also highlighted as slowing the devolatilisation process. Kiga et al. [1997] showed that the flame propagation speed in oxyfuel environments was slower than for air-fired cases and this was largely attributed to the higher specific heat capacity of CO_2. The majority of literature published in this area suggest [O_2] levels of 27–35% may be required for similar combustion properties - including ignition characteristics, flame luminosity and flame temperature - to those observed in air-fired cases, though the actual level is often seen as fuel dependent with lower rank fuels exhibiting greater responsiveness to changes in [O_2] [Davidson and Santos, 2010, Man and Gibbins, 2011].

Increased fuel reactivity in high [O_2] in oxyfuel environments has been observed in a wide range of bench-scale studies. Liu [2009] suggests that at slower heating rates present in TGA studies the effect on combustion when switching between between N_2 and CO_2 as the diluent is much reduced because the TGA device works to maintain constant temperatures. However, increasing [O_2] is reported to accelerate and intensify the combustion process. Towards the higher end of TGA heating rates many other published works show although [O_2] is more important, slight delays to ignition in CO_2-based atmospheres, for example [Wang et al., 2012, Yüzbaşı and Selçuk, 2012].

Experiments with coal in drop tube furnaces (DTF), EFRs and in TGA pyrolysis work have shown that during the devolatilisation process the presence of CO_2 increased the release of volatile components compared to an inert N_2 environment at temperatures near the combustion range [Gil et al., 2012*b*, Meng et al., 2013, Rathnam et al., 2009, Wang et al., 2012, Yüzbaşı and Selçuk, 2012]. This is largely attributed to the gasification reactions which as Liu [2009] highlights are unlikely to be witnessed in non-isothermal oxidising

TGA. This is because in TGA devices the combustion reactions tend to occur at lower temperatures than the gasification reactions [Wang et al., 2012]. Comparison between different temperatures, experimental set ups and gas compositions has caused some complexity with regards to the reactivity and ultimate burnout of chars in the combustion environment. Wall et al. [2009] found an increase in burnout in oxyfuel conditions in opposition to much reported literature, for example [Borrego and Alvarez, 2007]. Further work in this area has identified that most results comparing char combustion in N_2- and CO_2-based environments tend to indicate that the CO_2 environment creates a slightly more reactive char. However, the CO_2 boundary layer surrounding a particle reduces oxygen diffusivity and particle surface temperature compared to an N_2 surrounding environment. In addition, increased [O_2] increases char particle temperatures through faster oxidising of CO to CO_2, while the Boudouard reaction reduces particle temperature due to its endothermic nature [Hecht et al., 2011]. The extent to which each of these stages occur depend on local gas concentrations (including water vapour which is not considered in this work) and particular properties for a given fuel hence creating a complex overall effect balancing kinetics and mass diffusion to ascertain the overall rate of combustion [Scheffknecht et al., 2011, Shaddix and Molina, 2009]. Variation between experiments in temperature, residence time and [O_2] affect the competition between the chemical rate increase and mass transfer rate decrease which has led to the mixed results. In general, in order to equal or improve on ignition performance and burnout observed for air-firing, [O_2] of 27–35% is required with 30% often cited as the air-equivalent [O_2].

Tests at pilot scale tests tend to confirm most of the findings from smaller-scale experimentation. Liu et al. [2005] found that in similar [O_2] at 20 kW firing oxyfuel combustion tended to produce lower combustion temperatures, resulting in lower burnout of the coal. However, replacing the secondary air stream with [O_2] of 30% created similar combustion temperature profiles to air firing and operating the entire unit at 30% O_2 in CO_2 increased the gas temperatures along the furnace. Under staged and unstaged oxygen-enriched oxyfuel conditions, the combustion efficiency was found to increase compared to the air-firing case. Andersson [2005] similarly observed temperature reductions when firing coal at 21% O_2 at 100 kW scale; however, increasing [O_2] to 27% in CO_2 tended to result in similar gas temperatures to air-firing. Although temperatures were close to those experienced during air firing, the radiative flux was measured to be greater in the oxyfuel environment in the 100 kW tests. Tan et al. [2006] observed that temperatures

at 35% [O_2] were greater than air firing and resulted in greater heat transfer fluxes along the length of the furnace when oxyfiring at 0.3 MW.

2.7.2 NO_x emissions from oxyfuel combustion

The majority of experiments at a representative scale tend to show that NO_x emissions decrease in oxyfuel atmospheres compared to air-firing [Davidson and Santos, 2010, Fujimori and Yamada, 2013, Scheffknecht et al., 2011, Toftegaard et al., 2010, Wall et al., 2009]. For example, Liu et al. [2005] found reductions of 20% in unstaged conditions and reductions below those achieved in air-firing under staging (as low as 7.5% of fuel-N converted to NO_x) in their experiments at 20 kW with fuel-N content of 1.62%. Andersson [2005] also found reductions at 20 kW scale which where slightly more favourable than air-firing under staged and unstaged conditions. Under unstaged conditions tests with two coals showed emissions fell from 375–250 and 382 to 322 mg MJ^{-1} in a 27% [O_2] oxyfuel atmosphere. When staging was employed emissions under oxyfuel conditions were consistently lower than the air fired case finding a minimum at 71 mg MJ^{-1} for $\lambda = 0.75$ and a 3 s residence time in the reducing zone when firing a South African bituminous coal. Tan et al. [2006] fired a bituminous, a sub-bituminous and a lignite coal using a 0.3 MW facility. The first coal showed slightly higher NO emissions under oxyfuel conditions though this was explained by not optimising the burner to operate in low-NO_x mode under oxyfuel conditions ([O_2] = 35%, RR = 45%). For the second coal, although [NO] increased for oxyfuel conditions ([O_2] 35% RR = 37–38%) this was negated by the reduced flue gas volume in oxyfuel firing. When firing the third coal the burner was optimised for low-NO_x firing in oxyfuel operation which effected a 74% reduction in NO emissions on a mass/energy basis. This final finding agreed with Liu et al. [2005] that current low-NO_x technologies are expected to be applicable to oxyfuel firing and that recirculation of flue gas also provides significant reductions in NO emissions [Fujimori and Yamada, 2013].

Although experimentally reductions are observed, the complex interplay of NO_x formation detailed in Section 2.3.1 predicates reasoning for such reductions is still the subject of debate. Sarofim [2007] noted that the reduction is essentially due to either a reduction in the conversion of fuel-N to NO_x or due to increased destruction of NO_x formed. An analysis of mechanisms reducing NO_x emissions was reviewed by Normann et al. [2009]. Davidson and Santos [2010] combine this review with the work Mackrory and colleagues

Table 2.11: Suggested reasons for reductions in NO_x emissions during oxyfuel combustion [Davidson and Santos, 2010, Mackrory and Tree, 2009, Normann et al., 2009]

Mechanism	**Method of reduction**
N_2 reduction	prevents thermal- and prompt-NO formation
increased [O_2]	more attached flame
increased [NO]	limits conversion of fuel-N to NO
flue gas recycle	reduction of recycled NO_x to N_2 in the fuel-rich flame zone
temperature changes	high temperature and low [N_2] could promote reverse thermal (Zeldovich) mechanism
increased residence times in fuel-rich regions	greater opportunity for NO to be reduced to N_2
significantly lower [NO_x] in oxyfuel combustion	reduces propensity to form NO
increased volatile yields	increased ability to reduce NO from volatiles & reduced NO formation from char
reburning	increased soot, CO and char may provide mechanism for NO reduction
gasification reactions	increased importance of gasification reactions

undertook in proposing their oxyfuel NO_x model (given in [Mackrory and Tree, 2009]) and highlight ten possibilities for the reductions in NO_x emissions in oxyfuel combustion. A brief outline of the mechanisms presented is given in Table 2.11.

2.7.3 SO_x emissions from oxyfuel combustion

Oxyfuel combustion appears to have little effect on the formation of SO_2 when compared to air-firing in once-through systems but SO_2 emissions have been observed to reduce when FGR is employed. Both Liu et al. [2005] and Andersson [2005] report negligible changes to SO_2 emissions in once-through 20 kW systems. Tan et al. [2006] reports that the effect of recycling the flue gas without SO_2 removal and the reduced flue gas volume in oxyfuel combustion causes an increase in flue gas [SO_2] but that actual emissions were slightly lower than air-firing with more sulphur captured by ash and deposits upon furnace and heat transfer surfaces. In the results presented in the review paper by Scheffknecht et al. [2011] significant reductions of SO_2 emissions of up to a third compared to firing in air are noted. Toftegaard et al. [2010] and Fujimori and Yamada [2013] summarise that increased conversion of SO_2 to SO_3 is likely to occur on account of the higher [SO_2] which, along with the increased moisture content, could increase the acid dew point for flue gases potentially creating corrosion issues should H_2SO_4 be formed [Wall et al., 2009]. Increased [SO_2] also increases the propensity for sulphur to be taken up by ash or deposit

particles. While SO_2 emissions alone are similar or less than witnessed in air-firing, concerns have been raised with respect to both SCR and SNCR applications where removal of NO is favoured by excess of ammonia. Reactions between ammonia and SO_3 are known to create ammonium bisulphate which has a high propensity to stick to surfaces it impacts leading to increased fouling and potential clogging of catalysts in SCR [Nordstrand et al., 2008, Toftegaard et al., 2010]. The oxidation state of sulphur in oxyfuel systems has been linked to an increase in emissions of other trace elements, in particular mercury [Font et al., 2012]. Understanding of the interplay between mercury and sulphur emissions is still developing and, since biomass fuels contain very low levels of these elements, is considered beyond the scope of this thesis to explore this issue further.

2.7.4 Oxyfuel with biomass

Despite a large amount of work focussing on coal-fired oxyfuel and air-fired cofiring, relatively little information has been published investigating biomass combustion under oxyfuel conditions. Indeed the review paper by Toftegaard et al. [2010] reports only three papers on the subject [Arias et al., 2008, Borrego et al., 2009, Fryda et al., 2010]. Since 2010 increased attention for Bio-CCS at national and international level has driven more interest in the subject. This section details an overview of relevant published work. Findings of biomass oxyfuel combustion are separated into bench scale, pilot-scale and corrosion studies.

2.7.4.1 Bench-scale results

Borrego et al. [2009] performed fast pyrolysis at a temperature of 950 °C in N_2 and CO_2 environments in DTF experiments with two woody biomasses and rice husks. Unlike many other works, the results show for all fuels that although the mass loss in the DTF was greater than the volatile matter content found during proximate analysis (confirming increased devolatilisation at increased temperatures) a higher weight loss was observed in the N_2 environment compared to the CO_2 atmosphere.

Farrow and Snape [2010] studied the effect of pyrolysis of sawdust samples in a a TGA device ($\beta = 150\,\mathrm{K\,min^{-1}}$) with subsequent combustion of the chars formed in a 21% [O_2] environment. The work found that reducing particle size increased burnout reactivity

but had little effect on volatile yield which was much more dependent on temperature of devolatilisation. Increasing devolatilisation was reported to increase the amount of nitrogen released from the char.

Arias et al. [2008] used an EFR to study ignition and burnout properties of a high volatile bituminous coal blended with eucalyptus at 10 and 20 % BBR under air and three oxyfuel atmospheres (21, 30, 35% [O_2]). In air blending with biomass reduced ignition temperatures and had a marginally beneficial effect on burnout. At the 21% O_2 oxyfuel atmosphere ignition improved slightly with BBR though was considerably slower than firing under air. Increased [O_2] increased the ignitability of the blends and ignition temperature also fell slightly for increasing BBR in oxygen-enriched conditions. Under oxygen-enriched conditions the burnout of the blends was considerably improved by blending.

Riaza et al. [2012] performed experiments using similar atmospheres and BBR to Arias et al. [2008] with two different coals and olive waste burned in an EFR. Ignition (as defined by when 10% of the non-water material had left the particle) was delayed in an oxyfuel environment comparable to air, but accelerated in experiments at 30% [O_2]. Increases in BBR were also found to accelerate ignition and also burnout of the fuel. Compared to air-firing burnout was found to be reduced in 21% [O_2] oxyfuel environment but increased at 30 and 35% [O_2]. Reducing the excess O_2 in the EFR was found to reduce the burnout. NO emissions were reported as falling with increasing BBR with the less reactive coal which the authors suggest is due to the reduction of NO formed by CO and char particles as reported by other researchers. Variation of [O_2] had little effect on NO emissions in oxyfuel conditions which were found to be lower than air-firing in all cases. When firing with the more reactive coal, the decrease in NO emissions with increasing BBR was not witnessed for oxyfuel conditions despite being observed for air-firing case and both cases for the semi-anthracitic coal.

A number of similar experiments have been carried out using TGA to investigate reactivity of biomasses and their blends in oxyfuel environments. Details of these experiments are presented in Table 2.12. In summary, work at TGA scale complements the findings of the pyrolysis and EFR work reported above. Similar to findings for coal-firing in oxyfuel conditions, simply substituting N_2 with CO_2 as the comburent tends to reduce the reactivity of the combustion environment while increasing [O_2] to 30% seems to provide more favourable combustion conditions than observed for air firing. Similar to findings

for cofiring in air, biomass blending tends to improve the ignition properties of fuel mixes and in most cases the ultimate burnout. Biomasses were found to be less responsive to changes in combustion atmosphere than coals for most of the results reported. This may be explained by the increased dependency of O-diffusion in char combustion which forms a larger part of coal combustion than it does in the biomass cases.

2.7.4.2 Larger-scale results

Skeen et al. [2010] investigated NO emissions when cofiring sawdust waste and subbituminous coal under air and 30% [O_2] oxyfuel conditions at 30 kW_{th} scale. In an unstaged, non-swirling flame NO emissions were lower under oxyfuel conditions on a mass/ energy basis (reducing from $\sim$90 to $\sim$60 $ng\,J^{-1}$) but were not observed to reduce with increasing BBR (up to 40%$_{wt}$) when exit [O_2] was maintained at 3%. In later modelling work, Holtmeyer et al. [2012] suggest the coupling of the increased size of the biomass particles with the reduction in flame length due to the increased [O_2] and reduced secondary gas flow rate caused more of the biomass particles to breakthrough the flame envelope and devolatilise in the high temperature, high [O_2] zone increasing the conversion of fuel-N to NO as BBR increased.

Smart, Patel and Riley [2010] carried out work firing two coals with shea meal and sawdust at 0.5 MW_{th} scale. Both biomasses were fired at 20%$_{mass}$ BBR and shea meal was also fired with one of the coals at 40%$_{mass}$ BBR. The aim of the work was to investigate the effect on burnout and radiative and convective heat transfer (RHF and CHF, respectively) when varying the inlet gas composition to simulate variation in the flue gas recycle rate (RR). The results observed show similar trends to those reported for coal-firing [Smart, O'Nions and Riley, 2010] where increasing RR (and decreasing [O_2]) decreases RHF while increasing CHF. However, variations between fuels were observed with the shea meal found to be more sensitive to RR than the saw dust. In general the addition of biomass tended to reduce RHF compared to coal firing, particularly near the burner. The authors suggest this is due to the increased moisture content and reduced calorific value of the biomass volatiles compared to those from the coals, particularly for the high-moisture, larger sawdust particles. In their conclusions the authors suggest that since the calculation for oxygen requirement includes oxygen bound in the biomass, the coal 'sees' less oxygen in the flame which may also reduce flame temperature and subsequent RHF. Working

Table 2.12: Synthesis of results of published literature reporting TGA of biomass oxyfuel combustion

Reference	Fuels	Atmosphere	Heating Rate	Results
Yuzbasi and Selçuk [2011]	lignite & olive residue & 50% BBR	0, 21 & 30% $[O_2]$ in N_2 & CO_2	40 K min^{-1}	pyrolysis results similar up to 700 °C after which mass loss faster in CO_2 due to char gasification; CO_2 slightly delays combustion but elevated $[O_2]$ shifts combustion profiles to lower temperatures and increases the rate of weight loss; no synergy from blending in either pyrolysis atmosphere but some synergy during combustion
Lai et al. [2012]	mixed paper waste	$[O_2]$ of 20, 30, 40 and 50 % in N_2 & CO_2	20 K min^{-1}	replacing N_2 with CO_2 caused slight delay in ignition and slightly lower maximum weight loss; "with increasing $[O_2]$ ignition became easier, a lower temperature was needed to reach maximum of the DTG curves, and the curves gradually shifted to a lower temperature range"; air-equivalent of 30% $[O_2]$ in CO_2
Irfan et al. [2012]	bituminous coal & palm shell & 10 & 20% BBR	Air & oxyfuel with $[O_2]$ 22–100%	10 K min^{-1}	At equal $[O_2]$ ignition was delayed and burnout reduced slightly in oxyfuel compared to air but when $[O_2] \geq 30\%$ reactivity increased
Gil et al. [2012*c*]	semi-anthracitic coal & olive waste & 10 & 20% BBR	air & oxyfuel with $[O_2] = 21$, 30 & 35%	15 K min^{-1}	Biomass decreased characteristic temperatures and was less affected by change from N_2 to CO_2; combustion accelerated in oxyfuel when $[O_2] > 21\%$
Gil et al. [2012*a*]	2 coals & torrefacted pine sawdust chars	air & 30% $[O_2]$ oxyfuel	2,3 & 5 K min^{-1}	No interaction between chars; no real changes between char combustion kinetics in air and 30% $[O_2]$ oxyfuel
Tang et al. [2011]	microalgae & municipal solid waste	20% $[O_2]$ in N_2 & CO_2	20 K min^{-1}	Oxyfuel at same $[O_2]$ resulted in later ignition, delayed burnout and less intense maximum rate than observed in N_2-O_2 environment

ranges of approximately similar heat transfer fluxes to air-firing of coal were found to be achievable with all blends of coal and biomass with RR = 71–73%. However, the precise RR range to achieve this varied between fuels and blends. Carbon burnout was generally improved both by cofiring and oxyfuel conditions. The sawdust was found to be highly reactive in all environments while the addition of shea meal had a smaller impact on burnout with the authors suggesting this blend was more influenced by impact of cofiring on temperature reduction, particularly in oxyfuel firing. Combustion temperatures and exit gas species are not reported in this work.

2.7.4.3 Corrosion results

Although not a primary focus of this work, the impact of firing biomass in oxygen-enriched and oxyfuel conditions on metal corrosion is important to the ability of the technology to be deployed in commercial boilers. Thus, it is useful to include consideration of the little work published in this area in this review of relevant literature.

Fryda et al. [2010] investigated ash formation when cofiring two coals with shea meal in DTF experiments at 20%$_{wt}$ BBR. The results suggest the blend of fuels was more important at determining deposition behvaiour than the combustion environment, which suggested similar temperature profiles along the reactor and ash chemistry in a 30% [O_2] in CO_2 environment. The oxyfuel tests were found to increase the rate of deposition of fine, easily dispersed dusts on the sampling collector. Blending biomass with coal tended to reduce the deposition propensity, with reductions in deposition rates greater than would be expected solely due to the reduced ash content of the biomass.

Syed et al. [2011] investigated the effect on corrosion of a number of steels with a variety of coatings that may be expected to result from deposition in conventional boilers. Each of the samples was exposed to synthetic flue gases representing air and oxyfuel cofiring of coal and cereal co-product. In each situation the authors found that corrosion is enhanced by firing biomass under oxyfuel conditions and for the most aggressive deposits the corrosion levels are greater than the industrial targets. The high levels of SO_2 and HCl (6260 and 1700 ppmv, respectively) were thought to be responsible for the increased corrosion under oxyfuel conditions. The authors note that increasing alloy contents of chromium (Cr) and nickel (Ni) increase resistance to corrosion.

2.8 Estimating kinetic parameters using thermogravimetry

A method of comparing fuel reactivity in different atmospheres was required in order to qualitatively inform how different fuels may react under novel combustion environments when fired at pilot scale. The kinetics of combustion are an important factor that govern many aspects of the process; from the amount of heat generated for a given residence time or distance through the furnace to the efficiency of combustion overall. One way that kinetics can be investigated, which as the work in Tables 2.8 and 2.12 shows has often been used for analysing fuel combustion, is through use of bench-scale experimentation with thermogravimetric analysis (TGA).

During preliminary studies analysing TGA data it became apparent that commonly used procedures for comparing reactivity between fuel combustion experiments were not appropriate for this work. Some existing methods were found to involve a high amount of effort (either experimentally or during analysis) which was difficult to justify given the inherent limitations of modelling complex reaction as simple systems. Conversely, simpler methods were found to be less robust with varying transparency of results reported and unclear guidance of how multiple reaction systems can be analysed using methods derived for single-reactions.

This led to the development of a methodology for reactivity analysis, which is detailed in Chapter 4. This represents an extension of the work on TGA beyond that initially envisaged. Specific background material necessary for development of the method detailed in Chapter 4 is presented here.

A brief introduction to some of the most common methods for extracting rate parameters from TGA data is first presented drawing on several reviews and standard methods for single reactions (or processes simplified to pseudo-single reactions) occurring in isolation. Some widely known limitations of these methods are then presented with modifications made by researchers to reduce their errors.

2.8.1 Obtaining relevant kinetic data

The application of data derived from bench-scale techniques by procedures that apply homogeneous, single reaction step models to groups of heterogeneous, parallel reactions has been the subject of fierce debate in the literature [Flynn, 1997, Starink, 2003, Vyazovkin

et al., 2011, White et al., 2011]. While the use of TGA to identify activation energies for combustion of pure compounds is able to provide insight into combustion characteristics, to claim a precise extraction of activation energies of the decompostition of complex fuels such as coal or biomass is unhelpful. Defining an apparent activation energy is nevertheless useful for initial fuel screening applications and as a method of qualitatively explaining phenomena observed in larger scale applications. In using the apparent activation energy as a medium for comparison between fuels care should be taken to distinguish between a chemical and apparent activation energy. White et al. [2011] suggest the chemical activation energy, as derived for homogenous reactions, can either be defined as "*the energy threshold that must be overcome before molecules can get close enough to react and form products*" (as per molecular collision theory) or "*as the difference between the average energy of molecules undergoing reaction and average energy of all reactant molecules*" (as per transition state theory). Conversely, the apparent activation energy is interpreted as "*the whole complexity of processes occurring [. . .] under the given experimental conditions*". [White et al., 2011]

For kinetic analysis of the results of TGA an enormous number of methods have been suggested to calculate the apparent activation energy and remaining members of the kinetic triplet of the sample being tested. The wide range of options indicates a lack of an all-encompassing solution and Flynn [1997] suggests that significant disagreement between values calculated under different conditions and using different techniques renders comparison between literature values problematic. Here a non-exhaustive list of several of the methods most commonly applied to analysing the decomposition of fuels are presented drawn from three recent reviews of the subject [Starink, 2003, Vyazovkin et al., 2011, White et al., 2011].

2.8.2 Single-step Arrhenius equation

Almost all models to describe the kinetics of combustion assume the isoconversional principle and draw on the Arrhenius equation. This states that the rate constant for a reaction (k, s^{-1}) is a function of the pre-exponential function (A, s^{-1}), the energy of activation (E_A, $J\,mol^{-1}$), the universal gas constant (R, $8.314\,J\,mol^{-1}\,K^{-1}$) and the absolute temperature of the system (T, K).

$$k = Ae^{-E_A/RT} \tag{2.16}$$

For reactions considered in this work, the first three terms are considered to be independent of temperature over the temperature range of common combustion reactions thus the rate constant is dependent only on the temperature. Combining this with the reaction dependence on the conversion of reactant ($f(\alpha)$) gives the well known reaction for change of conversion with time ($\mathrm{d}\alpha/\mathrm{d}t$):

$$\frac{\mathrm{d}\alpha}{\mathrm{d}t} = kf(\alpha) = Ae^{-E_A/RT} f(\alpha) \tag{2.17}$$

where the extent of reaction (α) is calculated by comparing the initial mass (m_o), the mass a given time (m_t) and the mass at the end of the reaction (m_t):

$$\alpha = \frac{m_0 - m_t}{m_0 - m_f} \tag{2.18}$$

Following slight rearrangement, Equation (2.17) becomes:

$$\frac{\mathrm{d}\alpha/\mathrm{d}t}{f(\alpha)} = Ae^{-E_A/RT} \tag{2.19}$$

For non-isothermal TGA experiments carried out at a constant heating rate, the rate of temperature increase (β, $\mathrm{K\,s^{-1}}$) is defined as

$$\beta = \frac{\mathrm{d}T}{\mathrm{d}t} \tag{2.20}$$

And so

$$\frac{\mathrm{d}\alpha/\mathrm{d}T}{f(\alpha)} = \frac{A}{\beta} e^{-E_A/RT} \tag{2.21}$$

2.8.3 Differential isoconversional approach: the Friedman method

One method, described by Friedman [1964], of solving this equation used extensively due to its simplicity is to assume that the single-stage process is governed only by the order of

reaction (n) as:

$$f(\alpha) = (1-\alpha)^n \tag{2.22}$$

So

$$\frac{\mathrm{d}\alpha/\mathrm{d}T}{(1-\alpha)^n} = \frac{A}{\beta} e^{-E_A/RT} \tag{2.23}$$

Taking natural logarithms yields the following linear relationship.

$$\ln\left[\frac{\mathrm{d}\alpha/\mathrm{d}T}{(1-\alpha)^n}\right] = \ln\frac{A}{\beta} - \frac{E_A}{RT} \tag{2.24}$$

So plotting $\ln\left[\frac{\mathrm{d}\alpha/\mathrm{d}T}{(1-\alpha)^n}\right]$ against $1/T$ should yield a straight line with gradient $-E_A/R$ and intercept $\ln[A/\beta]$. A range of sensible values for the order of reaction (n) are plotted and a least squares regression coefficient is used to evaluate the best fit to the data.

2.8.4 Integral methods

An alternative that has been popular with many researchers is to integrate across the generalised reaction, yielding:

$$g(\alpha) = \int_0^\alpha \frac{\mathrm{d}\alpha}{f(\alpha)} = \frac{A}{\beta}\int_0^{T_\alpha} e^{\frac{-E_A}{RT}}\,\mathrm{d}T \tag{2.25}$$

If we define $\zeta = E_A/RT$ then

$$g(\alpha) = \frac{AE_A}{\beta R}\int_{\zeta_\alpha}^{\infty} \frac{e^{-\zeta}}{\zeta^2}\mathrm{d}\zeta = \frac{AE_A}{\beta R} p(\zeta) \tag{2.26}$$

Where $p(\zeta)$ is known as the temperature integral and has no analytical solution. Various approximations of this yield different methods of estimating the kinetic parameters using the orders of reaction presented in Table 2.13.

2.8.4.1 Flynn-Wall-Ozawa (FWO) method

One method of calculating the temperature interval is to use an approximation proposed by Doyle [1962] which is applicable if $20 \leq \zeta \leq 60$:

$$\log p\left(\zeta\right) \simeq -2.315 - 0.4567\zeta \tag{2.27}$$

which leads to the FWO method [Flynn and Wall, 1966, Ozawa, 1965] which has continued to be widely used and discussed in the literature, for example [Flynn, 1997, Ozawa, 1992, White et al., 2011]:

$$\log \beta = \log\left(A\frac{E_A}{R \cdot g\left(\alpha\right)}\right) - 2.315 - 0.4567\frac{E_A}{RT} \tag{2.28}$$

Plotting $\log \beta$ against $1/T$ yields a point for each heating rate and the slope of the line connecting these is is $-0.4567E/R$ and the value of the intercept is then used to calculate A.

2.8.4.2 Kissinger-Akahira-Sunose (KAS) method

Another approximation of the temperature interval by Doyle [1961] for $20 \leq \zeta \leq 50$ is:

$$\log p\left(\zeta\right) \simeq \frac{e^{-\zeta}}{\zeta^2} \tag{2.29}$$

which leads to the equally well-established KAS method [Akahira and Sunose, 1971, Kissinger, 1957, Starink, 2003]:

$$\ln\left(\frac{\beta}{T_m^2}\right) = -\frac{E_A}{R}\left(\frac{1}{T_m}\right) + C_2 + C_3 \ldots \tag{2.30}$$

Where T_m is the temperature at the maximum reaction rate and a plot of points from different heating rates of $\ln\left(\frac{\beta}{T_m^2}\right)$ against $1/T_m$ allows E_A to be determined from the slope of the line since the constants of integration (C_2 and C_3) are assumed not to depend on β or T_m [Starink, 2003].

2.8.4.3 Coats-Redfern (CR) method

Perhaps the most widely used procedure is the Coats-Redfern (CR) method [Coats and Redfern, 1964, 1965] which uses a Taylor series expansion to approximate the temperature interval. The reaction is commonly assumed to be first order which yields the following equation:

$$\ln\left(\frac{-\ln\left(1-\alpha\right)}{T^2}\right) = \ln\left[\frac{AR}{\beta E_A}\left(1-\frac{2RT}{E_A}\right)\right] - \frac{E_A}{RT} \tag{2.31}$$

This can be simplified since for normal values of E_A (where $80 < E_A < 260\,\mathrm{kJ\,mol^{-1}}$), as $2RT/E_A \ll 1$ to give

$$\ln\left(\frac{-\ln\left(1-\alpha\right)}{T^2}\right) = \ln\left(\frac{AR}{\beta E_A}\right) - \frac{E_A}{RT} \tag{2.32}$$

So, plotting $\ln\left[-\ln\left(1-\alpha\right)/T^2\right]$ against $1/T$ yields E_A and A from data at only one temperature heating rate.

2.8.4.4 Vyazovkin method

Vyazovkin and Dollimore [1996] suggest a more rigorous analysis using data from a number (q) of experiments at several (j and k) heating rates and a description of the temperature interval as:

$$p\left(\zeta\right) = \int_0^{T_\alpha} e^{E/RT}\mathrm{d}T \tag{2.33}$$

This function can then be approximated numerically or by use of the Senum-Yang approximation [Senum and Yang, 1977]:

$$p\left(\zeta\right) = \left(\frac{e^{-\zeta}}{\zeta}\right)\left(\frac{\zeta^3+18\zeta^2+88\zeta+96}{\zeta^4+20\zeta^3+120\zeta^2+240\zeta+120}\right) \tag{2.34}$$

The Vyazovkin procedure then iterates to minimise reduce the value of $\Gamma\left(E_A\right)$ which is defined as:

Table 2.13: Expressions for selected common reaction mechanisms in solid-state reactions [White et al., 2011]

Reaction Order (n)	$f(a) = (1-\alpha)^n$	$g(a) = \int_0^\alpha f(\alpha)$
Zero	1^n	α
First	$(1-\alpha)$	$-\ln(1-\alpha)$
n^{th}	$(1-\alpha)^n$	$(n-1)^{-1}(1-\alpha)^{(1-n)}$

$$\Gamma(E_A) = \sum_{j}^{q} \sum_{k \neq j}^{q} \frac{\beta_k p(\zeta_j)}{\beta_j p(\zeta_k)} \tag{2.35}$$

2.8.5 Non-isoconversional approach

A further alternative is provided by Zhang et al. [2009] who challenge the isoconversional assumption. Rather than estimating a constant activation energy across the entire reaction, this work modifies the Friedman method calculating activation energy and pre-exponential factor as the reaction proceeds. Disregarding the isoconversional principle and assuming a single reaction order yields the following relationship:

$$\frac{\mathrm{d}\alpha}{\mathrm{d}T} = \frac{A(\alpha)}{\beta} e^{\frac{-E_A(\alpha)}{RT}} f(\alpha) \tag{2.36}$$

The values of $A(\alpha)$ and $E_A(\alpha)$ are calculated using the B-spline curve fitting method and then the equation is integrated using a fourth order Runge Kutta algorithm. The work requires three separate sets of data at different values of β and then presents an averaged value for A and E_A.

2.8.6 Other considerations

Although the methods presented above differ in the way they estimate kinetic parameters, several common issues deserve consideration here. The impact of the rate of temperature increase (β), the compensation effect caused by non-unique kinetic triplets and methods of testing how well the data represent the observed results are discussed below.

2.8.6.1 Impact of rate of temperature increase

All of the methods above except the Friedman and Coats-Redfern procedures require repetition of the TGA experiments at different rates of temperature increase in order to generate the plots required to estimate the kinetic parameters. It is therefore implicit in their calculations that they assume the rate of temperature increase does not affect the apparent activation energy. For well-mixed homogenous reactions this assumption may be appropriate, though when considering heterogeneous reactions heat and mass transfer effects in real situations create gradients in temperature and species profiles within samples undergoing combustion. Lu et al. [2010] showed that for biomass particles devolatilising in an EFR the particles could not be modelled as spherical with effective diameters of greater than 200–300 μm suggesting that species and temperature gradients within and around the particle were non-uniform. Although TGA heating rates are generally orders of magnitude lower than EFR, DTF and scaled combustion tests, as White et al. [2011] note: *"The dependence of biomass pyrolysis kinetics on heating rate is still unresolved with some evidence supporting the notion that the use of different heating rates during biomass pyrolysis has minimal impact [. . .] and other data indicating that biomass conversion reactions are kinetically slower at higher heating rates."*

2.8.7 The compensation effect

The compensation effect arises from estimating the values of the parameters in the kinetic triplet from one data set which is known to produce non-unique solutions and is widely reported in the literature [De Jong et al., 2007, Vyazovkin et al., 2011, White et al., 2011]. Particularly when attempting to minimise a function it may be that several triplets are equally able to represent a line fitted to experimental data. Saddawi et al. [2010] note that even when one of the parameters is fixed, as is often the case when modelling biomass pyrolysis as a first order reaction, both high and low activation energies are reported for similar samples. Vyazovkin et al. [2011] and White et al. [2011] both detail further mathematical manipulations that allow approximation of unique solutions though these involve several repetitions of experiments. Another option is to reduce the degrees of freedom by fixing the value of one or two of the parameters within a range of known values. For example many researchers suggest first-order reactions are appropriate for fuel decomposition reactions while Li et al. [2008] fixed the pre-exponential function in

their work. However, these further assumptions necessarily increase the potential for error when predicting the values of kinetic parameters.

2.8.8 Method evaluation by reconstruction

In most examples of estimating the kinetic triplet from TGA experiments the accuracy of the method is usually defined by the linearity of the model line created to experimental data points. Realising that this does not necessarily evaluate how well the estimated parameters represent the experimental data (only the linearity of the line the model produces), several researchers have instead used the values derived from the model to reconstruct the decomposition data [Grønli et al., 2002, Skreiberg et al., 2011, Várhegyi et al., 2009]. The authors then compare this reconstructed data with the experimental data and thus indicate how well the estimated parameters predict the actual decomposition.

2.9 Research questions

From the review of relevant literature presented in this chapter a number of areas have been highlighted where knowledge is lacking regarding the technological development of combining biomass combustion with CCS, and in particular oxyfuel combustion. To date, very little work has been published that focusses on the combustion of biomass in CCS-relevant atmospheres at sufficient scale to usefully inform what will occur at industrial scale. This is precisely the type of work that is necessary for the development of Bio-CCS technology. In particular, very little work has focussed on the emissions of typical pollutants and the impact on combustion characteristics of blending biomass with coal in oxygen-enriched atmospheres. To explain results from such tests, it is useful to understand how the reactivity of the fuels fired change in novel combustion atmospheres. Analysing these changes in reactivity requires a robust method that can be rapidly applied without expending significant resources. In light of this summary of the gaps in the relevant areas of knowledge, the following research questions are proposed for this work:

1. Develop, test and evaluate a methodology to rapidly and robustly analyse variation in the decomposition behaviour of biomass fuels in TGA experiments;
2. Use the above methodology to investigate the variation in reactivity and decomposition behaviour of three UK-relevant energy resource biomasses in OEC and oxyfuel

atmospheres;

3. Investigate the impact of the biomass blending ratio on pollutant emissions and combustion characteristics for cofiring with coal in OEC conditions through cofiring UK-relevant energy resource biomasses, including brownfield-derived biomass, at 20 kW scale;
4. Investigate the impact of oxidant staging on pollutant emissions and combustion characteristics for cofiring with coal in OEC conditions through cofiring UK-relevant energy resource biomasses, including brownfield-derived biomass, at 20 kW scale;
5. Investigate the impact of CO_2-enrichment of the combustion atmosphere on pollutant emissions and combustion characteristics for cofiring with coal in OEC conditions through cofiring UK-relevant energy resource biomasses, including brownfield-derived biomass, at 20 kW scale;
6. Investigate the impact of dedicated biomass firing in OEC and CO_2-enriched combustion on pollutant emissions and combustion characteristics, at 20 kW scale;

Chapter 3

Experimental Methodology

3.1 Chapter overview

This chapter presents the experimental methodology used to generate the data presented in Chapters 4 to 6. The first of the following sections details fuel characterisation techniques that provide data which is used to inform experimental results such as proximate analysis, ultimate analysis and particle size distribution. The method for obtaining experimental data at TGA scale, the findings from which are used to help explain the results from the 20 kW facilities, is then presented before a comprehensive account of the 20 kW combustion facilities is provided.

3.2 Fuel characterisation

Five fuels were analysed in this work. Dr. Richard Lord supplied three biomasses grown in the North of England as part of the BioReGen project [Pratt and Lord, 2010]: short-rotation coppiced willow - *Salix spp.* - (SRC); miscanthus (MC) - *Miscanthus giganteus* - and reed canary grass - *Phalaris arundinacea* - (RCG). RWE NPower supplied the shea meal - *Vitellaris paradoxa* - (SM) which was included in the kinetics testing in order to compare to previous work [Munir et al., 2009]. SM was not involved in the pilot scale combustion tests which cofired the first three biomasses with Williamson coal (WC). All of the UK-grown biomasses were harvested, dried and milled to pass through a 500 μm seive, while the other fuels were presented as would be fired by commercial power plant operators.

3.2.1 Proximate analysis

Biomass proximate analysis was carried out by TGA analysis to estimate the amount of moisture, volatile matter, fixed carbon and ash in each sample. Approximately 20 mg was measured into a crucible of a Stanton Redcroft TGA device that was operated with a N_2 atmosphere. Once air had been purged from the system each sample was heated from ambient temperature to 388 K at a heating rate (β) of 20 K min^{-1}. The sample was then held at this temperature for ten minutes to ensure all moisture was removed. The sample was then heated at a rate of 20 K min^{-1} to 1173 K where it was held for 20 minutes to ensure pyrolysis was complete. Air was then introduced to the chamber and a further 20 minute period was allowed to permit full oxidation of the sample char. Examples of the mass loss and derivative thermogram (DTG) curves for the fuels are shown in Figure 3.1. The moisture content of the biomasses was calculated as the mass loss between the onset of the TGA and that at a temperature of 393 K to allow for mass loss observed during any temperature overshoot of the TGA device when approaching 388 K. Although the release of volatiles occurred across different temperature ranges for the samples, by a temperature of 873 K the DTG curves for each biomass sample suggested the main devolatilisation reactions had completed and the difference between mass at this temperature and at 393 K was taken as the mass attributed to volatile matter. The difference between the final mass and the mass at 873 K represents the fixed carbon. The final mass is attributed to ash. The masses were normalised to the starting mass to convert the amounts to the percentages presented in Table 3.1. Results for the biomasses were found to agree with ranges in the literature [Vassilev et al., 2010]. Confidence was also enhanced as results also agreed with those obtained for smaller samples tested under a higher heating rate ($\sim$5 mg at 40 K min^{-1}). All coal analysis data were provided by Knight Services.

The analysis shows on an as received basis SRC and MC both display relatively high levels of volatile matter (72.4 and 74.0%, respectively) with low amounts of ash (2.9 and 3.3%). RCG displays an ash content almost as high as coal (8.1% compared to 9.0%) though like SRC and MC about double the moisture content of coal (6% compared to 3%). SRC, MC and RCG contain approximately one third of the fixed carbon content of coal. The results of the SM analysis show it exists somewhere between the other biomasses and coal with a lower VM, higher FC and higher ash content than most of the biomasses.

The DTG for MC and SRC are very similar showing a distinct shoulder at $\sim$590 K which

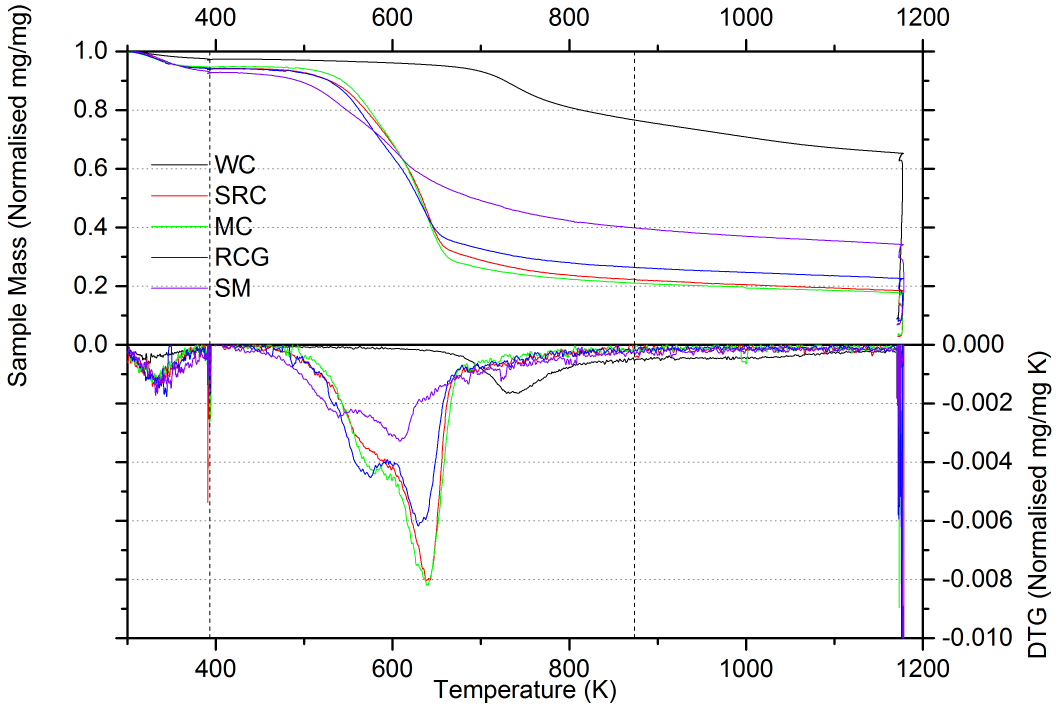

Figure 3.1: Results of biomass proximate analysis showing for increasing temperature the mass loss and its first derivative (DTG) with respect to temperature

is thought to represent the transition from hemicellulose to cellulose decomposition controlling the overall decomposition. RCG shows a similar decomposition profile though with slightly more decomposition attributed to the lower-temperature hemicullose decomposition and less to the cellulose stage. The onset of decomposition for all three of these biomasses is approximately 470 K with the highest rate of mass loss in the range 630–640 K. Between 670–873 K a slow, decreasing mass loss is observed for all samples. This is thought to represent the most thermally stable lignin compounds with the mass loss due to the more reactive lignin compounds being hidden behind the decomposition of hemicellulose and cellulose. SM decomposition begins ∼50 K earlier and displays a different profile to the other biomasses with less intense peaks and a wider temperature range over which decomposition is observed. WC shows a significantly different decomposition with a far lower amount of volatile matter being released mainly at temperatures >700 K with the decomposition showing a less defined peak and a continued slower mass loss until approximately 1100 K.

Table 3.1: Combined results of fuel characterisation studies

Fuel	WC	SRC	MC	RCG	SM
Proximate Analysis (%), ar:					
Moisture	3.4	6.0	5.5	5.8	7.5
Volatile matter (VM)	33.9	72.4	74	68.5	53.8
Fixed carbon (FC)	53.7	18.7	17.3	17.6	31.9
Ash	9.0	2.9	3.3	8.1	6.9
Lignocellulosic Content(%), ar:					
Hemicellulose	N/A	11.7	22.4	27.5	10.9
Cellulose	N/A	48.0	47.6	31.2	2.9
Lignin (ADL)	N/A	14.0	6.0	-2.0	24.4
Lignin (Klason)	N/A	27.2	23.0	20.0	41.6
Ultimate Analysis (%), ar:					
C	72.0	47.7	46.4	42.2	48.6 [a]
H	4.5	6.0	5.8	5.4	5.9 [a]
N	1.7	0.4	0.3	1.4	2.9 [a]
S	1.9	0.0	0.0	0.0	0.2 [a]
O[b]	10.9	43.0	44.3	42.8	37.5 [a]
C:H	15.9	8.0	8.0	7.8	8.3 [a]
C:O	6.6	1.1	1.0	1.0	1.3 [a]
Heating Value (MJ/kg), ar:					
Experimental NCV	28.3	17.6	17.8	15.8	17.2
Theoretical NCV	28.2	17.7	16.9	15.2	18.5

[a] Shea meal data from Nimmo et al. [2010]; [b] By difference

3.2.2 Ultimate analysis

Ultimate analysis was performed to measure the relative amounts of the main components in each sample. For each fuel 3.25 $\pm$ 0.3 mg of sample was accurately weighed out. Each sample was then tightly encapsulated in aluminium foil and loaded into a Thermo-Scientific Flash 2000 CHNS Analyser. Samples were run in duplicate and if the results did not corroborate a further analysis was run until reproducibility was achieved. Oxygen was calculated by difference. The averages of reproducible results are presented in Table 3.1.

3.2.3 Hemicellulose, cellulose and lignin content

Analysis of the lignocellulosic contents of biomass is conducted by several wet chemistry stages, detailed concisely by Carrier et al. [2011]. The (Klason) lignin content of a sample is that which remains insoluble in H_2SO_4 after two hours under concentrated conditions and then a further four hours of boiling of the diluted solution. The amount of neutral detergent fibre (NDF) is the organic matter not solubilised after one hour of heating under reflux in a neutral detergent solution of sodium laurylsulphate in presence of a 98 °C thermoresistant amylase. The acid detergent fibre (ADF) is the material not solubilised after one hour of heating under reflex in an acid detergent solution of acetyltrimethylammonium bromide in 0.5M sulphuric acid. The acid detergent lignin (ADL) is the amount of matter not solubilised after three hours of extraction with a 72%$_{wt}$ sulphuric acid solution and includes lignin and ash. The amount of hemicellulose, cellulose and lignin is then calculated according to Equations (3.1) to (3.3). This analysis was carried out by Dr Sue Lister at Aberystwyth University. The results are presented in Table 3.1. The negative value for lignin derived using the ADL method arises as the ADL measured value is less than the ash content of the fuel which suggests some of the ash components are solubilised by acid solutions. While this is less apparent for the samples containing lower amounts of ash, the relatively high ash content of the RCG (8.1%) and ability of acid solutions to solubilise ash compounds, particularly Ca and Na, shown by Kim et al. [2003]. While the Klason and ADL methods for measuring lignin appear similar differences of the magnitude observed in Table 3.1 are common, as shown by Carrier et al. [2011].

$$\text{Hemicellulose} = \text{NDF} - \text{ADF} \tag{3.1}$$

$$\text{Cellulose} = \text{ADF} - \text{ADL} \tag{3.2}$$

$$\text{Lignin (ADL)} = \text{ADL} - \text{Ash} \tag{3.3}$$

$$\tag{3.4}$$

3.2.4 Volatile species

During the data acquistion for the proximate analysis, analysis of the species evolved during devolatilisation was conducted by passing the exhaust stream to a Fourier-Transform Infra-red (FTIR) spectrometer as shown in Figure 3.2. The Gram-Schmidt absorbance is shown for all fuels in Figure 3.3 while a three-dimensional plot of relative absorbance and wavelength over time is shown for each fuel individually in Figure 3.6. Although direct comparison between the magnitudes of these data cannot be complete due to scaling differences attributed to variation in moisture, ash and FC content between the fuels, the Gram-Schmidt curves in Figure 3.3 allow general trends to be extracted. Comparison with TGA data suggests a short delay of up to two-minutes between products being released from the surface of the sample particles and being detected by the infra-red spectrometer. All of the biomasses show detection peaks during the holocellulose decomposition while the coal sample exhibits two peaks much later into the experiment. The spectra taken at the peak of the Gram-Schmidt curves for each biomass are shown in Figure 3.4.

The expected presences of a wide range of compounds produced a series of complex spectra for each fuel. In attempt to deconvolute the data characteristic wavelengths for typical pyrolysis products were analysed for each of the fuels as carried out by other researches [Han et al., 2010, Singh et al., 2012]. The evolution of CO, CO_2, methane (CH_4) and phenolic compounds over time are shown in Figure 3.5. The delay between devolatilisation from the particle and detection by the spectrometer may have allowed further decomposition reactions to occur which may have contributed to the observation for all samples that CO_2 is the dominant pyrolysis product. This was followed by phenolic compounds and CH_4 with CO observed to be slightly less common. The results agree with those discussed in Section 3.2.1 with CO_2 observed during the decomposition of hemicellulose and cellulose. The detection of the other species occurred at similar times to the detection of

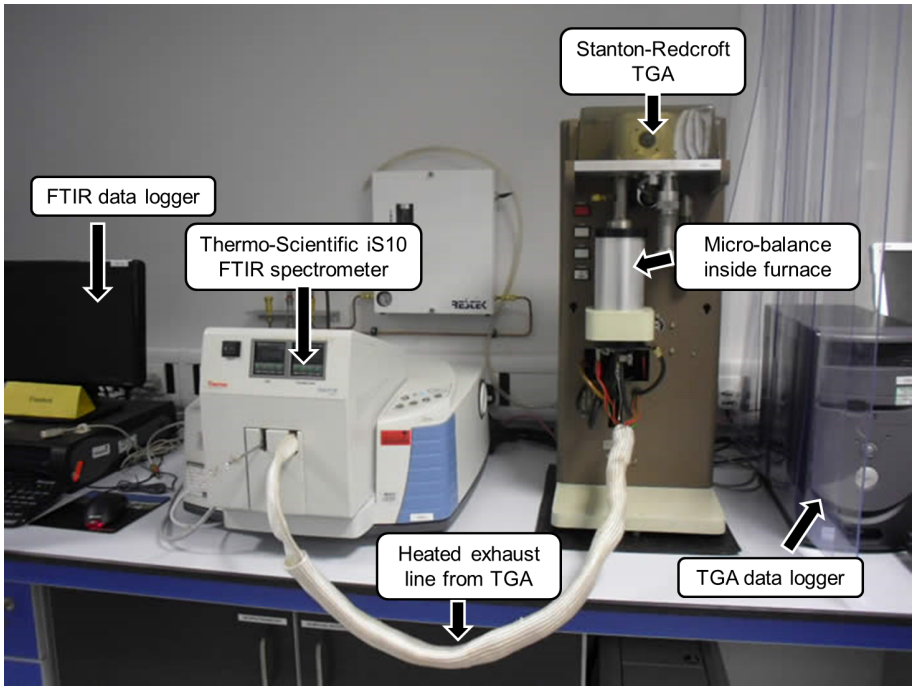

Figure 3.2: Photograph showing TGA-FTIR experimental set up. Photograph amended from [University of Leeds, 2013]

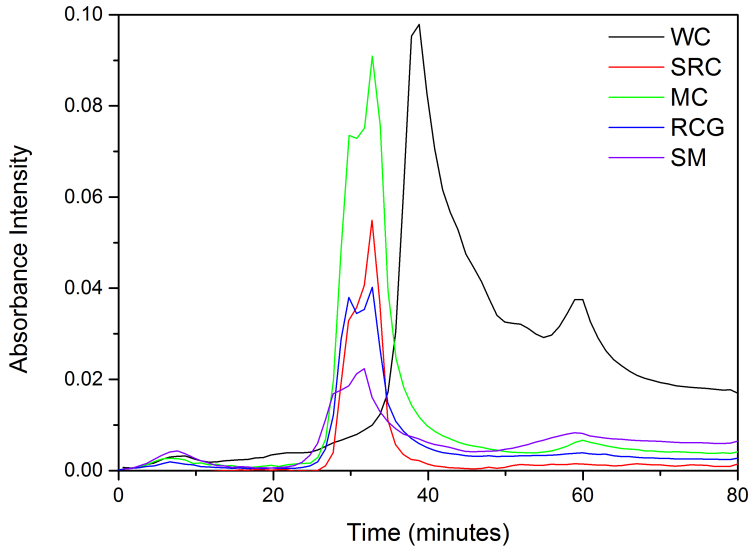

Figure 3.3: Gram-Schmidt evolution of materials over time during pyrolysis of fuels in TGA device

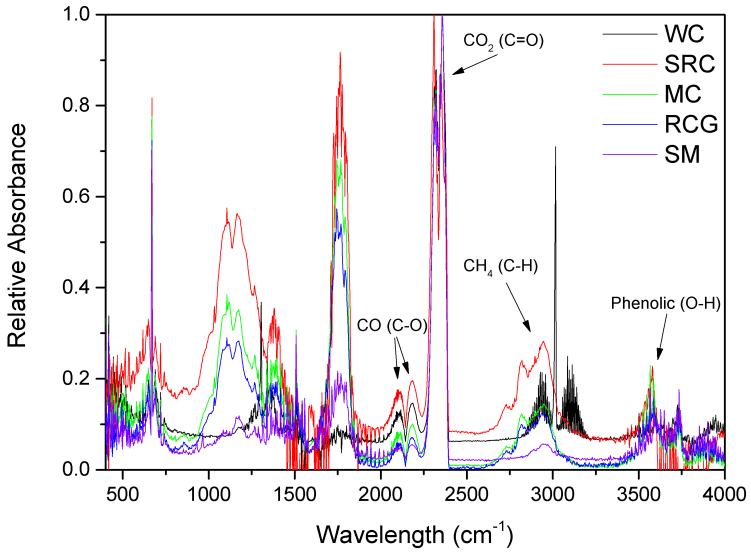

Figure 3.4: The absorbance spectra at the peak of the Gram-Schmidt curves during pyrolysis of fuels in TGA device

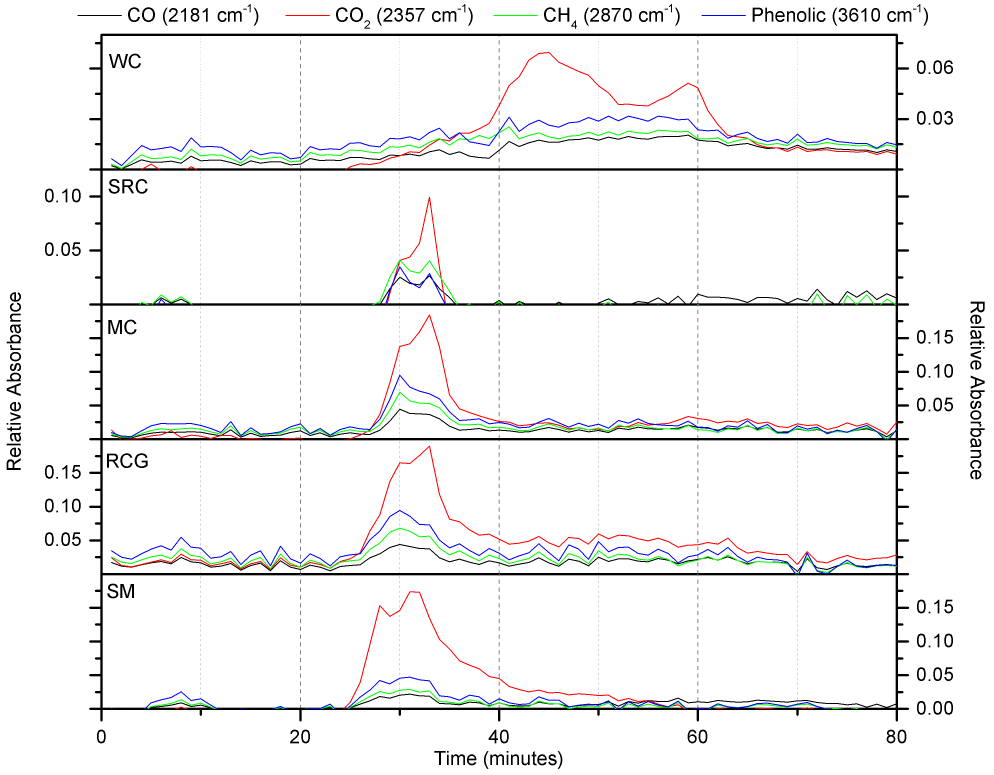

Figure 3.5: Comparison between fuels of detection of characteristic wavelengths for common pyrolysis products

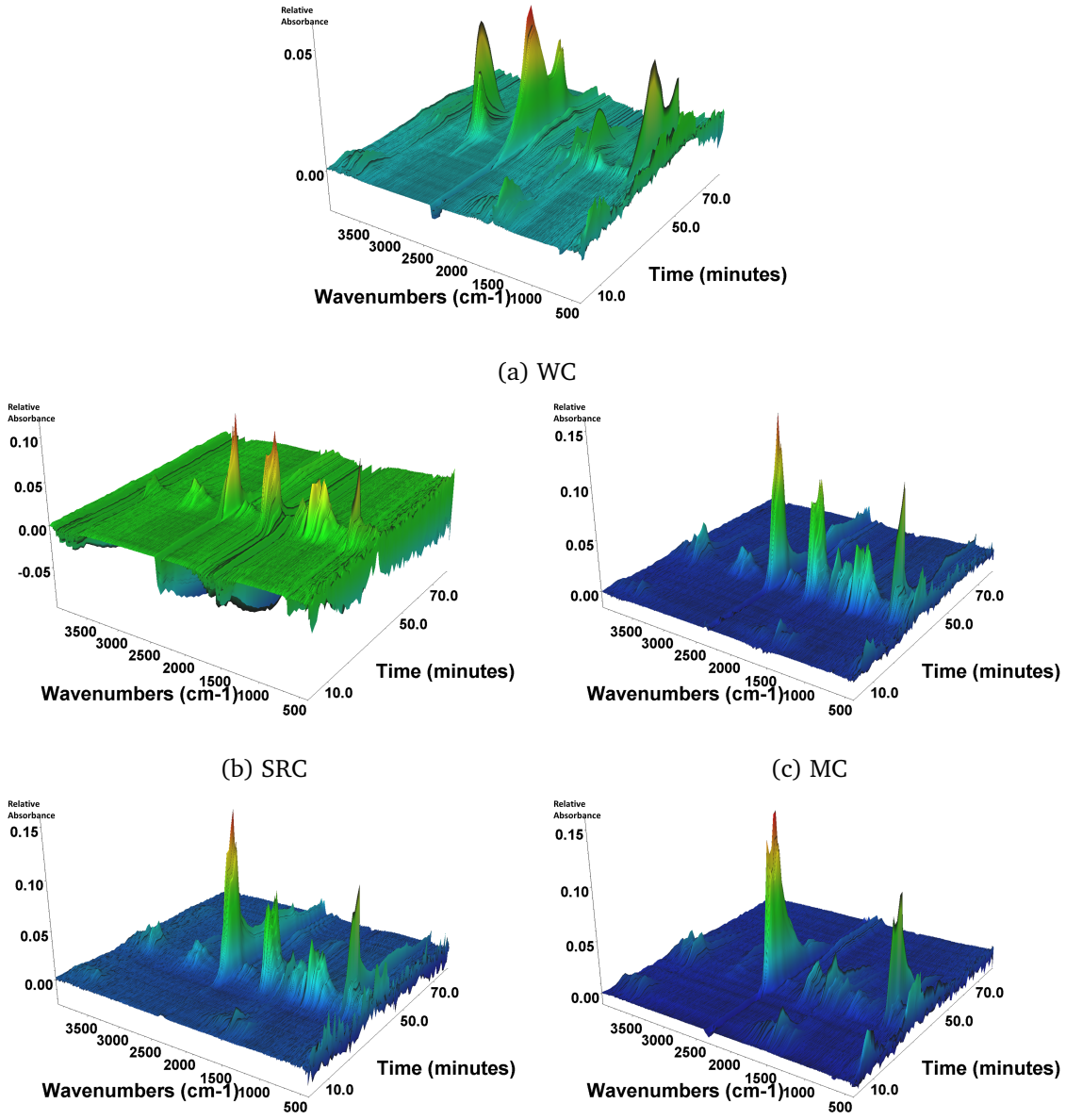

(a) WC

(b) SRC

(c) MC

(d) RCG

(e) SM

Figure 3.6: Three-dimensional plots showing the relative absorbance of different wavenumbers over time during the pyrolysis of different fuels. Poor baseline correction was observed for the SRC sample. However, since these results are not intended to be quantitative, and instead only illustrate the difference in emission profile during pyrolysis, a repeat experiment was not considered necessary

CO_2 suggesting these may also have been released from holocellulose molecules. For MC and RCG the detection of non-CO_2 species was at a maximum during the hemicellulose decomposition stage. SRC exhibited similar intensity during both hemicellulose and cellulose decompositions while SM and WC showed broader, less defined peaks in general which may be due to decomposition of more complex molecules. From Figure 3.6 it is also clear that the WC and SM pyrolysis products absorb far less in the 2250–1750 cm^{-1} range than the other biomasses. Although difficult to comprehensively identify what may cause absorbances in this range, the increased O_2 found in Section 3.2.2 could suggest the likelihood of an increased observance of C=O bonds in the SRC, MC and RCG with aldehyde and ketone bonds in cyclic arrangements known to absorb at 1750 and 1775 cm^{-1}, respectively. Increased oxygen content within holocellulose molecules may also explain the peaks in the range 1100–1200 cm^{-1} which may correspond to secondary and tertiary alcohols formed as cellulose molecules decompose.

3.2.5 Particle size

The particle size distribution of the biomass and coal particles was analysed for the samples used in the 20 kW combustion tests by Dr. S. S. Daood at IIT Technologies. The variation in biomass sizes predicated that samples were analysed for particle size distribution using both the Dry Malvern as well as MINOX air jet sieving (AJS) techniques. Dry Malvern analysis is recommended for particles $<100\,\mu$m in diameter [Daood, 2011]. Upon initial testing it was found that the majority of the biomass particles were $>125\,\mu$m in size and thus the AJS technique using 20 mbar suction for periods of four minutes was found to give more consistent results for the biomass samples. Dry Malvern analysis using laser diffraction was used for the coal samples. The Rosin-Rammler distribution was calculated according to Equation (3.5) which predicts the fraction of with a diameter greater than diameter d (Y_d) is given by the average diameter ($\bar{d}$) and the spread factor (z).

$$Y_d = e^{-(d/\bar{d})^z} \tag{3.5}$$

The results of the analysis presented in Figure 3.7 show SRC is substantially coarser than the other biomasses with over 50% larger than 250 μm, approximately double the corresponding size for MC and RCG and about five times larger than 50% passing for WC. The

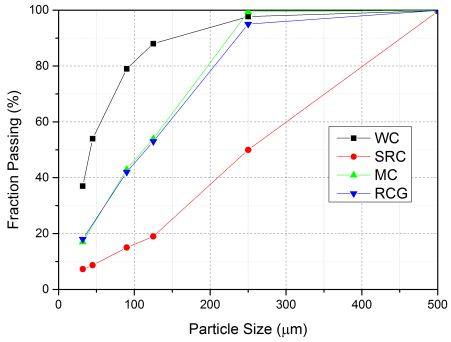

Rosin-Rammler Factor	WC	SRC	MC	RCG
Mean diameter ($\bar{d}$, μm)	60	312	142	150
Spread parameter (z)	1.00	1.80	1.72	1.51

Figure 3.7: Particle size analysis for the three biomass and one coal sample used during 20 kW pilot-scale combustion

grasses (MC and RCG) show very similar size distributions with over 90% of the particles smaller than 250 μm. WC is the finest of the fuels with over 80% of particles smaller than 100 μm.

3.2.6 Particle morphology

A Carl Zeiss EVO MA15 scanning electron microscope (SEM) was used to investigate the morphology of samples which were mounted on Leit carbon tabs and coated with a layer of $\approx$ 10 nm of amorphous carbon to aid conductivity. In addition to carbon coating, in order to reduce particle charging on the biomass samples the machine was operated under variable pressure mode while the coal sample was analysed under standard vacuum conditions. The images in Figure 3.8 corroborate the size distribution shown in Figure 3.7 showing that on average the coal particles are far smaller than their biomass counterparts but also that their morphology is markedly different. The coal particles are largely equi-dimensional particles while the biomass particles tend to include a range of particles of various sizes and shapes with a number of large cylindrical shapes present.

3.2.7 Calorific value

A Parr Bomb Calorimeter was used to establish the net calorific value of each for the samples. For the coal approximately 0.25 g and for the biomasses approximately 0.4 g was accurately weighed out for each sample. The sample was then enclosed in a pressurised

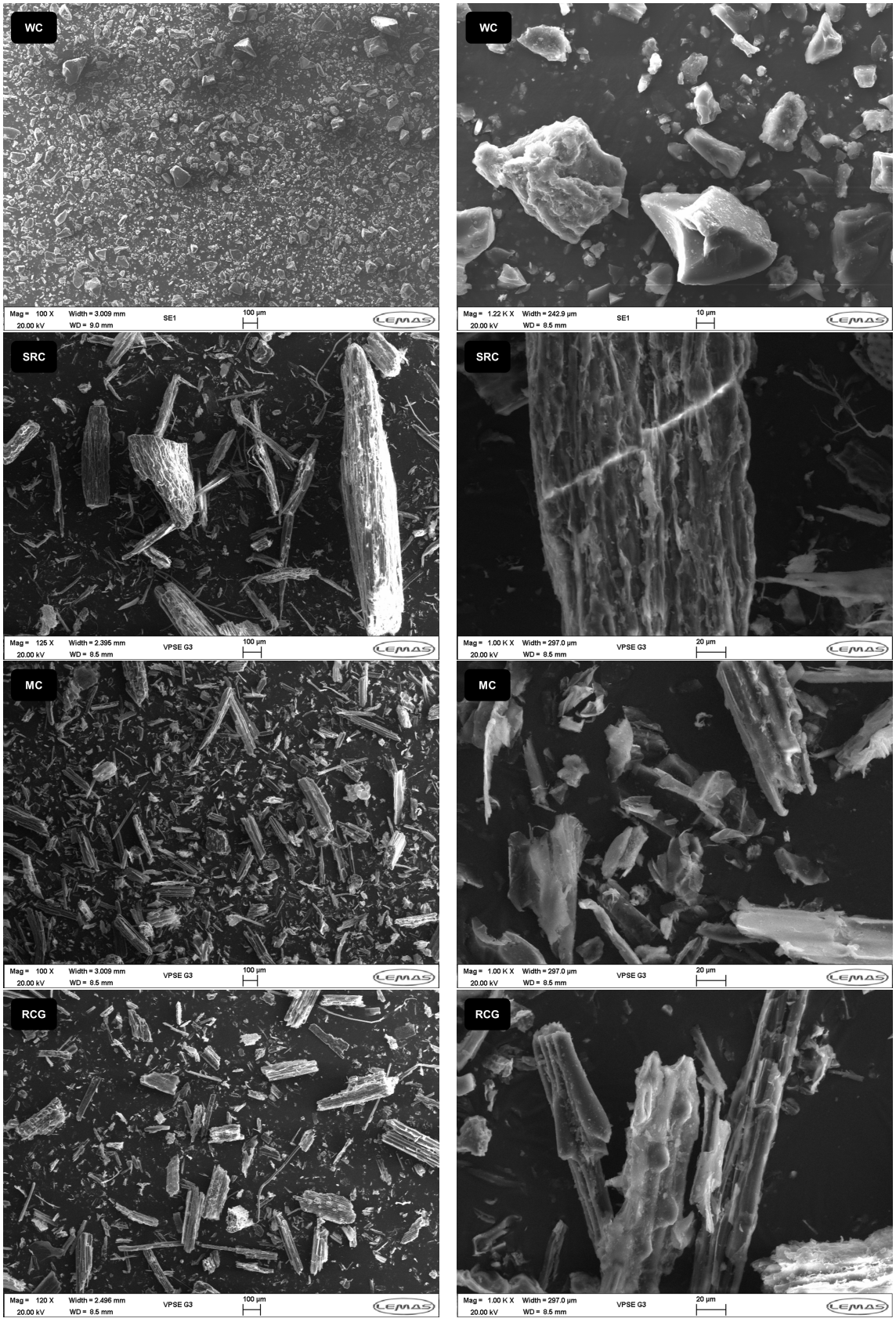

Figure 3.8: SEM images of fuels at approximately $100x$ and $1000x$ magnification

bomb vessel with a short length of fuse wire suspended just above the sample. The bomb is seated in a water bath filled with 2.000 kg of deionised water. The vessel is charged with O_2 and once pressurised an electric charge is passed through the fuse wire causing the sample to ignite and oxidise. The heat generated from combustion is transferred through the metal casing to the water bath where the temperature increase is accurately measured. Once the temperature has stabilised the energy released to the water (ΔE) is calculated according to the general heat transfer equation (shown in Equation (3.6)). Samples were run in duplicate and if the results did not corroborate a further analysis was run until reproducibility was achieved. The averages of reproducible results are presented in Table 3.1.

$$\Delta E = m_{\mathrm{H_2O}} \cdot C_{P,\mathrm{H_2O}} \cdot \Delta T \tag{3.6}$$

where $m_{\mathrm{H_2O}}$ is the mass of water, $C_{P,\mathrm{H_2O}}$ the specific heat capacity of deionised water and ΔT the change in temperature measured.

3.3 Bench-scale experimentation: TGA

3.3.1 Sample preparation

In an attempt to separate experimental physical characteristics from those of a chemical nature and to ensure homogeniety in small sample sizes it was necessary to further reduce the size of the particles. According to Lu et al. [2010] mass transfer effects during thermal treatment may be largely mitigated once particle size is reduced to approximately 200 μm. To avoid the escape of volatile species and/ or waxy deposits, the biomass samples to be investigated in TGA were milled using a SPEX 6770 Freezer Mill which uses liquid nitrogen to ensure samples remain solid during milling [Adams et al., 2011, Jones et al., 2012]. The coal was ground by hand in a pestle and mortar. The particle sizes of all samples were reduced until they passed through a 212 μm sieve.

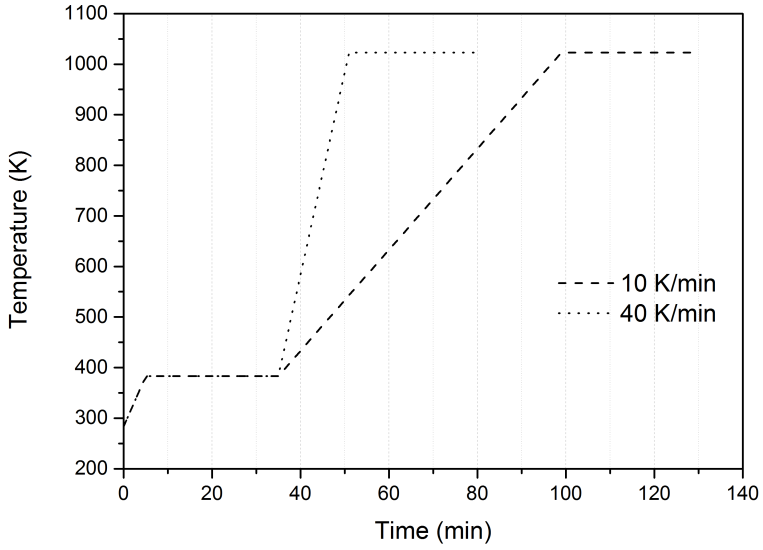

Figure 3.9: Time-temperature graph of TGA experiments

3.3.2 Experimental procedure

The experimental data was generated according to ASTM standards E1641 and E2550. For each experiment $5 \pm 0.5\,\mathrm{mg}$ of biomass sample was accurately measured into an open alumina crucible and the sample was introduced to a Mettler-Toledo TGA/DSC1 device. In this equipment, the thermobalance is coupled to a differential scanning calorimeter which measures the heat flux necessary to maintain the set temperature thereby providing an indication of the endo- or exothermicity of any occuring reactions. Once air was purged by the test atmosphere the sample was heated to 383 K and held for 30 minutes to drive off moisture. The sample was then heated at the test heating rate (β) to a temperature of 1023 K while the test atmosphere was pumped into the chamber at a rate of $50\,\mathrm{ml\,min^{-1}}$. The sample was held at the final temperature for a further 30 min to ensure combustion was complete. Although as White et al. [2011] note, the Coats-Redfern method only requires a single heating rate to generate reactivity parameters, each of the TGA tests was repeated at heating rates of 10 and $40\,\mathrm{K\,min^{-1}}$ to increase the robustness of the results. The time-temperature profiles for these heating rates are shown in Figure 3.9.

The combustion of each sample was studied in four oxidising atmospheres. Dry air (21% O_2, 79 % N_2) was the reference case. Similar to the work of Yuzbasi and Selçuk [2011], the composition of the oxyfuel atmosphere was chosen to be similar to that reported in the literature and consists of an enriched O_2 level compared to air and thus was labelled

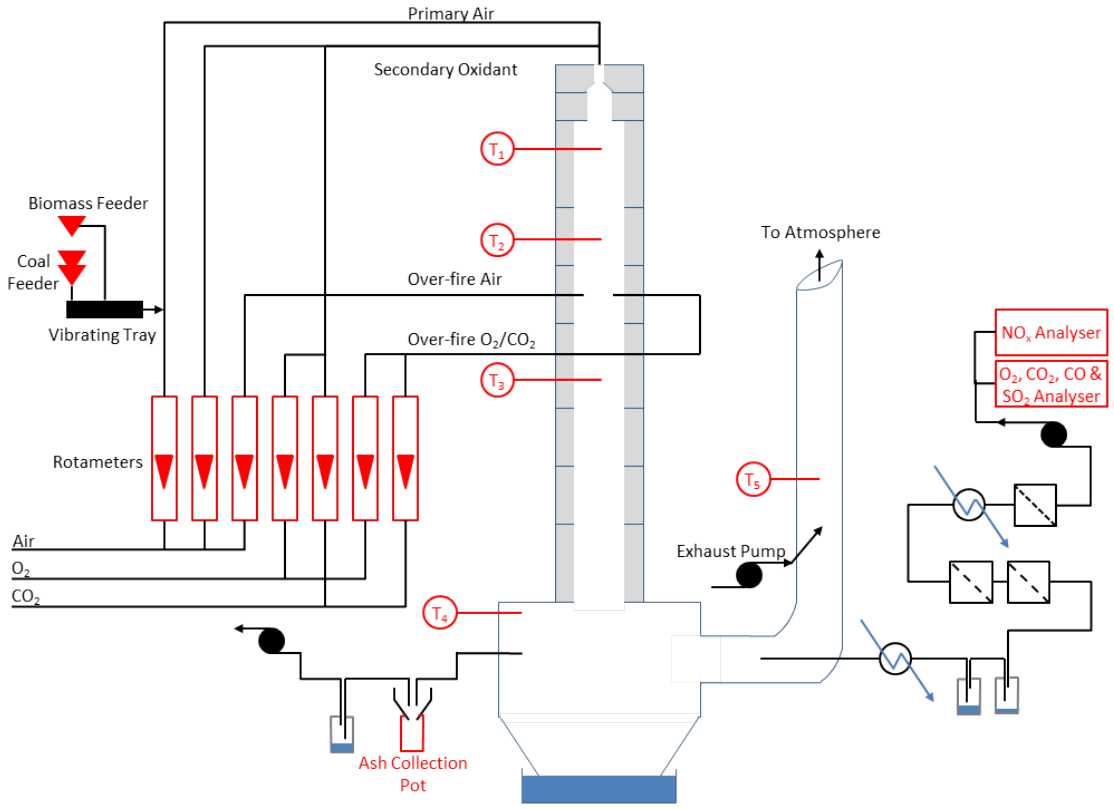

Figure 3.10: Schematic diagram of 20kW experimental rig. Black lines represent flows and red icons represent me asurement locations.

En-Oxy (30 % O_2, 70 % CO_2). In order to investigate the effect of increasing oxygen concentration and substituting N_2 for CO_2 separately an oxygen-enriched air (En-Air: 30 % O_2, 70 % N_2) and an un-enriched oxyfuel condition (Oxy: 21 % O_2, 79 % CO_2) were also included in the experimental design. Steam could not be included in the 20 kW experiments which were modelled on a dry-recycled system and thus, despite the practical likelihood of high steam concentrations for wet-recycled oxyfuel systems, it was not included in the TGA experiments either. All gases were supplied premixed by BOC.

3.4 20 kW-scale combustion

The 20 kW combustion rig used in this study has been documented by a number of previous literature publications, for example [Daood et al., 2011, Nimmo et al., 2010]. However this work features some small changes to those presented previously and thus a full description of the experimental set up is included below. A schematic diagram of the rig is shown in Figure 3.10.

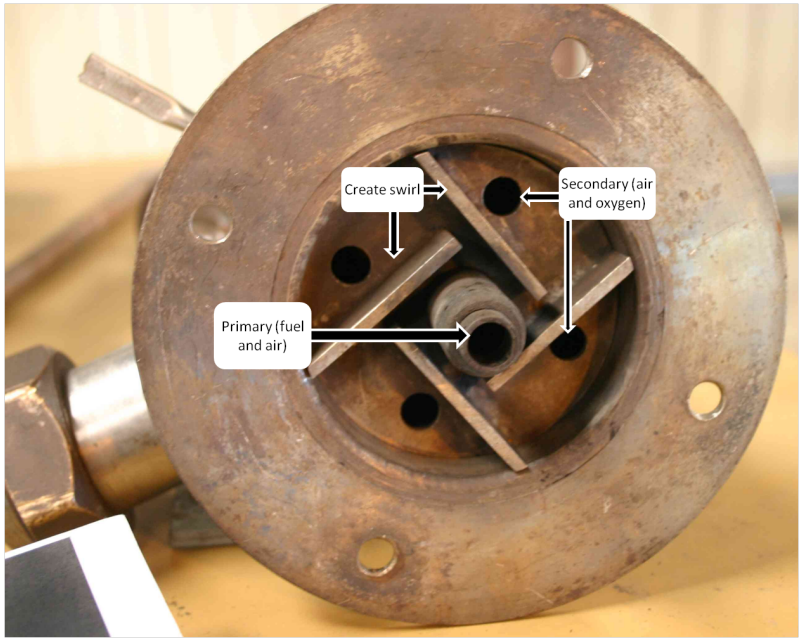

Figure 3.11: Photograph of the primary and secondary ports and the arrangement of flow-diverters to create swirl in the burner

3.4.1 Furnace

The pulverised fuel combustor used for this work is cylindrical and 3.5 m high with an internal diameter of 200 mm and operated in a down-fired configuration. The inside wall of the furnace is lined with 100 mm of refractory lining and the unit is capable of thermal throughput of approximately 20 kW when firing coal. It is operated at a slight negative pressure, with a sealing water splash tray used to prevent escape of combustion gases. The combustor features a single burner which includes a central non-swirling primary air port and a secondary swirling port (Figure 3.11). The furnace is divided into 9 sections. The top section is lined with cast alumina and houses the water-cooled burner and quarl which is conical, extending from a diameter of 28 mm to 140 mm over a distance of 265 mm. Each of the furnace sections contain several ports which may be used for either gas injection, or gas or particle sampling (Figure 3.15). An exhaust fan induces flow through the furnace and dilutes the combustion flue gases before they are vented to the atmosphere.

3.4.2 Fuel supply

Pulverised fuel is conveyed pneumatically to the furnace by the primary combustion air which collects the fuel from a vibrating plate that ensures homogeneity of the feed. The

Table 3.2: Gradient (l), intercept (c) and linearity (r^2) of calibration factors for fuel feeding systems

Fuel	l	c	r^2
WC 1	0.00999	-0.7655	0.9845
WC 2	0.01077	0.0445	0.9988
SRC	0.07591	-0.0615	0.9801
MC	0.08689	-0.0980	0.9939
RCG	0.15015	-0.2832	0.9889

fuel is fed to the plate by screw feeders: coal is fed by a twin-screw feeder while the biomass is fed by a single screw feeder. The biomass feeder was custom-built for the experimental rig. It consists of an angled lower section which forms an inverted apex. The biomass in the hopper is continually agitated by two sets of fins attached to the screw mechanism which prevents settling of the fuel and ensures homogeneity. The screw drives material horizontally from the centre of the hopper to ensure a representative sample of the fuel and to reduce bridging of the sample. For both feeders, adjustment of the screw rotational rate is used to modify the fuel feed rate. Coal is mechanically drawn into the feeder from a hopper above via a rotary valve while the biomass feeder requires regular refilling by hand. To ensure fuel mass flow rates did not change throughout the experiments fuel levels were maintained at set points. The level in the biomass feed hopper was maintained at approximately 2 cm above the agitator fins while the coal level was maintained through the use of a graduated dip stick. The fuel flow rates from both feeders have been calibrated from a series of measurements. The relationship between screw rate and flow of fuel was found to be linear for all fuels as shown by Figure 3.12. The linear relationship shown in Table 3.2 were derived from each of these lines and used to interpolate the screw settings necessary to achieve the correct biomass blending ratios.

3.4.3 Gas supply

Primary air is fed from a compressor and regulated at a pressure of 1.5 bar. Similar to the work of Smart, O'Nions and Riley [2010], due to carrying the fuel the [O_2] of this stream is never enriched, maintaining 21% by volume and abiding by Health and Safety procedures. The secondary and tertiary gas flows can consist of mixes of air, CO_2 or O_2. A fan provides the air while CO_2 and O_2 are delivered from bottles on site regulated to

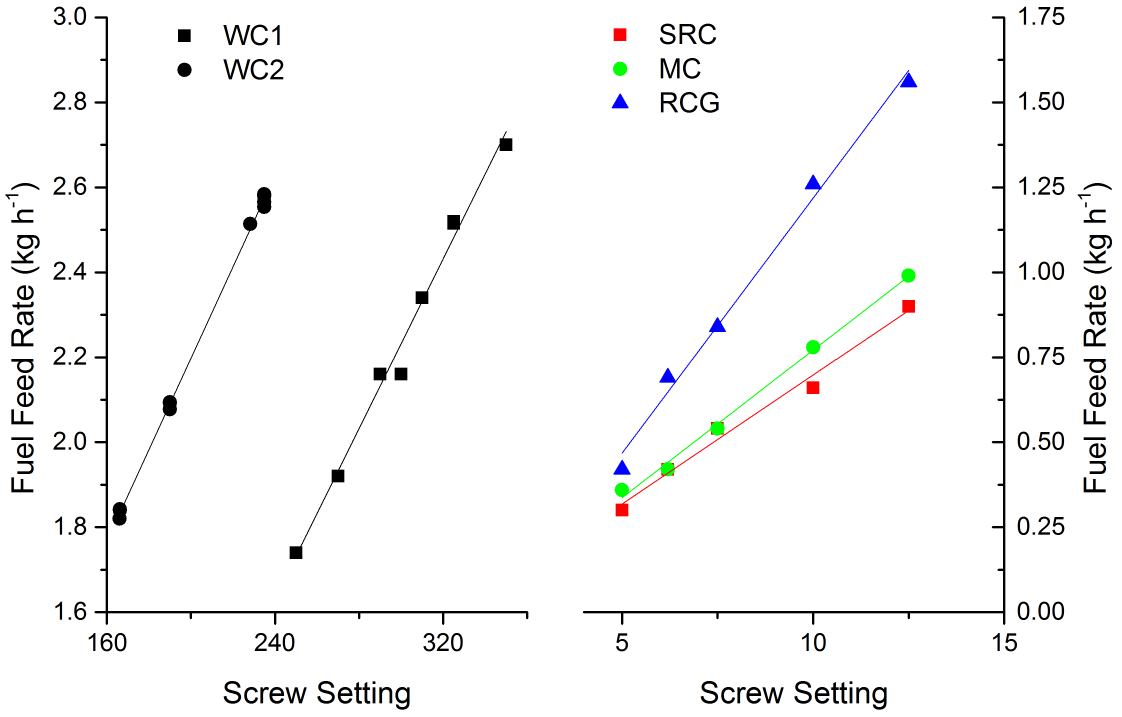

Figure 3.12: Calibration curves for feed rates of coal and biomasses. The equation of the line is used to calculate screw settings during for different blending ratios for each fuel

ambient temperature and a pressure of 1 bar. Each of the gases is metered individually before being injected to the furnace. Tertiary CO_2 and O_2 are mixed (if used together) and delivered in an oxygen-rated line which can be inserted at any of the ports shown in Figure 3.10. Tertiary air was injected to the fifth section of the combustor since this has been found to be the optimised level to reduce NO_2 emissions in previous work [Daood et al., 2011].

Gas flows (N, $\mathrm{L\,min^{-1}}$) are measured by rotameters which are pre-calibrated to specific gases (normally air) at 15 °C and 1 bar. Since the flowing gases are not always the same as the calibrated measurements a correction must be applied. Equation (3.7) is the generic equation used to calculate flow rates when the temperature, pressure or flowing gas through is different to conditions used during calibration. The temperature of the primary flow is approximated by the ambient temperature and pressure is controlled by a regulator. The temperature and pressure for the secondary and tertiary flows are measured upstream of the secondary air rotameter. During operation the temperature of the secondary and tertiary streams was typically in the region of 42–46 °C and the pressure ∼1.14 bar.

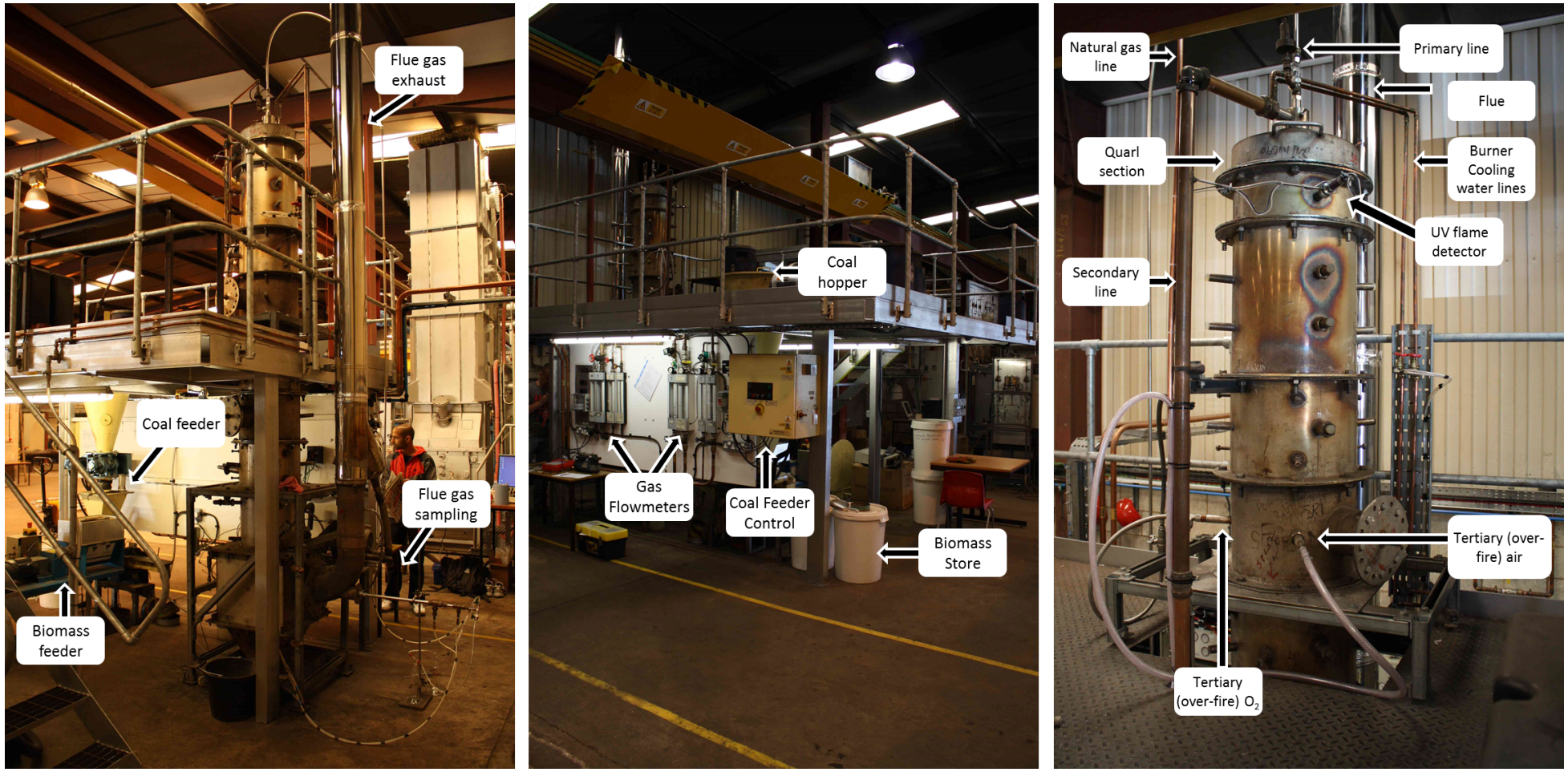

Figure 3.13: Annotated photographs of the 20 kW combustion rig

$$N_2 = N_1 \times \sqrt{\frac{\rho_1 P_2 T_1}{\rho_2 P_1 T_2}} \tag{3.7}$$

where N (L min^{-1}) represents flow rate, ρ (kg m^{-3}) density, P (bar) the absolute pressure and T (K) the absolute temperature of the flow.

3.4.4 Measurements

3.4.4.1 Temperatures

Three temperature measurements are made inside the furnace using ceramic-sheathed type R thermocouples. Temperatures are also measured in the flue section and for the water returning from the jackets using type K thermocouples. The in-furnace temperature measurements (1–3) are made 45, 90 and 165 cm, respectively, from the burner throat as shown in the schematic diagram in Figure 3.10. The locations of T_1 and T_2 are also shown in Figure 3.15.

3.4.4.2 Gaseous emissions

Gases are sampled using a customised, water-cooled probe which extracts sample gases from the centre of the flue. An auxiliary pump augments suction provided by the pump attached to the NO_x measurement unit and both act to draw gases through the sampling system. Gases are drawn into the probe and then pass through two water traps (Dreschel bottles) which remove the majority of entrained water and two glass wool filters which trap larger particles. After this filtration the gas is introduced to a refrigeration system to cause any remaining water vapour to condense and be retained in the cooling unit. Upon exiting the cooling unit the gas stream is drawn through a much finer filter to remove any remaining entrained particles. A manifold then divides the gases between the three analyser units. Bypass flows allow a constant flow of the necessary amount of gas to be drawn by the analysers by venting any excess. Small rotameters on these bypass lines provide a visual check of the state of the gas analysis line - which are susceptible to blockage by moisture and/ or particles - and a way of ensuring gas flows during calibration are representative of those during operation.

An ABB URAS26 non-dispersive infrared (NDIR) unit simultaneously measures CO_2, CO

and SO_2. An Analysis Automation Limited analyser measures NO_x by chemiluminescence while exit [O_2] was established using an ABB Magnos27 thermomagnetic analyser. The exhaust lines from the analysis equipment are collected with the bypass line and then vented to atmosphere.

Calibration of analysers was carried out depending on the frequency of testing and how recent the previous calibration had occurred. Pilot tests suggested that overnight analyser drift could be considered negligible if the analysers remained switched on. Thus, a typical week would involve testing on Thursday and Friday of the week and in this situation calibration would be carried out each Thursday prior to beginning analysis with the analysers switched on overnight. If a break of testing was expected the analysers were turned off and would be calibrated again at the next test date.

The calibration procedure was carried out manually and only once the analysers had been given enough time to warm up and their uncalibrated measurements stabilise (typically 3 hours after turning on). All calibration gases were introduced individually through the sampling line after the two Dreschel bottle water traps in order to simulate the gas flow during testing as closely as possible. Oxygen-free nitrogen was used as the zero calibration gas for all analysers. The NO_x analyser requires manual calibration through turning a calibration dial whereas the ABB analysers require a set-point to be input and then calibrate themselves at that level. Once the analysers were calibrated with the zero gas the voltage signal sent to Labview was noted in order to perform signal calibration. For each analyser in turn a span gas representative of testing environments was introduced through the sampling line. The calibration of the analysers was then carried out at the span range in the same way as for the zero gas and the span range and corresponding voltage signal sent to Labview was recorded. Once the analyser calibrations were complete the signal calibrations were then conducted. This involved using the measurement amounts and corresponding voltages received by Labview to calculate the slope and intercept of the signal curve for each gas. Once each of these factors was calculated the Labview operation was stopped and the values in Labview were updated to reflect the new data. The Labview process and datalogging was then restarted with the new signal calibration factors in place.

Three span gases were used for the calibration: a mixture of CO, CO_2 and O_2 in N_2; a mixture of NO and NO_2 in N_2; and SO_2 in N_2. Although interaction is expected between

CO_2 and O_2 when measuring $[O_2]$ thermomagnetically, it was assumed that no interactive effects occur between the separate span gas mixtures. Noting the effect on $[O_2]$ of CO_2 a correction factor for O_2 measurement at elevated $[CO_2]$ was required. Rather than recalibrating the O_2 analyser every time high levels of CO_2 were expected (requiring a number of span gases to be held in stock) a correction factor was derived. For this work 3% O_2 (equivalent to an oxidant excess of 16% in air) in a range of $[CO_2]$ atmospheres was used to investigate interference on the O_2 analyser. As span gas concentrations are often used to calibrate multiple experimental rigs the relative concentrations occasionally change. In light of this rather than deriving a calibration factor for a single O_2-CO_2 calibration gas the factors at maximum and minimum $[CO_2]$ were derived. Linear interpolation could then be used to calculate the slope and intercept values for mixtures between these extremes. Simultaneous calibrations and measurements were made using a borrowed Servomex analyser that measures $[O_2]$ using the paramagnetic method and is not thought to be influenced by CO_2. The O_2 analysers were first calibrated at 3% O_2 in N_2. Once calibrated, a span gas at 3% O_2 and 10% CO_2 in N_2 was then introduced and the O_2 measurement was recorded. This was repeated for 3% O_2 with 40 and 70% CO_2 in N_2. The analysers were then calibrated using 3% O_2 with 70% CO_2 in N_2 and the $[O_2]$ at 40, 10 and 0 % CO_2 was then measured. From these tests a linear relationship between measured $[O_2]$ and $[CO_2]$ was observed as shown in Figure 3.14 where the gradient and intercept values for the correction curves are also shown.

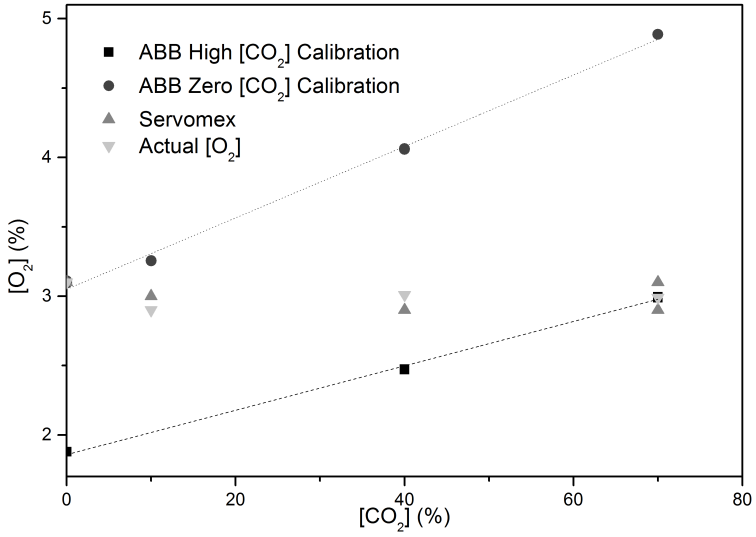

$[CO_2]$	l	c
0	0.0257	3.050
70	0.0160	1.858

Figure 3.14: Interference of CO_2 on O_2 measurements using ABB and Servomex analysers

3.4.4.3 Solid emissions

Fly ash is sampled from the flue box using a customised probe and cyclone arrangement that is connected to a vacuum pump with an intermediate water trap as shown in Figure 3.15. Measurements are taken over 15 to 20 minute periods with ash sampling over this period yielding approximately 1 g to 2 g of sample.

Ash samples are then analysed offline to calculate the Loss on Ignition (LOI) according to Equation (2.8). The value for LOI is then combined with the known ash content of the fuel mix m_{ash} in order to calculate the carbon burnout of the process as follows where m_{uc} represents the mass fraction of unburned combustibles in the ash and m_{tc} represents the mass fraction of total combustibles in fuel:

Noting: $LOI = m_{\text{uc}} / \left(m_{\text{uc}} + m_{\text{ash}}\right)$ and $m_{\text{tc}} = 1 - m_{\text{ash}}$

$$\begin{aligned} \text{Carbon burnout} &= 1 - \frac{m_{\text{uc}}}{m_{\text{tc}}} \\ &= 1 - \frac{m_{\text{uc}}}{m_{\text{tc}}} \times \frac{m_{\text{ash}} / \left(m_{\text{uc}} + m_{\text{ash}}\right)}{m_{\text{ash}} / \left(m_{\text{uc}} + m_{\text{ash}}\right)} \\ &= 1 - \frac{m_{\text{ash}}}{1 - m_{\text{ash}}} \times \frac{LOI}{1 - LOI} \end{aligned} \tag{3.8}$$

Further analysis was also carried out to determine the content of selected ash samples using Energy-Dispersive X-Ray (EDX) analysis which was coupled to the SEM equipment and using X-Ray Fluorescence (XRF) analysis conducted at the University of Leicester. Both EDX and XRF operate by subjecting a sample to high-energy beam that causes the sample to absorb and then emit energy. Since each element releases energy in a characteristic way, the overall energy released from the sample can be analysed to identify which elements are present in the sample. The SEM analysis was carried out using a Oxford Instruments AZtecEnergy EDX system which allowed elemental mapping of samples while XRF allowed more precise quantification of the sample and was carried out analysing fusion bead samples using a PANalytical Axios-Advanced XRF spectrometer at the University of Leicester.

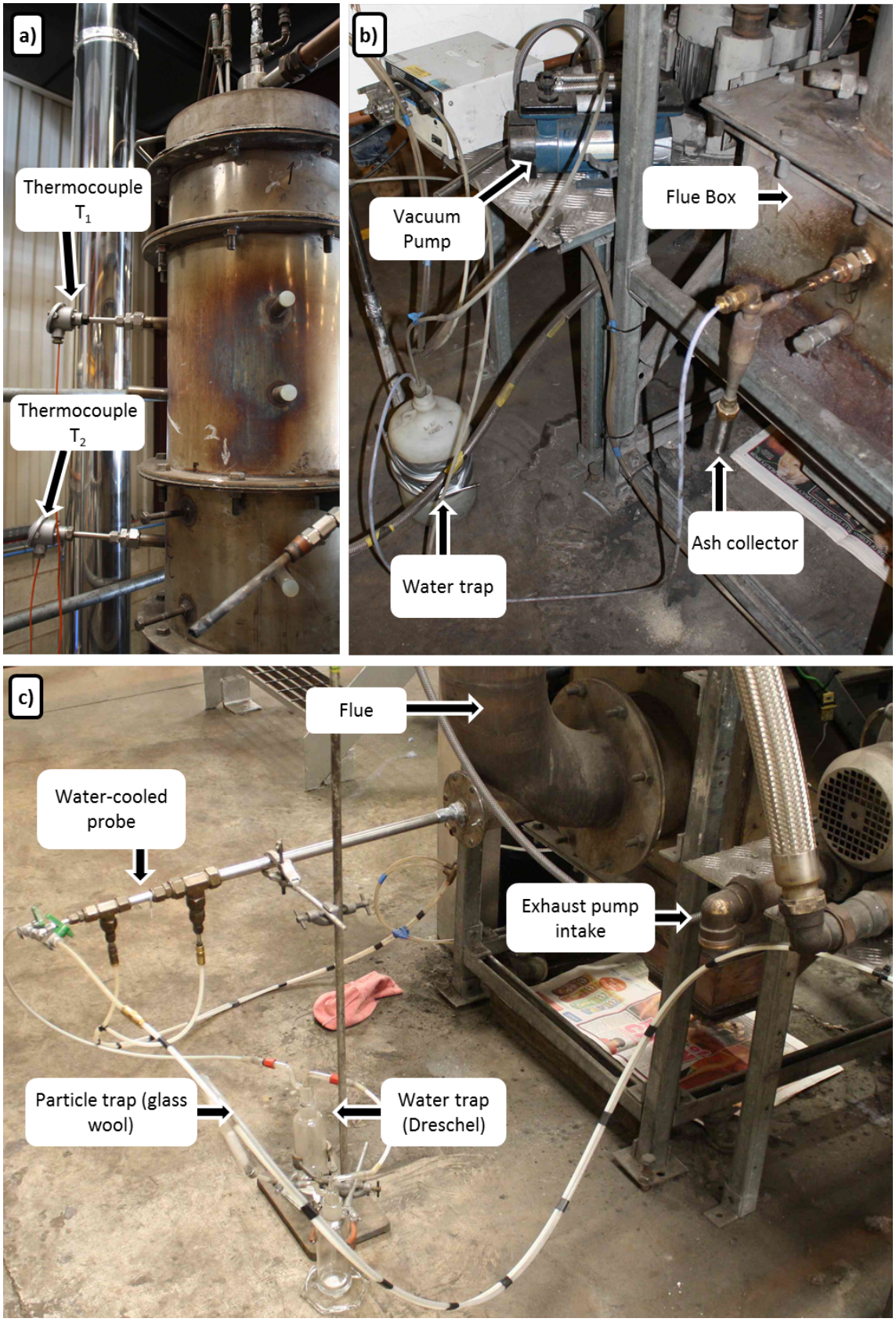

Figure 3.15: Sampling systems for (a) temperature, (b) ash and (c) flue gases

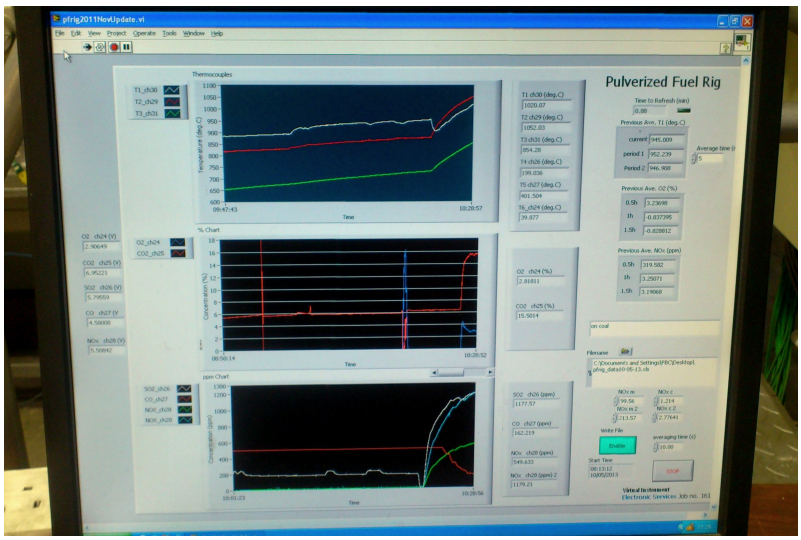

Figure 3.16: An example screenshot of Labview online data viewing showing the transition from gas to coal during rig start up. The top graph shows the temperature readings from thermocouples 1–3. The middle graph shows flue gas concentration in % of O_2 and CO_2 in %,. The bottom graph shows flue gas concentration of the lesser species NO, SO_2 and CO in ppm.

3.4.4.4 Data logging

All online measurements (temperatures and gaseous emissions) are connected to an data monitoring and logging system (LabView) and send voltage signals that are interpreted by a Data Acquisition (DAQ) device. A screenshot of a typical output is shown in Figure 3.16.

3.4.5 Estimating entrainment

For safe operation the furnace is operated at a slightly negative pressure. This leads to entrained air being drawn into the furnace at various points. Previous experience with the rig has indicated that the majority of the entrainment occurs through the primary line though damage to seals and deformation due to temperature stresses could lead to ingress between the separate furnace sections. In order to predict the required flow rates and outlet concentrations it is necessary to have a good approximation of this level of entrainment.

The first stage of the entrainment calculations is to calibrate the flue gas measurement system and ensure that the furnace has attained steady state while running on natural gas. Once complete the natural gas flow is set at a known value. From the combustion spreadsheet, the air requirement to deliver an excess of 15 % is calculated and from this

Table 3.3: Results from preliminary entrainment calculations

Stream	Test 1	Test 2	Test 3
Natural Gas ($L\,min^{-1}$)	28.7	28.7	28.7
Primary ($L\,min^{-1}$)	15.7	105.1	15.2
Secondary ($L\,min^{-1}$)	266.5	132.3	265.3
Total ($L\,min^{-1}$)	**282.2**	**237.4**	**280.5**

the target concentrations of O_2 and CO_2 are predicted. Then, maintaining a nominal primary flow (just enough to prevent backflow of natural gas) the secondary air flow is increased until the target concentrations are met. Once this reading has stabilised and the secondary flow rate has been noted, the second phase begins. The primary air flow is increased to $105\,L\,min^{-1}$; the value of this flow during testing which is assumed to be constant to ensure pneumatic conveyancing of the fuel in all tests. The secondary air flow is then decreased until the same target concentrations are realised. Once this has been attained, the first stage is repeated to check for hysteresis. The entrainment is calculated by subtracting the total known gas flow rate for the second test from the average total known gas flow rate from the first and third tests. The results of the entrainment calculation are presented in Table 3.3 where an entrainment of approximately $44\,L\,min^{-1}$ is found. During testing air is also entrained with the fuel feed, varying with fuel type and extent of blending. From comparing coal baseline data with these results it is estimated that a further $9\,L\,min^{-1}$ of air may enter the system in this way. Thus, an entrainment flow of $53\,L\,min^{-1}$ is assumed when calculating set flows for experimental design.

Experience of previous operators suggested the actual entrainment was found to vary on the rig and so during experiments the entrainment was calculated once on each day of testing. It was assumed that variation in entrainment was attributable only to ingress in the primary line. Once a stable coal baseline was reached, the gas flow rate through the secondary line was set to $\sim 230\,L\,min^{-1}$. The primary flow was then adjusted to give the correct flue gas concentrations. The deviation of the flow rate passing through the primary rotameter during this test and the original primary flow value ($105\,L\,min^{-1}$) was then found to be the practical entrainment. This was found to vary from 28–$63\,L\,min^{-1}$ with an average value of $42.2\,L\,min^{-1}$. A variety of reasons including ambient temperature, humidity, fuel blend, time between tests or seal damage on the rig may have been responsible for such variation.

Table 3.4: Typical combustion characteristics for baseline operation. The value presented is the average of the baseline readings with the corresponding standard deviation

Characteristic	Unit	Target	Value
Coal feed	$kg\,h^{-1}$	2.5	2.5
Primary air	$L\,min^{-1}$	105	110 ± 8
Entrained air	$L\,min^{-1}$	53	44 ± 11
Secondary air	$L\,min^{-1}$	230	229 ± 12
T_1	°C	1949[a]	1250 ± 24
T_2	°C	n/a	1241 ± 13
T_3	°C	n/a	1113 ± 13
O_2	%	2.96	2.94 ± 0.19
CO_2	%	15.82	15.63 ± 0.44
NO	ppmv	2882	818 ± 75
SO_2	ppmv	1549	1347 ± 50
CO	ppmv	0	32 ± 13

[a] Adiabatic flame temperature

3.4.6 Typical day of testing

A normal day of testing begins with lighting and warming up the rig using natural gas according the the start up procedure. Over the course of an hour the flow of natural gas and air into the furnace is steadily increased. Typically, after 60–90 minutes firing natural gas the temperature in the top sections of the furnace (T_1 and T_2) begins to approach 1000–1100 °C at which point coal is introduced to replace natural gas as the fuel. At least a further hour of warming is required before baseline data is sought which also allows the gas analysers to warm up, stabilise and be calibrated if not left on from the previous day. A steady baseline is established for at least 10 minutes prior to any testing in order to verify the correct operation of the rig. The baseline was unstaged coal firing in air at a 16 % excess and typical combustion characteristics for this are shown in Table 3.4. If the day's experiments use conditions far from the baseline - for example high levels of oxidant enrichment which lead to far higher temperatures near the burner - a second baseline is usually established at closer conditions and the data is compared to previously collected results. To conserve limited biomass reserves, baselines are carried out on coal only. For example, if a BBR of 20% RCG was to be fired in an oxygen-enriched air environment with oxidant staging, this setting would first be investigated on coal. Then, once combustion characteristics had stabilised, the BBR would be adjusted for the test.

Once the baseline has been established the parameters are changed to reflect the con-

ditions of the test which are calculated from the combustion spreadsheet in advance of testing. The predictive spreadsheet provides target flue gas concentrations and estimated inputs needed to achieve the conditions on the rig. However, the predictive spreadsheet is based on a series of simplifying assumptions and as a result the outputs are used only as a guide for the experiments. During experiments the exit gas concentrations - particularly O_2 and CO_2 - are used to monitor whether the correct level of combustion air is being introduced to satisfy the testing parameters. Real-time data is displayed in the Labview interface and steady state of measurements is established visually before sampling begins. The Labview interface was modified to display averaged values of T_1, O_2 and NO for the previous three 5-minute intervals. This allowed a quick check that steady state had been attained which can be difficult to observe from a continuous graph. Both the gas and ash sampling lines are purged prior to taking measurements. Typically measurements last for 20–30 minutes and conditions and points of interest are noted in the comments box in the Labview Interface which also appear on the output spreadsheet. Changes to conditions during sampling are largely avoided though it is occasionally necessary to make minor corrections during testing. If changes result in substantial deviations in the results the test is abandoned and restarted once steady state has again been attained. Following a successful test, the conditions are changed to another set of parameters and steady state is again sought. The sampling lines are again purged prior to the commencement of the next test. A successful day of testing may yield 4–6 sets of results which then require further processing.

After the final test of the day a closing baseline is established to check whether any underlying changes have occurred during the day's testing. Following this the fuel supply is shut off and the air flow through the furnace is increased in order to promote faster cooling of the rig. The gas sampling lines and analysers are purged with compressed air to remove debris and condensed water that may have accumulated through the day. Once temperatures in the flue box have fallen below 110 °C, the rig is considered safe to leave to cool down unattended as detailed in the shut down procedure.

3.4.7 Biomass blending ratio (BBR)

For consistency, the experimental design aims to maintain the thermal rating of the furnace at the level seen during the coal baseline (19.7 kW). So, for given blending ratios

Table 3.5: Mass fraction for each biomass at three BBR settings and the thermal input achievable at 100% BBR with the feeder running at full capacity

Setting	SRC	MC	RCG
BBR = 8%$_{th}$			
Biomass mass fraction (%)	12.3	12.2	13.5
Biomass mass flow (kg h^{-1})	0.322	0.318	0.359
Total fuel flow (kg h^{-1})	2.622	2.618	2.659
BBR = 15%$_{th}$			
Biomass mass fraction (%)	22.1	21.9	24.0
Biomass mass flow (kg h^{-1})	0.604	0.597	0.673
Total fuel flow (kg h^{-1})	2.729	2.722	2.798
BBR = 20%$_{th}$			
Biomass mass fraction (%)	28.7	28.5	31.0
Biomass mass flow (kg h^{-1})	0.805	0.796	0.897
Total fuel flow (kg h^{-1})	2.805	2.796	2.897
BBR = 100%$_{th}$			
Biomass mass flow (kg h^{-1})	3.500	3.981	4.485
Biomass screw setting	Max	46.9	31.8
Thermal rating (kW)	17.1	19.7	19.7

the amount of coal required decreases with increasing biomass usage. A spreadsheet uses the linear fit shown in Figure 3.12 and the NCV values shown in Table 3.1 to calculate the screw setting to deliver the correct mass flow of coal and biomass feeders for a given blending ratio. BBR of 8, 15 and 20% on a thermal basis were investigated in this work. Tests at 100% biomass were also investigated though for the only biomass with sufficient reserves to fire at 100% (SRC) the biomass feeder was unable to maintain the thermal input of the coal. The mass fraction for each biomass for each BBR is shown in Table 3.5 where the thermal input for 100% BBR at full biomass feeder screw rate is also shown.

3.4.8 Calculating gas flows

Gas flows for each experiment are calculated by a series of steps using a predictive spreadsheet. The process can be understood as follows. The BBR and mass flow rate from the previous section are taken as the starting point to ensure that each experiment maintains a constant thermal input of 19.7 kW. Then the composition by mass of the fuel blend is calculated using the ultimate analysis results in Table 3.1 and the fuel input is then

converted to a molar basis. Using the following equations it is then possible to calculate the total amount of oxygen required for stoichiometric combustion where all reactions are assumed to proceed to completion and are limited by the non-oxygen species.

$$\mathrm{C} + 2\mathrm{O} \rightarrow \mathrm{CO_2} \tag{3.9}$$

$$2\mathrm{H} + \mathrm{O} \rightarrow \mathrm{H_2O} \tag{3.10}$$

$$\mathrm{N} + \mathrm{O} \rightarrow \mathrm{NO} \tag{3.11}$$

$$\mathrm{S} + 2\mathrm{O} \rightarrow \mathrm{SO_2} \tag{3.12}$$

The theoretical molar oxygen requirement ($\sum n_{\mathrm{O},t}$) is then given by the composition of C,H,N,S and O in the fuel.

$$\sum n_{\mathrm{O},t} = 2n_{\mathrm{C},f} + \frac{1}{2}n_{\mathrm{H},f} + n_{\mathrm{N,f}} + 2n_{\mathrm{S},f} - n_{\mathrm{O},f} \tag{3.13}$$

The practical total amount of oxygen delivered as $\mathrm{O_2}$ ($n_{\mathrm{O_2},T}$) is then calculated from the theoretical oxygen requirement according to the excess oxidant to be supplied (XS, 16% in this study) according to the following relationship:

$$n_{\mathrm{O_2},T} = \frac{\sum n_{\mathrm{O},t}}{2} \times (1 + XS) \tag{3.14}$$

3.4.9 Oxidant staging

Increasing levels of oxidant staging are achieved by reducing the amount of oxygen delivered by the secondary stream while increasing the amount delivered by the tertiary (over-fired) stream. A mass balance indicated that the mass of oxygen diverted through the tertiary line was a function of the total required oxygen ($n_{\mathrm{O_2},T}$), the burner stoichiometric ratio (BSR) and the level of excess oxidant (XS). The first term is found from Equation (3.14) while BSR and XS are set by the experimental schedule. In order to calculate the amount of oxygen delivered by the tertiary flow ($n_{\mathrm{O_2},3}$) a mass balance of

the oxygen species entering the furnace is first completed:

$$\begin{aligned} n_{O_2,T} &= n_{O_2,e} + n_{O_2,1} + n_{O_2,2} + n_{O_2,3} \\ \therefore n_{O_2,3} &= n_{O_2,T} - (n_{O_2,e} + n_{O_2,1} + n_{O_2,2}) = N_3 \cdot x_{O_2,3} \end{aligned} \tag{3.15}$$

where the subscript e denotes the entrained flow and N represents the total volumetric flow for a stream.

BSR is defined as ratio of the amount of oxygen entering the burner (the sum of oxygen delivered by the entrained, primary and secondary flows) to the amount which is stoichiometrically required for combustion:

$$\begin{aligned} BSR &= \frac{n_{O_2,e} + n_{O_2,1} + n_{O_2,2}}{{}^{n_{O_2,T}}/_{1+XS}} \\ \therefore n_{O_2,e} + n_{O_2,1} + n_{O_2,2} &= \frac{n_{O_2,T} \cdot BSR}{1+XS} \end{aligned} \tag{3.16}$$

So substituting Equation (3.16) into Equation (3.15) yields:

$$\begin{aligned} n_{O_2,3} &= n_{O_2,T} - \frac{n_{O_2,T} \cdot BSR}{1+XS} \\ n_{O_2,3} &= n_{O_2,T}\left(1 - \frac{BSR}{1+XS}\right) \end{aligned} \tag{3.17}$$

For given values for XS and BSR, $n_{O_2,3}$ can then be calculated which permits calculation of all of the other streams for unenriched combustion since x_{O_2} is 21% for all streams. The table in Table 3.6 may then be completed using:

$$n_{O_2,2} = n_{O_2,T} - n_{O_2,e} - n_{O_2,1} - n_{O_2,3} \tag{3.18}$$

$$N_3 = {}^{n_{O_2,3}}/_{x_{O_2,3}} \tag{3.19}$$

$$N_2 = {}^{n_{O_2,2}}/_{x_{O_2,2}} \tag{3.20}$$

The actual inlet compositions are then calculated depending on whether N_2 or CO_2 is the dilution gas in the secondary and tertiary air streams.

3.4.10 Oxidant enrichment

The primary and entrainment feeds are considered to be a fixed flow of air (21% O_2) while both the flowrate and composition of the secondary and tertiary flows can be varied

Table 3.6: Demonstration of procedure to calculate inlet gas flows

Stream	**Stream total flow (N)**	**Stream O_2 flow (n_{O_2})**	**Steam O_2 concentration (x_{O_2})**
Unit	$L\,min^{-1}$ @ STP	$L\,min^{-1}$ @ STP	%
Entrainme	$N_e = 53$	$n_{O_2,e} = 11.13$	$x_{O_2,e} = 0.21$
Primary	$N_1 = 105$	$n_{O_2,1} = 22.05$	$x_{O_2,1} = 0.21$
Secondar	N_2	$n_{O_2,2}$	$x_{O_2,2}$
Tertiary	N_3	$n_{O_2,3}$	$x_{O_2,3}$
Total	$N_T = {}^{m_{O_2,T}}/_{x_{O_2,T}}$	$n_{O_2,T}$	$x_{O_2,T}$

as any mixture of O_2, CO_2 or air. Oxygen-enriched combustion was defined as referring to the total oxygen concentration entering the combustor and similar to much work in the literature was set at a value of 30%. Since the primary and entrained streams cannot be enriched, calculating flow rates for combustion with oxygen enriched streams requires an extra assumption to be made regarding how to enrich the secondary and tertiary streams. Initially an equal split of enrichment between the streams was considered so that $x_{O_2,2} = x_{O_2,3}$. However, the minimum measurable flow through the secondary rotameter is $\sim$25 $L\,min^{-1}$. Preliminary calculations suggested that for deep-staged oxygen-enriched cofiring (where according to the calculations more oxygen was 'available' from the biomass) the required air flow would be below this limit. Thus, the decision was taken to ensure the tertiary stream was enriched to a greater degree than the secondary stream thereby ensuring the flow of air was measurable on the rotameter. Rather than changing both the value of both $x_{O_2,2}$ and $x_{O_2,3}$ for every calculation a value of $x_{O_2,3} = 45\%$ was set as constant as this always ensured the secondary flow was less enriched than the tertiary. Through setting the value of $x_{O_2,3}$ the remaining unknowns in Table 3.6 can then be calculated as detailed in the previous section.

3.4.11 Prediction of outlet gas concentrations

Once the fuel and gas flows into the furnace are known the spreadsheet performs a simple mass balance across the furnace and from this produces a prediction of the outlet gas concentrations according to the reactions in Equations (3.9) to (3.12). The outlet gas concentrations are given on a volume basis and represent the relative molar concentrations of the gases. Both wet and dry targets are calculated. The concentrations of O_2 and CO_2 are the most important target concentrations and during experiments input parameters

are varied in order to approximate these as closely as possible. Targets for the baseline settings are shown alongside the averages of the results in Table 3.4.

3.4.12 Processing of results

Online data for each experimental run underwent a series of stages to ensure the data presented in the following section is representative of the experiments and comparable using a common framework.

3.4.12.1 Ensuring representative data

Once data had been collected and separated into individual tests it was visually and statistically inspected to assess whether the reported average well-represented the experimental period. Simultaneous plots of all online data allowed definition of steady state periods and also the identification of any significant deviations from the average values. If such deviations were found, a search of the comments log was then conducted to attempt to understand why the deviation may have occurred, for example if a fuel feeder cut out or a sample line became blocked and was purged with compressed air to clear the blockage. Periods of unsteady state (typically at the beginning of experimental runs) or explainable deviations were then removed from the data noting any adjustments in the comments section. The stability of the data was then assessed on the basis of the standard deviation values. Compared with the baseline of unstaged coal combustion in air, biomass cofiring, oxygen enrichment or oxidant staging typically increased the variability within an experiment and thus accepting or rejecting data was based on judgement from experience rather than a rigid acceptance value. Typically, during experiments standard deviations for temperatures were found to vary by no more than 10 K, for measurements of O_2 and CO_2 by no more than 0.3% and for measurements of SO_2 and NO by no more than 30 ppm though in occasional circumstances more variable data was permitted though in these cases the variability was typically less than 5% of the averaged reported value.

3.4.12.2 Ensuring fair comparisons

In order to discuss results fairly it was necessary to compare data using a standard framework. This was considered in two ways. First, variations in results due to the experimental

design were accounted for and then variation of external factors between experiments is addressed.

3.4.12.3 Controlling for variation due to experimental design

Gaseous emissions are measured as volume fraction of the bulk exhaust gas. Thus, changes to this volume would affect the apparent emissions reported for NO and SO_2. For air-firing this dilution effect is normally negated by reporting an emissions value corrected to 6% [O_2] in the flue gas using Equation (3.21) which uses NO as an example.

In this work the flue gas volume may also be reduced due to both the amount of biomass being blended (due to its contributing a higher oxygen content to the fuel blend) and due to oxygen enrichment of the combustion atmosphere. To correct for this the measurement is multiplied by the ratio of the delivered gas volume for that experiment (N_{exp}) to that delivered during air firing (N_{air}). Presenting results on a volume basis was preferred here due to current reporting practices and legislation and for easier comparison with the published literature. However, as oxygen-enriched combustion and oxyfuel combustion develop it is suggested that mass of emissions per unit of energy generated would be a better metric to account for the reduced flue gas volumes and increased concentrations due to flue gas recycling.

$$\text{NO}_{6\%\text{O}_2\text{ in air}} = \text{NO}_{\text{O}_2,\text{measured}} \times \frac{21-6}{21-\text{O}_{2,\text{measured}}} \times \frac{N_{\text{exp}}}{N_{\text{air}}} \tag{3.21}$$

3.4.12.4 Controlling for variation due to external factors

As will be shown in the following section, variation also exists between experiments due to changes in ambient conditions, such as air temperature, density and humidity, and experimental conditions such as air entrainment. In order to quantify the effects of changes to the combustion system it is useful to compare experimental results with baseline values. However, variation in the baseline values may serve to convolute this data if all data were to be compared to a single baseline value. Instead, as well as reporting actual values, to take account of external variability between experimental days, results in the following section are also normalised to the baseline values for that day of testing. For gaseous emissions this also has the effect of reducing the error associated with the measurement

as noted in Section 3.4.13.2.

3.4.13 Baseline characterisation

Establishing a baseline (control) set of of results is essential for evaluating the effects variation in experimental parameters brings. As part of each day's experimental schedule an opening set of baseline data was recorded and for most testing days a closing baseline was also conducted to ensure there had been no significant changes to the combustion set up throughout the day's testing. Although mitigating measures are taken where possible, unlike small-scale experiments pilot-scale testing involves accounting for many parameters that are outside of the control of the experimenter. For this reason, a small amount of variation in baseline data was to be expected since the experiments detailed in this work spanned a period of nearly two years. It would be unpractical to continually retest and recalibrate all of the measurement equipment so several assumptions, detailed below, were made regarding accuracy and consistency.

3.4.13.1 Assumptions

i) Having calibrated the coal feeder as described in Section 3.4.2, at a given feeder screw setting the feed rate of coal is constant so long as the coal level in lower hopper is maintained at a consistent level as monitored by a marked dip-stick.

ii) The majority of entrained air enters through the the primary port and any entrained air that leaks in elsewhere does so at a constant rate. Thus, since the primary flow is constant throughout the testing procedure, the amount of entrained air may vary between days of experiments but during a single day it is assumed to be constant. For every day of testing the actual entrainment is calculated using the procedure in Section 3.4.5.

iii) The compressor and humidifier together provide a primary air stream of constant temperature and humidity thus the inputs for the predictive calculations in Sections 3.4.8, 3.4.9 and 3.4.11 are not varied between experiments.

In light of the assumptions a coal input of $2.5\,\mathrm{kg\,h^{-1}}$ (equating to 19.7 kW net thermal basis) was established as the only fixed input for the furnace. Variation of the primary and secondary gas flows were then carried out in order to result in a flue gas $[O_2] \simeq 3.0\%$ and

[CO_2] $\simeq 15.8\%$ on a dry basis as designated as the baseline in Table 3.4. These critical parameters were set to ensure consistent thermal input and operation of the furnace at $\approx$ 16 % excess air when the temperatures reported by thermocouples T_1, T_2 and T_3 had stabilised.

3.4.13.2 Errors and variation in results

As noted in the previous section, variation in measurements can be viewed in two ways: variation during measurement of each experimental baseline and variation between the averaged baselines for different testing days. Errors may also affect the reporting of results. Tables 3.7 and 3.8 show the results of attempting to identify and quantify the errors due to observation and accuracy of measurement equipment along with a comparison of this to the magnitude of typical baseline values. Comparing this data with the variability ranges for the baseline in Table 3.4 suggests that measurement errors are substantially smaller than variation between experiments due to external factors though similar to variability within experiments. This is illustrated for the furnace temperatures in Figure 3.17 where the grey shaded area shows the variation in the data between tests alongside variability during tests.

The total error (Err_{tot}) in a given value (X) is calculated from the individual errors according to Equations (3.22) and (3.23) based on the general formula for error propagation. The errors identified in Table 3.7 are used with these equations to calculate the errors in raw data presented in Table 3.8. For emissions of NO and SO_2 corrected to 6% [O_2] the error was calculated as $\pm$ 7.4%. For gaseous emission results that are normalised in order to reduce variability, the error associated with the calibration gas is negated since the same error is present in the measurement and the daily baseline and that the error manifests as a proportional shift in the calibration curve in the measurement device. Thus, for results normalised to the daily baseline, only the two errors arising from accuracy of the measurement device to measure the concentration is included which results in an error calculated as $\pm$ 1.4%.

For additional errors that are independent of other measurements:

$$Err_{tot} = \sqrt{Err_1^2 + Err_2^2 + Err_3^2 + \dots} \tag{3.22}$$

Table 3.7: Sources of measurement error [ABB, 2009, Omega, 2013, Signal, 2010]

Measurement	Source of Error	Error	Percentage of Baseline Value
Rotameters	Float movement and measurement by eye	1 minor graduation	$\leq$ 5% measured value
Thermocouples	Measurement accuracy	0.25% R-type, 0.75 % K-type	
Analyser calibration gases	Rate accuracy (certified)	$\leq$ 5% full scale	
NO, SO_2, CO & CO_2	Measurement accuracy	$\leq$ 1% calibration span	
O_2	Measurement accuracy	$\leq$ 2% calibration span	
Coal Feed Rate	Feeder variations	$\leq$ 5% measurement	
Biomass Feed Rate	Feeder variations	$\leq$ 10% measurement for very low BBR, typically $\leq$ 5%	
Balance (for LOI and burnout calculations)	Balance accuracy	$\pm$0.000 05 g	0.26%

For multiplication and division of errors (as used in normalising against other values):

$$Err_{tot} = X \times \sqrt{\left(\frac{Err_1}{X_1}^2\right) + \left(\frac{Err_2}{X_2}^2\right) + \left(\frac{Err_3}{X_3}^2\right) + \dots} \tag{3.23}$$

As noted in Section 3.4.12.4, it is useful to compare experimental data to the coal baseline data though it is useful to appreciate the variability in the baseline data. In the results in this chapter where data is presented in its raw form the following conventions are used:

- a grey band illustrates the variability in the baseline data
- points on a graph represent the arithmetic mean for a given experimental result, averaged over the data collection period
- error bars attached to points represent calculated error where the error depends on the measurement value
- in some cases where the error is independent of the measured value or where the change in error is negligible across the measured values a maximum error is included on the graph which aids in clarity of presentation.

Table 3.8: Comparison of estimated errors, variation during experiments and variation between experiments for baseline conditions for raw experimental data

Measurement	Baseline Value	Maximum Estimated Error	Variation during experiment	Variation between experiments
Gas flow	380 L min^{-1}	19 L min^{-1}	N/A	11 L min^{-1} [a]
T_1	1250 °C	2.5 °C	5.2 °C	24.0 °C
T_2	1241 °C	2.5 °C	2.5 °C	12.8 °C
T_3	1113 °C	2.8 °C	2.8 °C	12.9 °C
O_2	2.94 %	0.16 %	0.18 %	0.19 %
CO_2	15.63 %	0.82 %	0.20 %	0.44 %
SO_2	1119 ppmv[b]	83 ppmv[b]	17 ppmv[b]	42 ppmv[b]
NO	679 ppmv[b]	50 ppmv[b]	18 ppmv[b]	61 ppmv[b]
CO	32 ppmv[b]	2.4 ppmv[b]	4 ppmv[b]	13 ppmv[b]
Burnout	99.51%	0.001%	NA	0.10%

[a]Entrainment; [b]at 6% O_2

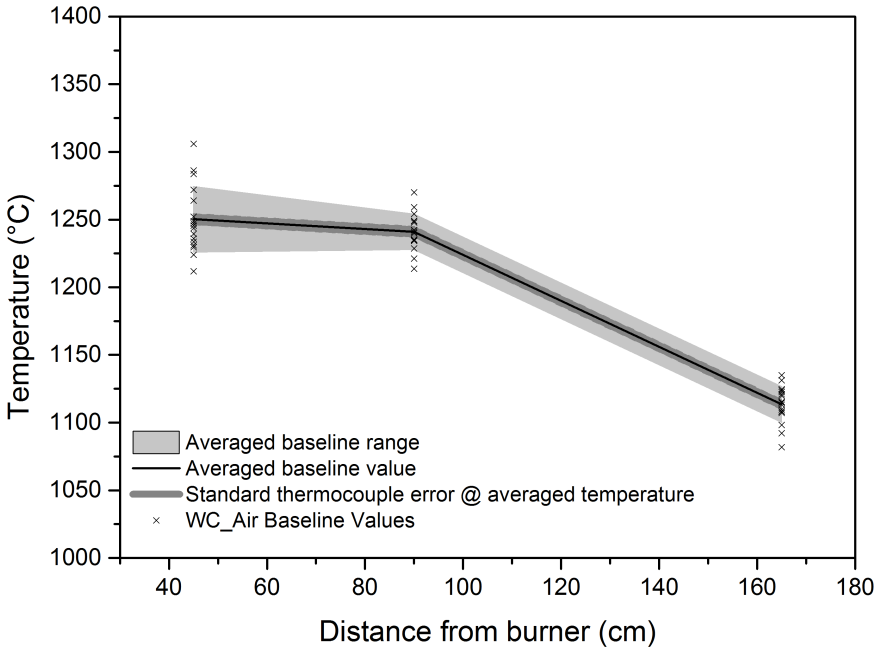

Figure 3.17: Axial furnace temperature profile for coal (WC) baseline at 20kW Unstaged, Un-Enriched Conditions. The crosses show data points, the grey light gray section shows standard deviation of the averaged baseline values (the black line), the darker gray shading represents the error associated with standard thermocouples at that temperature

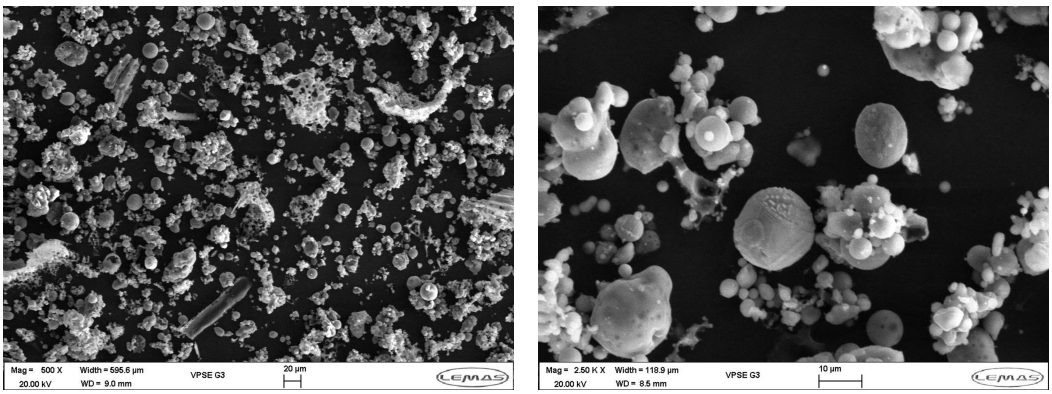

Figure 3.18: SEM images of ash collected from baseline experiments at 500x and 2500x magnification

3.4.13.3 Ash analysis

As well as analysing the ash using loss on ignition calculations to calculate the carbon burnout, selected ash samples were also further analysed according to the procedures detailed in Section 3.4.4.3. Ash morphology was analysed using SEM imaging. These images were coupled with EDX analysis to create elemental maps of samples and some selected samples underwent XRF analysis in order to quantify the oxide content of the ash samples. These quantifications are then used to calculated the fouling propensity of the ashes using the equations for Alkali Index and Base-to-Acid ratio given in Sections 2.3.3.1 and 2.3.3.2. SEM images of typical baseline ash is presented in Figure 3.18 while Figure 3.19 shows EDX elemental mapping for the sample. The XRF analysis of baseline is presented with results for other ashes in Figure 6.12.

The SEM images shown in Figure 3.18 illustrate that the coal ash particles tend to form a mixture of sizes of spherical particles with many of the smaller particles aggregating together or on the surface of larger particles. The lower magnification image suggest that as well as ash particles the sample contains several non-spherical particles which are thought to be either dust fragments present in the air during sampling or particles of refractory lining that have become detached during firing as occasionally larger particles of this type were also identified in the ash sample.

The EDX element maps of the ash samples presented in Figure 3.19 illustrate that particles exhibiting different morphologies also may contain different elements. The vast majority of the sample consists of oxides with aluminum and silicon being the most common elements. Potassium and titanium are also widely distributed, though appear less intensely than Si and Al with the Ti signal less intense than that for K. Some of the particles also ap-

pear to contain relatively high concentrations of iron, calcium and sulphur with the latter two being found together suggesting capture of S by Ca.

3.4.14 Summary

This chapter has provided the necessary detail for experimental techniques, fuel characterisation and baseline data in order to analyse and discuss the experimental results in the following chapters.

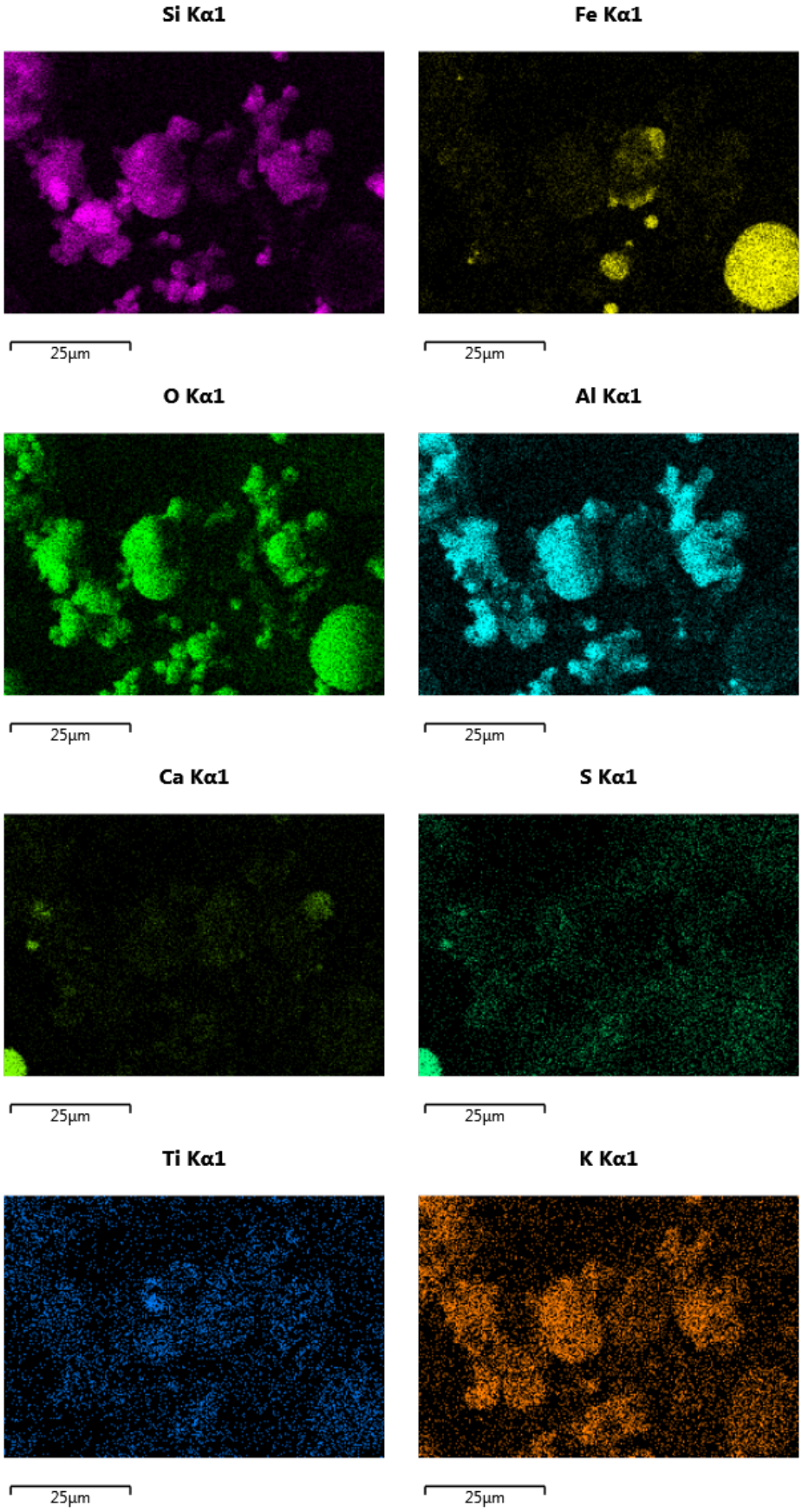

Figure 3.19: EDX mapping of elements present in ash collected from baseline experiments

Chapter 4

Development of a TGA Reactivity Assessment Methodology

4.1 Chapter overview

The work in this chapter was borne out of a need to rapidly and economically assess the probable effects on reactivity of combusting a variety of fuels in a variety of atmospheres in order to help explain the results presented in Chapter 6. The research matrix for this series included four biomasses and one coal burning in four different combustion atmospheres at two different heating rates, thus an expensive set of characterisations was not feasible. Instead a robust method was needed to estimate with relative confidence the effect of altering the reaction atmosphere on the decomposition of each of these fuels. Analysis of published literature suggested the use of the Coats-Redfern technique would be best able to provide reactivity data using a minimal number of heating rates. However, available methods and published literature contained little detail on application of the Coats-Redfern method to parallel reactions which has resulted in a range of 'kinetic data' reported for similar samples. In investigating the method and answering the first research question in Section 2.9, this chapter highlights that for graphical methods, such as those proposed by Coats and Redfern, a temperature range which the linear fit is made across is essential in providing robustness of the data. A simple method of overcoming the compensation effect is presented before it is demonstrated that while the square of the Pearson product moment correlation coefficient (r^2) is necessary for the data fitting section, to provide an overview of the whole reaction it is equally useful to provide the

correlation between collected data and that reconstructed from predicted reactivity parameters.

In this work, the initial case examines the effect of smoothing and how subjective curve fitting can affect the estimated parameters. The work is then extended to include a decomposition consisting of two independent parallel reactions with minor overlap and finally a decomposition that includes three reactions with substantial overlap. Finally, having established the method is able to estimate the kinetic parameters for the idealised data, the procedures are applied to experimental results from biomass decomposition tests, comparing the reactivity of short rotation coppiced willow (SRC) and shea meal (SM) in two oxidising atmospheres. The results indicate that as long as pseudo-reactions within the decomposition data can be identified, the method is able to extract the reactivity parameters for the decompositions with high confidence.

4.2 Research need

Although originally, and often still, used to characterise single reactions, at some point the method of estimating kinetic parameters from TGA was applied to fuels, despite fuels exhibiting more complex behaviour. Much reported research claims to estimate with a relatively high degree of accuracy, kinetic rates of decomposition for complex fuels decomposing due to a range of parallel and series reactions. There are several reasons why the technique continues to be popular, notable among them being that few other options exist for characterisation; that despite limited scientific precedent, the characterisation appears to be applicable to some degree; and equally a lack of guidance in the academic literature to extend guidelines for simple extraction of TGA-derived data for single reactions to more complex decompositions comprised of parallel reactions. In addition, despite the availability of clear methods for, and the limitations of, extracting rate constants from TGA data, non-adherence is common in the research community. It is unfortunate that many examples exist in which 'kinetic rates' are extracted from TGA data which cannot claim to model precisely the reactions they are attempting to characterise perhaps explaining: "*the rampant inconsistencies in published biomass kinetic data*" [White et al., 2011]. It is believed researchers working with complex reactions (such as pyrolysis or combustion of multi-component fuels) will continue to use TGA data since it offers rapid, indicative results rendering it particularly useful for comparative studies. Thus, a formalisation of

the procedure which is difficult to find in the literature is reported herein. The availability of several comprehensive works which detail the procedure for individual reactions [ASTM, 2007, Vyazovkin et al., 2011, White et al., 2011] and recent work by Moukhina [2012] identifying mechanisms for decompositions due to series and parallel reactions is acknowledged. In this work, the methods explained and collected therein have been extended to demonstrate applicability to parallel reactions in the decomposition of complex fuels.

Isoconversional methods such as the Kissinger-Akira-Sunose [Akahira and Sunose, 1971, Kissinger, 1957] and Flynn-Wall-Ozawa [Flynn and Wall, 1966, Ozawa, 1965] methods may provide more accurate rate parameter estimates but at the cost of at least three temperature ramp rates [Starink, 2003, White et al., 2011]. Equally, the development of distributed activation energy models (DAEM) and extensive curve-fitting techniques have been employed elsewhere in an attempt to further increase the accuracy of predicting pyrolysis and oxidative reactions of fuels with varying degrees of success [Hillier et al., 2010, Saloojee, 2011, Shen et al., 2011, Várhegyi et al., 2009, Varhegyi et al., 2012, Zhang et al., 2009]. In short, it is acknowledged that a considerable amount of work exists that aims to extract rate parameters for reactivity analysis from TGA data. However, while other methods are reported to display marginal increases in accuracy, this is invariably at the cost of at least three heating rates or the application of relatively complex solver techniques. Dissimilar to work which can actively employ the TGA results in modelling studies, it is noted that while rate data extracted from TGA experiments show correlation with larger scale combustion [Davini et al., 1996], the orders of magnitude difference in heating rate predicate that any extrapolations can only be qualitative [Gil et al., 2012*c*]. Furthermore, it is widely accepted that the 'rate' data extracted from TGA devices is dependent on the experiment and so it is felt that TGA results should realistically only be used for comparison within the confines of an experiment and not compared with external data as to extrapolate further would be beyond the limitations of the procedure. Thus, for comparative work between experiments with various fuels and atmospheres emphasis is placed on rapid, indicative techniques which are more likely to be useful to industry and screening of fuels by assessing trends rather than providing data which may be precise by not strictly relevant to actual combustion. Since the use of TGA-derived data in accurately predicting full-scale combustion is qualitative in nature, it is felt methods which involve substantial extra effort (either by repeated experiments or through complex curve

fitting) are difficult to justify. In summary, this chapter does not intend to duplicate available literature which details the potential for pitfalls during TGA studies. Instead, it aims to provide a method which can sit within the guidance provided by standards, which is powerful, rapid, traceable and therefore useful. It is also noted that for a non-specialist TGA literature can be misleading and contradictory and so this work attempts to provide a method for which those who adopt it clearly understand the inherent limitations.

Providing estimates for rate data using only a minimal number of heating rates restricted the choice of method for analysing reactivity to either the Coats-Redfern or the Friedman methods. In their work comparing several methods of estimating kinetic variables from TGA data Pérez-Maqueda et al. [2005] concluded that integral methods are preferred over those of a derivative nature due to avoiding noise produced in derivative versions. In addition, the Coats-Redfern analysis was observed to display the smallest error across experimental ranges and is thus chosen as the basis for developing a procedure here.

Rather than a completely new method, the following work details a rigorous procedure for applying the Coats-Redfern technique to parallel reactions. The procedure also includes robust reporting of an increased amount of experimental data used for comparisons between experiments. At present, data reporting is often lacking in literature where in some cases it has become common practice to omit reporting of the pre-exponential constant in the Arrhenius equation. Moreover, even where reported, this important parameter is rarely used in discussions regarding comparisons of reactivity which are normally reduced solely to the activation energy. This approach could prove erroneous as compensation effects between the kinetic triplet derived from a single experimental set up may not yield a unique solution for any of the individual parameters [White et al., 2011]. Similarly, although the standard methods detail the application of graphical methods to single reactions, how such methods are applied and reported in the literature is less clear. The following method creates a robust procedure to identify and distinguish between parallel reactions which is fully traceable with the above increase in reported data.

4.3 Method Development

Idealised and experimental data are used to develop and test the method which is the focus of this chapter. Experimental data was generated according to methods detailed in

Chapter 3. Idealised data involves artificial construction of mass and DTG curves from known kinetic parameters, which allows the accuracy of the method to be tested. Having introduced the method of generating idealised data, the outputs of which are then used in the majority of this chapter, the process of identification of reaction zones is then included. The effects of curve fitting, data smoothing and overlapping data are all discussed in the following sections.

4.3.1 Experimental data

Experimental data for this work was generated according to the procedure detailed in Section 3.3.2. Results from experimental work using two biomass samples - short rotation coppiced willow (SRC) and shea meal (SM) - decomposing in two combustion atmospheres - air (21% [O_2] in N_2) and oxygen-enriched air (30% [O_2] in N_2) - were used to test the model during development. Experiments of each combination of sample and combustion environment was conducted at heating rates (β) of 10 and 40 $\mathrm{K\,min^{-1}}$.

4.3.2 Idealised data

Throughout this section recommendations are made regarding how TGA data should be treated. Similar to the work of Hillier et al. [2010], as a basis for these recommendations an idealised set of TGA results has been created that aims to test the method and illustrate the potential problems and errors associated with data processing. For simplicity, the initial case assumes a single, irreversible, first order reaction described by the Arrhenius relationship that consumes all of the solid reactant. This concept is then extended to include two and then three non-competitive parallel reactions in the decomposition with a differing extent of overlap between reactions. A heating rate (β) of 1 $\mathrm{K\,s^{-1}}$ is assumed and mass remaining at each time-step (M_i) is calculated according to the following equations. Each pre-exponential activity coefficient and activation energy is considered to remain constant across the relatively narrow temperature range of each reaction. The parameters used in the idealised reactions are presented in Table 4.1.

4.3.3 Arrhenius model

The general Arrhenius equation (shown previously in Equation (2.16)) is shown for individual components in Equation (4.1). Equation (4.2) demonstrates how during decomposition the remaining reactant mass (M_i) is calculated at each time-step for the idealised and reconstructed datasets. The model assumes a solid fuel of total mass M decomposes according to a number (θ) of independent, non-competitive, first-order reactions on constituent reactants (m_a). The reaction rate constant (k_a) and according decomposition of each reactant is calculated according the temperature (T) at each time-step (i) and the results are summed to give the overall mass at that time-step (M_i). The calculated values are then substituted into the next time-step's calculation to calculate the progress of the reaction with increasing temperature.

$$k_{a,i} = A_a e^{\frac{-E_{A,a}}{RT_i}} \tag{4.1}$$

$$M_i = \sum_{a=1}^{a=\theta} [m_{a,i-1} - k_{a,i} m_{a,i-1}] \tag{4.2}$$

where

- k is the rate constant
- a denotes the reaction number k and m are related to
- i is the time-step

Table 4.1: Rate parameters for generating idealised TGA data

Reaction (a)	m_i	$E_{A,i}$ (kJ mol^{-1})	ln(A_i)
1 Reaction Decomposition			
1	1.00	100	15.2
2 Reaction Decomposition			
1	0.25	100	15.2
2	0.75	120	13.8
3 Reaction Decomposition			
1	0.10	135	23.9
2	0.15	190	32.0
3	0.75	110	13.0

- A is the pre-exponential constant
- E_A is the activation energy
- R is the universal gas constant
- T is the absolute temperature
- θ is the number of reactions occurring in the decomposition (1 - 3 in the following examples)
- m_a is the mass of reactant decomposing in reaction a, the sum of which (M) is the total mass decomposing.

4.3.4 Identifying reactions and leading edges

One of the biggest problems with using the Coats-Redfern technique to analyse TGA data from fuel decompositions is that single reactions often cannot be isolated from the overall decomposition. Indeed from the derivative thermogram (DTG) graphs presented throughout this work it can be seen that the rising edge of the tail of initial reactions often overlap with the falling leg of the onset of a subsequent reaction. Thus, it is necessary to investigate how well the kinetic parameters may be estimated using only a small part of the data.

In this work identifying reactions is completed by adopting the following method where it is assumed that all decompositions comprise of non-competitive, first-order reactions obeying Arrhenius laws. The following procedure is demonstrated with the 3-reaction decomposition illustrated in Figure 4.1.

Starting from the top left of the DTG graph the horizontal line (L_1) is drawn at the tangent to the zero line. The tangent to the leading edge of the first reaction (L_2) is then drawn and extended to ensure it will cross L_1 and L_3. The start of the first reaction is defined as the point where the bisecting line through the intersection of L_1 and L_2 meets the DTG curve (A). The leading edge of reaction 1 (B-C) is the section of the tangent L_2 that is in contact with the DTG. Since the first and second reaction in this case overlap significantly, a shoulder is formed in the DTG curve. Here, a line of best fit is drawn to the shoulder zone (L_3) which is extended to ensure it intersects L_2 and will intersect L_4. The tangent to the leading edge for the second reaction (L_4) is then drawn and extended to ensure

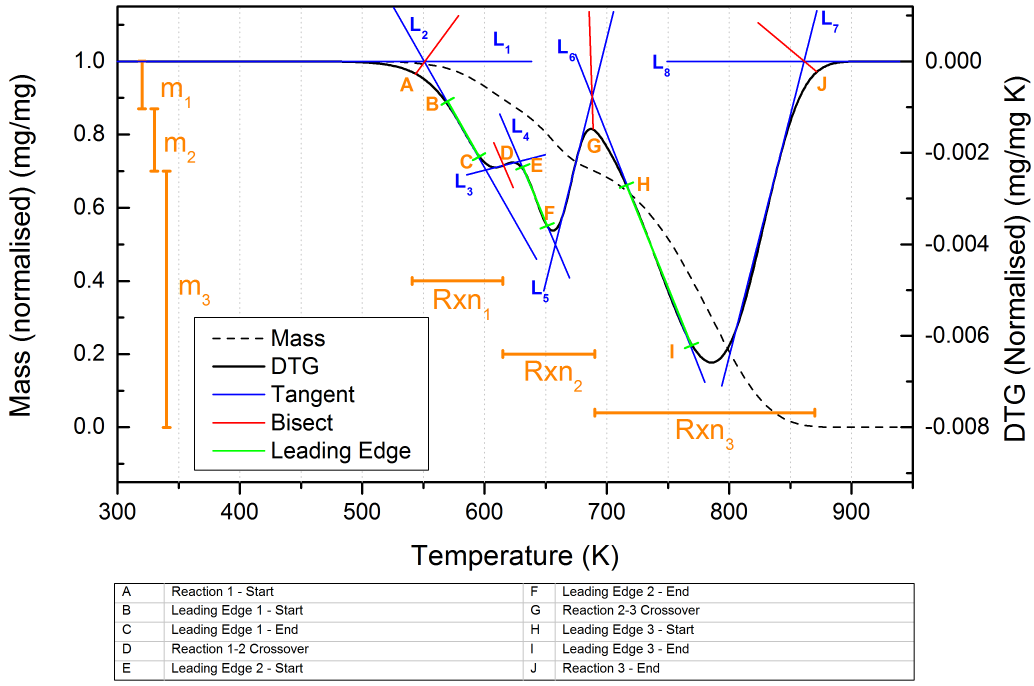

A	Reaction 1 - Start	F	Leading Edge 2 - End
B	Leading Edge 1 - Start	G	Reaction 2-3 Crossover
C	Leading Edge 1 - End	H	Leading Edge 3 - Start
D	Reaction 1-2 Crossover	I	Leading Edge 3 - End
E	Leading Edge 2 - Start	J	Reaction 3 - End

Figure 4.1: An example of the graphical procedure for identifying reactions from DTG data using idealised three-reaction decomposition as an example

it intersects L_3. The crossover point between reactions 1 and 2 (D) is determined as the midpoint of the line between where L_3 intersects L_2 and L_4. The leading edge of reaction 2 (E-F) is the section of the tangent L_4 that is in contact with the DTG. To determine the crossover between reactions 2 and 3 the tangents to the trailing edge of reaction 2 (L_5) and the leading edge of reaction 3 (L_6) are drawn and extended to ensure they intersect. The crossover between reactions 2 and 3 is defined as the point where the bisecting line through the intersection of L_5 and L_6 meets the DTG curve (G). The leading edge of reaction 3 (H-I) is the section of the tangent L_6 that is in contact with the DTG. To determine the end of reaction 3 the tangents to the trailing edge of reaction 3 (L_7) and the final zero line (L_8) are drawn and extended to ensure they intersect. The end of reaction 3 is defined as the point where the bisecting line through the intersection of L_7 and L_8 meets the DTG curve (J).

4.3.5 Assigning reactions compositional mass

When reconstructing decompositions comprising parallel reactions, as will be performed later, it is necessary to estimate the fraction of the total mass consumed by each reaction.

If experiments are conducted under different heating rates the temperature ranges which the reactions occur across may change. However, at the heating rates which can be studied in TGA devices and within the tolerance of experimental errors, the mass loss due to each reaction should be similar at different heating rates for most cases of interest. Thus, as well as providing data for reconstruction, this additional procedure builds confidence that data is being compared between experiments fairly. The mass attributed to each reaction is derived from the change in mass within temperature ranges of the reactions calculated in the previous section.

4.3.6 Applying the Coats-Redfern procedure

For each reaction the Coats-Redfern procedure is then applied as detailed in Section 2.8.4.3. Assuming all reactions follow first-order kinetics this involves calculating the extent of reaction ($\alpha = {}^{m_0 - m_i}/_{m_0 - m_f}$) and then plotting $\ln\left(-\ln\left(1-\alpha\right)/T^2\right)$ against $1/T$. The the slope of the line is then $-E_A/R$ and the intercept equal to $\ln\left(AR/\beta E_A\right)$.

4.3.7 Method evaluation by reconstruction

In the literature the robustness and accuracy of the Coats-Redfern method at predicting kinetic parameters is often described by linearity of the Coats-Redfern plot or a section of it. In order to test the accuracy of the technique presented here it is more useful to reconstruct the entire mass and DTG curves (since these are the focus of the method). To do this, the estimated values for activation energy, pre-exponential constant and mass fraction for each reaction within a decomposition are substituted into Equations (4.1) and (4.2) to generate mass and DTG curves which can be directly compared to the original data, a process similar to work in biomass pyrolysis [Grønli et al., 2002, Skreiberg et al., 2011, Várhegyi et al., 2009]. Although useful for the researcher, it would be impractical to provide a graph of every plot in a publication, so the square of the Pearson product moment correlation coefficient (r^2) between the initial and the reconstructed data for the mass loss and DTG profiles is instead calculated. This procedure protects against false-confidence in the data which could occur if the Coats-Redfern plot, or a section of it, was highly linear but not necessarily appropriate for the reaction. Also, if sufficient data is provided (temperature range, mass loss, activation energy, pre-exponential constant and order of reaction for each reaction) the mass and DTG profiles may be reconstructed

using Equations (4.1) and (4.2) to a degree of accuracy provided by the correlation coefficient. This is not possible with the majority of data available in the literature which either provides an overall activation energy encompassing several decomposition reactions or, alternatively, individual reactivity parameters without the constituent masses consumed by each reaction within the decomposition. It is believed the approach in this work is considerably different to much combustion literature which only reports the linear fit to the Coats-Redfern plot.

It is important to note that the comparison of the data should only be carried out in the region of the reaction and the original data should be normalised to this range since the method focusses on each reaction separately. Any temperature range included where no reaction is occurring will artificially boost the value of r^2. Equally, if other reactions are occurring outside of the studied reaction zone, such as the continued mass loss seen in biomass ashes, this will not have a detrimental effect on the coefficient.

4.3.8 Overcoming the compensation effect

The existence of the compensation effect, as detailed in Section 2.8.7, suggests that the output of this model should be only compared qualitatively with TGA data already in the literature since when using a graphical technique to estimate a function, especially when a degree of freedom such as the order of reaction being modelled is fixed, a numerical output of the model cannot be viewed singularly. In short, although widely practised, it is judged that comparison of activation energies alone is insufficient to describe relative reactivities and can even be misleading. For example, a more reactive decomposition may be represented by a higher activation energy than a less reactive decomposition so long as the pre-exponential constant is sufficiently higher than that of the less reactive case. Since in this method the order of reaction is fixed to unity, the model output only requires evaluation of two terms. This allows reactivity comparisons to be simply completed by normalising the reactivity to a reference case value for activation energy ($E_{A,0}$) and pre-exponential function (A_0). Once the reference case is established, the following simple equation can be used to discern the reactivity of a fuel relative to the reference case (S_i).

$$S_i = 1 - \frac{E_{A,i}/E_{A,0}}{\ln A_i/\ln A_0} \tag{4.3}$$

where if

- $S_i < 0$ then the reaction is less reactive than the reference case
- $S_i = 0$ then the reaction and the reference case are equally reactive
- $S_i > 0$ then the reaction is more reactive than the reference case

To provide a basis for comparison for the trends presented by any variation found in S_i, the temperature at which maximum rate of reaction ($T_{\text{max},i}$) for each reaction was also calcuated. This was then normalised to the reference case ($T_{\text{max},0}$) to indicate a change in reactivity as $\delta T_{max} = (T_{\text{max},0} - T_{\text{max},i}) / T_{\text{max},0}$.

4.3.9 Model limitations

While the assumptions made in the above method are often valid for the oxidative and pyrolysis decomposition of some complex fuels, the limitations of the method stated should also be noted. As presented above the method cannot reliably evaluate reactivity for reactions that are not first-order or those reactions which are competitive, series or in any way interactive in nature.

4.4 Method testing

4.4.1 Effect of fitting range (one-reaction decomposition)

Simulated plots of the mass and DTG shown in Figure 4.2 generated by substituting the data in Table 4.1 into Equations (4.1) and (4.2) for a decomposition comprising a single reaction were analysed according to the procedure. The Coats-Redfern plot for this example is shown in Figure 4.3. In order to investigate the usefulness of fitting data to the leading edge of the reaction, the figure also shows the fitting ranges that are used to produce the parameter estimates displayed in Figure 4.4. Here, although the α value is calculated for the entire reaction, the range of data the Coats-Redfern line is fitted to is varied as the lines of best fit are fitted to all the data, the central 90, 80 and 60 % of the data and the leading edge respectively. From this it can be concluded that the 'tail' of the Coats-Redfern plot created at the start of reaction (which appears at the right in Figure 4.3 as the plot is against $1/T$) has the largest effect on the slope of the line and

therefore most distorts the parameter predictions arising from it. It is also clear that the estimated parameters are dependent on the amount of data fitted to. For example, reducing the fitting range from all of the data to 60 % reduces the values of activation energy predicted by approximately 10 % and reduces the value of logarithm of the pre-exponential constant from 19.7 to 16.7. The parameters estimated are then used to reconstruct the mass and DTG curves, the correlation between these curves and the original is presented as the unsmoothed data series in Figure 4.6. In this instance, due to the compensation effect detailed in Section 2.8.7, the Coats-Redfern method tends to overestimate both the activation energy and the pre-exponential factor emphasising the need for caution when comparing with reactivity data obtained by other methods. However, it can be confidently stated that relative to fitting to the entire dataset, a single-reaction decomposition may be well-estimated by simply fitting the Coats-Redfern line to the reaction's leading edge temperature interval.

4.4.2 Effect of smoothing (one-reaction decomposition)

During TGA, variability present in the results due to experimental variations and feedback loops that control the TGA device manifest as noise in the data. Despite being regularly employed, the amount to which data is smoothed to reduce this variability is rarely reported and is not mentioned in standard methods for extracting kinetics from TGA data. To analyse the effect of smoothing on the estimation of rate parameters a 10% random error as shown in Equation (4.4) is applied. Prior to undergoing the Coats-Redfern technique, various levels of smoothing are employed using a moving point average (Equation (4.5)).

$$M_i = \sum_{a=1}^{a=\theta} \left[m_{a,i-1} - (0.9 + 0.2 \times Z)\, k_{a,i} m_{a,i-1} \right] \tag{4.4}$$

where Z is a random number between 0 and 1 and the average mass $\bar{M}_t$ is given by

$$\bar{M}_t = \frac{\sum_{i=t-\tau}^{t+\tau} M_i}{2\tau + 1} \tag{4.5}$$

The idealised data with random noise along with an either-side smooth of 10, 20, and 50 points (τ) (respectively corresponding to 10%, 19% and 46% of the data for this reaction at this heating rate) are shown in Figure 4.5. Following the same data-fitting procedure

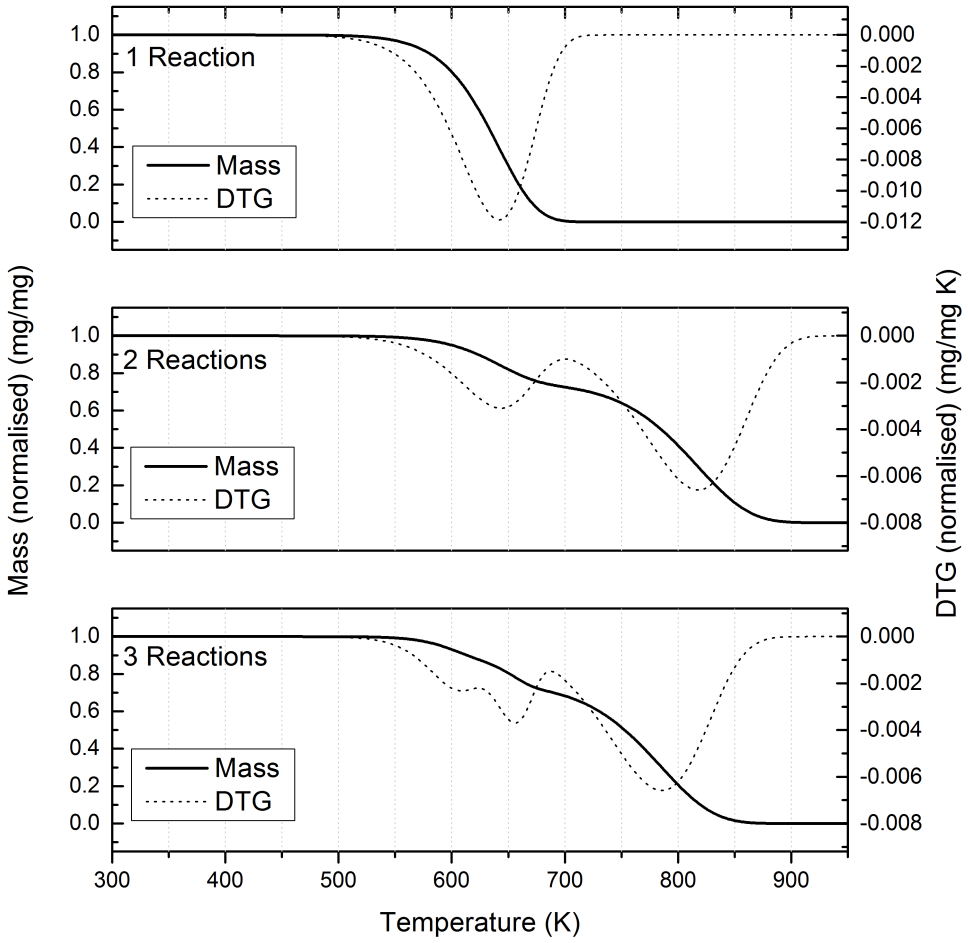

Figure 4.2: Idealised mass and DTG data for 1-, 2- and 3-reaction decompositions

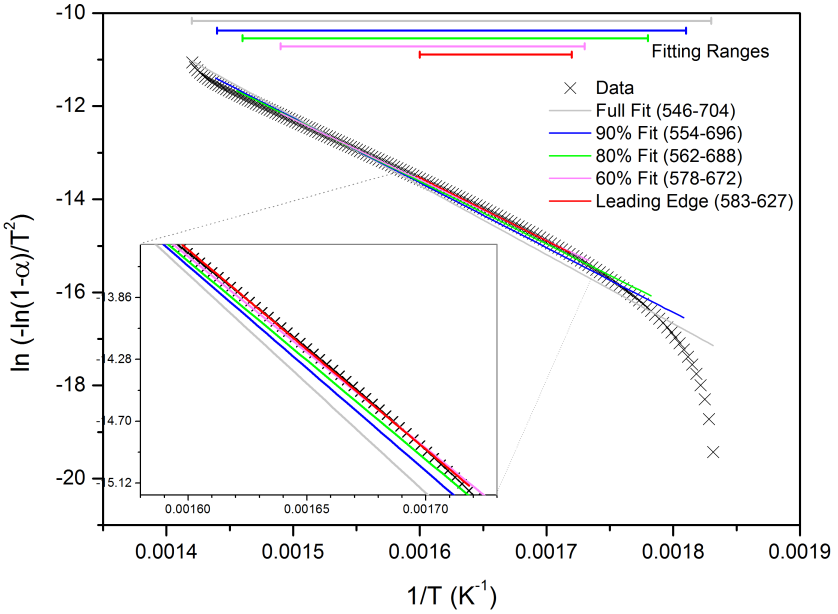

Figure 4.3: Coats-Redfern plot for dataset fitted to various proportions of the data

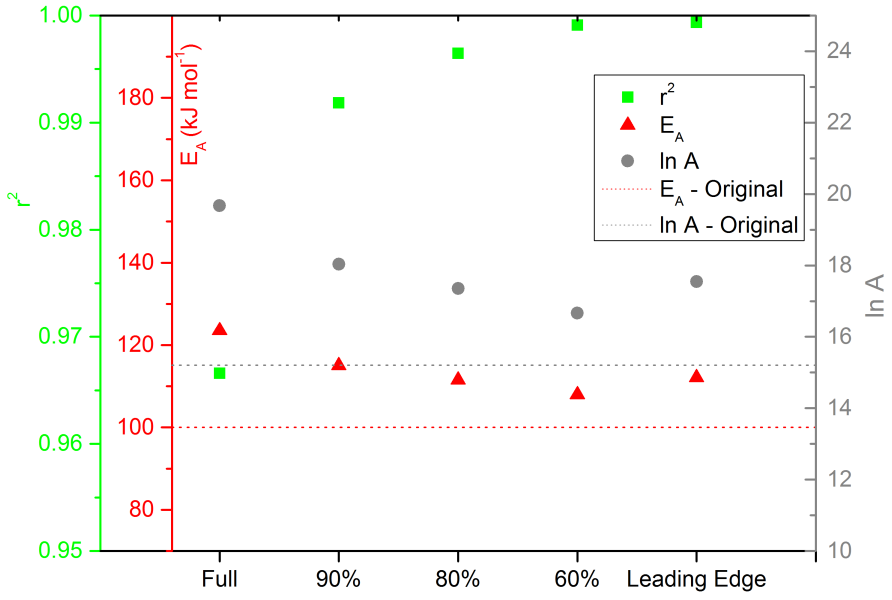

Figure 4.4: Effect of fitting width on Coats-Redfern parameter estimation

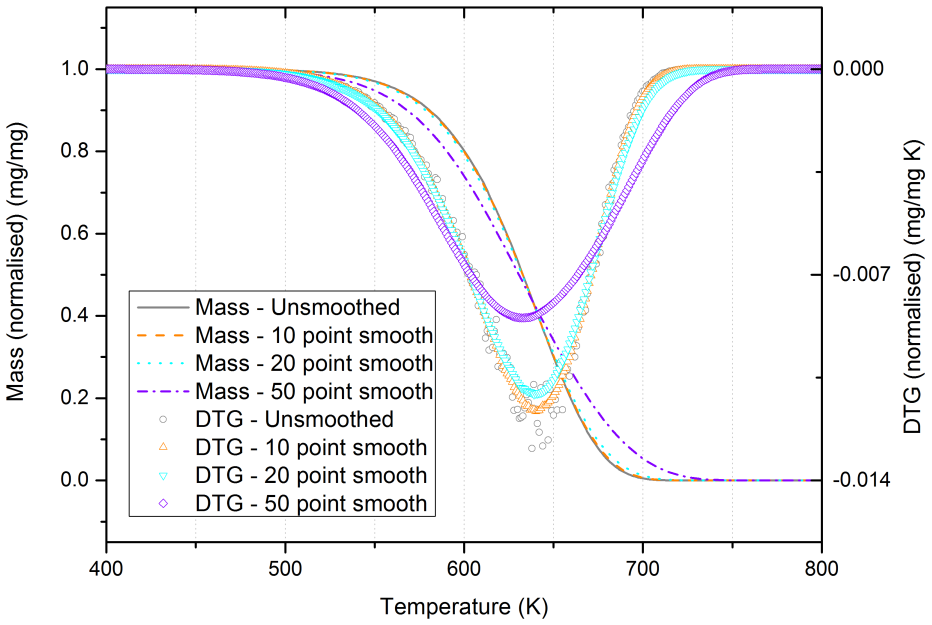

Figure 4.5: Effect of smoothing on mass and DTG data

employed without smoothing allowed parameter estimation and subsequent reconstruction of the mass and DTG curves. Comparing these reconstructed curves with the original data produced the results shown in Figure 4.6 where it is apparent that an increased degree of smoothing of the mass reading can have a substantial effect on not only the DTG profile but also the parameters that are predicted. Although focusing on the leading edge appears to lessen the impact of smoothing, it is suggested here that a small amount of smoothing may be employed to graphically identify reaction zones more easily, but that any smoothing causes the Coats-Redfern method's accuracy to diminish and as such if used should be reported with the data and should be kept to a minimum function of the dataset or, if possible, avoided completely.

4.4.3 Two-reaction decomposition with slight overlap

Having established that fitting the Coats-Redfern method only to the leading edge is able to estimate the rate parameters for one-reaction decomposition, it is now useful to simulate overlapping reactions as is the case in most fuel TGA data. This was completed by considering mass loss due to two non-competitive, parallel reactions that overlap slightly as presented by the data in Table 4.1 and shown in Figure 4.2.

Separating the decomposition into two reactions and then following the same procedure as

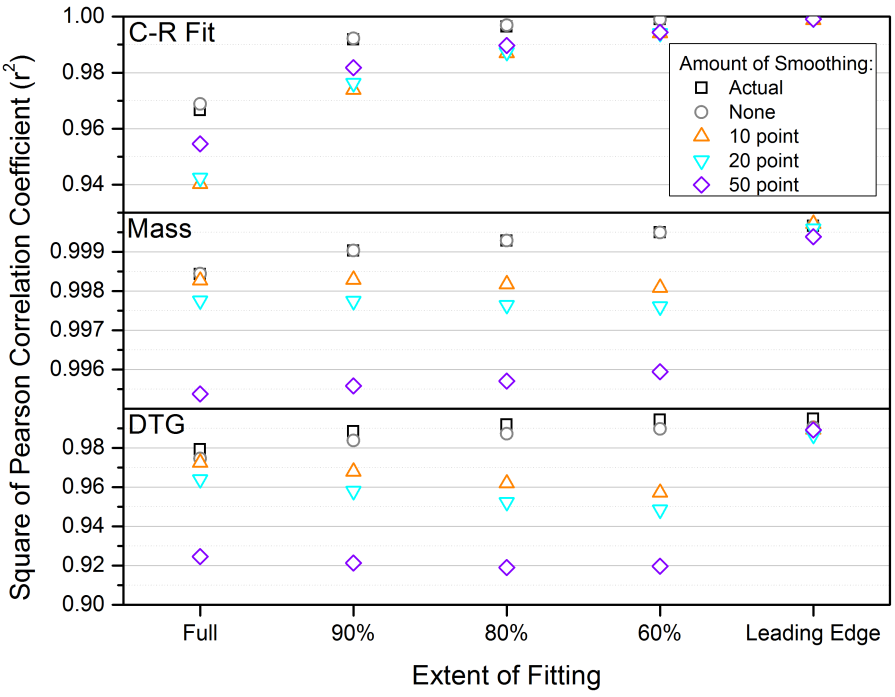

Figure 4.6: Variation in correlation between original data and that reconstructed by parameter estimation depending on level of smoothing performed prior to undergoing the Coats-Redfern procedure

for the single-reaction decomposition for each of the reactions, the estimates of parameters shown in Table 4.2 were derived where trends similar to those seen for the single-reaction decomposition were found. These figures indicate that modelling the leading edge using the Coats-Redfern technique is able to provide a relatively good approximation of the reactivity even when individual reactions cannot be fully resolved using graphical methods. In fact, in this case, the overlap acts to reduce the overestimation of parameters by the Coats-Redfern method compared to the single-reaction predictions. Using the results from the estimation procedure for the leading edge, the mass loss and DTG for the sample were reconstructed and compared with the original data displaying good agreement with r^2 values of 0.9990 and 0.9842 for correlation between the original and model-derived mass and DTG curves respectively. Figure 4.7 shows the reconstruction of the mass and DTG curves for estimates derived from fitting to the full range of data and just to the leading edge. Data fitted to the leading edge better captures the decomposition profile shown in the DTG which is reflected in the higher r^2 value.

Table 4.2: Estimated rate parameters for 2-reaction decomposition for varying widths of fit to the Coats-Redfern plot

	Full	90%	80%	60%	Leading Edge	Model
Reaction 1: (545 K to 704 K), Leading Edge (590 K to 630 K)						
$E_{A,i}$ (kJ mol^{-1})	119.0	111.8	107.0	104.2	108.3	100
ln(A$_i$)	18.60	17.20	16.28	15.78	16.64	15.20
CR Fit, r^2	0.9584	0.9842	0.9933	0.9978	0.9996	n/a
Reaction 2: (704 K to 903 K), Leading Edge (746 K to 793 K)						
$E_{A,i}$ (kJ mol^{-1})	152.9	142.9	136.7	132.0	143.8	120
ln(A$_i$)	18.68	17.17	16.24	15.53	17.46	13.81
CR Fit, r^2	0.9607	0.9881	0.9956	0.9988	0.9989	n/a
Correlation between original and reconstructed data:						
Mass, r^2	0.9970	0.9980	0.9985	0.9989	0.9990	n/a
DTG, r^2	0.9629	0.9745	0.9807	0.9855	0.9842	n/a

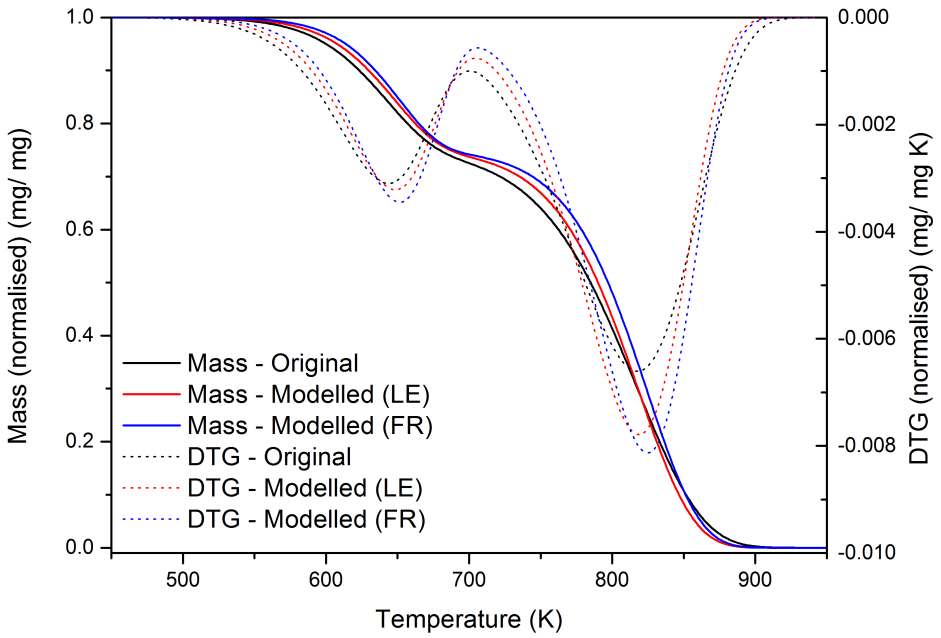

Figure 4.7: Mass and DTG curves for 2-reaction decomposition comparing original values with estimates based on full-range (FR) CR fit and fitting only to the leading edge (LE)

4.4.4 Three-reaction decomposition with overlap

Further extending the previous work, a scenario that involves two initial reactions with considerable overlap followed by a third reaction set mostly apart from the first two was simulated using the values in Table 4.1 which created the mass loss and DTG curves shown in Figure 4.2.

In this scenario, the three reactions were identified and following the same procedure as detailed previously the results shown in Table 4.3 were generated again displaying a similar trend to the single-reaction decomposition results (Figure 4.4). The plot in Figure 4.8 was generated for the values estimated from the leading edge temperature range. Similarly to the previous section, Figure 4.8 shows the reconstruction of the mass and DTG curves for estimates derived from fitting to the full range of data and just to the leading edge. The significant overlap between reactions in this example convolutes the data and reduces the ability of the method to accurately estimate single rate parameters. Data fitted to the leading edge again better captures the decomposition profile shown in the DTG which is reflected in the higher r^2 values of 0.9992 and 0.9597 for mass and DTG for the leading edge compared to 0.9984 and 0.9379 for full-range fitting. However, in this scenario Table 4.3 shows that fitting to 80% and 60% of the data derives estimates that perform slightly better than those generated from the leading edge. Despite the minor improvements from fitting to 60 or 80% of the data, the rigorous method for defining the fitting range detailed in Section 4.3.4 and the relative accuracy of the parameters derived permit the conclusion that fitting to the leading edge is shown to be a robust method for estimating reactivity parameters from TGA data containing overlapping, parallel reactions.

Table 4.3: Estimated rate parameters for 3-reaction decomposition for varying widths of fit to the Coats-Redfern plot

	Full	90%	80%	60%	Leading Edge	Model
Reaction 1: (537 K to 617 K), Leading Edge (570 K to 595 K)						
$E_{A,i}$ (kJ mol^{-1})	192.0	182.5	169.5	161.5	154.0	135
ln(A$_i$)	35.89	33.89	31.16	29.47	27.89	23.94
CR Fit, r^2	0.9628	0.9814	0.9948	0.9985	0.9999	n/a
Reaction 2: (617 K to 688 K), Leading Edge (635 K to 650 K)						
$E_{A,i}$ (kJ mol^{-1})	217.2	204.7	191.0	185.3	199.9	190
ln(A$_i$)	36.75	34.42	31.88	30.83	33.65	32
CR Fit, r^2	0.9486	0.9762	0.9930	0.9978	0.9995	n/a
Reaction 3: (688 K to 873 K), Leading Edge (720 K to 760 K)						
$E_{A,i}$ (kJ mol^{-1})	146.5	136.6	129.5	124.5	147.6	110
ln(A$_i$)	18.58	17.03	15.92	15.16	19.05	13
CR Fit, r^2	0.9529	0.9838	0.9941	0.9982	0.9977	n/a
Correlation between original and reconstructed data:						
Mass, r^2	0.9984	0.9990	0.9994	0.9995	0.9992	n/a
DTG, r^2	0.9379	0.9555	0.9682	0.9754	0.9597	n/a

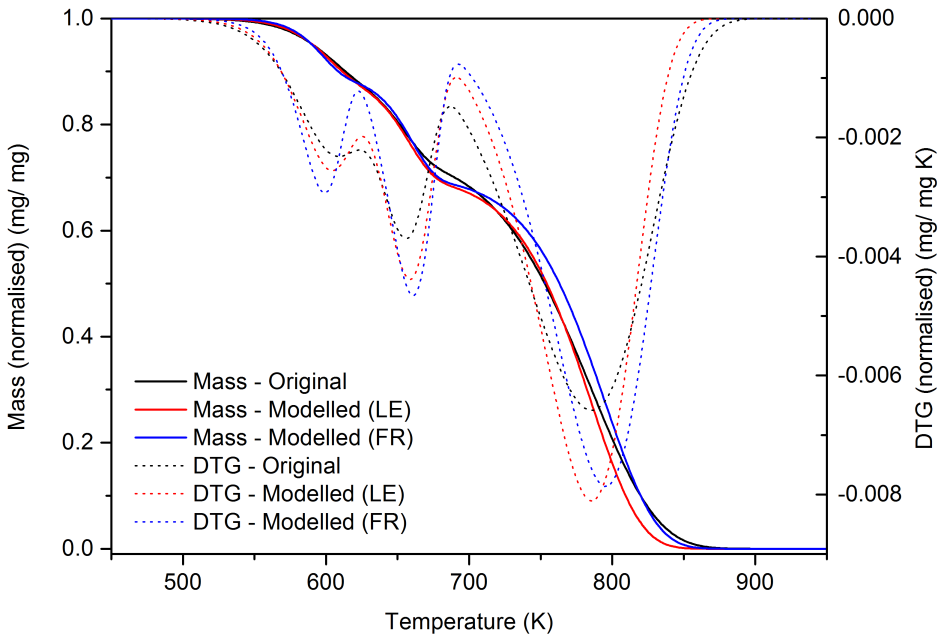

Figure 4.8: Mass and DTG curves for 3-reaction decomposition comparing original values with estimates based on full-range (FR) CR fit and fitting only to the leading edge (LE)

4.4.5 Testing the model with real data

From the collected data, the mass and its first derivative with respect to temperature were plotted in order to identify the reaction zones, leading edges and mass fraction per reaction which are presented in Table 4.4. Using this data, the Coats-Redfern procedure as detailed above was then applied for three identified reactions. An example plot for each of the three reactions along with the fitting range for the leading edge are shown in Figure 4.9 for SRC decomposing in air at a heating rate of $10\,\mathrm{K\,min^{-1}}$. Estimates for activation energies and the pre-exponential factors are presented in Table 4.4 for each reaction of the four decompositions studied. These parameters and the mass attributed to each reaction were then substituted into Equations (4.1) and (4.2) to reconstruct the mass and DTG profiles that are shown in Figure 4.10 for SRC and in Figure 4.11 for SM decomposing at $10\,\mathrm{K\,min^{-1}}$ in air in both cases. The reconstructed SRC data was generally found to correlate well with the experimental data across the reaction temperature range with r^2 typically greater than 0.997 and 0.842 for the mass and DTG curves respectively. However, the inability to identify distinct reaction zones for the SM sample rendered the model less able to predict this decomposition with r^2 values greater than 0.976 for the mass curve and in the region of 0.55 for the DTG curve. The relative reactivity (S_i) was then calculated using the air case at each heating rate as the reference case. The results shown in Figure 4.12 also include the normalised difference between the temperature at which maximum rate was found for each sample and the air case (δT_{max}). Comparing these two sets of results with the actual DTG profiles (Figures 4.13 and 4.14) it can be concluded that although the SM is relatively poorly characterised by the kinetic parameters (illustrated by the poor reconstruction correlation), the change in reactivity assessed by the procedure correlates well with changes in DTG. However, for the variation in the value of δT_{max} on unsmoothed data this is not the case as measurement noise can cause the maximum rate loss to be artificially predicted due to an outlier. Slight smoothing of the DTG data removes the outlier but has been shown also to affect the estimation of rate parameters. In this case, if smoothing is not employed it appears the model output (S_i) is a better indication of change in reactivity than δT_{max}. However, if δT_{max} is found from slightly smoothed data the changes in this value and S_i correlate well as the effect of noise on δT_{max} is avoided. Moreover, although comparison of the rate parameters with external data would be questionable, comparison with trends in reactivity assessed by S_i is possible even with decompositions that comprise overlapping reactions. For the SRC sample the

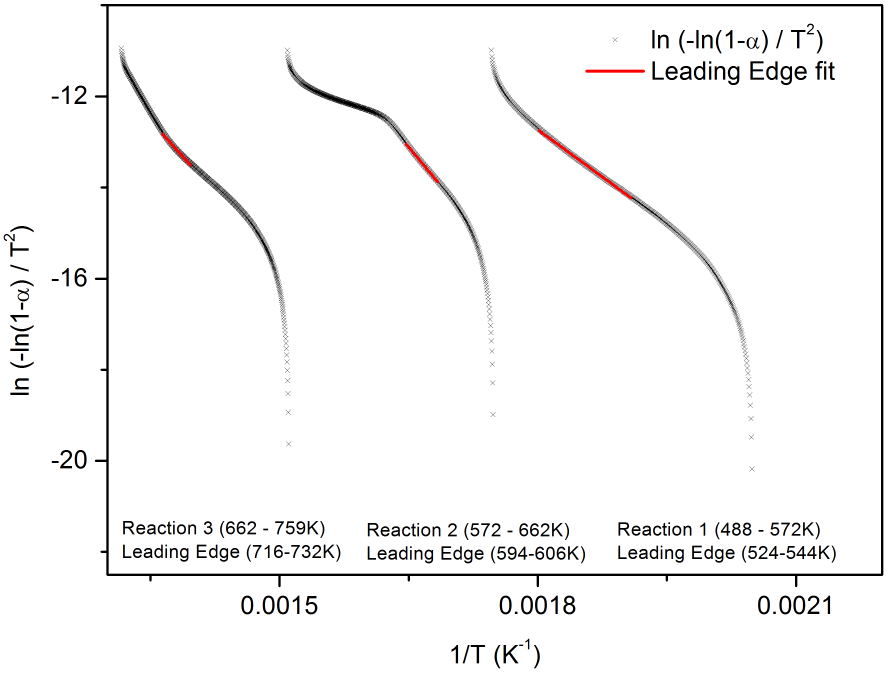

Figure 4.9: Coats-Redfern plots for SRC reacting in air at 10 K min^{-1}

trends for both S_i and unsmoothed δT_{max} correlate well.

4.4.6 Comparison of results with published literature

As the r^2 values suggest, the actual parameters generated by the Coats-Redfern technique may not necessarily well-reflect changes in reactivity when compared separately and may not well reflect the decomposition they are modelling when considered individually. For this reason it is felt only the trends found in reactivity and not the actual parameter values should be compared with wider literature.

The findings for both biomasses broadly indicate an overall increase in reactivity with an increase in oxygen concentration which is in agreement with published literature [Yuzbasi and Selçuk, 2011]. This is even the case for reactions where the activation energy increases, emphasising the need for comparison of activation energy and pre-exponential values together. Figure 4.12 also shows that relatively small differences in reactivity are seen for the first two (devolatilisation) reactions, which may even be considered negligible, while the reactivity during the final char oxidation reaction substantially benefits from the increase in oxygen concentration.

Table 4.4: Parameters derived for SRC and SM decomposition

O_2 (%)	β (K min^{-1})	Reaction Number (θ)	Reaction Range (K)	Leading Edge (K)	m_i	CR Fit (r^2)	E_{Ai} (kJ mol^{-1})	ln A_i	Mass Reconstruct (r^2)	DTG Reconstruct (r^2)	$T_{max,i}$ (K)
Willow (SRC)											
21	10	1	488–572	522–544	0.25	0.9992	114.7	19.85			572.9
21	10	2	572–662	594–606	0.51	0.9994	188.4	32.51	0.9977	0.8332	608.3
21	10	3	662–759	716–732	0.24	0.9946	173.7	23.83			734.0
21	40	1	510–594	546–576	0.23	0.9994	118.4	21.06			593.8
21	40	2	594–688	616–632	0.50	0.9999	175.8	29.90	0.9983	0.8809	633.6
21	40	3	688–808	756–774	0.26	0.9976	143.8	18.70			777.2
30	10	1	496–570	530–552	0.24	0.9996	124.7	22.15			569.6
30	10	2	570–660	592–604	0.53	0.9993	196.6	34.38	0.9970	0.8242	605.6
30	10	3	660–750	714–724	0.24	0.9962	196.8	28.05			724.0
30	40	1	514–594	548–576	0.24	0.9996	122.0	21.83			593.3
30	40	2	594–690	614–628	0.50	0.9998	178.6	30.49	0.9976	0.8895	632.1
30	40	3	690–794	746–766	0.25	0.9964	163.1	22.11			766.7
Shea Meal (SM)											
21	10	1	454–534	494–524	0.12	0.9975	100.3	18.38			530.2
21	10	2	534–686	548–578	0.55	0.9911	116.2	18.25	0.9766	0.4936	578.3
21	10	3	686–784	738–752	0.33	0.9914	208.8	28.47			757.4
21	40	1	462–554	503-540	0.14	0.9989	98.6	18.51			549.3
21	40	2	554–698	570–596	0.43	0.9932	119.4	19.56	0.9874	0.5912	606.6
21	40	3	698–868	760–788	0.44	0.9984	97.5	10.18			796.0
30	10	1	445–532	504–518	0.12	0.9985	101.8	18.85			532.3
30	10	2	532–685	548–578	0.57	0.9936	111.4	17.25	0.9797	0.5298	575.7
30	10	3	685–776	734–748	0.31	0.9925	218.1	30.31			750.3
30	40	1	460–554	500–540	0.14	0.9989	96.2	17.95			550.2
30	40	2	554–708	570-596	0.47	0.9936	117.9	19.19	0.9839	0.5829	601.3
30	40	3	708–842	758–776	0.39	0.9988	138.1	16.90			793.1

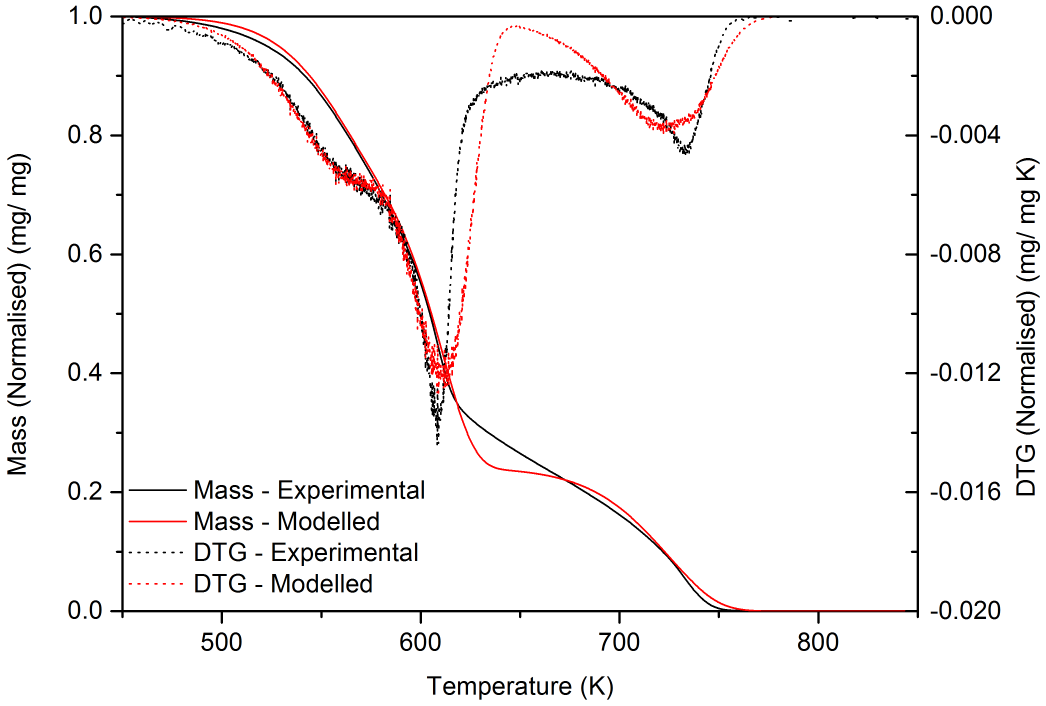

Figure 4.10: Comparison of experimentally derived and modelled mass and DTG data against temperature for SRC decomposing in air

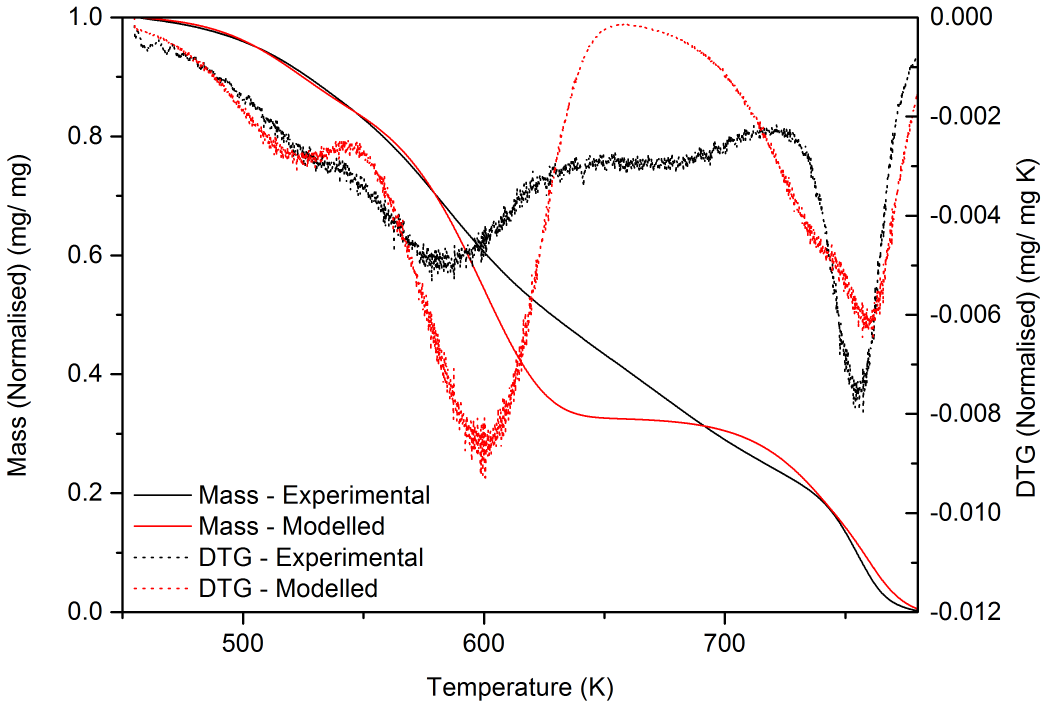

Figure 4.11: Comparison of experimentally derived and modelled mass and DTG data against temperature for SM decomposing in air

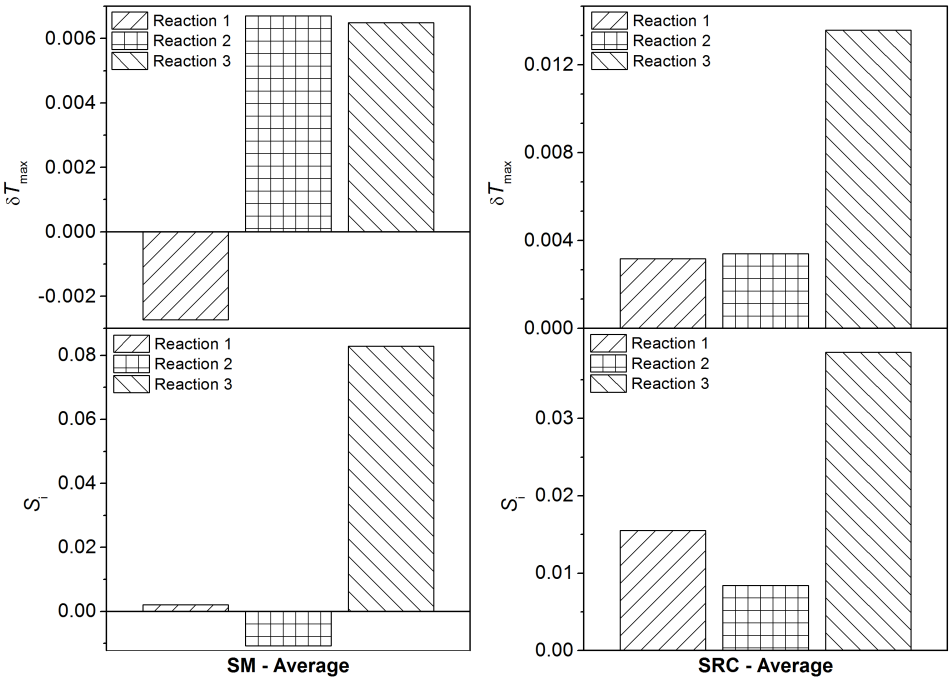

Figure 4.12: Reactivity (S_i) and change in maximum rate temperature (δT_{max}) of SRC and SM decomposing in oxygen-enriched air relative to air averaged between 10 and 40 K min^{-1} heating rates

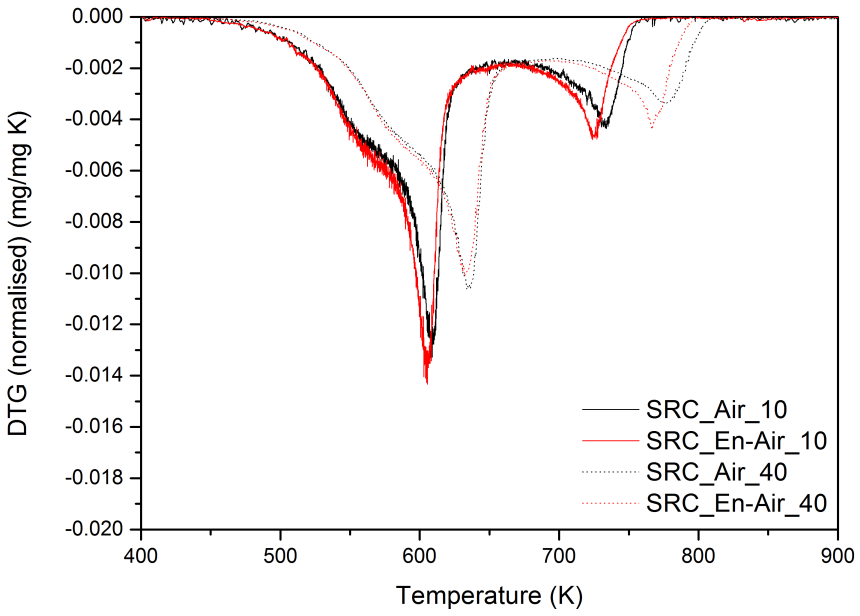

Figure 4.13: DTG against temperature for SRC decomposing in Air and oxygen-enriched air (En-Air) at 10 and 40 K min^{-1}

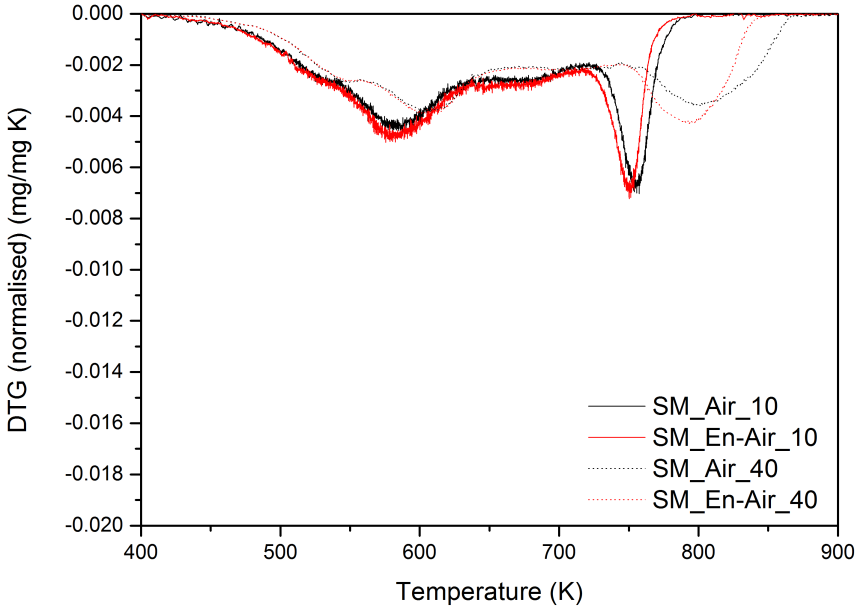

Figure 4.14: DTG against temperature for SM decomposing in Air and oxygen-enriched air (En-Air) at 10 and 40 K min^{-1}

4.5 Summary

The simple, rapid Coats-Redfern procedure which is widely used by academe and industry has been formalised and further developed. This method's ability to estimate rate parameters for overlapping, multi-reaction decompositions has been demonstrated by testing it on a variety of idealised decompositions where greater rigour in evaluating predictions against real data, and greater reporting of results than currently practiced is employed. The method was extensively tested using a theoretical idealised dataset to understand the effects of data treatment - such as data smoothing, the temperature range for the fit of the Coats-Redfern plot and a technique to overcome the compensation effect - and identification of reactions on the reactivity of the mixture of fuel and combustion atmosphere. The ability of the method to estimate reactivity parameters was judged based on the correlation between the original data and data recreated by substituting the predicted parameters in a multicomponent Arrhenius decomposition. The results suggested that data smoothing reduces the ability of the method to estimate reactivity parameters. Testing with mildly-overlapping parallel reactions illustrated that a fit of the Coats-Redfern plot to the leading edge of the reaction on the DTG plot was able to accurately predict the reactivity parameters of the total decomposition. The method's ability to identify changes in reactivity for real samples was demonstrated by comparing the decomposition of two biomass samples

in two combustion atmospheres. The model was found to characterise the decomposition of SRC well, while an inability to distinguish separate reactions in more complex SM rendered the method less able to characterise its decomposition. Nevertheless, changes in reactivity of the samples between the two combustion atmospheres were identified where the char reaction in particular was found to be more reactive in a combustion atmosphere with a higher oxygen concentration. More detailed analysis of the effects of O_2-enrichment on biomass combustion is one of the focuses of the following chapter.

Chapter 5

Bench-Scale Results and Discussion

5.1 Chapter overview

Reactivities of four biomass samples and one coal sample under thermal treatment were investigated in four combustion atmospheres by subjecting the samples to non-isothermal thermogravimetric analysis (TGA) under two heating rates. The combustion atmospheres were chosen to reflect carbon capture and storage applications and include oxygen-enriched air and oxyfuel combustion systems in order to inform the results generated from the 20 kW experiments in Chapter 6 and answer the second research question in Section 2.9. The standard Coats-Redfern method was applied to results from the coal samples alongside the extension of the standard Coats-Redfern method detailed in Chapter 4 which was applied to analyse changes in reactivity of the reaction stages involved in the decomposition of each of the biomasses. Although some variation was observed between the results, the overall trends suggest increasing oxygen concentration increases combustion reactivity and that in temperature-controlled TGA instruments substituting N_2 for CO_2 as the comburent has a modest benefit on combustion reactivity during oxygen enriched conditions. A typical oxyfuel combustion environment was found to be more reactive than an air equivalent for all fuels studied.

5.2 Experimental procedure

The decomposition of four biomass samples and one coal in four different combustion atmospheres were analysed using non-isothermal thermogravimetry (TGA) at two heat-

ing rates (10 and 40 $K\,min^{-1}$). Characteristics of Williamson coal (WC), short-rotation coppiced willow (SRC), miscanthus (MC), reed canary grass (RCG) and shea meal (SM) are detailed in Section 3.2. The combustion atmospheres studied include air - 21% O_2 in N_2- (Air), oxygen-enriched air - 30% O_2 in N_2 - (En-Air), unenriched oxyfuel - 21% O_2 in CO_2 - (Oxy) and oxygen-enriched oxyfuel - 30% O_2 in CO_2 - (En-Oxy). Without the ability to include steam in the 20 kW experiments, which the results in this chapter are used to inform, it was decided to conduct these tests also without steam, representing a dry-recycle process. Experimental results presented in this chapter were produced according to the methodology detailed in Section 3.3.2 where each of the samples was introduced to Mettler-Toledo TGA/DSC1 equipment producing TGA and heat flux data. While not used in analysing reactivity, the latter data was used alongside the TGA data to highlight the various reaction stages that occur during combustion.

5.3 Results and discussion

The coal and four biomass resources were processed in the TGA instrument for the four combustion atmospheres at two heating rates. The changes in mass and DTG with temperature for each of these experiments are shown in Figures 5.1 to 5.5 for each of the fuels. Similarity between experimental conditions and repetition of experiments at different heating rates suggested that should anomalous or erroneous data be found it would be easily highlighted.

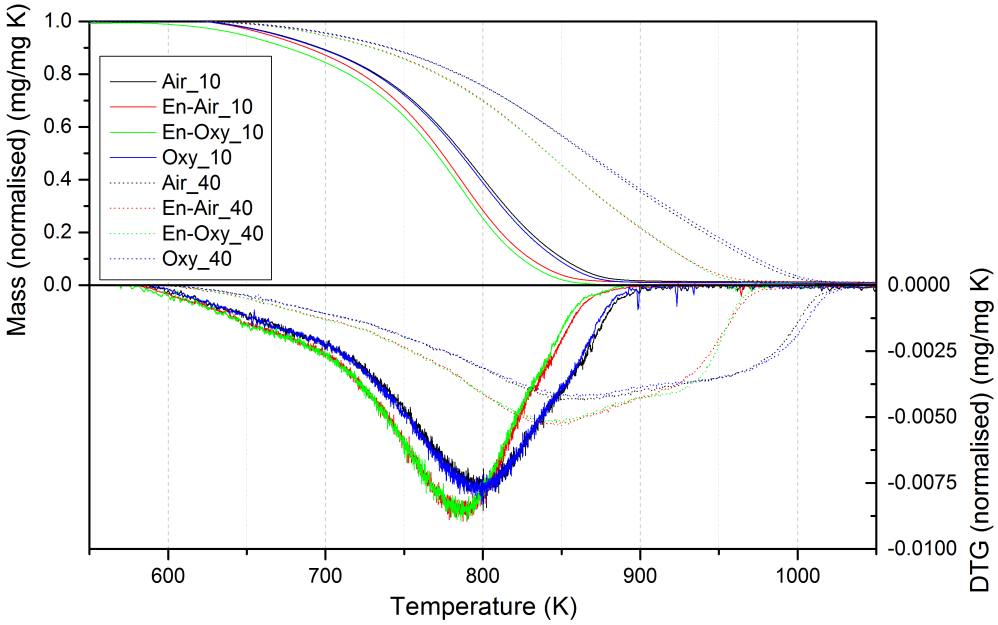

Figure 5.1: Change in mass and DTG with increasing temperature for WC decomposing in a range of atmospheres at heating rates of 10 and 40 K min^{-1}

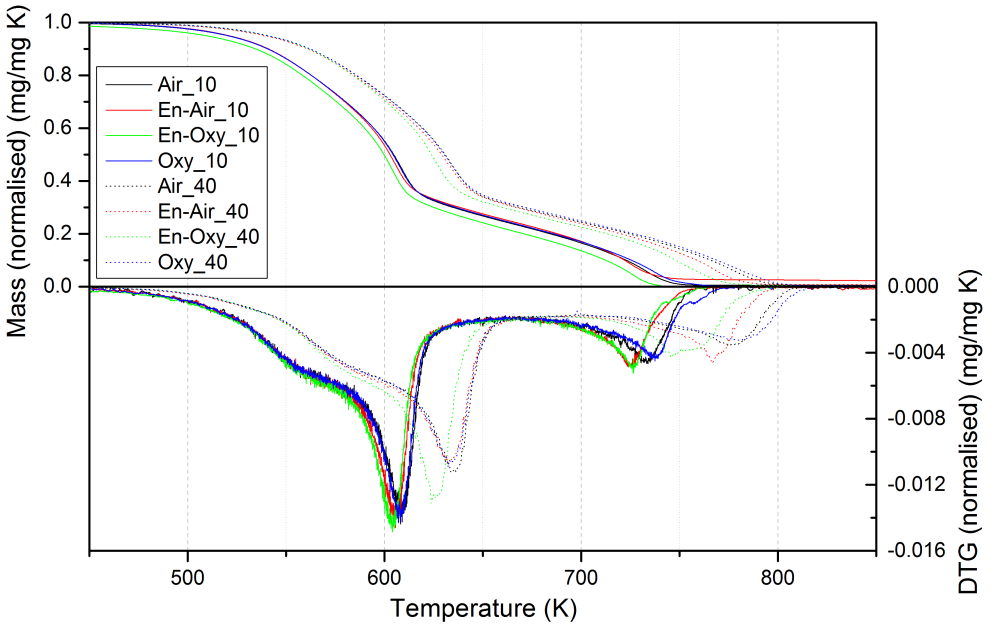

Figure 5.2: Change in mass and DTG with increasing temperature for SRC decomposing in a range of atmospheres at heating rates of 10 and 40 K min^{-1}

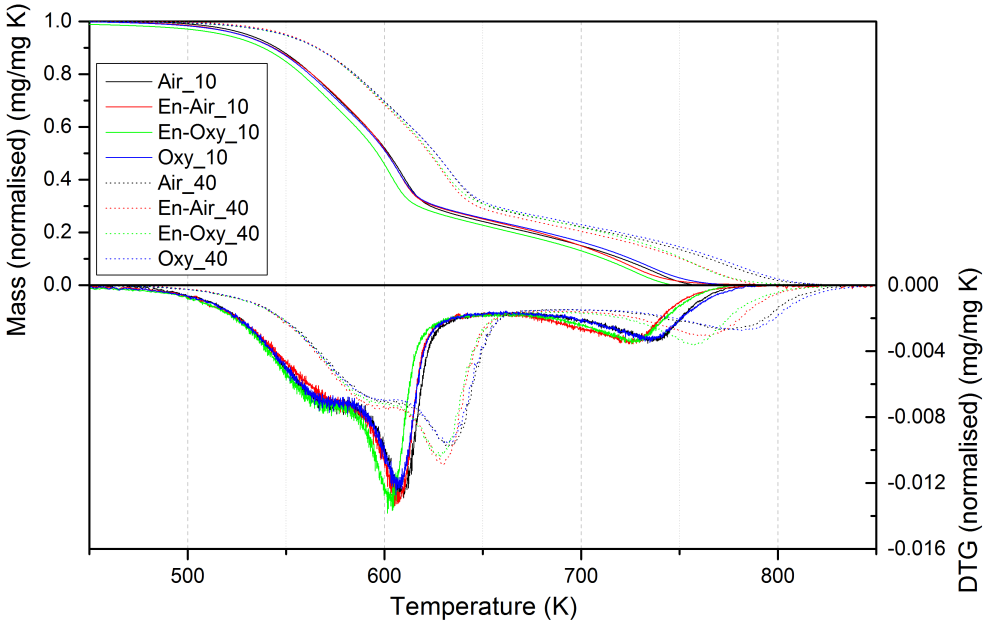

Figure 5.3: Change in mass and DTG with increasing temperature for MC decomposing in a range of atmospheres at heating rates of 10 and 40 K min^{-1}

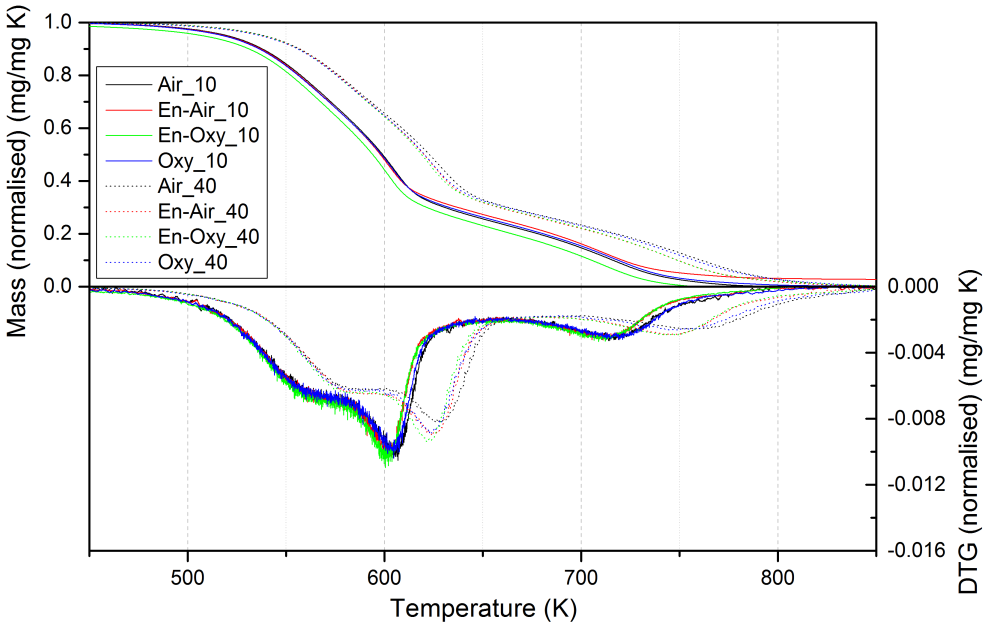

Figure 5.4: Change in mass and DTG with increasing temperature for RCG decomposing in a range of atmospheres at heating rates of 10 and 40 K min^{-1}

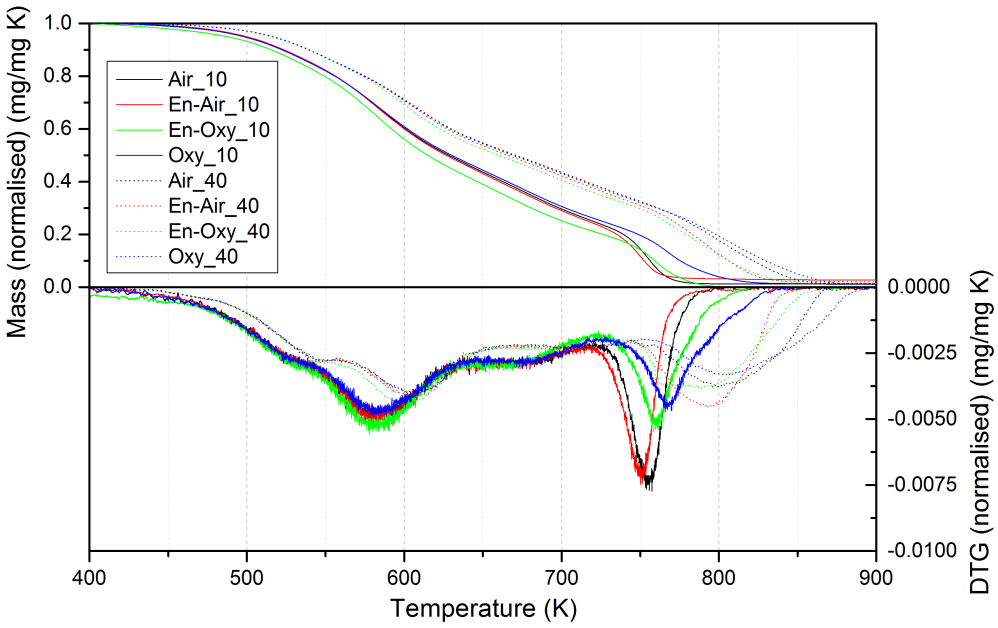

Figure 5.5: Change in mass and DTG with increasing temperature for SM decomposing in a range of atmospheres at heating rates of 10 and 40 K min^{-1}

5.3.1 Identifying reactions from DTG curves

Although in reality fuels decompose due to large number of reactions, each of which may compete and interfere with one another, for modelling purposes it is commonly assumed to be necessary to aggregate reactions occurring at similar temperatures into a smaller number of pseudo-reactions that occur independently. From the DTG profiles and DSC data the biomass samples were observed to decompose due to 3 pseudo-reactions while the WC decomposition was identified as having two pseudo-stages that exhibit considerably overlap in the DTG profile. An example of using the DSC data to corroborate reactions identified from the DTG data is shown in Figure 5.6 for RCG decomposing in air at a heating rate of $10\,\mathrm{K\,min^{-1}}$. The DTG curve at the the transition between the first two pseudo-stages (located at approximately 560 K to 580 K) corresponds with the overall reaction changing from endothermic to exothermic which can be interpreted as suggesting parallel non-competing reactions are occurring; one endothermic and one exothermic. At temperatures below 560 K the endothermic reaction dominates the total mass loss. As the temperature increases the reactant concentration for the endothermic reaction is consumed and this begins to limit the total mass loss occurring. However, rather than the rate of mass loss decreasing, the exothermic reaction begins to take control of the mass loss and for a period the decline in the endothermic reaction rate is matched by the increase in rate of the exothermic reaction rate which results in the relatively unchanged overall rate of mass loss observed across the shoulder. As the exothermic reaction continues to accelerate with increasing temperature a peak rate of reaction is reached at 605 K after which this reaction rate declines and at 635 K the final pseudo-stage takes over. The final reaction is less sharply defined than the first two and as the reactant for this final pseudo-stage is increasing depleted the reaction rate falls until eventually this reaction is completed at approximately 770 K. The peak rate as measured by the DSC data occurs approximately 10 K later than in the DTG suggesting either one or both of a time lag between mass loss and combustion of volatile products and a potential delay in the feedback response of the TGA instrument.

It was initially planned to carry out the same procedure for identifying reactions in the WC samples as was the case for the biomass, which resulted in two reactions with substantial overlap being identified. However, initial testing of the method developed in Chapter 4 suggested this was not the most robust way to model WC decompositions. Analysis of how

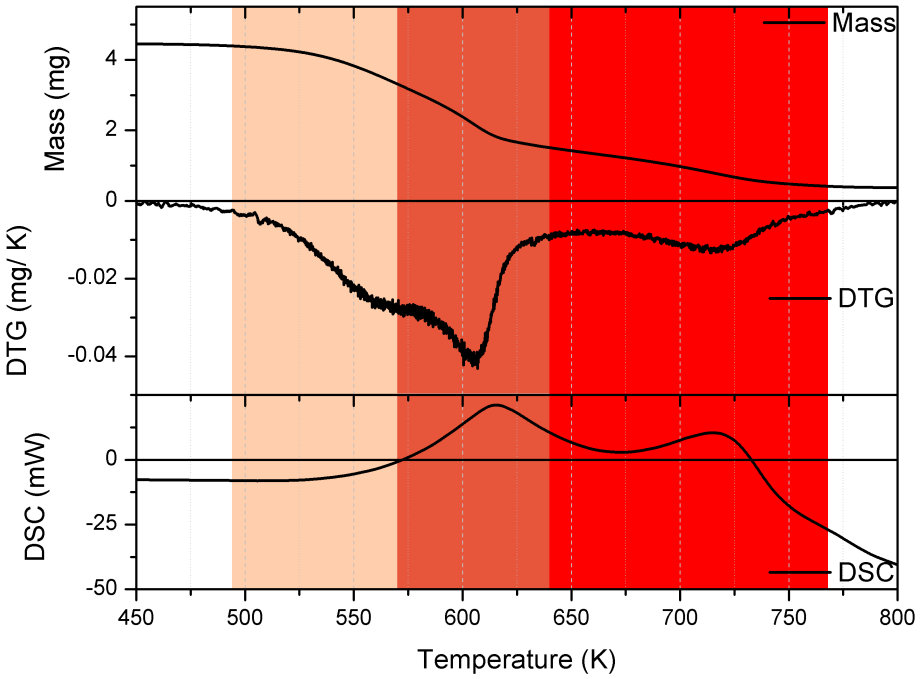

Figure 5.6: Results showing effect of increasing temperature on mass loss, DTG and DSC profiles for RCG decomposing in air at $10\,\mathrm{K\,min^{-1}}$ with identified decomposition pseudo-stages overlaid

well variations of the Coats-Redfern technique model WC decomposition were therefore carried out. First, the method as applied to the biomasses was performed. Here, the extent of reaction for the overall decomposition (α) was divided between the two identified reactions and kinetic parameters determined from the leading edge (LE) fit to each of these curves. Since the two individual pseudo-reactions cannot be resolved due to significant overlap it was also decided to fit to the leading edge ranges using a single extent of reaction. Finally, a fit was made to the full range of the single reaction as is commonly practiced in the literature. These approaches are shown graphically in Figure 5.7 using the decomposition of WC in air at $\beta = 10\,\mathrm{K\,min^{-1}}$ as an example. The analysis was conducted separately for the two heating rates and the reconstructed mass and DTG curves are shown in Figures 5.8 and 5.9 for $\beta = 10$ and $40\,\mathrm{K\,min^{-1}}$, respectively. How well the different reconstructed profiles match the experimental profile is given by the r^2 values in Table 5.1.

Figures 5.8 and 5.9 and Table 5.1 show that for WC, where it is not possible to resolve the two pseudo-reactions, modelling the decomposition with a single extent of reaction results in the best approximation of the experimental data. However, for the slower heating rate a full fit of the Coats-Redfern data was found to better approximate the data while for

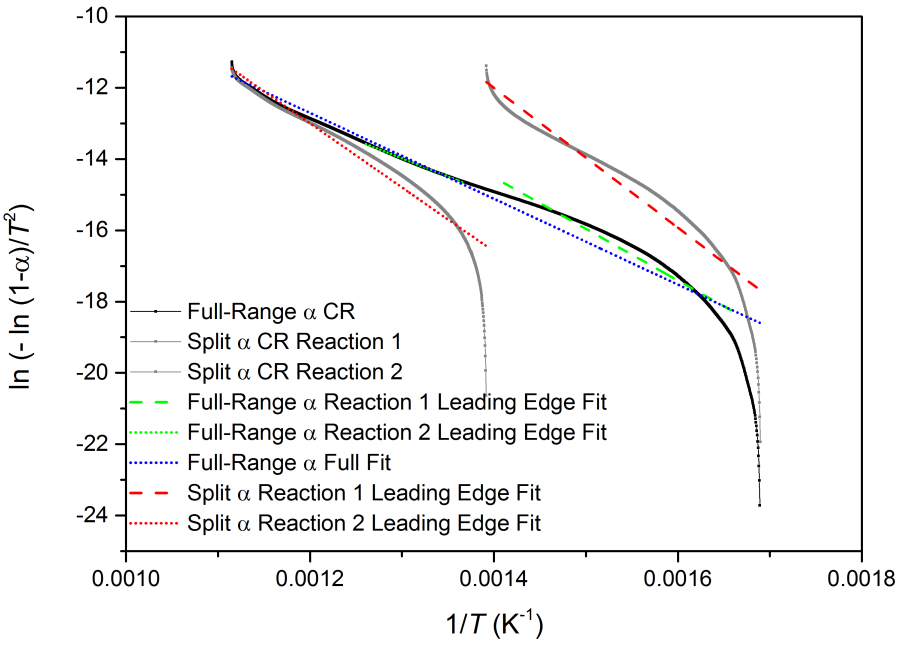

Figure 5.7: Variation on the fitting range for the Coats-Redfern method for WC decomposing in air at 10 K min^{-1}

the faster heating rate modelling using one extent of reaction with two fitting ranges was observed to best capture the decomposition profile. Since both techniques appear equally useful, the coal samples will be modelled using both of these techniques for the work in this chapter.

Table 5.1: Results of various techniques of applying the Coats-Redfern method to WC decomposing in air

Extent of reaction	Number of Reactions	Fitting Range	Mass r^2	DTG r^2
	10 K min^{-1}			
Split α	2	leading edge	0.9946	0.8389
Full range α	2	leading edge	0.9985	0.9475
Full range α	1	full fit	0.9988	0.9867
	40 K min^{-1}			
Split α	2	leading edge	0.9730	0.5321
Full range α	2	leading edge	0.9994	0.9648
Full range α	1	full fit	0.9953	0.9182

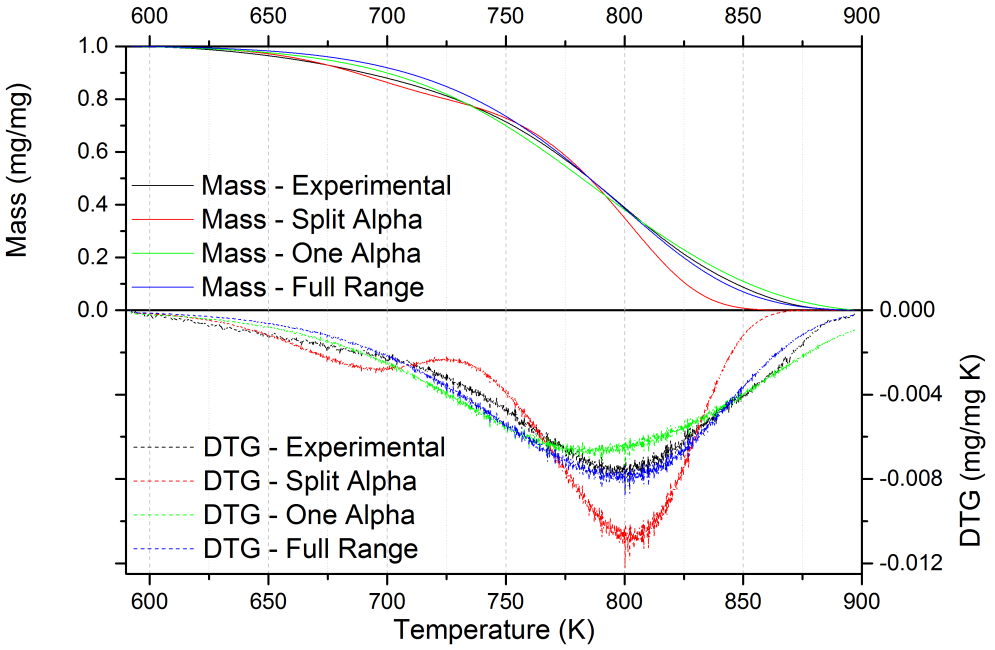

Figure 5.8: Experimental and reconstructed data for the effect of increasing temperature on mass and DTG for WC decomposing in air at $10\,\mathrm{K\,min^{-1}}$

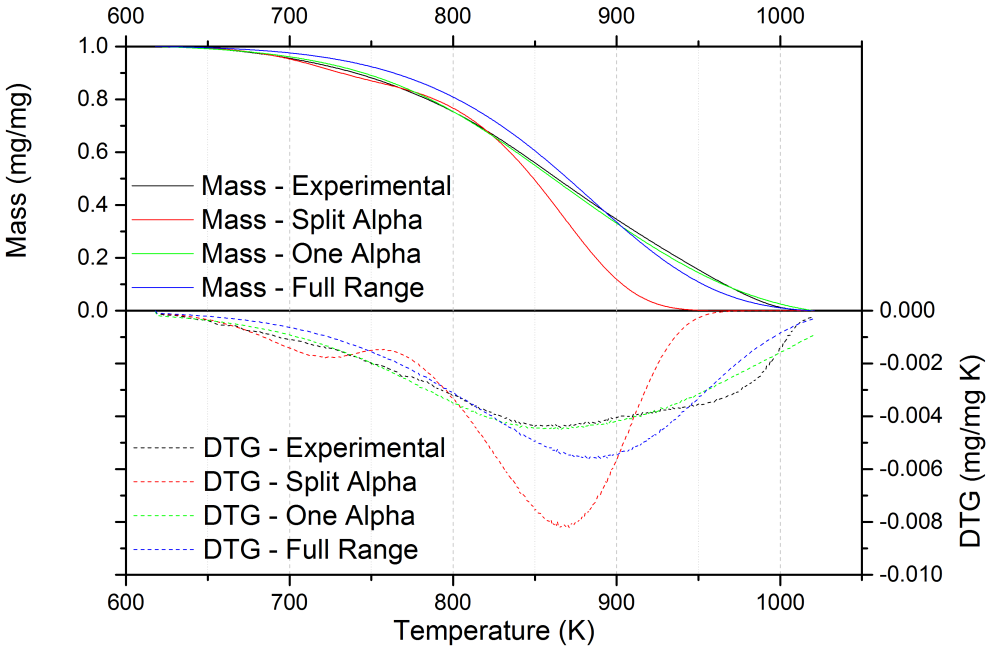

Figure 5.9: Experimental and reconstructed data for the effect of increasing temperature on mass and DTG for WC decomposing in air at $40\,\mathrm{K\,min^{-1}}$

5.3.2 Baseline decompositions in air

The decomposition of each sample in air was designated as the baseline value for each heating rate both for qualitative comparison between DTG profiles and evaluation of change in reactivity (S_i). An overview of the baseline profiles of the energy crops, SM and WC is presented below.

5.3.2.1 Energy crops (SRC, RCG and MC)

The three energy crops - SRC, RCG and MC - display similar decomposition DTG profiles and temperature ranges for the three reactions. Considered alongside the similarities in proximate and ultimate analyses (Table 3.1), this may indicate the substructures of each of these samples may also be comparable. In air these decompositions can be broadly described by the onset of an initial endothermic reaction at approximately 490 K for $\beta = 10\,\mathrm{K\,min^{-1}}$ and ≈ 515 K for $\beta = 40\,\mathrm{K\,min^{-1}}$. Comparison of the temperature range of this reaction with literature suggests this reaction may be due to the release of volatiles during the breakdown of hemicellulose materials [Borrego et al., 2009, Di Blasi, 2008, Yang et al., 2007]. The decline of this initial reaction then overlaps slightly with an increase of the rate of an exothermic reaction forming a shoulder in the DTG curve in the region of 575 when heated at $10\,\mathrm{K\,min^{-1}}$ and 595 K at $40\,\mathrm{K\,min^{-1}}$. Comparison with literature Di Blasi [2008], Yang et al. [2007] suggests this may be due to the oxidation of volatiles released due to the decomposition of cellulose materials. At temperatures of approximately 650 and 675 K the final reaction - which is also exothermic - is found to take control of the decomposition continuing until $\approx$ 765 and 820 K for 10 and $40\,\mathrm{K\,min^{-1}}$, respectively. Reactions in this temperature range are often attributed to the oxidation of char and from comparison with the proximate analysis also some of the more stable lignin-derived volatlile components [Di Blasi, 2008]. The fastest mass loss for each of the energy crops occurs during the second pseudo-reaction in all oxidising atmospheres at temperatures ranging from 590 K to 610 K and 615 K to 640 K for $\beta = 10$ and $40\,\mathrm{K\,min^{-1}}$, respectively.

5.3.2.2 Shea meal (SM)

Dissimilar to the grasses and willow, SM tends to begin devolatilisation at a lower temperature (approximately 35 K and 50 K) than the other biomasses and the transition between

the endothermic and exothermic devolatilisation stages also occurs at significantly lower temperature (535 K for $\beta = 10\,\mathrm{K\,min^{-1}}$ and 555 K for $\beta = 40\,\mathrm{K\,min^{-1}}$). Yuzbasi and Selçuk [2011] suggest a lower temperature devolatilisation may be due to weaker macromolecular bonds which may also be relevant here.

The overall DTG profile for the decomposition of SM has less defined reaction peaks and, particularly in the temperature interval of 650 K to 750 K, a complex series of reactions that convolute the DTG seem to be occurring. If it is assumed that the complex decomposition for SM can be represented by 3 pseudo-reactions, this has the effect of increasing the temperature range of the second and third reactions in SM's decomposition causing the reactions identified for the decomposition of SM to span the widest temperature range.

The SM DTG profile shows far more gradual changes in rate of mass loss than the energy crops and as a result the peak reaction rate is lower than the other samples with a mass loss sustained across a wider temperature range. Indeed, when SM was heated at the slower heating rate the peak reaction rate is found for the char oxidation stage rather than the volatile combustion reaction which displays the fastest mass loss in the other samples. This may be explained as the SM displays a higher char:volatiles ratio than the grasses and willow and a significantly higher ration of lignin to holocellulose.

5.3.3 Reaction temperature ranges

Figure 5.10 illustrates the variation due to heating rate and combustion atmosphere on the temperature ranges of each of the reactions. The temperatures quoted in the following discussion relate to the identified temperature ranges found by following the procedure and not directly to changes observed on the DTG.

5.3.3.1 Effect of heating rate

For the vast majority of samples reactions were retarded and elongated when the heating rate (β) was increased from 10 to $40\,\mathrm{K\,min^{-1}}$. For the energy crops the averaged temperatures for the start of reaction one increased from 495 K to 512 K and the temperature at which crossover between the first two reactions occurred increased from 572 K to 591 K when the heating rate was increased. The span of temperatures for the final, char oxida-

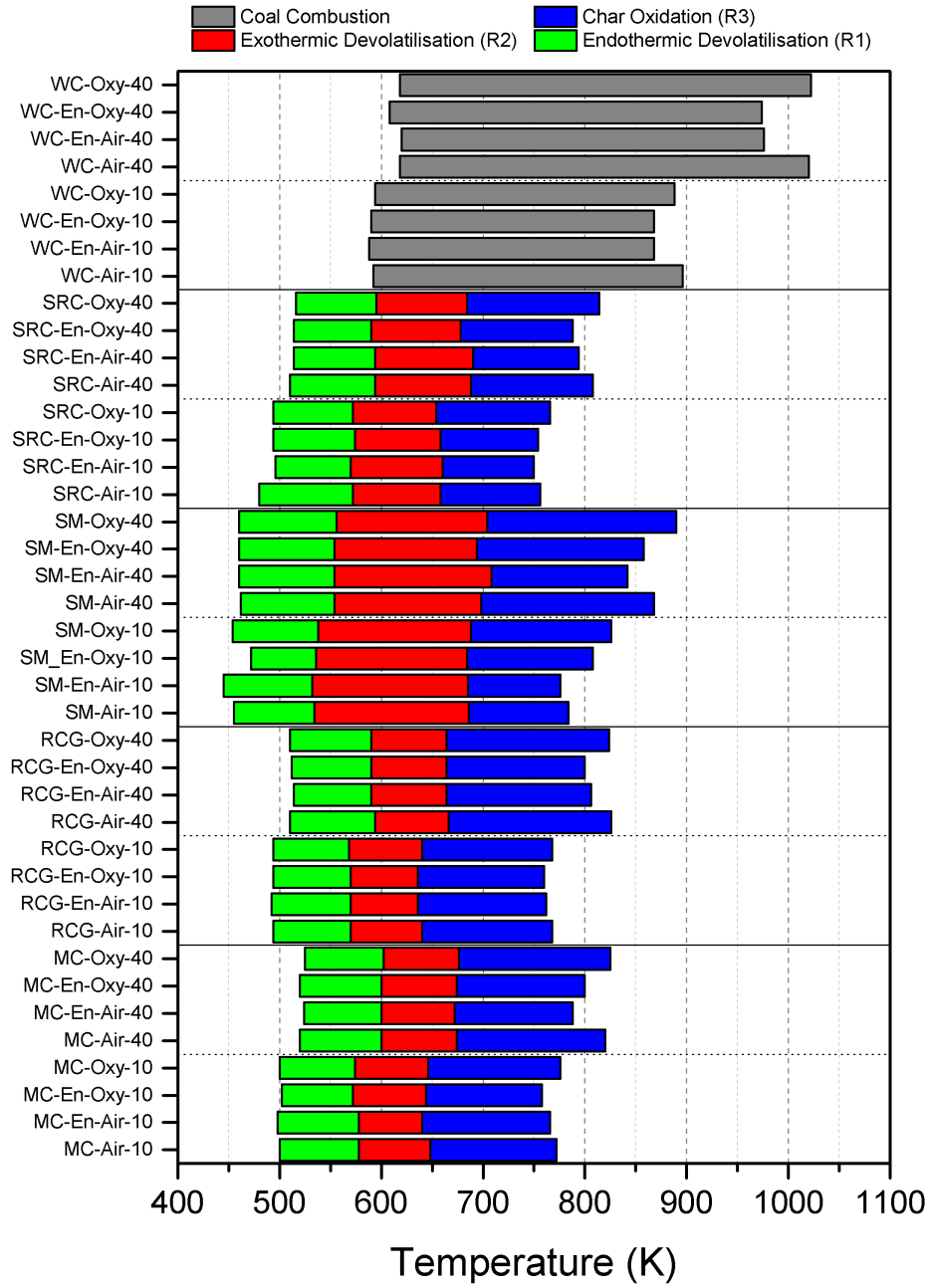

Figure 5.10: Variation in identified temperature reaction zones for each of the coal and biomass samples decomposing in different combustion atmospheres under 10 and 40 $\mathrm{K\,min^{-1}}$

tion reaction increased from an average of 649 K to 765 K for $\beta = 10\,\mathrm{K\,min^{-1}}$ to 676 K to 818 K when $\beta = 40\,\mathrm{K\,min^{-1}}$. The larger fixed carbon content of SM and WC caused the final reaction in their decompositions to be extended further than for the energy crops (by $\sim$50 and $\sim$100 K, respectively). Elongating the reaction over a wider temperature range suggests the reaction may not be kinetically controlled by the bulk system temperature and instead dependent on other experimental factors, as further discussed in Section 5.3.4.1. It is however interesting as this shift occurred despite reducing the particle size and the small mass of sample used. Without further study it is unclear whether the reason for the retardation and elongation of the decomposition profiles is due to mass and heat transfer diffusion in the particle or whether a disparity exists between the particle temperature and that recorded by the TGA thermocouple. However, since the TGA instrument used is very modern it is suggested the former is more likely. A possible recommendation for further work could be to determine a limit for the heating rate (β) at which the decomposition profile begins to change (thereby indicating where mass and temperature diffusion rate begins to control as opposed to kinetics). However, this would likely be different for every fuel sample and dependent on fuel proximate properties as well as particle size.

5.3.3.2 Effect of reaction atmosphere

Figure 5.10 suggests that changes to the combustion atmosphere have a negligible effect on the endothermic devolatilisation of the biomass samples (R1). However, in atmospheres with an enriched level of oxygen reactions two and three tended to span a reduced, narrower temperature range for a given heating rate than their unenriched counterparts suggesting increased [O_2] allows both more intense combustion of volatiles and oxidation of chars. This is in broad agreement with the literature - see the work of Gil et al. [2012*c*] for example - though whether the volatile combustion or char oxidation is more affected was observed to vary between experiments. This does however suggest that in these experiments the rate of delivery of oxygen to the particle surface affects the rate of release of the volatile components as well as affecting char oxidation.

Substituting the bulk gas of N_2 with CO_2 seems to have a complex but considerably smaller effect on the temperature range across which the reactions occur than increasing [O_2]. The temperature range for the RCG reactions appears to show almost no effect of changing from N_2-based to CO_2-based atmospheres while the SM results suggest a slight elongation

of the reaction temperature range in CO_2-based environments. In unenriched conditions substituting N_2 with CO_2 either had no effect or elongated slightly the total temperature range for the biomass samples, similar to that found by Gil et al. [2012*c*] and Liu [2009]. However, in WC combustion and biomass combuston in enriched atmospheres no clear trends can be extracted from the results perhaps suggesting that despite following the procedure detailed in Section 4.3.4, uncertainty in identification of reactions reduces the accuracy of this technique to robustly investigate subtle differences, requiring instead further analysis of the data, such as that detailed in the following section.

5.3.4 Relative reactivity (S_i)

The activation energy (E_A) and pre-exponential factor (A) for each of the reactions in each decomposition and how well the estimated parameters characterise the total decomposition (r^2) were calculated according to the procedure in Chapter 4. These results are tabulated in Table 5.2. However, noting the compensation effect discussed in Section 2.8.7, it is felt undesirable to discuss the changes in kinetic parameters separately and instead this work will only discuss the changes in total reactivity (S_i) which incorporates both E_A and A. For the following results, each of the total decompositions of fuels are divided into several individual pseudo-reactions and their reactivity compared to that of a baseline value. On the graphs a positive value for S_i indicates greater reactivity than the baseline.

It has already been remarked that little similar work exists in the literature and comparisons with that which does is somewhat problematic. For example the work of Gil et al. [2012*c*] compares characteristic temperatures between air and oxyfuel only but does not estimate reactivity parameters, the work of Liu [2009] compares air and oxyfuel combustion of coal chars by estimating the activation energy of the char reaction using multiple heating rates but only at at 10 % [O_2], and while the work of Yuzbasi and Selçuk [2011] evaluates biomasses decomposing in the same atmospheres as presented here the work did not estimate reactivity parameters from the TGA analysis. Nevertheless, where possible literature comparable with the findings are discussed below.

Table 5.2: Results for fuel decompositions in various combustion atmospheres

Identifier	Rxn #	Temperature Range (K)		Mass	CR Fit	E_A	ln A	Reconstruct (r^2)	
(Atmosphere_β)	(θ)	Reaction	Leading Edge	Fraction	r^2	kJ mol^{-1}		Mass	DTG
WC									
Air_10	1	592–896	Full range	1.00	0.9463	100.10	9.35	0.9988	0.9867
Air_10	1	592–896	602–708	0.17	0.9539	119.87	13.45	0.9985	0.9475
	2	592–896	730–792	0.83	0.9984	84.65	6.69		
Air_40	1	618–1020	Full range	1.00	0.9489	84.1	6.66	0.9953	0.9182
Air_40	1	618–1020	638–736	0.11	0.9760	112.3	12.14	0.9994	0.9648
	2	618–1020	758-832	0.89	1.0000	67.04	4.04		
En-Air_10	1	588–868	Full range	1.00	0.9446	103.09	10.17	0.9988	0.9808
En-Air_10	1	588–868	590–700	0.17	0.9044	138.92	17.34	0.9954	0.8754
	2	588–868	720–780	0.83	0.9973	88.29	7.56		
En-Air_40	1	620–976	Full range	1.00	0.9559	90.39	8.04	0.9974	0.9561
En-Air_40	1	620–976	640–734	0.15	0.9762	109.52	11.86	0.9995	0.97145
	2	620–976	770–820	0.85	0.9998	73.84	5.41		
En-Oxy_10	1	590–868	Full range	1.00	0.9598	99.53	9.63	0.9990	0.9765
En-Oxy_10	1	590–868	614–700	0.18	0.9827	99.04	9.85	0.9991	0.9569
	2	590–868	720–784	0.82	0.9971	88.82	7.69		
En-Oxy_40	1	608–974	Full range	1.00	0.9452	92.56	8.39	0.9961	0.9166
En-Oxy_40	1	608–974	626–718	0.10	0.9744	123.56	14.53	0.9994	0.9554
	2	608–974	736–828	0.90	0.9999	71.73	5.08		
Oxy_10	1	594–888	Full range	1.00	0.9402	103.08	9.87	0.9986	0.9849
Oxy_10	1	594–888	598–700	0.15	0.9128	146.20	18.43	0.9961	0.8898
	2	594–888	720–792	0.85	0.9981	84.62	6.71		
Oxy_40	1	618–1022	Full range	1.00	0.9454	82.83	6.43	0.9946	0.9080
Oxy_40	1	618–1022	634–728	0.08	0.9746	118.48	13.30	0.9994	0.9643
	2	618–1022	728–840	0.92	0.9997	67.42	4.10		
SRC									
Air_10	1	488-572	524-554	0.24	0.9992	114.74	19.85		
	2	572-662	594-606	0.51	0.9994	188.25	32.48	0.9978	0.8194
	3	662-759	716-732	0.24	0.9944	173.66	23.82		
Air_40	1	510-594	546-576	0.23	0.9993	118.67	21.12		
	2	594-688	615-632	0.50	0.9998	175.10	29.74	0.9984	0.8698
	3	687-808	755-774	0.27	0.9967	143.75	18.68		
En-Air_10	1	496-570	530-552	0.24	0.9996	124.76	22.16		
	2	570-660	592-604	0.52	0.9992	196.67	34.39	0.9971	0.8055
	3	660-750	714-724	0.24	0.9959	196.92	28.07		
En-Air_40	1	514-594	548-576	0.24	0.9995	122.23	21.87		
	2	594-690	614-628	0.50	0.9999	177.50	30.26	0.9978	0.8515
	3	689-794	746-766	0.26	0.9937	162.03	21.92		
En-Oxy_10	1	494-574	524-552	0.27	0.9997	115.12	19.85		
	2	574-658	594-606	0.49	0.9998	230.74	41.36	0.9961	0.8221
	3	658-754	720-740	0.24	0.9945	229.00	33.60		
En-Oxy_40	1	513-590	551-576	0.23	0.9988	131.46	24.01		
	2	590-678	612-620	0.51	0.9999	194.40	33.95	0.9981	0.8410
	3	678-788	726-748	0.27	0.9955	154.14	20.96		
Oxy_10	1	494-572	526-556	0.24	0.9995	120.90	21.24		
	2	572-654	594-604	0.49	0.9995	193.74	33.67	0.9985	0.8293
	3	654-750	716-738	0.27	0.9877	164.79	22.35		
Oxy_40	1	516-595	551-572	0.24	0.9998	123.18	22.04		
	2	595-684	615-628	0.48	0.9999	183.28	31.38	0.9911	0.8920
	3	683-814	755-778	0.28	0.9978	130.15	16.38		

Table 5.2: Results for fuel decompositions in various combustion atmospheres (cont.)

Identifier	Rxn #	Temperature Range (K)		Mass	CR Fit	E_A	ln A	Reconstruct (r^2)	
(Atmosphere_β)	(θ)	Reaction	Leading Edge	Fraction	r^2	kJ mol^{-1}		Mass	DTG
RCG									
Air_10	1	494-570	520-556	0.28	0.9999	132.09	23.82		
	2	570-640	590-606	0.45	1.0000	171.61	29.43	0.9990	0.9360
	3	640-768	672-710	0.27	0.9999	109.80	13.06		
Air_40	1	510-594	538-576	0.30	0.9999	132.12	24.07		
	2	594-666	607-626	0.41	0.9981	190.60	33.17	0.9989	0.9641
	3	666-826	700-754	0.29	0.9995	97.55	11.24		
En-Air_10	1	492-570	524-556	0.29	0.9997	129.82	23.32		
	2	570-636	586-598	0.44	0.9997	188.19	32.99	0.9989	0.9370
	3	636-762	670-710	0.28	0.9997	108.88	13.05		
En-Air_40	1	514-590	539-574	0.28	0.9999	139.59	25.80		
	2	590-664	606-620	0.44	0.9991	184.95	32.26	0.9989	0.9509
	3	664-806	703-742	0.28	0.9999	108.70	13.42		
En-Oxy_10	1	494-570	524-554	0.29	0.9998	128.84	23.11		
	2	570-636	586-598	0.44	0.9997	190.39	33.46	0.9988	0.9335
	3	636-760	668-712	0.27	0.9996	109.16	13.14		
En-Oxy_40	1	512-590	539-576	0.29	0.9998	140.93	26.11		
	2	590-664	606-618	0.43	0.9995	197.71	34.87	0.9986	0.9402
	3	664-800	700-740	0.28	0.9999	111.94	14.02		
Oxy_10	1	494-568	526-554	0.26	0.9998	133.48	24.23		
	2	568-640	588-600	0.46	1.0000	166.23	28.39	0.9990	0.9280
	3	640-768	678-716	0.28	0.9997	108.21	12.78		
Oxy_40	1	509-590	539-570	0.28	0.9998	134.61	24.74		
	2	590-664	605-620	0.43	0.9993	186.94	32.67	0.9989	0.9571
	3	664-824	700-746	0.29	0.9996	101.22	11.97		
MC									
Air_10	1	500-578	528-562	0.31	0.9999	136.16	24.31		
	2	578-648	596-608	0.44	0.9999	216.26	38.25	0.9988	0.9482
	3	648-772	700-738	0.25	0.9953	121.07	14.72		
Air_40	1	520-600	554-587	0.30	0.9997	140.52	25.47		
	2	600-674	614-630	0.44	0.9989	199.77	34.69	0.9988	0.9691
	3	673-820	730-772	0.26	0.9986	104.61	12.18		
En-Air_10	1	498-578	526-568	0.30	0.9997	123.43	21.61		
	2	578-640	592-606	0.43	0.9999	228.21	40.80	0.9992	0.9408
	3	640-766	672-728	0.27	0.9986	116.52	14.19		
En-Air_40	1	524-600	560-588	0.31	0.9996	148.68	27.21		
	2	600-672	612-626	0.44	0.9983	230.95	40.96	0.9984	0.9636
	3	672-788	724-760	0.25	0.9973	122.32	15.48		
En-Oxy_10	1	502-572	530-560	0.28	0.9997	141.72	25.80		
	2	572-644	590-604	0.46	0.9998	210.10	37.37	0.9985	0.9223
	3	644-758	688-728	0.26	0.9970	120.77	14.87		
En-Oxy_40	1	519-600	552-584	0.31	0.9998	140.28	25.40		
	2	600-674	612-624	0.43	0.9982	236.86	42.15	0.9982	0.9562
	3	674-800	729-754	0.26	0.9978	133.41	17.35		
Oxy_10	1	500-574	528-560	0.28	0.9999	138.09	24.90		
	2	574-646	592-604	0.46	0.9999	194.64	33.98	0.9990	0.9307
	3	646-776	692-738	0.27	0.9964	113.70	13.39		
Oxy_40	1	525-602	552-578	0.31	0.9998	145.30	26.43		
	2	602-676	618-628	0.42	0.9995	215.78	37.77	0.9981	0.9593
	3	676-825	730-770	0.27	0.9991	100.20	11.33		

Table 5.2: Results for fuel decompositions in various combustion atmospheres (cont.)

Identifier	Rxn #	Temperature Range (K)		Mass	CR Fit	E_A	ln A	Reconstruct (r^2)	
(Atmosphere_β)	(θ)	Reaction	Leading Edge	Fraction	r^2	kJ mol^{-1}		Mass	DTG
SM									
Air_10	1	455-534	494-524	0.12	0.9975	100.31	18.38		
	2	534-686	548-578	0.55	0.9911	116.18	18.25	0.9766	0.4936
	3	686-784	738-752	0.33	0.9914	208.79	28.47		
Air_40	1	461-554	504-540	0.14	0.9989	98.63	18.51		
	2	554-698	569-596	0.43	0.9932	119.43	19.56	0.9874	0.5912
	3	698-868	760-788	0.44	0.9984	97.52	10.18		
En-Air_10	1	445-532	504-518	0.12	0.9985	101.76	18.85		
	2	532-685	548-578	0.57	0.9936	111.44	17.25	0.9797	0.5298
	3	685-776	734-748	0.31	0.9925	218.14	30.31		
En-Air_40	1	460-554	500-540	0.14	0.9989	96.22	17.95		
	2	553-708	570-596	0.47	0.9936	117.95	19.19	0.9839	0.5829
	3	708-842	757-776	0.39	0.9988	138.10	16.90		
En-Oxy_10	1	472-536	494-518	0.13	0.9998	112.45	21.17		
	2	536-684	550-572	0.57	0.9935	131.65	21.67	0.9708	0.5002
	3	684-808	742-756	0.30	0.9938	152.17	18.86		
En-Oxy_40	1	460-554	498-540	0.14	0.9990	97.98	18.34		
	2	554-694	569-594	0.44	0.9936	130.38	21.97	0.9872	0.6559
	3	693-858	748-768	0.42	0.9941	110.97	12.64		
Oxy_10	1	454-538	486-524	0.14	0.9993	91.60	16.15		
	2	538-688	548-570	0.53	0.9881	147.06	24.97	0.9677	0.5134
	3	688-826	750-766	0.33	0.9956	139.24	16.45		
Oxy_40	1	460-556	502-540	0.14	0.9990	95.52	17.72		
	2	556-704	572-594	0.44	0.9941	125.92	20.86	0.9854	0.5861
	3	703-890	767-792	0.42	0.9988	94.31	9.52		

5.3.4.1 Effect of heating rate

One assumption regularly employed during the extraction of kinetic parameters from non-isothermal TGA work is that the parameters are independent of the experimental heating rate so long as the magnitude of variation is small. To investigate this a comparison between the results at different heating rates is presented in Figure 5.11 where $\beta = 10\,\mathrm{K\,min^{-1}}$ is used as the reference case for the higher heating rate. This figure shows that the reactivities predicted for the grasses - RCG and MC - at the higher heating rate are typically within 5 % of those estimated at the lower heating rate. However, the results for WC and SM suggest in all cases the final reaction peak is substantially less reactive at the higher heating rate. Taking all the results together this supports the claim by White et al. [2011] that no consensus has emerged whether increases in heating rate reduces the kinetic rate of reactions. However, in almost all cases it is the char combustion stage that is observed to be less reactive at the higher heating rate with the reduction in react-

ivity appearing correlated to the fixed carbon content of the fuels (WC shows the largest reductions and the grasses show the least). It could therefore be argued that the devolatilisation reactions are less affected by heating rate suggesting that temperature profiles at these heating rates are relatively uniform. However, the reduction in apparent reactivity of the char oxidation stage suggests that another factor is rate limiting as the temperature ramp rate is increased. It is suggested that the rate of oxygen diffusion to the char surface limits the reaction since increasing [O_2] appears to reduce the reduction in apparent reactivity for the samples with higher fixed carbon contents (WC and SM).

Noting that this work is considered as an indicator to help explain phenomena observed in Chapter 6 it is considered beyond the scope of this work to investigate the effect of heating rate on reactivity parameters or the methods of estimating them in further detail as performed by Hayhurst [2013] among others, since such work requires extensive effort, requiring both a number of experiments and complex computer solvers, which in this work are not justified as detailed in Section 4.2. Instead the following discussion focusses on the trend changes due to changing combustion atmospheres which have been shown to be robust in Chapter 4. Rather than increasing the uncertainty by averaging the results for S_i the relative reactivities are calculated and presented for each heating rate individually in Figures 5.12a and 5.12b and the results are discussed by fuel before more general conclusions are drawn.

5.3.4.2 Williamson coal (WC)

The WC samples results for both methods suggest the reactivity changes at both heating rates display good agreement. When kinetic parameters were extracted from modelling the full range of the CR data apparent reactivity was observed to increase with oxygen-enriched atmospheres. This increase was observed to be greater at the higher heating rate supporting the suggestion in Section 5.3.4.1 that oxygen-diffusion may have a larger rate-limiting impact at higher heating rates and that increasing the bulk concentration of O_2 increases its rate of delivery to the char surface. The results from the modelling approach that fits the data according to two reaction leading edge broadly agrees with the results for a single reaction fit. When dividing the decomposition into two pseudo-stages the first reaction is only responsible for $\sim$ 10% of the total mass and so behaviour of the second reaction is considered more important in terms of the overall reactivity. Increasing [O_2]

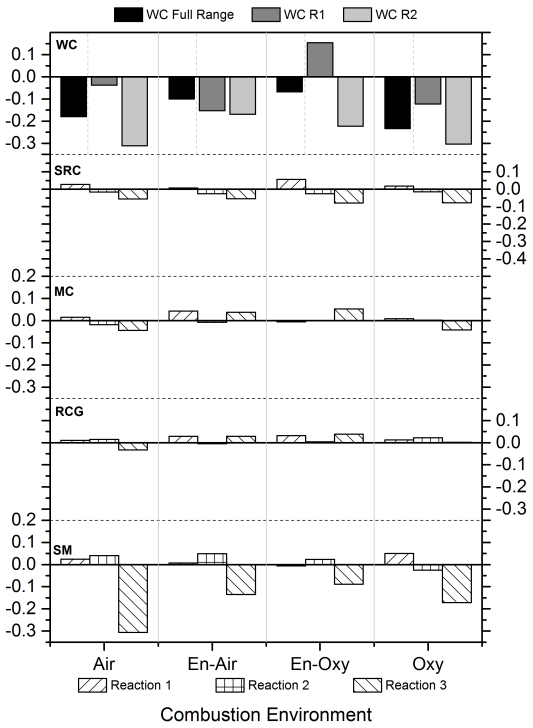

Figure 5.11: S_i comparison between estimated reactivity of sample results from $\beta = 40\,\mathrm{K\,min^{-1}}$ compared to $10\,\mathrm{K\,min^{-1}}$ for Williamson coal (WC), willow (SRC), miscanthus (MC), reed canary grass (RCG) and shea meal (SM) decomposing in different oxidative atmospheres

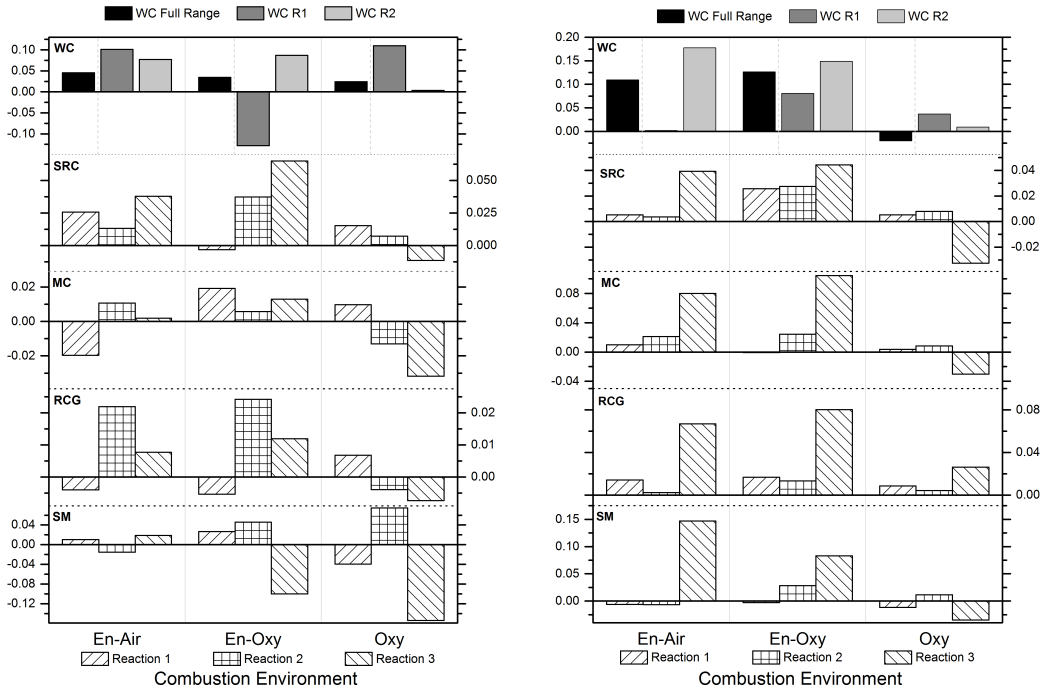

(a) $\beta = 10\,\mathrm{K\,min^{-1}}$ (b) $\beta = 40\,\mathrm{K\,min^{-1}}$

Figure 5.12: Changes in reactivity and temperature of maximum rate for Williamson coal (WC), short-rotation coppiced (SRC) willow, miscanthus (MC) reed canary grass (RCG) and shea meal (SM) decomposing in different combustion atmospheres at heating rates (β) of 10 and 40 $\mathrm{K\,min^{-1}}$

has a significant positive benefit on apparent reactivity while no clear trend is observed when substituting N_2 for CO_2 as the comburent, as is similar to work reported elsewhere [Gil et al., 2012*a*, Irfan et al., 2012, Liu, 2009].

5.3.4.3 Short-rotation coppiced willow (SRC)

The SRC samples are observed to broadly behave in a similar fashion under both heating rates. In atmospheres with enriched [O_2] the final char reaction was observed to be more reactive than the corresponding unenriched scenarios. In the oxyfuel (CO_2-based) atmospheres enriching [O_2] also caused an increase in the reactivity of the second reaction though this was less readily observed in N_2-based environments. No trend can be determined concerning how reactivity changes for the first reaction depending on the combustion environment though most changes observed are small corroborating the findings shown in Figure 5.10. At the slower heating rate for unenriched atmospheres replacing N_2 with CO_2 tended to have a small effect on each of the reactivities while at the faster heating rate a substantial reduction in reactivity of the char oxidation was witnessed perhaps suggesting slower diffusion of O_2 in CO_2 is to some extent limiting the reaction. However, that this reduction was not seen at higher [O_2] where small increases in S_i were observed may suggest the enrichment of O_2 sufficiently counters the reduction in its mobility. The second reaction stage is responsible for $\sim$ 50% of the total mass loss and in all atmospheres this was observed to be more reactive than combustion in air. Substitution of N_2 for CO_2 tended to have a small increasing effect on S_i for this reaction in all conditions tested.

5.3.4.4 Miscanthus (MC)

At the slower heating rate increasing [O_2] was observed to slightly increase the reactivities of reactions 2 and 3. However, at 40 K min^{-1} these oxidative reactions greatly benefitted from the increased oxygen concentration. The second reaction was again the most important in terms of total mass representing approximately 45% of the total mass loss during the decomposition. In O_2-enriched conditions the apparent reactivity for this reaction increased. Particularly under faster heating rates, the reactivity of the final pseudo-reaction was also increased with increasing [O_2]. In the char oxidation stage substituting N_2 for CO_2 reduced reactivity in unenriched conditions but slightly increased the value of S_i

when [O_2] was enriched.

5.3.4.5 Reed canary grass (RCG)

RCG shows the same trend as above in the second reaction, which is responsible for a similar amount of the total mass loss, with the value of S_i increasing in O_2-enriched conditions at lower heating rates and in the char oxidation stage at the higher heating rate. Comparison with the DTGs suggest the reason for this shift in increased S_i from R2 to R3 may be due to changes in the way the DTG is analysed rather than changes in S_i between the reactions. At low heating rates substituting N_2 for CO_2 was observed to have a relatively minor effect on the reactivities; however, at $40\,\mathrm{K\,min^{-1}}$ reactions 2 and 3 were observed to increase in reactivity when switching to an oxyfuel environment of comparable [O_2].

5.3.4.6 Shea meal (SM)

The relatively poor correlation between the reconstructed mass and DTG curves for the SM samples indicate the method can less robustly analyse the changes in relative reactivity for this sample and emphasise the need for care when attempting to interpret the results. Comparing S_i with the DTGs in Figure 5.5 it can be observed that when increasing the oxygen concentration compared to the unenriched state the reactivity of the final reaction increases while the same reaction was reduced when the atmosphere was changed to be CO_2-based.

5.3.5 Overall results

Although the results for the different fuels show some variation, some overall conclusions may be drawn. The energy crops behaved in a similar fashion while changes to the reactivity of SM and WC were unique to those fuels. Overall, S_i, reaction temperature ranges and DTG results show that enriching the concentration of oxygen in the combustion atmosphere is the most important factor affecting reactivity and increases the reactivity of combustion occurring during either one or both of reactions 2 or 3. This is in agreement with the findings of Liu [2009], though with only two oxygen concentrations here it is not possible to predict dependence of the reaction on the concentration as is carried out in

that work as to do so would require a large number of repeated experiments which cannot be justified here where the focus is to provide supporting evidence to analyse the results in Chapter 6. The impact on reactivity was found to be greater at the higher heating rate where it is suggested [O_2] has a stronger rate-limiting effect due to the diffusion of O_2 to the char surface required for char oxidation.

Similar to the findings in the literature, no clear trends were observed when substituting N_2 with CO_2 which appeared to be dependent on the experimental set up. At a heating rate of $10\,K\,min^{-1}$ in unenriched conditions replacing air with a CO_2-based atmosphere tends to reduce the reactivity relative to air of the final char-oxidation reaction. However, this trend was not observed for all fuels at the fastest heating rate. Conversely, in O_2-enriched conditions the oxyfuel environment appeared to be marginally more reactive than that with N_2as the base gas. This result is unlikely to be observed in practical combustion because the operation of the TGA instrument involves ensuring a given temperature within the combustion chamber. Therefore, as noted by Liu [2009], unlike in a furnace where the higher heat capacity of CO_2 would reduce gas and particle temperatures (hence depressing apparent reactivity), the temperature depression is not witnessed in the TGA instrument thus this depression of reactivity is not seen. As for the slight increase in reactivity, although the CO_2-gasification reaction does not significantly affect decomposition until 1073 K this could also contribute a small amount to an increased reactivity or the increased heat capacity of CO_2 could lead to marginally higher particle temperatures as more energy is contained in the system at any given temperature.

Comparing a typical oxyfuel combustion atmosphere (30 % O_2 in CO_2) with combustion in air finds that the former is more reactive during both the combustion of volatiles and char oxidation stages during TGA. However, the extent to which this phenomenon exists at large-scale combustion with much more rapid heating rates is unclear. One the one hand the increased heat capacity of CO_2 is likely to reduce the gas and particle temperatures compared to a N_2-based environment. However, in practice, oxyfuel combustion will likely be carried out in oxygen-enriched conditions that elevate the furnace temperatures by reducing the thermal diluent and intensifying the combustion process promoting higher reaction rates.

5.4 Conclusions

Four biomass samples and one coal decomposing in air, oxygen-enriched air and oxyfuel atmospheres were analysed by TGA at two heating rates. An extended Coats-Redfern method was applied to assess changes in reactivity due to the different combustion conditions in order to answer the second research question in Section 2.9. Relative reactivity was observed to change due to heating rate suggesting the apparent reactivity of the char oxidation stage was lower at higher heating rates while the devolatilisation reactions were less affected. However, in general it can be concluded that increasing [O_2] increased combustion reactivity. This was particularly the case at the higher heating rate where it is suggested [O_2] contributes more to limiting the overall rate of reaction. A lesser effect was observed when substituting N_2 for CO_2 as the comburent though in unenriched conditions this tended to reduce char oxidation reactivity while in oxygen-enriched conditions the same substitution marginally increased reactivity. A typical oxyfuel environment was found to have increased combustion reactivity compared to combustion in air in an externally heated TGA atmosphere. The work in the next chapter investigates whether similar behaviour occurs during combustion of these fuels in a 20 kW furnace.

Chapter 6

20 kW-scale Furnace Results and Discussion

6.1 Chapter overview

This chapter presents the results of the testing on the 20 kW furnace which is the focal point of this part of the thesis. In order to answer research questions 3–6 detailed in Section 2.9 the results are divided into four separate experiments for which a description of the results is presented individually before the results are discussed together for that experiment. During all of the experiments, the effects on combustion conditions and gaseous and solid emissions are investigated. The first experiment investigates the effects of increasing the biomass blending ratio (BBR) of three biomasses during unstaged combustion in air and oxygen-enriched air. The second experiment investigates the effect of cofiring three different biomasses at 15% (on a thermal basis) with various levels of oxidant staging in air and oxygen-enriched air. The third experiment investigates unstaged combustion of the three biomasses where the secondary air stream is replaced with one of two synthetic oxyfuel mixtures. The fourth section of the results investigate dedicated biomass firing under air and partial-oxyfuel conditions. Results in each section are compared to existing literature that was presented in Chapter 2 and discussed individually using the fuel characterisation results (Chapter 3) and findings from the TGA analysis (Chapter 5). Finally, conclusions drawn from each of the discussions of the experimental results are presented.

6.2 Impact of variation of biomass blending ratio (BBR) on combustion in air and oxygen-enriched air

6.2.1 Experimental design

In order to answer research question 3 in Section 2.9, the amount of biomass blended with coal was studied in combustion experiments with 0, 8, 15 and 20% on a thermal basis for each of the three biomass samples. The tests were conducted in air and oxygen-enriched air (30% [O_2]). For each of these tests the furnace was operated in an unstaged fashion with oxidant delivered by the primary and secondary lines. In the following figures, BBR Error represents the combined experimental error associated with the two fuel feeders, calculated as described in Section 3.4.13.2.

6.2.2 Combustion characteristics

Figure 6.1 shows how the combustion temperatures in the furnace varied with increasing biomass blending in both air and oxygen-enriched air combustion atmospheres. In general, increasing BBR in air-firing tends to slightly reduce temperatures close to the burner (T_1), but by the time the combustion mixture has travelled further along the furnace (T_2 and T_3) small increases in temperature were observed in a very similar fashion to that reported by Spliethoff and Hein [1998]. Under oxygen enrichment combustion temperatures were observed to increase significantly for coal firing and combustion with RCG and MC and low BBR of SRC. Near the burner, the combustion temperature appeared sensitive to increasing BBR of SRC under oxygen-enriched conditions reducing by $\sim$125 °C when BBR increased from 8% to 20%. However, at other measurement locations with SRC, and with both other fuels at all measuring locations, increasing BBR had relatively little impact on temperature though small increases were generally observed for increasing BBR with RCG and MC. In general, oxygen-enriched combustion resulted in increasing temperatures by $\sim$125 °C, $\sim$100 °C and $\sim$75 °C at T_1, T_2, and T_3, respectively.

Figure 6.2 illustrates the variation in carbon burnout and CO emissions with increasing biomass blending in both air and oxygen-enriched air combustion atmospheres. For all fuel mixtures combustion in oxygen-enriched conditions resulted in a higher carbon burnout, as reported elsewhere [Nimmo et al., 2010, Smart and Riley, 2012], while for all ex-

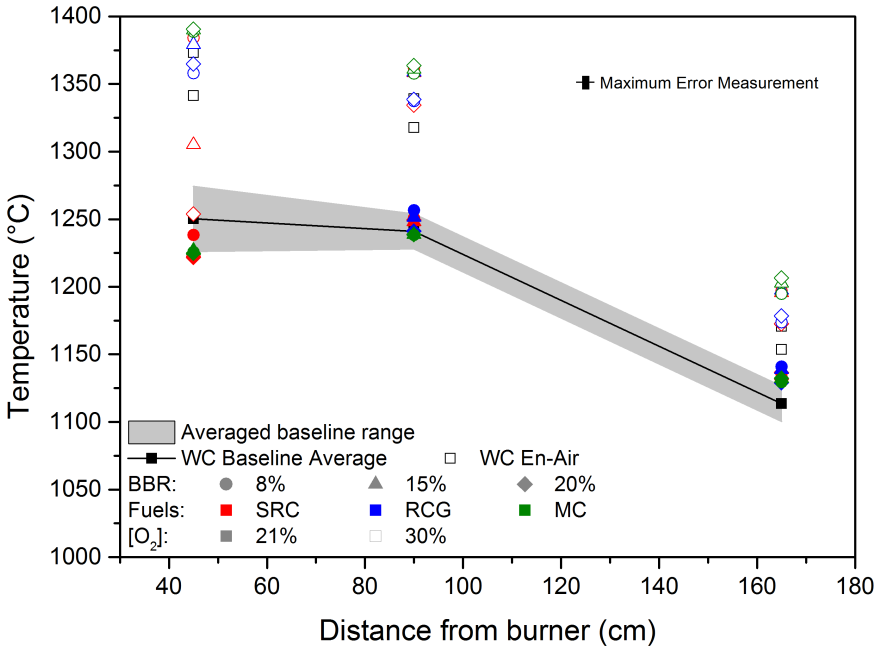

Figure 6.1: Variation in temperatures at various distances along the furnace with increasing biomass blending ratio (BBR)

periments CO remained largely unchanged. Although little change was observed during combustion in oxygen-enriched when BBR was increased, blending of biomass in air was also observed to increase burnout for all fuels. The increase in burnout found in this work is similar to the findings of Munir et al. [2011] when using similar equipment who found a general increase in burnout with increasing BBR up to a maximum of 15% for cofiring most biomasses. In the present work the change in burnout in air firing was slightly dependent on the biomass being blended with SRC the most beneficial to burnout, followed by RCG and then MC. At the lowest BBR level of 8% the increase in carbon burnout barely exceeded the range observed for the baseline values. However, when BBR was increased to 15% burnout increased from 99.5% for coal-firing to an average of 99.7% for the cofired mixtures. As BBR was increased to 20% carbon burnout values were reduced slightly compared to the 15% BBR though were still greater than for coal-firing and 8% BBR. The reduction between 15 and 20% BBR was most apparent for SRC cofiring.

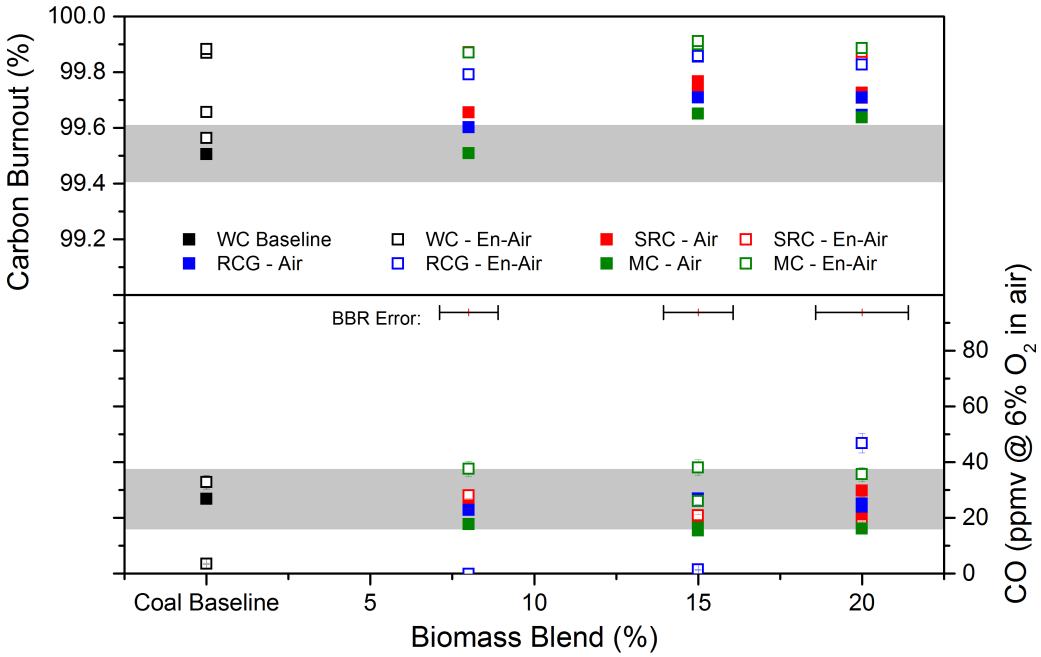

Figure 6.2: Variation in carbon burnout and CO emissions with increasing biomass blending ratio (BBR)

6.2.3 Gaseous emissions

The effect on NO_x emissions due to increasing BBR in air and oxygen-enriched air conditions is presented in Figure 6.3. Although emissions measurements corrected to 6% [O_2] in the flue gas of an air-fired case are presented for completeness, on account of the variability detailed in Section 3.4.13.2 this work will discuss the results compared to the daily baseline.

In air, for both RCG and MC increasing BBR tended to slightly reduce NO_x emissions though by less than 10% which is approximately the limit of variation observed between experiments and similar to results found with fuels with similar fuel-N content [Munir et al., 2010, 2011]. Conversely, when cofiring with SRC at 8 and 15% emissions of NO_x tended to increase compared to their daily baseline and reduced to approximately the same amount as coal-firing for BBR of 20%. oxygen-enriched combustion increased NO_x emissions in all experiments compared to their air-fired counterparts except for high BBR of SRC where levels were similar. The largest increase of approximately 30% compared to the daily baseline was observed for 8 and 15% BBR of MC.

Variation in SO_2 emissions due to increasing BBR in air and oxygen-enriched air conditions are shown in Figure 6.4. Here, increasing BBR overwhelmingly led to a reduction in emissions of SO_2 for all biomasses in both combustion conditions. At BBR of 8 and 15%, combustion in air was observed to generally reduce SO_2 emissions more than in oxygen-enriched air, though a reversal of this trend was found for BBR of 20%. During air firing the reduction in emissions of SO_2 was almost linear with increasing BBR similar to that reported elsewhere [Bartolomé and Gil, 2013]. For oxygen-enriched conditions a precise trend is more difficult to identify though reductions in SO_2 of approximately 10% and 20% were observed with BBR of 15% and 20%, respectively.

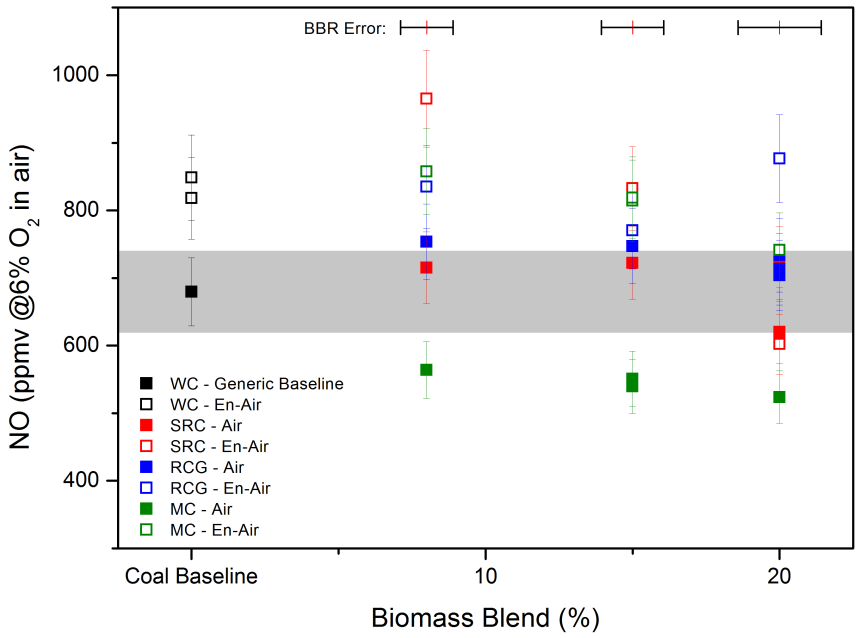

(a)

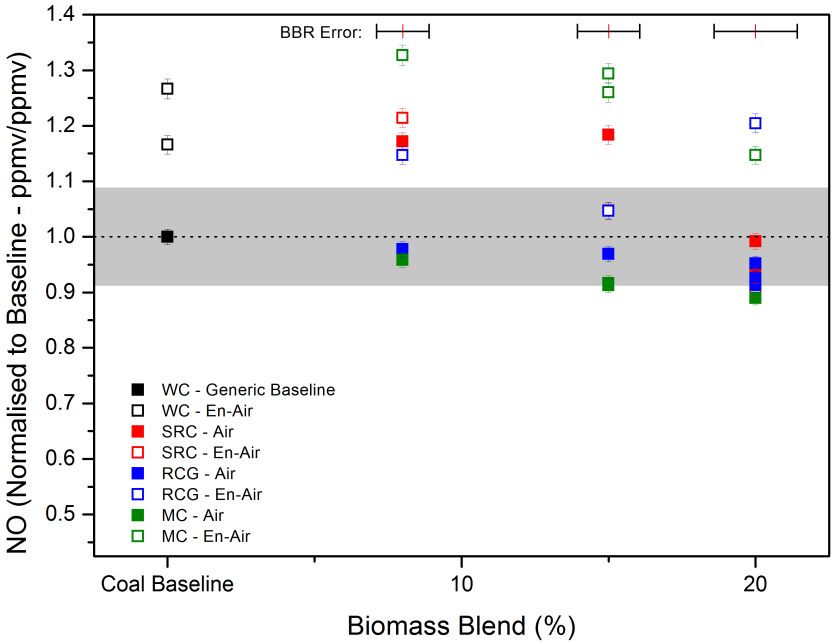

(b)

Figure 6.3: Variation in emissions of NO with increasing biomass blending ratio (BBR) in (a) absolute terms and (b) compared to the daily baseline value

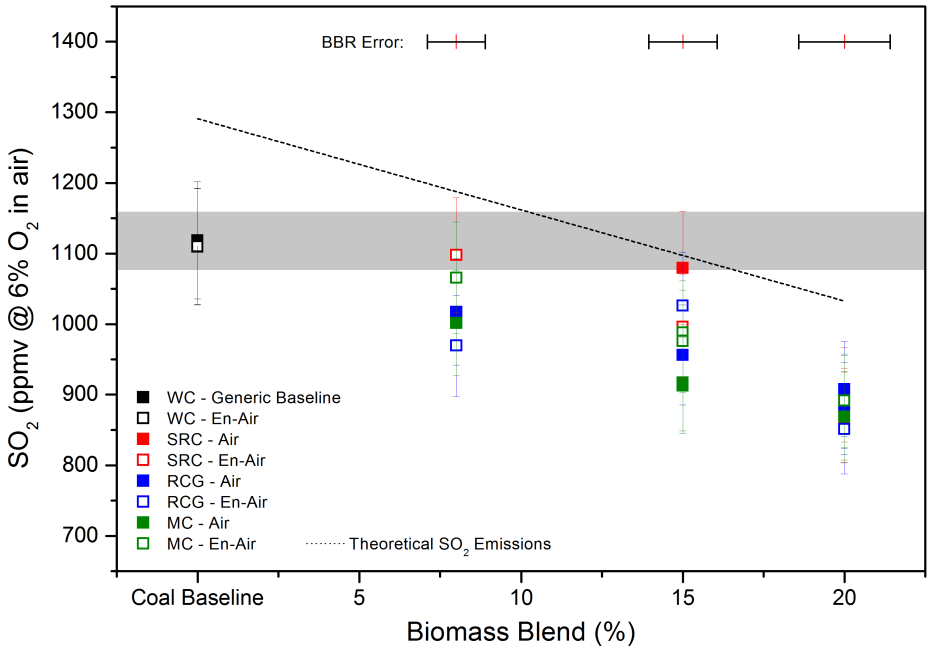

(a)

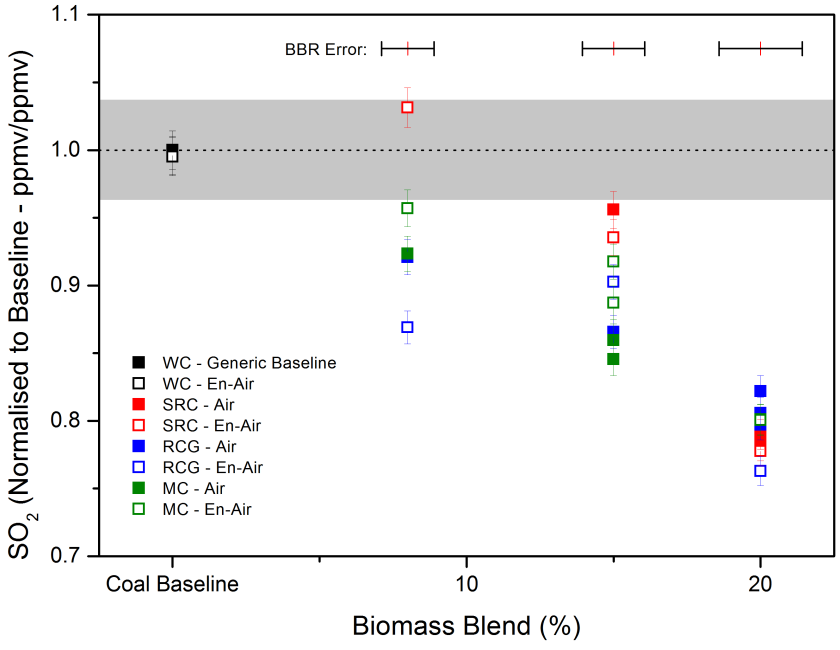

(b)

Figure 6.4: Variation in emissions of SO_2 with increasing biomass blending ratio (BBR) in (a) absolute terms and (b) compared to the daily baseline value

6.2.4 Ash analysis

Figures 6.6 and 6.7 show SEM images for the ashes collected in air and oxygen-enriched air combustion for coal firing and cofiring with SRC, RCG and MC at 15% BBR. Elemental maps generated by EDX analysis are shown for coal and 15% BBR in air and oxygen-enriched air combustion in Figures 6.8 to 6.11. Figure 6.12 presents the results of XRF analysis and the alkali index and base-to-acid ratio fouling indicators calculated for each of the ashes.

Comparison between the SEM images for air and oxygen-enriched air suggests combustion in increased [O_2] tends to result in higher number of spherical particles observed. In air-fired ashes, although the majority of particles observed are spherical, a broader mixture of particle shapes and sizes are observed than in oxygen-enriched firing ashes. Although some larger spherical particles are observed in the coal ashes, the number of these appears to increase during biomass firing alongside a larger number of smaller spherical particles. In air the ashes of RCG and MC appear similar to the coal ash while the SRC cofired ash displays larger, more aggregated, non-spherical particles than the other ashes. In oxygen-enriched combustion all of the ashes contain fewer non-spherical particles and RCG and SRC ashes tend to exhibit a greater degree of attachment of small particles to each other as well as adhering to larger particles than observed in the coal ash. The ash for MC cofired in oxygen-enriched conditions appears very similar to the coal.

As with the WC baseline ash sample (Figure 3.19), Si, Al and K dominate the element maps with Fe, S and Ca also observed but less ubiquitously. However, the XRF results suggest that in terms of composition the oxides of Si, Al and Fe dominate with Ca, K, S, Mg and Ti also representing $>$1% of the total mass. This discrepancy is explained by the fact that EDX estimates composition based on a molar basis while the XRF results are presented as mass fractions. For all fuel mixtures when oxygen-enriched air was used to fire the samples the relative amount of Fe in the ash typically increased slightly while the relative amounts of Si and Al reduced. For coal, the oxides of Si, Al and Fe constituted approximately 89% of the ash content which reduced to approximately 85%, 87% and 84% when cofiring with SRC, MC and RCG, respectively. This reduction in the major compounds was compensated by an increase in the amount of K, Ca and Mg from approximately 7.5% of the coal as to 9.8%, 8.5% and 11.0% for SRC, MC and RCG cofiring reflecting similar results with cereal co-product [Hussain et al., 2013]. For coal, firing in oxygen-enriched conditions

increased the amount of sulphur in the ash while when cofiring biomasses the amount of SO_3 detected in ash reduced in oxygen-enriched combustion. Cofiring of SRC and RCG significantly increased the amount of Ca and S compared to coal firing in air though the reduction when cofiring in oxygen-enriched conditions discussed above caused the relative amount of S in ash to fall to equal or below that observed for the coal firing. The level of potassium observed increased when cofiring with all of the biomasses compared to coal firing from 2% to 3–4%. The increase in the level of alkali and alkaline earth metals is one of the reasons for the increase in the Alkali Index and Base-to-Acid ratio observed when cofiring SRC and RCG in particular. Figure 6.5 shows a sulphur balance across the furnace for the range of experiments where the concentration of SO_3 measured in the fly ash is assumed to be representative of the sulphur content in all ash species. The results suggest during coal-firing approximately 10% of the sulphur present in the fuel cannot be accounted for and is therefore assumed to have been deposited on the furnace walls or, in much lesser amounts, emitted as gaseous SO_3. During cofiring of SRC and RCG the amount of sulphur accounted for approaches (and even appears to exceed) the amount entering in the fuel. This is driven by an increase in the sulphur content of the sampled ash and the reduced amount of sulphur entering in the cofired mixtures. Cofiring with MC, which has a very low ash content, produces similar results to coal-firing. Particularly in equipment operating with recycled flue gas, the ratio of SO_2 and SO_3 is important due to the potential effects on the acid dew point. Although SO_3 could not be measured in the current set up and no flue gas was recycled, it would be interesting in future work to investigate the impact of cofiring on the production of SO_3 in such situations.

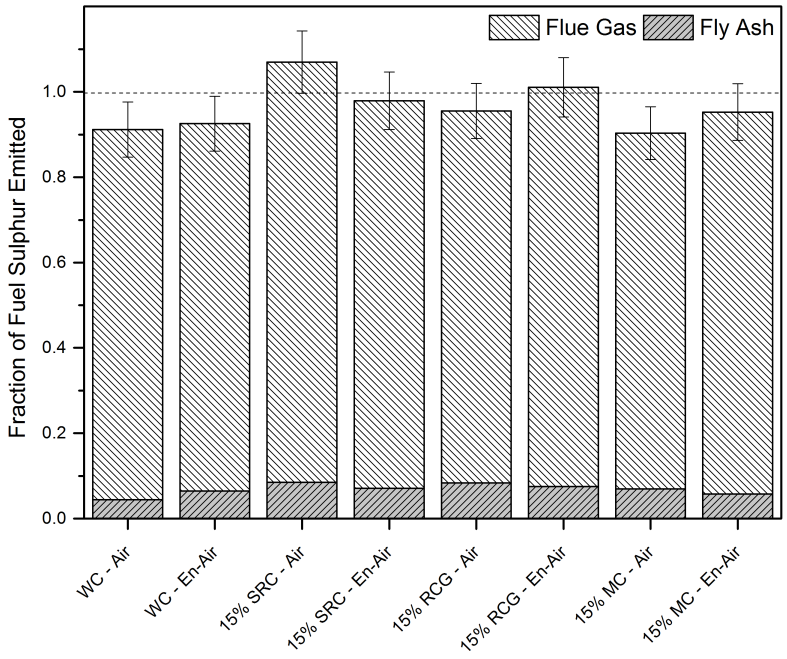

Figure 6.5: Sulphur balance across the furnace comparing sulphur emitted as gaseous SO_2 and as SO_3 in the fly ash. The error bars represent the error associated with the SO_2 measurement presented in previous figures.

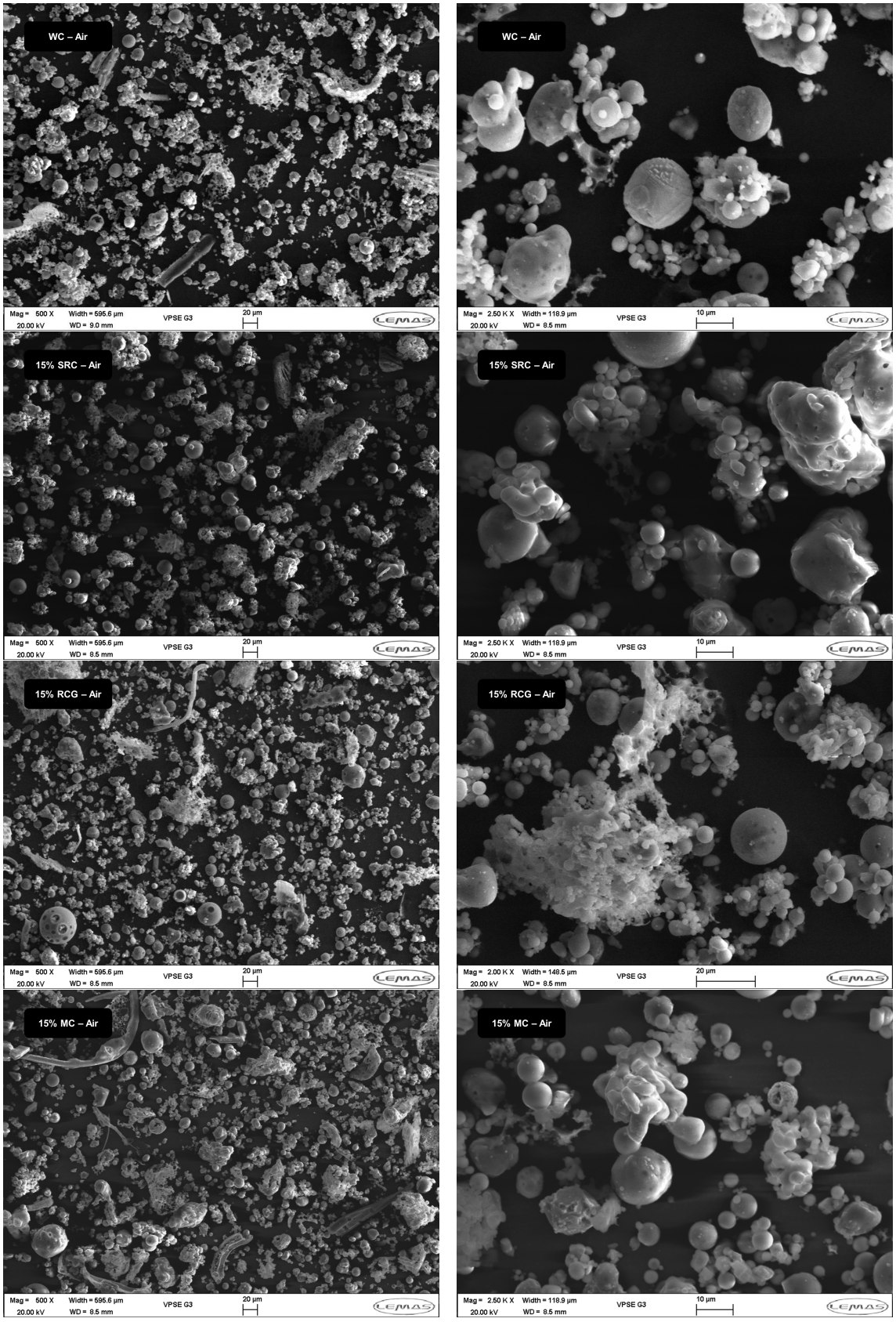

Figure 6.6: SEM images of the ash residue from combustion in oxygen-enriched conditions for WC and 15% BBR of SRC, RCG and MC at approximately 500x and 2500x magnification

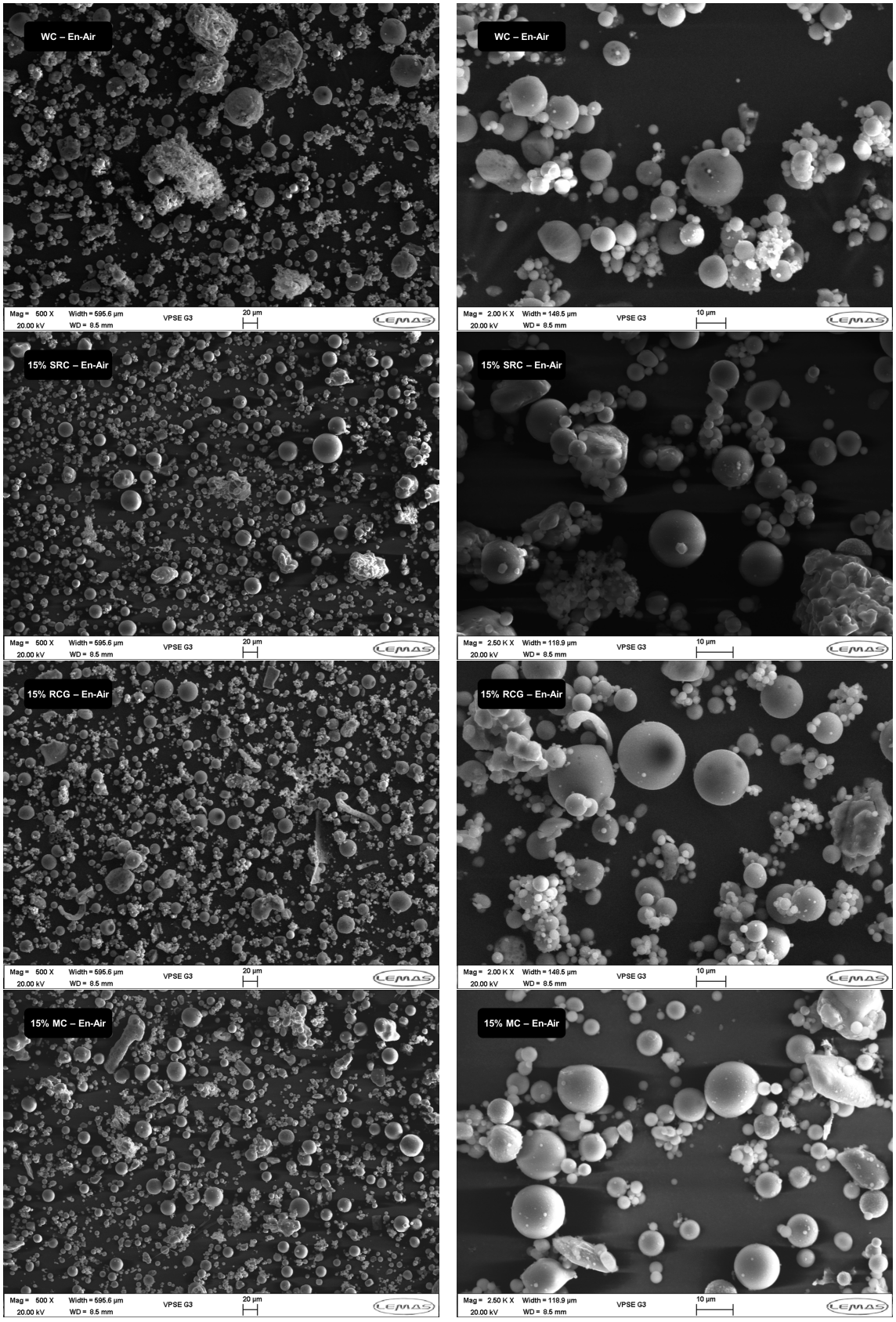

Figure 6.7: SEM images of the ash residue from combustion in oxygen-enriched conditions for WC and 15% BBR of SRC, RCG and MC at approximately 500x and 2500x magnification

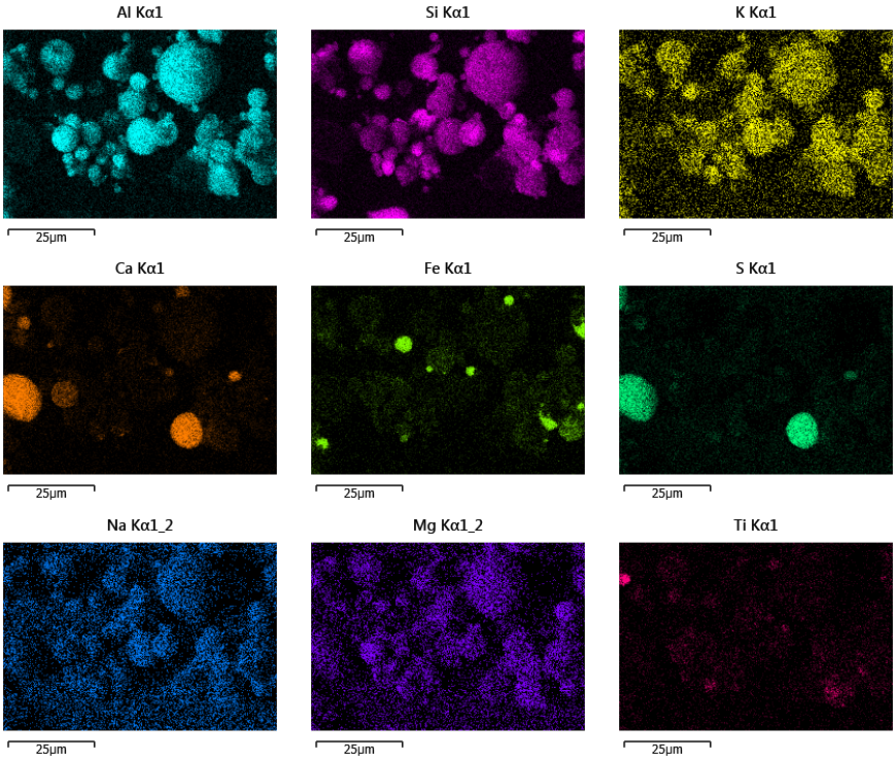

Figure 6.8: Elemental mapping of elements present in ash collected from experiments firing WC in unstaged, oxygen-enriched air experiments

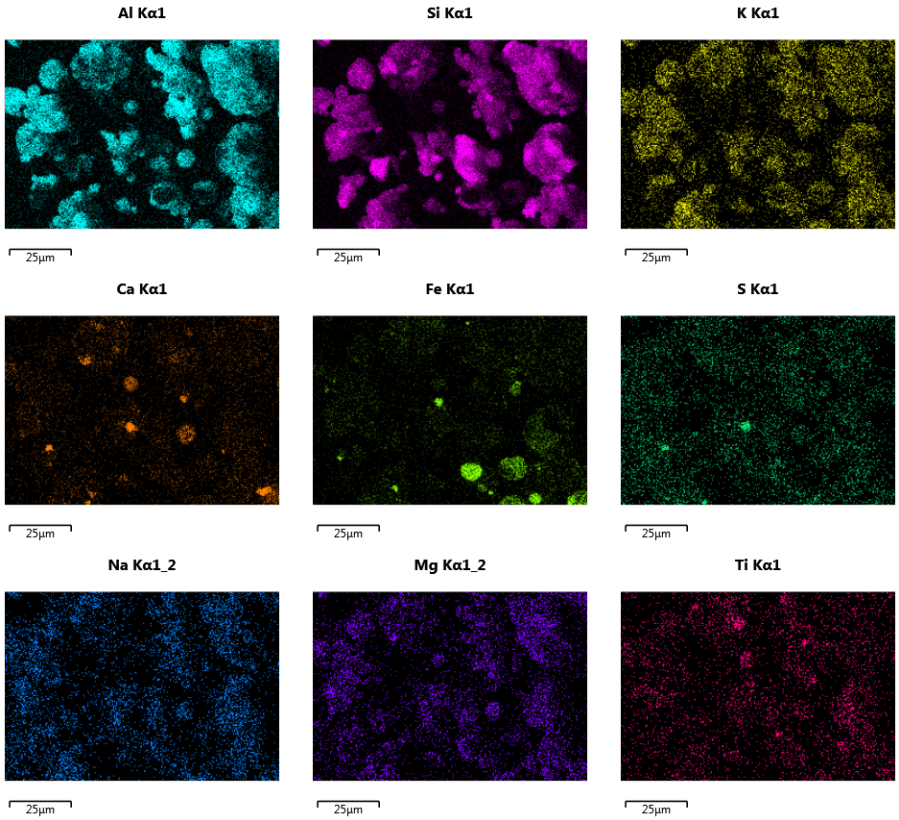

(a) Air

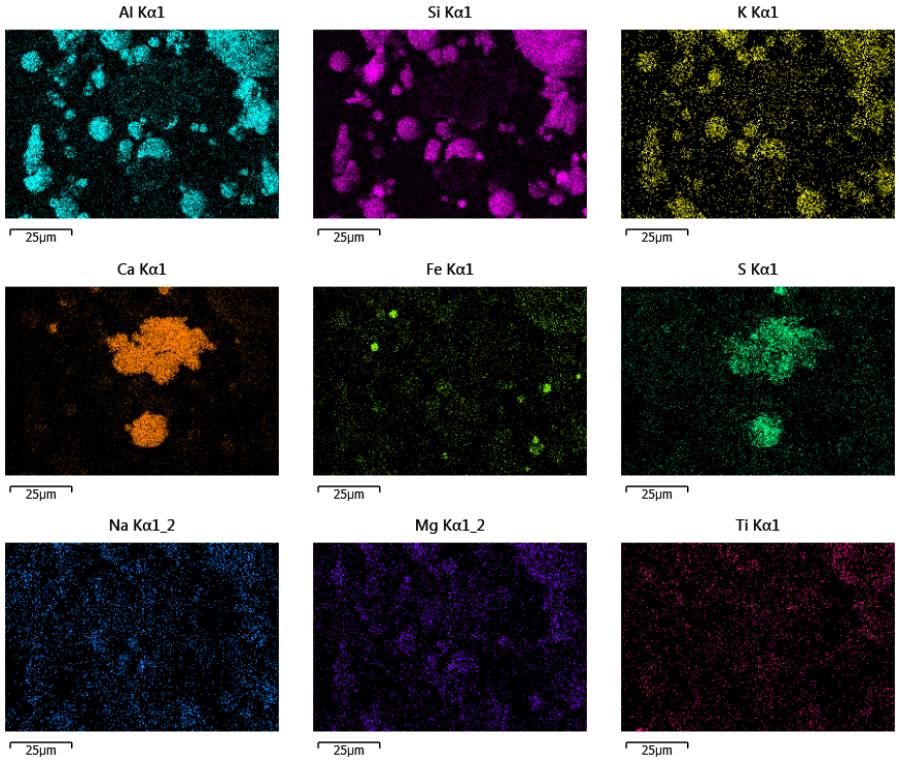

(b) Oxygen-Enriched Air

Figure 6.9: Elemental mapping of elements present in ash collected from experiments cofiring WC and 15% SRC in unstaged air and oxygen-enriched air experiments

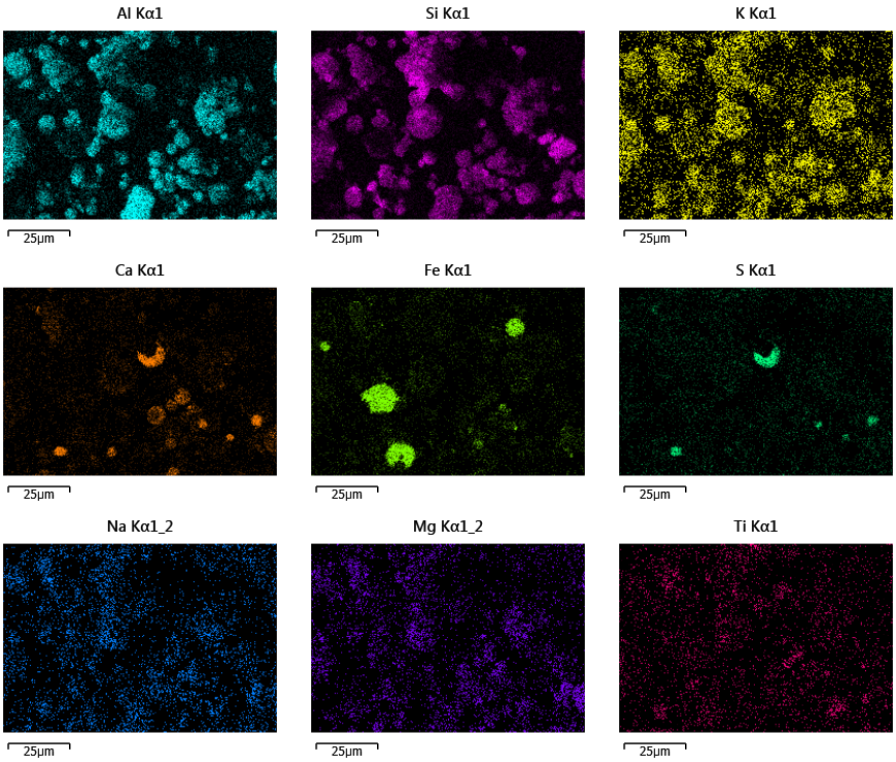

(a) Air

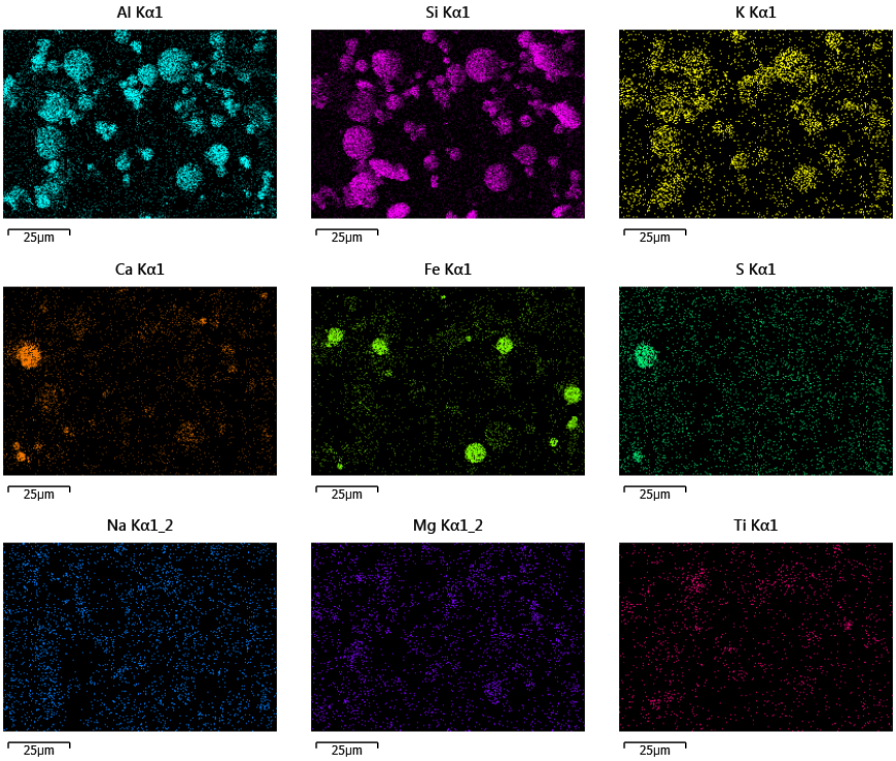

(b) Oxygen-Enriched Air

Figure 6.10: Elemental mapping of elements present in ash collected from experiments cofiring WC and 15% MC in unstaged air and oxygen-enriched air experiments

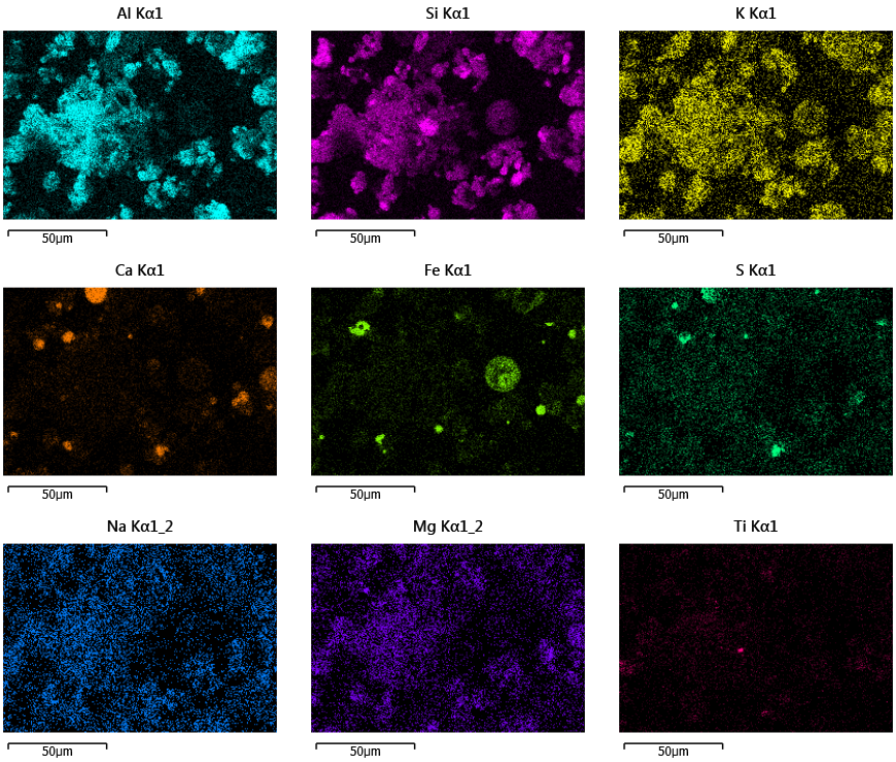

(a) Air

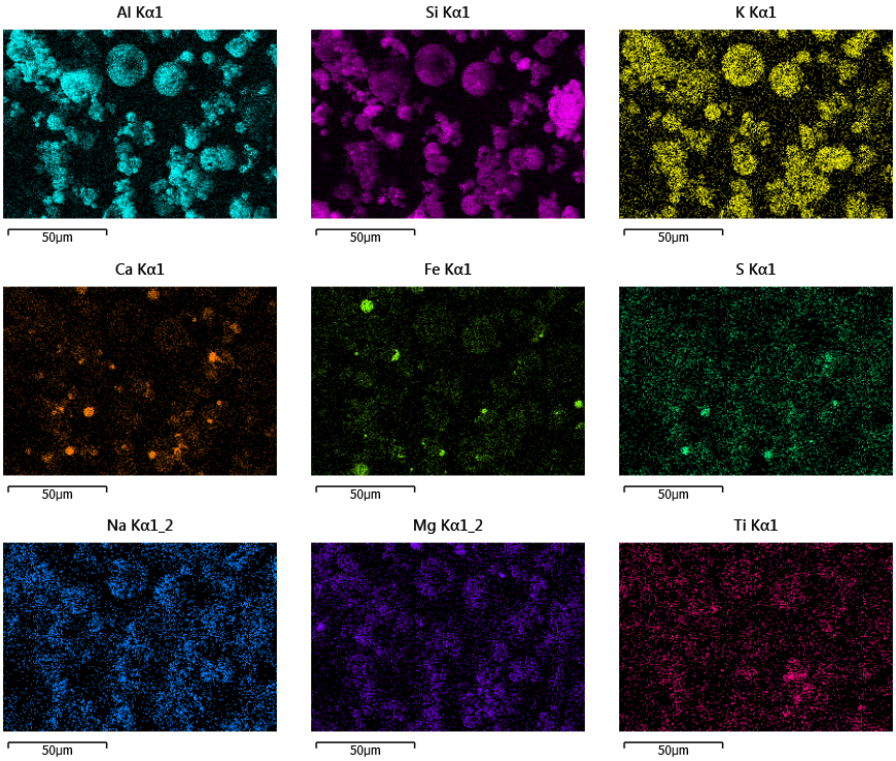

(b) Oxygen-Enriched Air

Figure 6.11: Elemental mapping of elements present in ash collected from experiments cofiring WC and 15% RCG in unstaged air and oxygen-enriched air experiments

Mass fraction of oxide (%)								
Oxide	**WC Air**	**WC En-Air**	**SRC Air**	**SRC En-Air**	**MC Air**	**MC En-Air**	**RCG Air**	**RCG En-Air**
SiO_2	52.71	51.92	50.69	50.52	53.93	53.52	53.70	53.91
TiO_2	1.16	1.09	1.13	1.12	1.09	1.06	1.04	1.01
Al_2O_3	21.22	21.10	20.92	20.71	20.16	19.87	18.52	17.84
Fe_2O_3	14.60	14.94	13.26	14.10	12.80	13.93	11.80	12.29
Mn_3O_4	0.08	0.07	0.08	0.07	0.07	0.07	0.10	0.10
MgO	1.03	0.97	1.20	1.18	1.21	1.19	1.37	1.39
CaO	4.19	4.01	4.98	5.14	4.11	4.10	5.49	5.69
Na_2O	0.71	0.75	0.76	0.76	0.74	0.75	0.73	0.71
K_2O	2.20	2.65	3.69	3.45	3.14	3.23	4.05	4.03
P_2O_5	0.13	0.12	0.44	0.52	0.40	0.32	0.77	0.81
SO_3	1.39	2.04	2.44	2.05	1.98	1.63	2.03	1.83
V_2O_5	0.05	0.04	0.05	0.05	0.05	0.04	0.05	0.04
Cr_2O_3	0.08	0.03	0.02	0.02	0.03	0.03	0.02	0.03
SrO	0.04	0.04	0.04	0.04	0.04	0.03	0.04	0.04
ZrO_2	0.07	0.06	0.07	0.07	0.06	0.06	0.06	0.06
BaO	0.05	0.04	0.05	0.05	0.05	0.04	0.05	0.06
NiO	0.05	0.02	0.02	0.02	0.02	0.02	0.02	0.02
CuO	0.09	0.03	0.03	0.02	0.03	0.02	0.02	0.02
ZnO	0.11	0.05	0.08	0.07	0.06	0.05	0.08	0.07
PbO	0.03	0.03	0.03	0.03	0.03	0.03	0.03	0.03
HfO_2	0.01	0.01	0.01	0.00	0.00	0.01	0.01	0.01

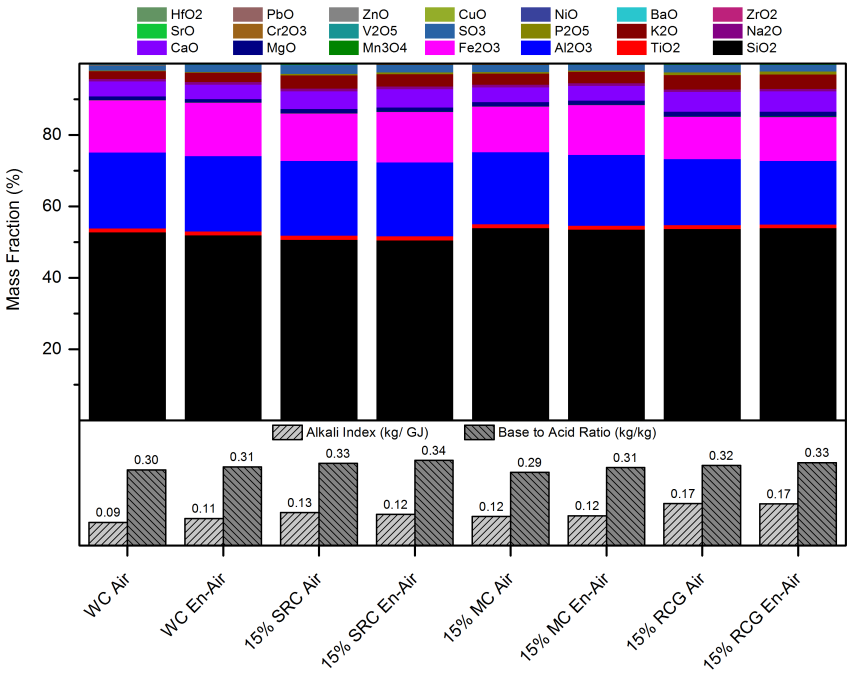

Figure 6.12: Results of XRF analysis presenting relative composition and calculated fouling indicators for coal and cofired ashes fired in air and oxygen-enriched atmospheres

6.2.5 Discussion of impact of BBR

The results in the previous subsections confirm that the substitution of coal with biomass has consequences during combustion, affecting combustion temperatures, carbon burnout and solid and gaseous emissions from the process. This subsection answers research question 3 in Section 2.9 by discussing and concluding from the results presented in this section using the combustion theory presented in Chapter 2, the fuel characterisation data presented in Section 3.2 and the findings of the bench-scale experiments presented in Chapter 5.

During combustion in air, increasing the amount of biomass tended to reduce the temperature observed nearest the burner (T_1 = 45 cm from burner throat) though as the combustion mixture travelled further along the furnace the temperatures in the cofired mixture tended to increase compared to the coal baseline. Together these temperatures suggest substituting coal with biomass delayed the combustion process and pushed it further along the furnace as is consistent with the literature reported in Section 2.5 [Splieth-off and Hein, 1998, Williams et al., 2012]. There are several reasons that may contribute to the observation of this effect.

First, the increased moisture content of all of the biomass resources compared to the coal would increase the amount of heat required to dry each fuel particle and heat it and the surrounding gases. The increase in moisture is multiplied as the lower CV of the biomass requires a larger mass of biomass fuel to be delivered to compensate for the amount of coal it is replacing.

Second, the significantly larger, less spherical particle sizes of the biomasses, as shown in Figures 3.7 and 3.8, are likely to extend particle heating times. This potentially delays the release of volatiles and reduces the rate of char burnout as oxygen from the bulk atmosphere must diffuse further into the particle to react with the fixed carbon (assuming the large particles do not explode when heated). Although the proximate analysis in Section 3.2.1 and the TGA experiments in Chapter 5 indicate that biomass samples devolatilise at lower temperatures than coal particles, the particle sizes of the fuel samples in the TGA experiments were reduced and they were heated at a much slower heating rate negating the thermal and species gradients that may have occurred during firing at 20 kW scale.

Third, although the biomass fuels display a higher volatile matter content than coal, the FTIR analysis in Section 3.2.4 and the significantly lower oxygen content of the coal suggest that the coal volatiles may contain a greater calorific value than those of the biomass, which were more likely to consist of simpler molecules with a greater degree of carbon oxidation. Thus, the combustion of these molecules may lead to a reduction in the increase in temperature compared to the temperature increase from combustion of coal-derived volatiles reducing the temperature nearest the burner. The considerably larger SRC sample displays considerably different behaviour to the other biomass samples which is mainly attributed to the difference the distribution in size and shape of its particles. However, due to the many possible reasons for accelerating or delaying combustion, it is difficult to compare between the MC and RCG biomass samples. For example, while the temperature profiles in air show that the temperature at T_2 for MC blends was slightly lower than for RCG blends, ascribing the particular reason for this includes complex and opposed reasoning. Combustion at T_2 may be higher with RCG as it is likely that on account of having a lower NCV than MC more fuel particles are added to the burner for every kW of energy which would act to increase the overall surface area for reaction. However, counter to this is the fact that RCG displays a slightly larger particle size than MC which would act to reduce the active surface area. Similarly, although MC particles comprise of more hemicellulose and cellulose than RCG particles, the high ash content in RCG may offer catalytic properties to the combustion reactions.

Despite the reduction in temperature near the burner, the increase in overall carbon burnout observed when cofiring suggests that the slight increase of temperatures further downstream in the furnace permit a greater proportion of combustion than in the coal-firing case. This could be due to an increased proportion of combustion occurring as volatile combustion (albeit delayed compared compared to coal) or due to the increased reactivity of biomass chars due to their catalytic content and intrinsic oxygen content as suggested by Williams et al. [2012]. The results in Figure 6.2 show that while up to 15% BBR increased the burnout of the blend, increasing BBR from 15 to 20% begins to reduce the burnout. It is suggested that the maximum burnout values at 15% BBR reflect an optimum trade off between increased reactivity of the biomass chars when heated mainly by the combustion of the coal particles and the decreasing temperature of combustion due to the increased biomass content, which contains higher moisture in larger particles which delay combustion. That this reduction is most acutely observed when firing the largest bio-

mass particles (SRC), which also show the largest reduction in combustion temperatures at T_1 with increasing BBR is thought to support this.

When firing with oxygen-enriched air, the trend observed for air firing is exaggerated for the SRC but the reduction in temperature observed at T_1 is no longer apparent for the other biomasses which, along with coal, combust at a substantially higher temperature. In the case of oxygen-enrichment it is suggested that the delay in combustion caused by the increased moisture and particle size of the biomasses is sufficiently countered by the higher temperature of the combustion system. This increased temperature provides a more intense combustion reaction as the volume of the combustion gases, and therefore the impact of thermal and chemical dilution, is reduced which leads to higher particle temperatures and devolatilisation rates as reported [Khatami et al., 2012, Murphy and Shaddix, 2006]. Since burnout values are already higher in oxygen-enriched conditions (typically $\sim$99.8%), there is less scope for improvement by blending biomass. However, a similar trend to that described for air firing is observed, though the effect on carbon burnout with varying BBR is of a considerably smaller magnitude.

Both cofiring and oxygen-enriched combustion appear to impact the ash produced from the furnace with the increased burnout in both situations leading to an increased number of smaller, spherical ash particles than observed for the baseline. Direct comparisions between the ashes are complicated by the variation in ash content and particle size of each fuel mix. For example, although the burnout calculation normalises for differing ash content of the fuels, the low ash content of SRC and MC means despite contributing $\sim$ 22% of the mass to the fuel mix they contribute only $\sim$ 9% to the ash mass while RCG contributes approximately 22%. Conversely, other things being equal, the larger particles of SRC compared to the other biomasses are more likely to be carried through the furnace uncombusted. In light of this, it is unsurprising that the ashes for cofiring with MC are very similar to the coal firing and that the ashes from the RCG blend show the largest changes in the XRF results. Similarly, when comparing the sizes of some of the SRC particles shown in Figure 3.8 it is not surprising that some of the particles in the air-fired SRC ashes appear larger and less spherical than those observed in the baseline. In oxygen-enriched conditions, the disappearance of these irregular particles suggest, in agreement with the increased burnout values, that the large SRC char particles are more fully oxidised by exposure to the increased temperatures and local [O_2].

Increasing BBR for RCG and MC tended to slightly reduce NO_x emissions but by a lower amount than comparison with the ultimate analysis in Table 3.1 might suggest (WC N-content is 1.7%, RCG is 1.4% and MC is 0.3%) though MC did consistently reduce NO_x emissions slightly more than RCG. Similarly, the increase in NO_x emissions that occurred when cofiring SRC indicates that the ultimate content of the fuel is not the most important factor in understanding NO_x emissions, as suggested by Kazagic and Smajevic [2009]. Indeed, that the emissions are significantly lower than predicted if all of the fuel-bound nitrogen was converted to NO_x (as detailed in Table 3.4) suggests that chemical pathways during combustion are more important than fuel inputs in determining NO_x emissions. Since no oxidant staging or other NO_x-reducing strategies are employed until the following set of experiments it is perhaps unsurprising that within the range of variability little differences are observed in NO_x emissions when BBR is increased.

Combustion in oxygen-enriched conditions was observed to increase NO_x emissions most probably because of the increased local concentration of O_2 available to fuel-N volatiles when they are released from the particles. The increased [O_2] increases the likelihood that volatile N-containing intermediate compounds will be oxidised to NO rather than reduced to N_2 and agrees with published data for unstaged flames [Daood et al., 2011, Thompson et al., 2004]. It is also possible that the reduction in thermal diluent may elevate temperatures in the burner sufficiently to promote thermal-NO formation though without temperature measurements closer to the burner this cannot be verified. Although reducing the amount of N_2 entering the furnace may also be expected to reduce the amount of prompt-NO formation the large excess of N_2 still likely to be available indicates any change would be negligible. In addition, were a reduction to occur, this is likely to occur alongside and be dominated by the other NO-formation mechanisms, particularly the increased fuel-N pathway, which are likely responsible for the higher observed NO emissions in oxygen-enriched conditions owing to the typical proportions of NO formation discussed in Section 2.3.1.

That emissions of NO_x are generally higher than those for coal when cofiring with SRC up to 20%, despite the lower fuel-N content (0.4%), may be explained by considering again the large particle size of the SRC fuel (Figure 3.7). In this situation, devolatilisation of the SRC sample would be delayed due to a delay in particle heating and an increased amount of moisture compared to coal-firing. Together these factors would reduce the competition for O_2 when the coal particles are devolatilising effectively increasing the

local [O_2] which would lead to an increase in coal-derived N-intermediates being oxidised to NO rather than reduced to N_2. This effect is not observed for the other biomasses which have mean particle diameters approximately half the size of the SRC sample and therefore are able to devolatilise more rapidly and compete with the coal volatiles for O_2. Increasing BBR past 15% tends to reduce temperatures near the burner which would act to reduce thermal-NO formation and the rate of devolatilisation somewhat negating the phenomena described above. At higher BBR it is suggested the impacts of temperature reduction begin to dominate and ultimately reduce NO emissions compared to lower levels of BBR.

Unlike the relationship between BBR and NO_x emissions, emissions of SO_2 are directly related to the ultimate composition of the fuel mix entering the furnace and reduce with increasing BBR due to two factors. First, the reduction in fuel-S reduces the amount of S available to be oxidised to SO_2. In unstaged air-firing, unlike NO_x emissions, which in practice were found to be far less than predicted had all of the fuel-N been oxidised, practical emissions of SO_2 were observed to reflect $>$85% conversion of fuel-S to SO_2. This higher conversion indicates that a reduction in fuel-S is more likely to reduce the amount of sulphur than can be oxidised and emitted as SO_2. Second, the increasing amount of alkaline earth metals in the biomass samples, in particular Ca as identified in the EDX element mapping and XRF analysis in Figure 6.12, increased the amount of sulphur retained in the ash. In fact, despite reductions in the amount of sulphur entering the system, in all air-firing situations the ash-S content for cofired tests observed in XRF testing was greater than when firing coal alone, as shown in Figures 6.5 and 6.12.

It is difficult to draw specific trends from oxygen-enriched conditions that suggest changes from air-fired cases suggesting, unlike NO_x emission formation, combustion chemistry is less important than the amount of sulphur entering the furnace in affecting SO_2 emissions in the flue gas.

The base-to-acid ratios presented in Figure 6.12 were observed to change little from that observed during coal-firing. However, as Salour et al. [1993] note, the addition of biomass may reduce the base-to-acid ratio that least desirable ash behaviour is observed at and so it is not clear from these results alone whether ash deformation is significantly more likely when cofiring.The results of the alkali index calculations also shown in Figure 6.12 suggest that when cofiring the biomasses at 15% in air and En-Air the MC and SRC ensure ashes that are unlikely to form sticky deposits. The alkali index value of 0.17

for 15% RCG is on the lower threshold for the possibility of fouling for both combustion environment suggesting further testing in this area may be required to fully identify ash behaviour.

6.3 Impact of oxidant-staging while cofiring in air and oxygen-enriched air

6.3.1 Experimental design

This section is designed to answer research question 4 in Section 2.9. Here, the amount of oxidant-staging in combustion experiments was investigated at a burner stoichiometric ratio (BSR) of 1.16. 1.0, 0.9 and 0.8 with coal alone and cofired with each of the three biomass samples at 15% BBR. The tests were conducted in air and oxygen-enriched air (30% [O_2]). Since the oxygen in the primary line could not be enriched, enrichment was carried out in the secondary and over-fired air (OFA) lines only, as detailed in Section 3.4.9. In the following figures, BSR Error represents the combined experimental error associated with the rotameters used to control the gas flows and that associated with the fuel feeders, calculated as described in Section 3.4.13.2.

6.3.2 Combustion characteristics

Figure 6.14 shows the temperature profiles recorded in the furnace for combustion of coal and coal-biomass blends (15% BBR) at various levels of oxidant staging, which is measured as decreasing burner stoichiometric ratio (BSR). When firing coal in air, increasing the amount of oxidant staging (reducing BSR) tends to increase the temperature nearest the burner (T_1) and reduce temperatures towards the end of the furnace (T_3) while temperatures midway along the furnace (T_2) tended to remain relatively constant or reduce slightly as BSR reduced.

Under oxygen-enriched conditions temperatures were substantially higher for all cases studied. At T_1 reducing BSR from 1.16 tended to very slightly increase temperature until BSR = 0.9, when further staging tended to slightly reduce observed temperatures. At T_2, a similar trend was observed though temperatures began decreasing at staging levels

beyond BSR = 1.0. Conversely to findings in air-firing, at T_3 the temperature increased by approximately 40 °C in a linear fashion when BSR reduced from 1.16 to 0.8.

The temperature trends for each biomass blend were similar to those observed for coal-firing though trends were observed to shift slightly differently for each biomass.

Similar to the findings for unstaged combustion, cofiring with SRC tended to reduce the combustion temperatures at T_1 particularly at unstaged and deep-staged oxygen-enriched combustion conditions, have little change at T_2 and slightly increase temperatures at T_3 compared to coal firing for most levels of oxidant-staging. However, during deep-staging (BSR = 0.8) of SRC in En-Air the temperature was significantly reduced throughout the furnace compared to coal-firing.

Cofiring of MC similarly reduced temperatures in air firing at T_1 and slightly reduced temperature at T_2 and T_3 compared to coal-firing. In oxygen-enriched conditions the temperatures at T_1 and T_2 were very similar to those observed during coal firing while temperatures at T_3 were found to be slightly elevated for all levels of staging.

Unlike the other biomasses, cofiring with RCG in air increased temperatures in the early stages of combustion but, similar to MC, did effect a reduction in temperature at T_2 compared to coal firing along with a slight elevation of temperature at T_3 when staging was employed. In oxygen-enriched conditions temperatures were generally slightly greater than those for coal-firing at T_1, similar to coal-firing at T_2 and slightly greater again at T_3.

The effect on carbon burnout and CO emissions due to variation in oxidant staging for the coal and coal-biomass blends in air and oxygen-enriched air is shown in Figure 6.13. CO emissions showed a slight increase with extensive staging though emissions were generally less than 50ppm. However, during oxidant staging the burnout of all cofired mixtures was found to reduce compared to unstaged conditions with SRC and MC most sensitive to reducing BSR with burnout falling by as much as 0.5% for MC cofired at BSR = 0.85 which represented an increase in LOI from 3.5% for unstaged conditions to 7.6% for BSR = 0.85. Although the burnout levels under oxygen-enriched combustion were also observed to decrease with increasing oxidant staging, the reduction compared to the baseline conditions was generally smaller than in air-firing and even under deep staging (BSR = 0.8) the burnout for all fuel mixtures was at least as good as the unstaged, air-fired baseline conditions.

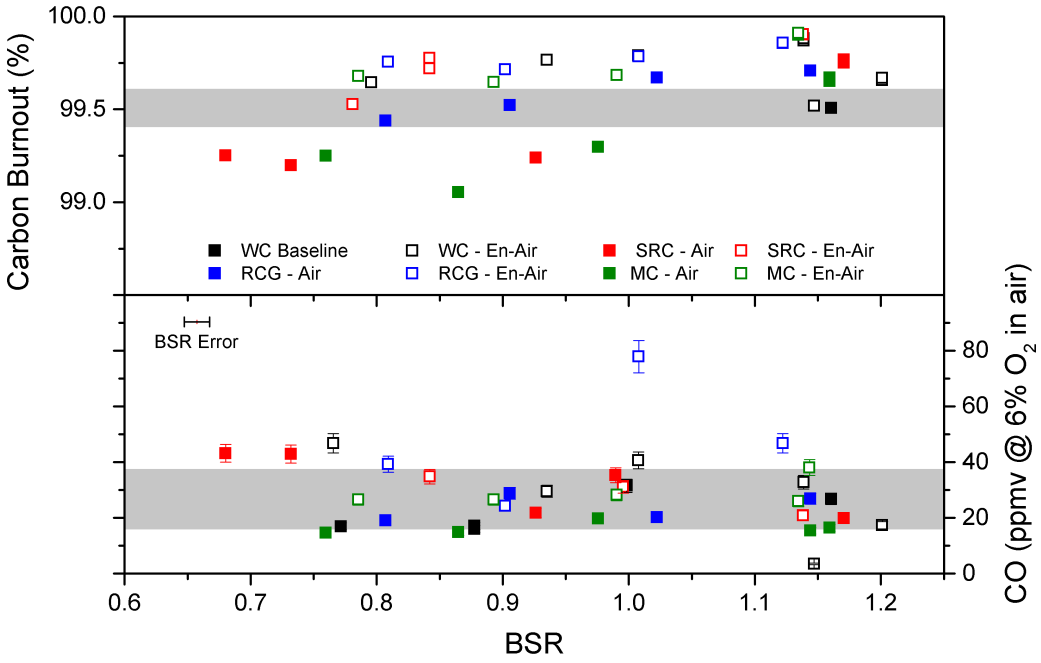

Figure 6.13: Variation in carbon burnout and CO emissions with increasing oxidant staging (reducing BSR)

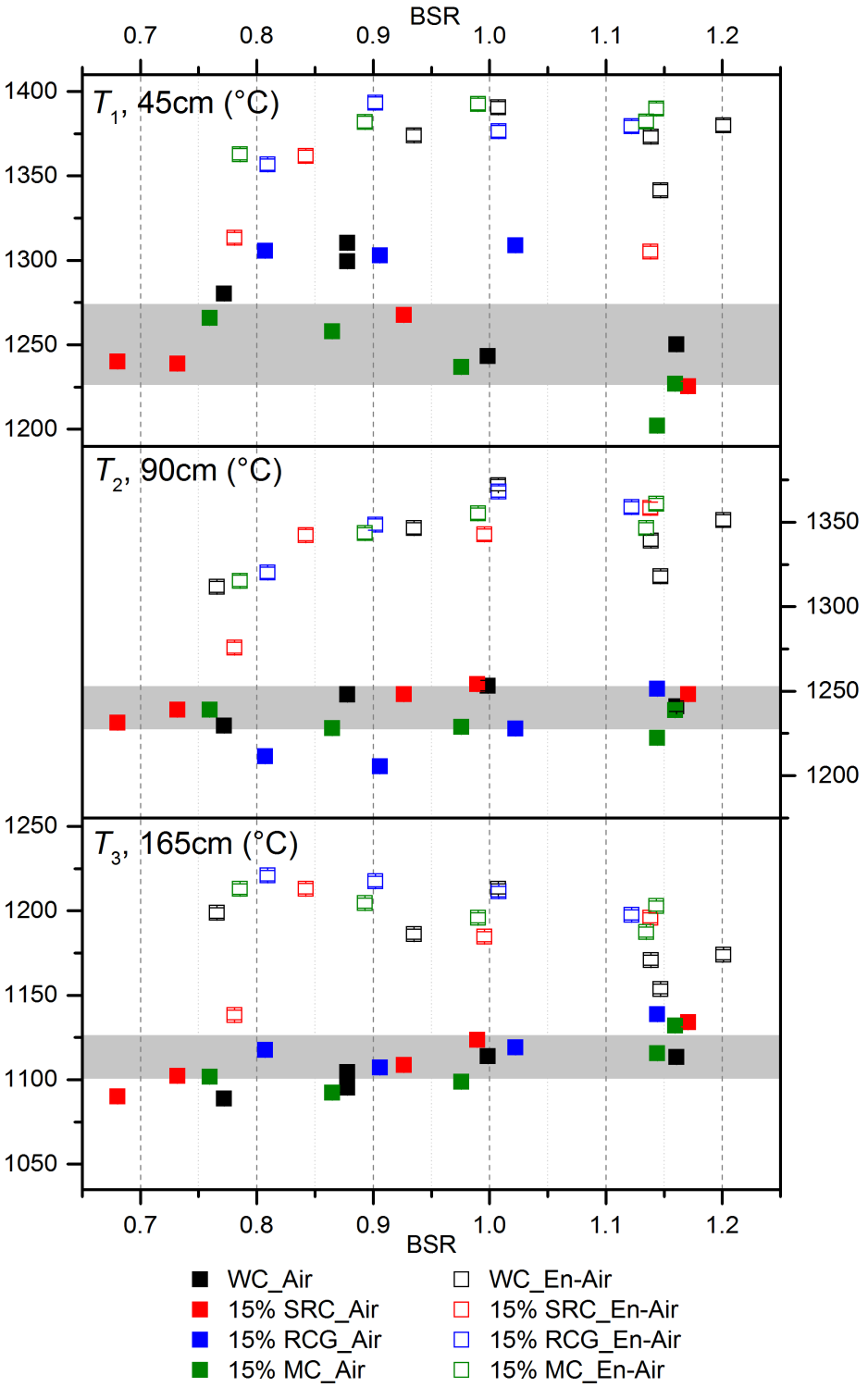

Figure 6.14: Variation in combustion temperatures at T_1, T_2, and T_3 with increasing oxidant staging (reducing BSR)

6.3.3 Gaseous emissions

Figure 6.15 shows the effect of oxidant staging on emissions of NO for firing coal and coal-biomass blends (at 15% BBR) in air and oxygen-enriched air. For coal-firing in air reducing BSR reduces NO emissions by approximately 60–70% in a linear fashion when BSR is reduced from 1.16 to ∼0.8. As reported in the previous section, in oxygen-enriched, unstaged conditions NO emissions are as much as 30% greater than observed for air firing of coal. However, as BSR is reduced NO emissions reduce more rapidly under oxygen-enriched conditions and at BSR = 1.0 NO emissions from oxygen-enriched combustion are similar to those for air firing. During oxygen-enriched combustion increasing staging past BSR = 0.9 cases the emissions of NO begin to level out as BSR is further decreased. In air firing emissions continued to decrease across this range resulting in similar NO emissions, which are about 70% lower than the daily baseline values, for coal in air and oxygen-enriched air when staging at BSR = 0.8.

During combustion in air, cofiring biomasses under oxidant-staged conditions appears to have little effect on NO emissions compared to coal-firing. However, in oxygen-enriched conditions when BSR <1.0 cofiring tended to slightly reduce emissions compared to coal-firing with NO emissions reduced by 80% compared to the daily baseline for cofired mixtures with BSR = 0.9–0.8.

Figure 6.16 shows the effect of oxidant staging on emissions of SO_2 for firing coal and coal-biomass blends (at 15%) in air and oxygen-enriched air. When firing coal in air reducing BSR tends to have little effect on SO_2 emission with only a slight increase observed as BSR decreases. In oxygen-enriched conditions a similar trend is observed but shifted slightly higher so that emissions in oxygen-enriched conditions are typically ∼10% greater than the daily baseline value at higher levels of oxidant staging. As noted in Section 6.2.3, in unstaged conditions biomass blending tends to reduce SO_2 emissions by approximately 5–15% in both air and oxygen-enriched air firing. However, as the level of oxidant staging is increased in both of these combustion atmospheres SO_2 emissions increasingly tend towards the results observed for coal firing. In air-firing emissions from coal and coal-biomass blends converged under deep staging at close to the value for the daily baseline. However, in oxygen-enriched combustion emissions from cofired fuel mixtures remain ∼5% lower than those from coal-firing under deep staging conditions.

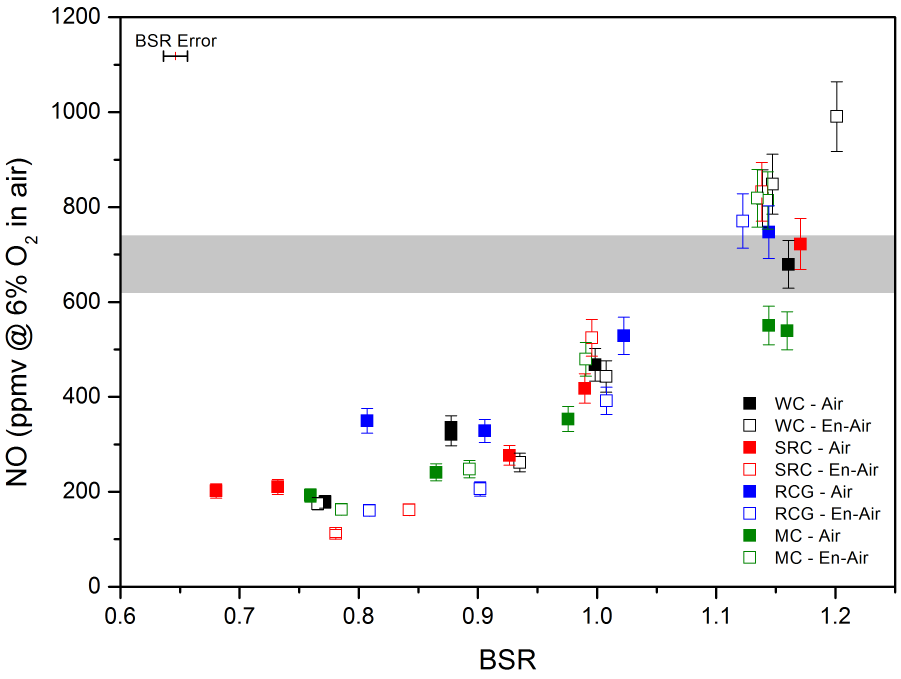

(a)

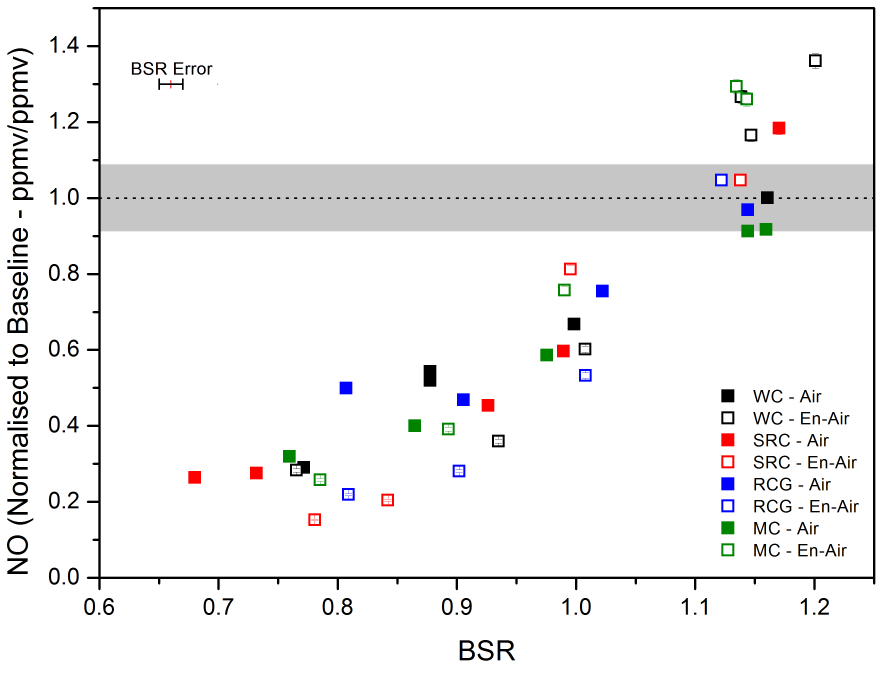

(b)

Figure 6.15: Variation in emissions of NO with variation in oxidant staging - measured as burner stoichiometic ratio (BSR) - in (a) absolute terms and (b) compared to the daily baseline value

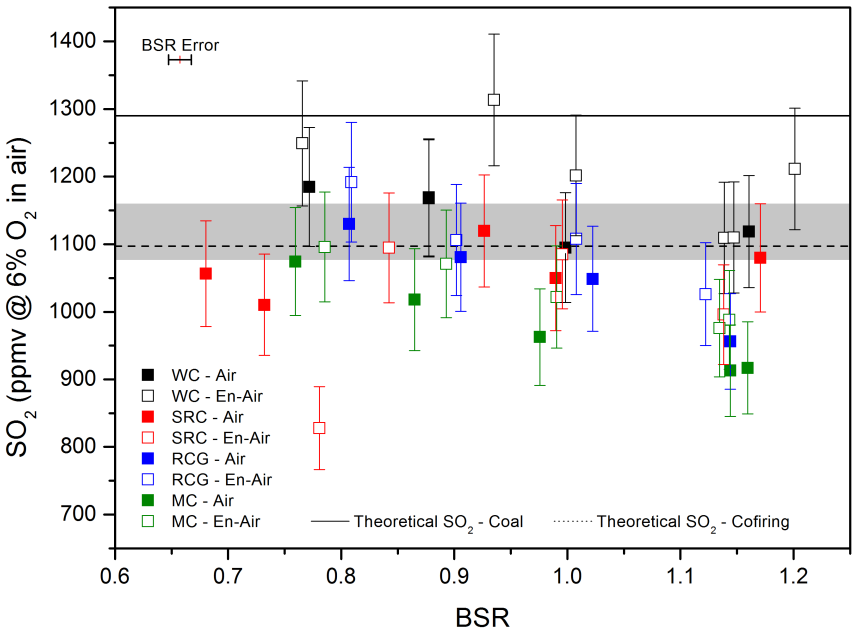

(a)

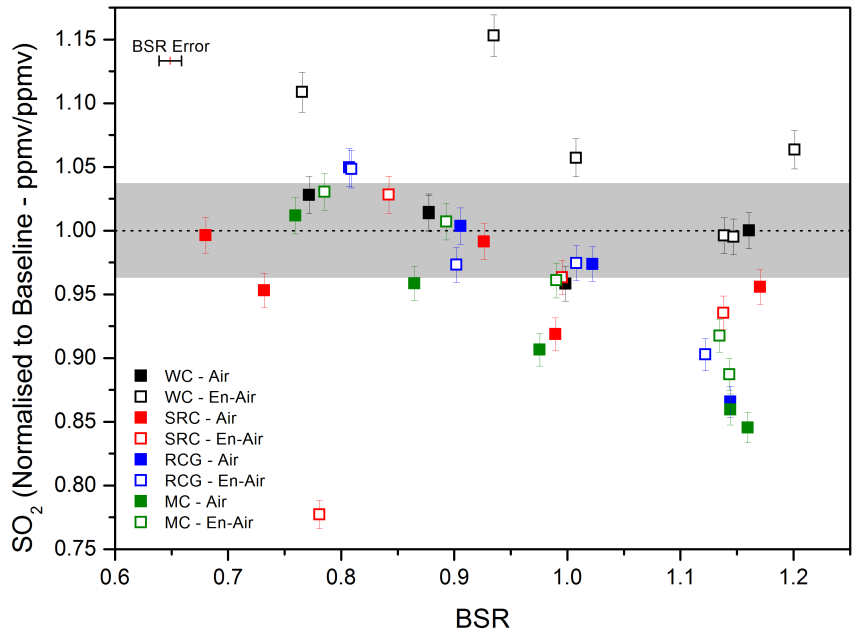

(b)

Figure 6.16: Variation in emissions of SO_2 with variation in oxidant staging - measured as burner stoichiometic ratio (BSR) - in (a) absolute terms and (b) compared to the daily baseline value

6.3.4 Discussion of impact of oxidant-staging

The results shown in the previous subsections illustrate that the practice of oxidant staging of coal and coal-biomass blends in air and oxygen-enriched air affects many aspects of the combustion process, including combustion temperatures, burnout and gaseous emissions from the process. Similar to the format of the previous experiment, this section will now attempt to explain the results using the combustion theory, fuel characterisation data and TGA experiments presented in Chapters 2, 3 and 5 to answer research question 4 in Section 3.4.9.

The process of oxidant staging essentially divides the furnace into a fuel-rich, zone with a sub-stoichiometric amount of oxygen and an oxidant-rich zone with a super-stoichiometric amount of oxygen present to ensure complete combustion. This has several implications for the combustion of fuels and as such affects the combustion characteristics and emissions from the furnace. In this work the injection of over-fired air (OFA) occurs in between thermocouples T_2 and T_3.

During air firing, as the extent of oxidant staging was increased, the temperatures at T_1 were also observed to increase. Such an increase in temperature during combustion could be due to two main factors: an increase in the amount of heat released from the combustion reactions or a decrease in the heat capacity of the flowing fluid. As the amount of staging increases, the mass flow of the fluid in the fuel-rich section of the furnace is reduced compared to that in unstaged combustion which, if the amount of heat released by combustion was constant, would lead to an increase in fluid temperatures if no other reactions are assumed to occur. This is thought to mainly explain the increase in the temperature observed at T_1. However, since temperatures at T_2 are similar to unstaged combustion despite the lower mass flow rate (and lower flowing heat capacity of the fluid) suggests the extent of combustion at this point is less than observed in unstaged combustion. Since the amount of fuel in the fuel-rich section is unchanged it is suggested this delay in combustion is due to the reduction in oxidant in this section of the furnace. At T_3 the mass flow in staged and unstaged combustion is the same so here the reduction in temperature with increasing staging is also thought to be due to a reduction in the heat released by combustion. This is supported by the reduced combustion burnout values observed for deep-staged air-fired fuel mixtures compared to their unstaged counterparts which echoes most results in the wider literature [Lin et al., 2009, Munir et al., 2011,

Ribeirete and Costa, 2009].

The reduction in oxidant available during the early stages of the reaction is also responsible for the reduction in emissions of NO observed as detailed in Section 2.4.1.4. Oxidant staging operates by reducing NO production from all three NO-formation mechanisms. Most importantly, as the fuels devolatilise releasing volatile-N compounds they are less likely to come into contact with oxygen and therefore more likely to follow the reductive pathway to form N_2. In addition, any volatile-N that is oxidised to NO is more likely to be reduced to N_2 due to the overall reducing nature of the atmosphere and the increased residence time any created NO spends in this environment as noted in Section 2.4.1.4 and the literature [EC, 2006, UNECE, 2012]. The reduction of local [O_2] also creates less opportunity for any prompt-NO formation and by limiting combustion and reducing the local temperature reduces the likelihood of O_2 dissociation leading to thermal-NO production. The fact that, similar to the findings of Ribeirete and Costa [2009], emissions of NO appear to plateau at approximately 20% of the baseline value once BSR is reduced below 0.8 may be due to the fact that NO is also likely to be formed when the OFA is injected and any char-N is exposed to an oxygen-rich atmosphere that promotes conversion to NO. In addition, the reduction in temperature observed with increasing staging may act to reduce the amount of N released with the volatiles, instead retaining it in the char as suggested by Glarborg [2003]. Any gains made in reduction of emissions of NO formed from volatile compounds are therefore offset by the increase in NO formed from the char.

In oxygen-enriched combustion, although the total amount of oxidant is reduced, the local [O_2] may actually increase due to the removal of the N_2 diluent. Therefore, in situations where nitrogen volatiles continue to have access to relatively high levels of O_2 and are not subject to long residence times in this environment it is understandable that the NO emissions may be higher than those in air firing, as is observed for unstaged and slightly-staged combustion in these results and in the wider literature [Daood et al., 2011, Nimmo et al., 2010, Thompson et al., 2004]. Moreover, the increased temperature in oxygen-enriched conditions promotes thermal-NO production. However, as oxidant staging increases competition for O_2 between the elements in the fuel mixture increases and the effective local [O_2] reduces, especially since an increasing proportion of oxidant supplied to the fuel-rich zone is supplied by the unenriched primary stream which therefore increases the relative amount of thermal diluent present in this section of the furnace. As oxidant staging increases, combustion proceeds less rapidly, the combustion atmosphere tends further to-

wards a reducing nature and residence times in this zone increase which all reduce the propensity for NO formation and increase the likelihood of any NO formed to be recycled and reduced to N_2. This causes NO emissions to fall more sharply than in air with increasing staging, analogous to that presented by Thompson et al. [2004]. As in air-firing, emissions appear to plateau at approximately 20% of the daily baseline value and thus may support the hypothesis above that any further reduction in NO formation from the volatile section is offset by an increase in NO formed from char-bound N. The levels of oxidant staging employed by Thompson et al. [2004] are not available from their data though it is thought that the minimum in NO emissions occurs in range λ = 0.9–0.7 which corresponds to the plateau in the current work. The continually high levels of carbon burnout and increasing temperature at T_3 as staging is increased suggest that despite having only a relatively short residence time in the super-stoichiometric environment the char particles combust very rapidly due to higher particle temperatures as suggested in bench-scale experiments by Murphy and Shaddix [2006] and observed for oxygen-enriched combustion in TGA devices in Chapter 5. Since this behaviour was not observed in air-firing it is suggested that enriching [O_2] to 30% is sufficient to compensate for and overcome the reduction in residence time for combustion in the super-stoichiometric section of the furnace which was responsible for reducing burnout values in air-firing.

The fact that in air the temperatures observed for the MC and RCG blends were generally similar or greater than coal-firing at T_1, lower than coal-firing at T_2 and similar at T_3 suggest that these fuel mixtures were able to mitigate some of the delay in combustion that occurred during coal-firing in air. In oxygen-enriched air the differences in temperature before OFA were injected were less readily observed suggesting, as noted above, that the increase in [O_2] was sufficient to overcome the reduction in combustion due to the reduced amount of oxidant available. At T_3 the RCG and MC blends tended to show higher temperatures suggesting that combustion intensity was greater during the period between OFA injection and the thermocouple than in coal-firing, which was supported by the increased carbon burnout of the blends. Cofiring SRC generally showed a similar trend to the other blends except at the deep-staging conditions where it appears in air and oxygen-enriched air that combustion was delayed compared to the coal-firing case. As discussed in the previous section this is perhaps due to the large particle size of the SRC sample. This would delay combustion and increasingly constrict the rate of combustion as the extent of staging increased as particle heating, devolatilisation and char-oxidation

times would all increase as is suggested by the results in air firing reported by Spliethoff and Hein [1998]. Comparing the results of MC with RCG shows that although the fuel-N content is considered to be less important than the combustion chemistry in predicting NO emissions, the lower fuel-N of the biomasses was observed to slightly reduce NO emissions under staged conditions though by an order of magnitude less (if at all) than the process of oxidant staging.

Emissions of SO_2 tended to slightly increase with increased oxidant staging for all fuel mixtures in both combustion environments though the magnitude of change was far lower than the decrease observed in NO emissions compared to the unstaged conditions. The increase was particularly apparent for the cofired mixtures. As reported in the previous section, the reduction in SO_2 emissions due to increased biomass blending were almost linear for unstaged conditions and was attributed to the reduced S content of the biomass and the increased ability of the alkali and alkaline earth metals in the biomass ash to capture sulphur. One reason for the increasing emissions of S as SO_2 may be due to a decrease in the amount of sulphur captured in the ash as SO_3. This could be brought about by the increased competition for O_2 during the fuel-rich section of the furnace and, in oxygen-enriched conditions particularly, the increased temperatures may cause an increase number of the alkali metals to volatilise and be released from the ash particles themselves. These possibilities could lead to a reduced ability for the ash to retain sulphur negating the reduction observed compared to the baseline values when biomass blends were fired in an unstaged manner.

6.4 Cofiring in air, oxygen-enriched air and partial oxyfuel environments

6.4.1 Experimental design

Research question 5 is addressed in this section where the impact of enrichment of the combustion atmosphere with O_2 and CO_2 is investigated while cofiring the three biomasses in unstaged conditions. Table 6.1 shows the predicted compositions for the feed and exhaust streams for the furnace when operated under air (Air), oxygen-enriched air (En-Air), partial oxyfuel (Oxy) and oxygen-enriched partial oxyfuel (En-Oxy) combustion atmospheres. Since the primary and entrained streams were restricted to be air, a mixture of N_2 and CO_2 was used as the comburent in the two oxyfuel cases. On account of this,

counter-intuitively, in the oxyfuel cases the concentration of CO_2 in the oxygen-enriched environment is lower than in the unenriched environment.

6.4.2 Combustion characteristics

Figure 6.17 shows the variation of the temperature recorded at several furnace locations for unstaged combustion of coal and coal-biomass blends (15% BBR) in the four combustion environments detailed in Table 6.1. The results for air and oxygen-enriched air firing are the same as those presented and discussed in Section 6.2, which can be summarised in two points. First, oxygen-enrichment of air was observed to substantially increase temperatures throughout the furnace. Second, biomass blending tended to reduce temperatures near the burner and increase them further along the furnace in air firing, while in oxygen-enriched air temperatures were elevated throughout the furnace during cofiring compared to firing coal.

In the oxyfuel environments temperatures were observed to be lower than those recorded during their air-fired counterparts. During the unenriched oxyfuel environment (inlet [O_2] = 21%) the temperature profile through the reactor was observed to change. In all other experiments temperatures generally were observed such that $T_1 \geq T_2 > T_3$. However, in the Oxy environment the temperature observed at T_1 was approximately 150 °C lower than that observed during air firing and 50 °C lower than that observed at T_2 in the Oxy case, which was itself approximately 100 °C lower than the air case. Temperatures at T_3 were only slightly lower than both those observed during air firing of coal and also those observed at T_1 when firing in the Oxy environment so the Oxy temperature profile is better described as $T_2 > T_1 \geq T_3$. Cofired blends tended to slightly increase temperatures

Table 6.1: Typical feed and exhaust compositions for Air, En-Air, Oxy and En-Oxy combustion atmospheres

Gas	Air - Feed	Air - Flue	En-Air - Feed	En-Air - Flue	Oxy - Feed	Oxy - Flue	En-Oxy - Feed	En-Oxy - Flue
O_2 (%)	21.0	3.0	30.2	4.3	21.0	3.0	30.2	4.3
N_2 (%)	79.0	80.7	69.8	72.1	32.1	32.8	46.1	47.6
CO_2 (%)	0.0	15.8	0.0	22.9	46.9	63.7	23.7	47.4
NO (ppm)	0	2882	0	4179	0	2882	0	4179
SO_2 (ppm)	0	1549	0	2246	0	1549	0	2246

at T_1, reduce them at T_2 and have a mixed effect at T_3. In oxygen-enriched oxyfuel conditions the temperature profile through the furnace was more similar to the air-based environments. Temperatures were greater than those for air firing though lower than those recorded for oxygen-enriched air firing. At T_1 the increase in temperature compared to air firing was 50–100 °C (200–250 °C greater than unenriched oxyfuel conditions) though these temperature differences were then reduced to $\sim$ 50 °C and $\sim$ 25 °C at T_2 and T_3, respectively.

The carbon burnout for the unstaged combustion of coal and biomass-coal blends (at 15% BBR) in the four combustion atmospheres experiments are displayed in Figure 6.18. It is unfortunate that for these experiments it was only possible to collect a smaller amount of ash for each experiment[1]. In light of this, the usual requirement for at least 1 g of sample was relaxed to $>$0.25 g for these experiments. Despite the belief that the results represent a good sample, on account of this reduced mass, these results should be interpreted only indicatively.

As discussed in previous sections of this chapter, cofiring of biomass and oxygen enrichment both act to increase the carbon burnout of fuel mixtures fired under unstaged conditions. Firing in unenriched oxyfuel conditions was observed to decrease the burnout of both coal and a blend of coal and RCG compared to their respective burnout values under air firing. However, in the Oxy conditions, cofiring was again observed to increase carbon burnout compared to firing coal alone. When firing in an oxygen-enriched oxyfuel atmosphere the carbon burnout for coal and biomass blends was also observed to fall compared to oxygen-enriched air case though the reduction was less than that observed between the unenriched conditions. Despite the reduction compared to oxygen-enriched air, carbon burnout for the En-Oxy atmosphere was observed to be greater than that for air-firing. Cofiring of SRC was observed to increase carbon burnout under an En-Oxy atmosphere while for the blends of coal with RCG and MC no change was detected compared to the coal firing tests.

[1]The reduced sample mass collected was due to a reduction in suction power from the vacuum pump attached the ash collection pot as well as dwindling biomass resources ensuring that experimental runs could not be extended

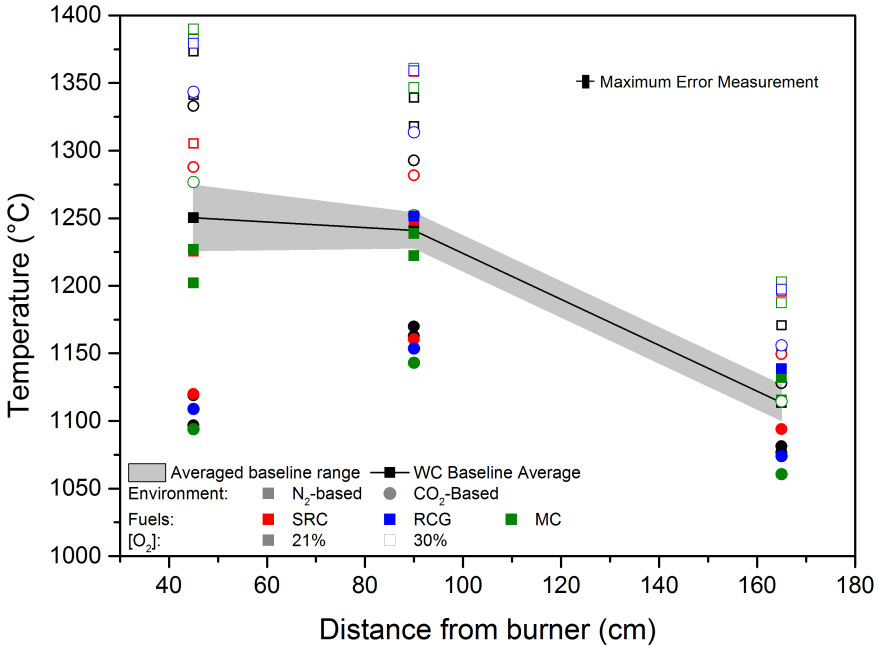

Figure 6.17: Variation in temperatures at various distances along the furnace between air and partial-oxyfuel fired unstaged systems for at 21 and 30% [O_2]

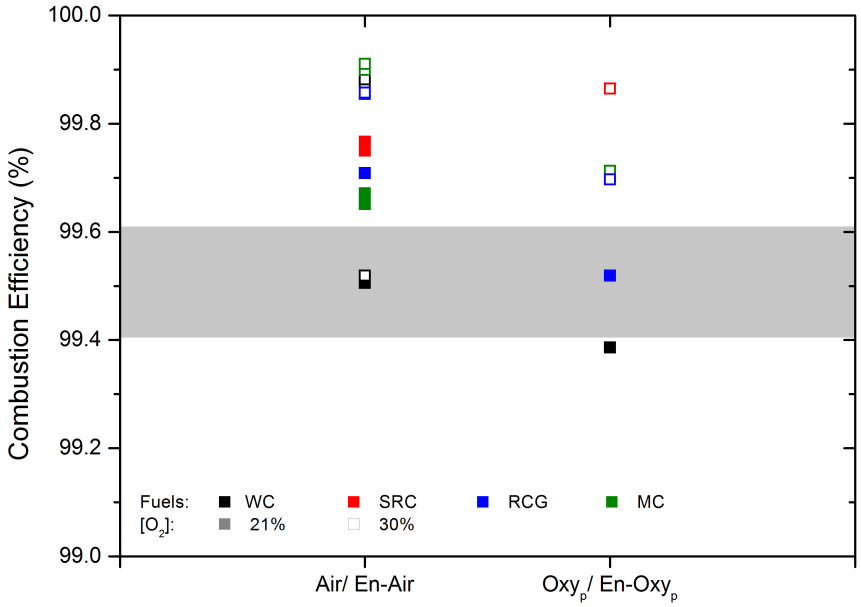

Figure 6.18: Variation in carbon burnout between the air and oxyfuel fired unstaged systems for at 21 and 30% [O_2]. Unlike previous experiments, CO emissions for this experiment are not presented on account of unreliable analyser performance during these tests.

6.4.3 Gaseous emissions

Figure 6.19 presents the emissions of NO from firing coal and biomass blends in the four combustion atmospheres. As observed in Section 6.2, cofiring of RCG and MC in air tended to slightly reduce NO emissions while SRC tended to increase NO emissions under unstaged conditions. Firing the fuels in oxygen-enriched air tended to increase NO emissions by up to 25% compared to the daily baseline values. When firing in the oxyfuel conditions, emissions of NO were observed to reduce compared to those recorded for their air-based equivalents. In unenriched conditions emissions from coal firing were approximately 30% lower than the baseline value while for the biomass blends this reduction was increased to 40–45%. Under oxygen-enriched oxyfuel conditions emissions of NO were broadly similar to those observed for coal-firing in air and lower than those observed for combustion in oxygen-enriched air.

Figure 6.20 presents the emissions of SO_2 from firing coal and biomass blends in the four combustion atmospheres. As observed in Section 6.2, biomass cofiring tended to reduce SO_2 emissions in both air and oxygen-enriched conditions while emissions for coal fired in both environments were observed to be very similar. In unenriched oxyfuel environments little change was observed compared to air firing while in oxygen-enriched oxyfuel environments a significant reduction in SO_2 emissions was observed for coal and cofired fuel mixes.

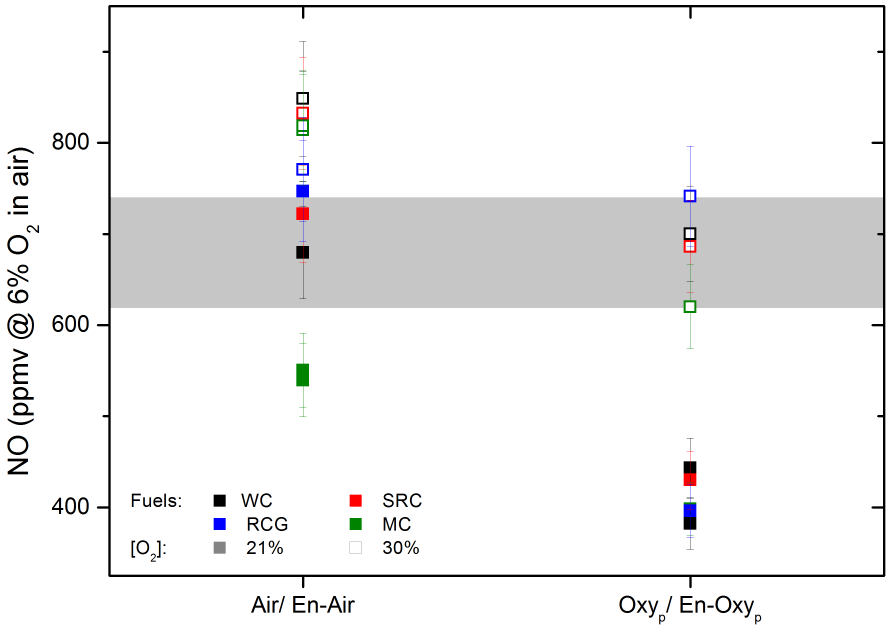

(a)

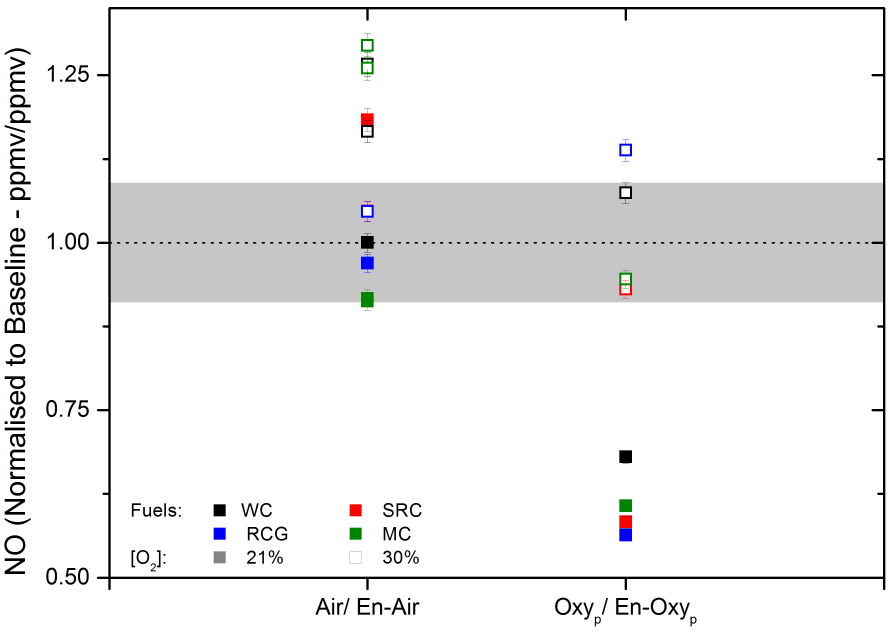

(b)

Figure 6.19: Variation in emissions of NO between nitrogen- and CO_2-based (oxyfuel) combustion atmospheres - in (a) absolute terms and (b) compared to the daily baseline value (b)

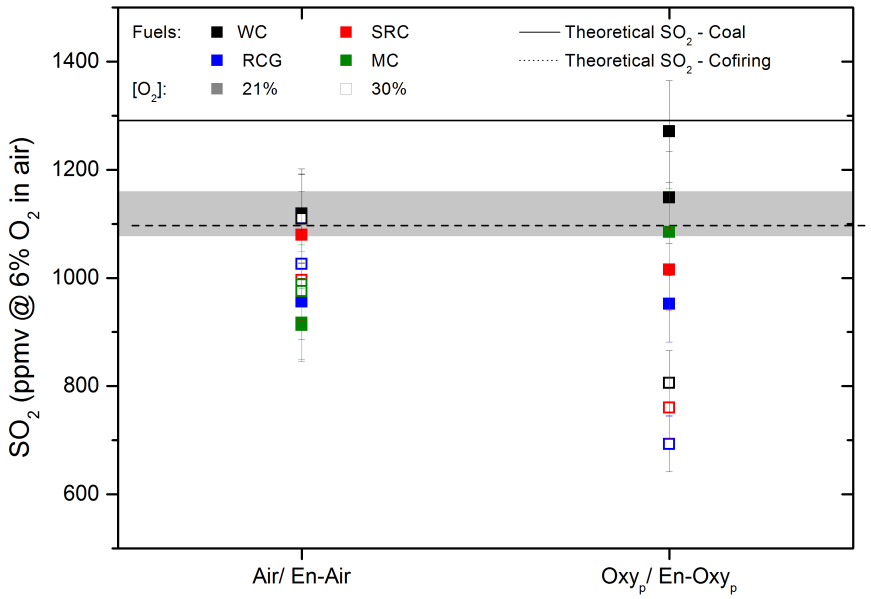

(a)

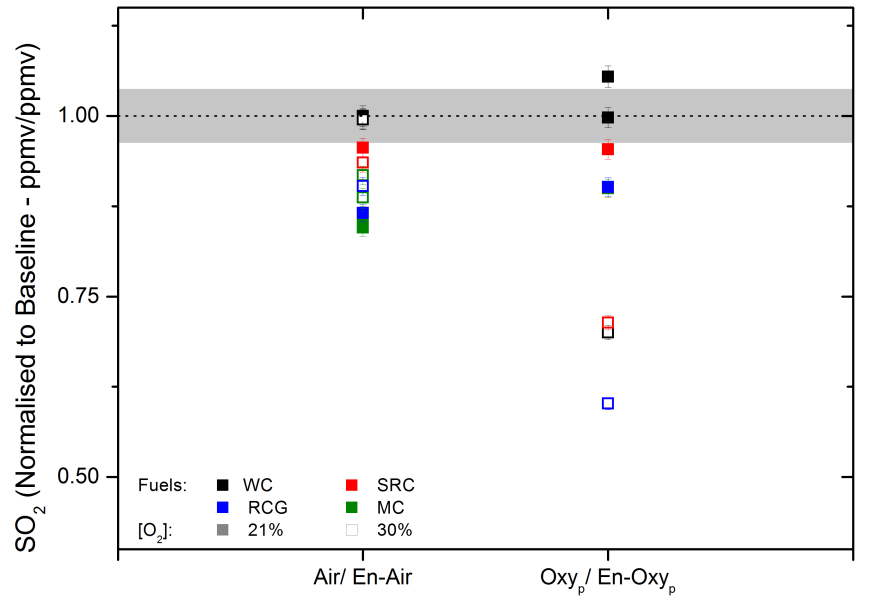

(b)

Figure 6.20: Variation in emissions of SO_2 between nitrogen- and CO_2-based (oxyfuel) combustion atmospheres - in (a) absolute terms and (b) compared to the daily baseline value

6.4.4 Ash analysis

As noted previously ash collection during these experiments was less effective than in previous cases resulting in lower quantities of ash available for analysis. An example of ashes collected for SRC cofired in Oxy and En-Oxy environments are shown in Figure 6.21 while the EDX maps for these samples are shown in Figure 6.22. The SEM images for the ash fired in Oxy conditions contains a large number of aggregated, non-spherical particles while the En-Oxy image suggests a larger number of smaller, more spherical particles. Aside from a greater intensity observed in the Oxy environment, no significant differences can be drawn between the Oxy and En-Oxy cases.

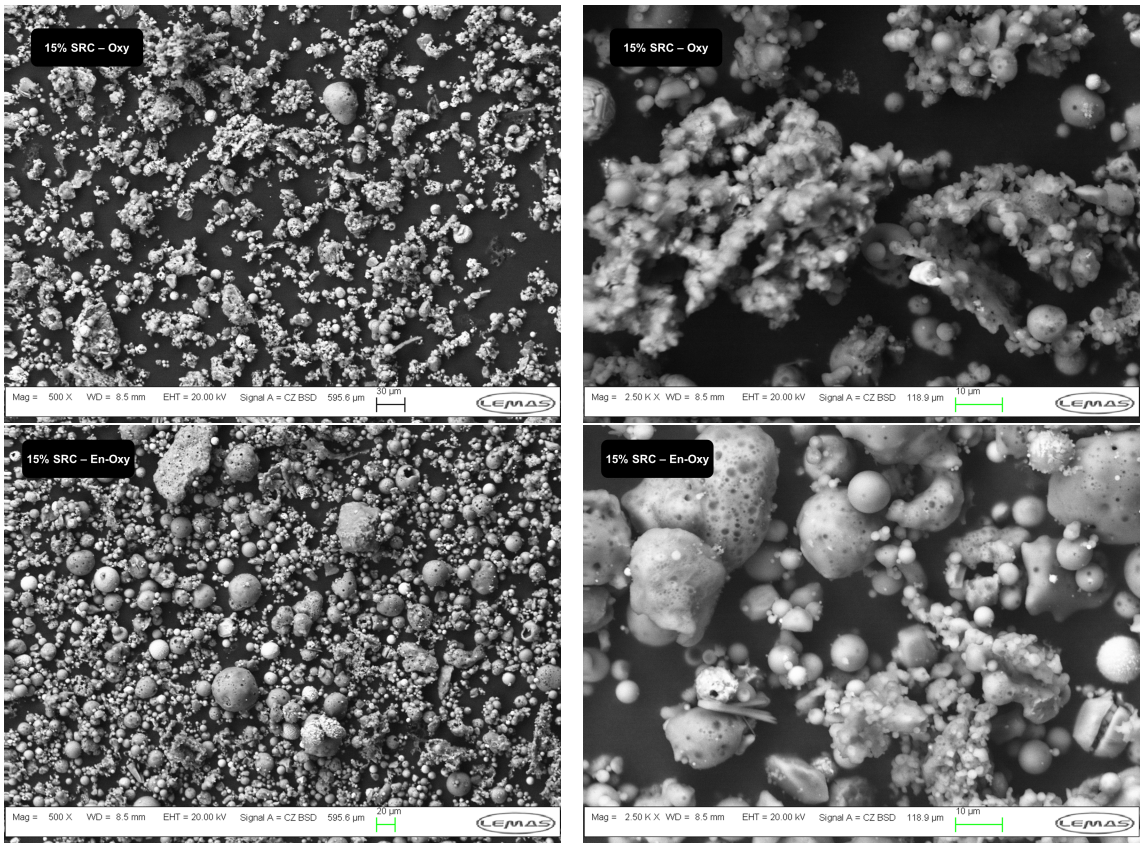

Figure 6.21: SEM images of ash residue from combustion in Oxy and En-Oxy conditions for WC and 15% BBR of SRC at 500x and 2500x magnification

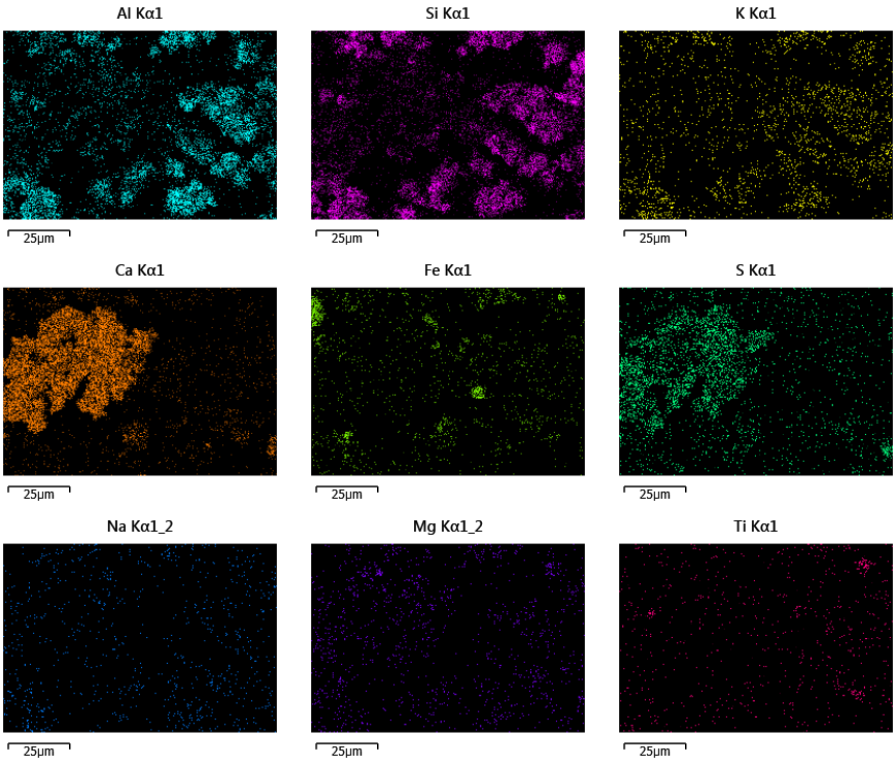

(a) Oxy

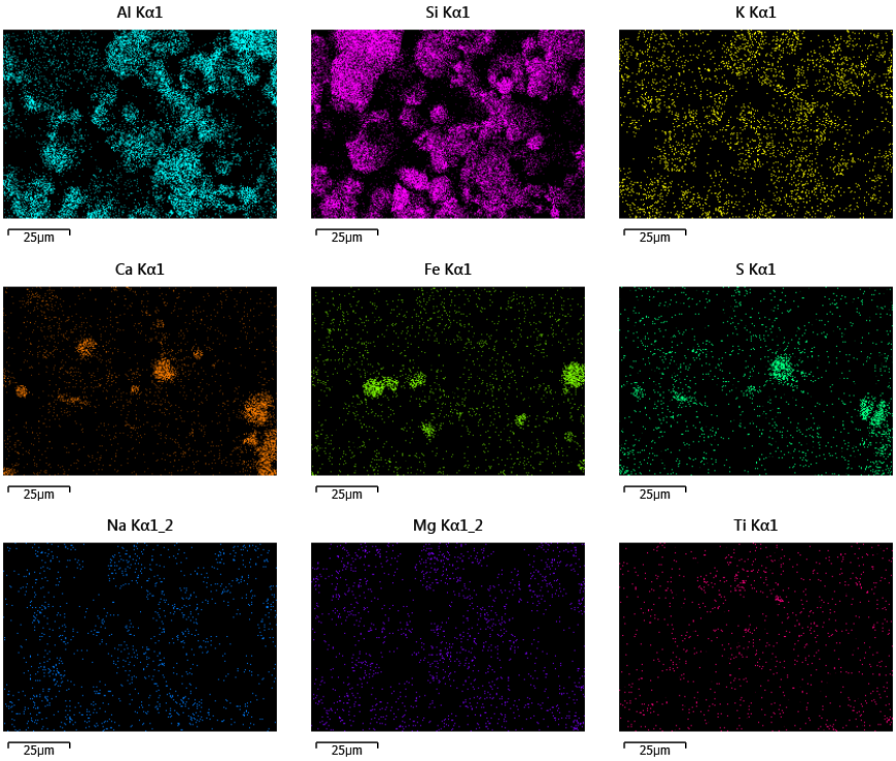

(b) Oxygen-Enriched Oxy

Figure 6.22: Elemental mapping of elements present in ash collected from experiments cofiring WC and 15% SRC in unstaged Oxy and oxygen-enriched Oxy experiments

6.4.5 Discussion of impact on combustion of O_2 and CO_2 enrichment

The previous subsections have presented results that suggest combustion of coal and coal-biomass blends in various O_2 and CO_2-enriched atmospheres alter many of the combustion characteristics and emissions. Where possible, the following subsection aims to provide reasoning for these changes by incorporating the literature, fuel characteristics and bench-scale results presented in earlier chapters to answer the penultimate research question (5) in Section 3.4.9.

In the unenriched Oxy environment combustion was considerably delayed in the furnace, changing the shape of the temperature profile as well as significantly reducing temperatures throughout the furnace. The delay in combustion appeared to reduce the carbon burnout of the combustion process resulting in higher amounts of combustible material remaining in the ash. Although the results in Chapter 5 suggest only a small reduction in ignition in TGA environments (where temperature reduction is largely negated), the furnace results agree with the many presented in the literature for coal-firing where the delayed temperature response is attributed to delayed fuel ignition on account of the higher heat capacity of CO_2 and decreased particle temperatures as volatiles evolved combust further from the particle due to the reduced mobility of O_2 in this atmosphere [Davidson and Santos, 2010, Kiga et al., 1997, Liu et al., 2005, Shaddix and Molina, 2009]. The reduction in temperatures is also likely to have reduced the rate and ultimate level of devolatilisation of the fuel particles as described by Farrow and Snape [2010]. Reducing devolatilisation therefore increases the need for oxygen to diffuse to the char surface to react with char-bound elements and since O_2 diffusivity is reduced in CO_2 compared to N_2 it is unsurprising that the carbon burnout in Oxy environments was lower than that in air. This reduction is smaller than others reported in the literature though this is perhaps due to the fact this work does not represent a total oxyfuel system and continues to contain a large amount of N_2 as the comburent.

In this thesis, blending of biomass with coal was generally observed to increase the ignitability of the coal samples similar to that reported by both Arias et al. [2008] and Riaza et al. [2012] during TGA experiments and agrees with the findings in Chapter 5 which suggest that coal is more sensitive to changes in combustion atmosphere than the biomass samples. Smart, Patel and Riley [2010] found near-burner temperatures tended to decrease when cofiring reasoning increased moisture, a reduction in heat given out from

combustion of the biomass volatiles and a decreasing amount of available O_2 for the coal volatiles to react with as more is intrinsically held in the biomass. However, this work generally used lower BBR ($15\%_{thermal}$ compared to 20 and $40\%_{mass}$) with far more reactive biomass samples (as shown in the DTG curves in Chapter 5 for example) and was not fired using wet recycled flue gas.

Emissions of NO were substantially lower in the Oxy environment compared to air-firing as reported by Liu et al. [2005]. Of the nine reasons listed in Table 2.11, it is suggested that the reduced temperature and increased likelihood of NO destruction were most responsible for reducing the ultimate emissions of NO during firing in the Oxy environment. As with all previous tests, cofiring of SRC, MC and RCG derived a modest further reduction in NO emissions.

In oxygen-enriched oxyfuel (En-Oxy) systems the delay in combustion observed in Oxy environments was no longer apparent and temperatures for the reduced gas volume were higher than for air though less than those observed for En-Air with the higher heat capacity of the En-Oxy environment mitigating the effect of reduced gas volume compared to En-Air temperatures. As a result of these increased temperatures, due to the many reasons discussed in the previous subsections, carbon burnout in En-Oxy was slightly greater than for air-firing though less than that in En-Air combustion. The increased temperature in En-Oxy compared to Oxy increased NO emissions, though the reduced mobility of O_2 and increased propensity to destroy NO in the CO_2-enriched environments caused NO emissions to be lower than those in En-Air and similar to those in Air. Although several authors have reported reductions in NO emissions in oxygen-enriched oxyfuel atmospheres, direct comparisons to the present work are complicated by the range of combustion conditions employed. For example, although Liu et al. [2005] and Andersson [2005] both reported a reduction of 10–20% in unstaged conditions, the first atmosphere consisted of 30% O_2 in CO_2 and the second was only enriched to 27% O_2. Thus, unstaged combustion in a higher [O_2] than the work by Andersson [2005] with a lower [CO_2] than the experiments by Liu et al. [2005] could be argued to not effect such large reductions in NO as those two experiments. It should also be noted that Tan et al. [2006] reported increased emissions in oxygen-enriched oxyfuel atmospheres before the burner in use was optimised to low-NO_x operation. Since it was not possible to alter the burner in the current work it may be that compared to the other works it is less-well optimised for low-NO_x firing in oxyfuel systems. Biomass blending in En-Oxy conditions tended to have a relatively modest impact

on NO emissions with reductions of the order of $<$10% observed for most cases.

Similar to the findings of Liu et al. [2005], little change was observed in SO_2 emissions when switching from the Air to Oxy environments. However, in oxygen-enriched oxyfuel conditions significant reductions in SO_2 emissions were observed with biomass blending effecting even larger emissions reductions. Although some published literature suggests slight reductions in SO_2 emissions during oxygen-enriched oxyfuel firing the magnitude of the reduction in this work appears considerably larger. Tan et al. [2006] notes increased concentrations of SO_2 will likely lead to increased deposits of S in the ash and slag and since the results in Section 6.2 show an increased tendency for the biomass ash compounds to capture S it may be that this mechanism is accelerated in oxygen-enriched oxyfuel atmospheres. Unfortunately insufficient ash collection and a lack of instrumentation to measure other sulphur species predicates that it is not possible to analyse the other emissions more fully to understand whether reductions in observed SO_2 emissions are offset by increases in other emission pathways.

6.5 Unstaged biomass combustion in O_2 and CO_2-enriched atmospheres

Once the main experimental programme detailed in the previous sections was complete a small surplus of SRC was available for firing in a short, dedicated biomass combustion testing regime. On account of the high propensity of SRC to slag compared to WC these tests were necessarily conducted last. As mentioned in Table 3.5, the biomass feeder was only able to provide enough SRC to provide 17.1 kW input. In light of this it is difficult to compare directly between the results for dedicated biomass and the coal and coal-biomass blends which were fired at 19.7 kW. However, results for dedicated biomass firing in air, and En-Oxy environments are presented in Table 6.2. During experiments it was noticed that increasing the BBR tended to affect the stability of results during experimental runs. Figures 6.23 and 6.24 show raw experimental results for dedicated SRC firing alongside other levels of BBR and the combustion atmosphere for temperatures and flue gases, respectively, which allows the drawing of answers to the final research question in Section 3.4.9.

6.5.1 Combustion measurements

The combustion of the lower thermal input of SRC generates a lower temperature profile throughout the furnace with temperatures ∼150, ∼120 and ∼75 °C lower than the coal baseline at T_1, T_2 and T_3, respectively. In the En-Oxy atmosphere the temperatures increase compared to air-firing of SRC but remain ∼80, ∼75 and ∼70 °C lower than the coal baseline value. NO emissions reduced considerably and were observed at ∼40 and ∼25% of the coal baseline value for air and En-Oxy firing of SRC. SO_2 emissions were found to be less than 5% of the baseline value in both cases. Unfortunately CO measurements are not reported due to unreliable analyser performance during these tests.

6.5.2 Combustion stability

From the results presented in Table 6.2 and Figures 6.23 and 6.24, it appears that in air-firing the temperature at T_1 and T_3 is relatively stable during 100% SRC firing but that temperatures at T_2 are considerably more variable than when firing coal. In the En-Oxy atmosphere increased variability is observed at T_1 and less so at T_2 for the dedicated biomass firing. Measurements of the flue gas suggested that the variability increases with higher SRC blending ratios, with O_2 and CO_2 in particular exhibiting a higher variability within experiments compared to the measured value in both air and En-Oxy environments.

Table 6.2: Experimental results for dedicated biomass combustion experiments

Measurement	Baseline Range (variation during experiment)	Maximum Estimated Error @ Baseline	SRC Air (variation during experiment)	SRC En-Oxy (variation during experiment)
T_1 °C	1226–1274 (± 5.2)	2.5	1100 (± 3)	1168 (± 4)
T_2 °C	1228–1253 (± 2.5)	2.5	1123 (± 5)	1164 (± 7)
T_3 °C	1100–1126 (± 2.8)	2.8	1037 (± 2)	1042 (± 2)
O_2 %	2.75–3.13 (± 0.18)	0.16	4.15 (± 0.61)	5.19 (± 0.92)$^{\alpha}$
CO_2 %	15.19–16.07 (± 0.20)	0.82	16.44 (± 0.79)	47.4 $^{\beta}$ (n/a)
NO ppmv @6% O_2 in air	619–740 (± 18)	32	259 (± 18)	180 (± 16)
SO_2 ppmv @6% O_2 in air	1077–1160 (± 3)	33	43 (± 0)	27 (± 1)

$^{\alpha}$ CO_2 corrected; $^{\beta}$ predicted

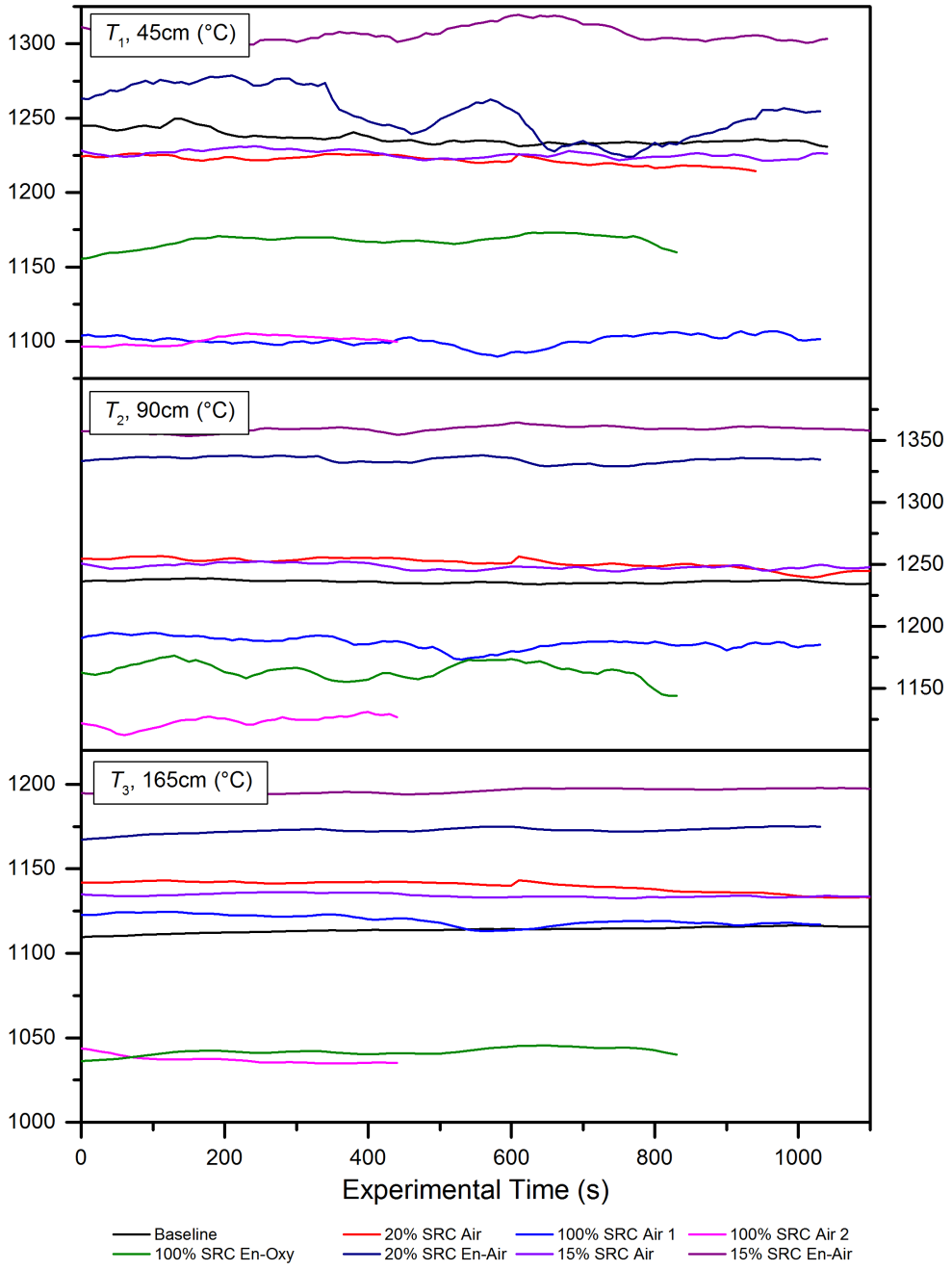

Figure 6.23: Experimental data showing stability of measurement of combustion temperatures at T_1, T_2, and T_3 with various blending ratios of SRC in various combustion atmospheres

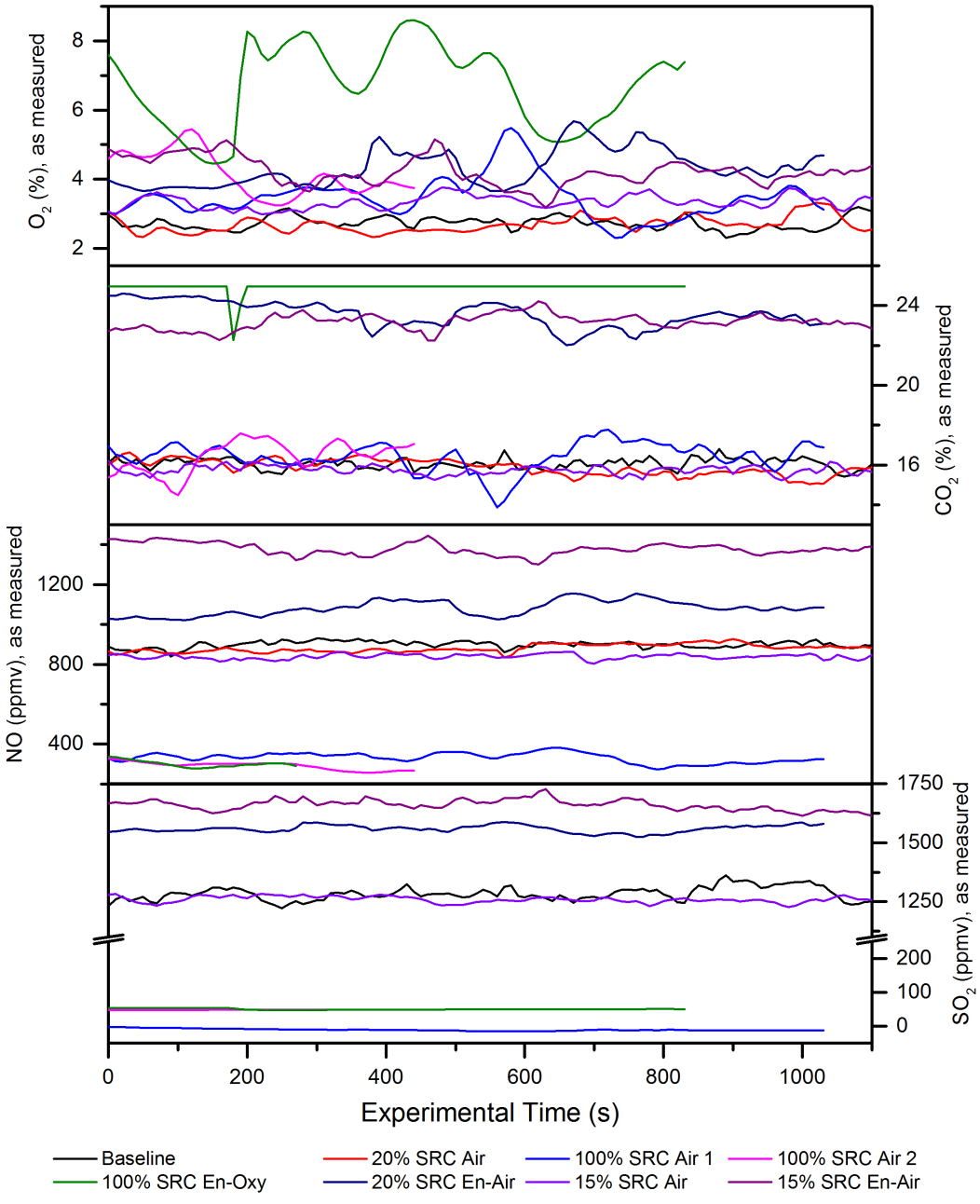

Figure 6.24: Experimental data showing stability of measurement of flue gas concentrations with various blending ratios of biomass in various combustion atmospheres

6.5.3 Discussion

Although the thermal input to the furnace is slightly lower in the results presented here, significant variation in combustion measurements and combustion stability have been observed under dedicated firing of SRC. Although the lower thermal input will likely somewhat reduce the furnace temperatures, the significant reduction observed at T_1 and T_2 especially indicate that combustion is delayed during SRC firing. This is particularly the case in air as the temperature profile through the furnace changes showing higher temperatures at T_2 than T_1 suggesting that the combustion process is being forced further along the furnace than in coal-firing in agreement with the results presented in Section 6.2 where the increased particle size, reduced calorific value and increased moisture content were suggests as reasons for delay in combustion. As well as being supported by the change in temperature profile, this theory is also supported by the change in variability of temperatures measured at T_1 and T_2 as an increased level of variability implies the thermocouple is closer to the flame. As noted above, delayed combustion would cause the flame to elongate and potentially shift further downstream. If more combustion is occurring near T_2 than T_1 then it would be expected that a reduction in volatility at T_1 is balanced by an increase in measurement volatility at T_2 as is observed for the case of firing 100% SRC in air. In the En-Oxy atmosphere the reduced gas volume and greater [O_2] accelerates combustion relative to air-firing and promotes combustion closer to the burner as is supported by an increase in measurement volatility at T_1, reduction in measurement volatility at T_2 and the fact that $T_1 > T_2$. However, the difference between the temperature measured at the first two thermocouples is less than that observed when firing coal or coal-biomass blends in oxygen-enriched atmospheres suggesting combustion is occurring less intensely before T_1 in the dedicated biomass-firing cases. In addition, the volatility of measured O_2 and CO_2 suggests the combustion process is unstable as it is for dedicated SRC firing in air. Considered together, it may be the case that the large particle size of the SRC - which delays ignition of the fuel - and the use of a burner designed for coal-firing combine to delay combustion to such an extent that the flame becomes detached resulting in highly variable combustion which is difficult to control. The length of the flame and its degree of attachment cannot be investigated with the experimental facilities used in the current work.

Unfortunately the limited supply of SRC, coupled with its low ash content and a fault that

caused reduced suction for the ash collection vacuum pump, meant that it was not possible to collect sufficient ash samples to be able to analyse the carbon burnout. However, it is suggested that the lower temperatures and very delayed mixing of fuel-N with oxidant resulting from the slow devolatilisation process together contribute to the significant reduction in NO emissions observed. The reduction in SO_2 is due to the very low sulphur content of the SRC.

6.6 Conclusions

A large number of experiments using a 20 kW facility have investigated a range of impacts on combustion when using coal and three biomass fuels - short-rotation coppiced willow (SRC), reed canary grass (RCG) and miscanthus (MC) - in a variety of air, oxygen-enriched air and CO_2-enriched combustion atmospheres to answer research questions 3–6 presented in Section 3.4.9. The following conclusions can be drawn from the results presented in this chapter:

- Increasing the biomass blending ratio (BBR) during unstaged combustion in air tends to delay and elongate combustion relative to the coal-fired baseline. This is due to the increased moisture content of the biomass, the slower devolatilisation of the larger biomass particles and the lower calorific value of the biomass volatiles.
- Increasing BBR increases the carbon burnout of the fuel mixture in the furnace up to a maximum of 15%. This is thought to be due to the higher reactivity of the biomass char and the larger proportion of combustion occurring in the gas phase. Increasing BBR above 15% appears to reduce burnout as the increased moisture content begins to reduce flame temperatures, reducing devolatilisation rates and delaying and extending the combustion process.
- Increasing BBR of MC and RCG reduces NO emissions relative to the coal baseline at unstaged firing in air, while blending of SRC initially increases NO emissions but as BBR increases NO emissions reduce to similar levels to the coal-fired baseline. The difference in behaviour is attributed to the substantially larger particle size of the SRC fuel which is unable to devolatilise rapidly enough to compete with coal-volatiles near the flame essentially increasing the local $[O_2]$ available for NO production from the coal volatiles. As noted above, at higher BBR the higher moisture

content of the biomass reduces flame temperatures therefore reducing NO formation.

- Increasing BBR reduces SO_2 emissions for all unstaged combustion conditions due to the significantly lower sulphur content of the biomass fuels compared to the coal. In addition, gaseous emissions of SO_2 were also reduced due the increased content of alkali and alkaline earth metals in the biomass ashes which appear react with and retain an increased amount of sulphur in the ash compared to coal-fired ashes.

- In oxygen-enriched atmospheres (En-Air: 30% [O_2], 70% [N_2]) combustion temperatures throughout the furnace are increased due to the reduced heat capacity of the reduced gas flow and the intensified combustion caused by the increased [O_2].

- Carbon burnout values in En-Air atmospheres are higher than those in unenriched conditions due to the increased devolatilisation rates driven by higher temperatures and the higher [O_2] facilitating increased diffusion of O_2 to react with combustible elements at the char surface. The increased [O_2] also acts to increase the char particle temperature as gas-phase combustion occurs closer to the char particle. SEM images of the ashes suggest a greater breakdown and increase in homogeniety of ash particles than in air-firing.

- Biomass blending in En-Air increased combustion temperatures compared to coal-firing for MC and RCG which were able to devolatilise and combust more rapidly due to the elevated temperatures and [O_2]. The large particle size of SRC again delayed combustion compared to the other fuels and increasing BBR of SRC reduced temperatures near the burner. However, temperatures quickly recovered and the burnout values for all biomasses were at least as high as those seen for coal-firing in En-Air and greater than air-firing of all fuel mixtures.

- The increased temperatures and associated devolatilisation rate of the fuel mixtures in En-Air increased emissions of NO compared to the baseline of coal-firing in air.

- Conventional ash slagging and fouling indicators suggest that cofiring the biomasses studied would result in manageable ashes with BBR up to 15% for MC and SRC while at this BBR RCG cofired ashes are located on the threshold of probable fouling and therefore require further analysis to be certain of behaviour.

- In air-firing employing the practice of oxidant-staging - reducing burner stoichiomet-

ric ratio (BSR) - tended to delay combustion, reduce combustion temperatures and reduce the overall carbon burnout of all fuel mixtures.

- Oxidant staging in air-firing was highly effective at reducing NO emissions with deep staging achieving reductions of up to 70% compared to the coal baseline with the reduction attributed mainly to a lack of O_2 available for volatile-N compounds to react with in the fuel-rich zone.

- In En-Air oxidant staging had a similar effect on combustion temperatures and carbon burnout to unstaged conditions with the increased combustion temperatures and [O_2] maintaining high burnout values despite increasing oxidant staging.

- Oxidant staging in En-Air situations was able to reduce NO emissions more rapidly than in air-firing and was able to achieve emissions reductions of up to 80% compared to the air-fired, coal baseline.

- Increasing oxidant staging tends to reduce the ability of biomass fuels to reduce SO_2 emissions compared to coal-firing in both air and En-Air conditions which may be due to a reduction in the ability of the ash compounds to capture gaseous sulphur compounds due to the reduced [O_2] in the fuel-rich section.

- Firing of all fuels in an unenriched oxyfuel environment (Oxy: 21% [O_2], 47% [CO_2], 32% [N_2]) significantly delayed combustion, reduced temperatures and tended to reduce carbon burnout compared to air-firing under unstaged conditions.

- Blending of biomass at 15% in the Oxy environment tended to accelerate the combustion process compared to coal-firing resulting in higher combustion temperatures near the burner but reduced temperatures further along the furnace. Blending of RCG marginally improved the carbon burnout compared to firing coal alone.

- Emissions of NO from combustion in the Oxy environment were considerably lower than air-firing due to the reduced temperatures, reduced amount of N_2 available for thermal-NO formation and increased likelihood of any NO formed to be reduced to N_2. Biomass blending was observed to effect slight further reductions in NO emissions.

- Firing of all fuels in an unstaged, oxygen-enriched oxyfuel environment (En-Oxy: 30% [O_2], 24% [CO_2], 46% [N_2]) accelerated combustion, increased combustion temperatures and improved carbon burnout compared to air-firing but by less than

achieved in the En-Air environment due to the increased heat capacity of CO_2 and reduced diffusivity of O_2 in En-Oxy compared to En-Air.

- NO emissions from combustion in En-Oxy environments were generally lower than those observed for En-Air and similar to those for air-firing. In general, blending of biomass had little effect or slightly reduced NO emissions compared to En-Oxy coal-firing.

- Emissions of SO_2 were similar to air-firing in the Oxy environment but significantly reduced in the En-Oxy environment. It was not possible to be certain as to why this reduction in SO_2 emissions in En-Oxy may have occurred though an increase in emissions as SO_3 and an increased amount of sulphur captured in ash and deposited on the furnace walls may be responsible though these factors were not measured.

- SEM images of ash samples suggest incomplete combustion in Oxy environments may have led to larger, non-spherical ash particles while results for En-Oxy suggested a more uniform particle shape that was similar to firing in En-Air.

- Firing 100% SRC in air was observed to significantly delay combustion and reduce furnace temperatures due to the high moisture content and large particle size of the fuel. The lower temperatures were mainly responsible for reducing NO emissions to approximately 40% of the coal-fired baseline.

- In En-Oxy conditions the combustion temperatures for 100% SRC firing were greater than air-firing of SRC but still lower than those observed during air-firing of coal. A combination of reduced propensity for NO formation through the thermal-NO route and increased likelihood of NO reduction to N_2 resulted in NO emissions approximately 25% of those observed for coal-firing in air.

- SO_2 emissions from 100% SRC firing in both combustion atmospheres were less than 5% of those observed during air-firing of coal due to the significantly lower content of sulphur in the fuel.

- Significantly increasing BBR without making burner modifications resulted in increased variability in combustion measurements due to unstable combustion that was difficult to control. Although not possible to verify with the experimental set up, it is suggested that under high BBR the flame may become detached resulting in the instability observed in temperature and flue gas measurements.

Part II

Analysis of the UK CCS Industry

Chapter 7

Innovation and Development of a UK CCS Industry

7.1 Introduction and background

7.1.1 Chapter overview

As well as marked shifts in individual, corporate and national behaviour, novel implementation of traditional and innovative technologies are key to the development of a global low-carbon economy as the title the Climate Change Committee's report: "*Building a low-carbon economy – the UK's innovation challenge*" suggests [CCC, 2010]. Similar to strategies published elsewhere, the report makes clear that the UK should *"develop and deploy"* CCS in order to meet the climate change goals. However, the route CCS development takes from an industry which doesn't currently exist to being widely deployed at a meaningful scale is far from certain. It is useful to understand how such development may be supported or hindered by analysing historical and current innovation in the UK CCS industry.

In order to explain how the analysis that follows fits with the wider scope of the industry this section of the thesis is structured to provide a narrative of the development of CCS in the UK. The UK CCS industry has changed considerably in the last decade or so and particularly over the period during which this work was carried out (2010–2013). To document these changes, a concise background of the industry's development from a policy view is provided up until mid-2011 when an expert-survey was performed. This survey provides

a snapshot of the industry at that time and is compared to similar work carried out previously in other nations using the same methodology. As a part of this survey, experts were asked to articulate recommendations for the removal of blocking mechanisms present in highlighted areas of the industry. An analysis of CCS in the UK from the time of the survey until mid-2013 is then used to evaluate whether the development of the industry since has moved to counter these blocking mechanisms.

While the focus of this thesis combines biomass firing with CCS, the following chapter aims to gauge the development of the UK CCS industry as a whole. This is because, although often cited as necessary for meeting low carbon energy targets, Bio-CCS is rarely separated from CCS in general in the UK. Thus, although likely to encounter some unique challenges, it is assumed that the development of Bio-CCS in the UK will follow the development of a more general UK CCS industry. To provide an insight on the potential for development of a Bio-CCS industry, a separate discussion on the potential of UK Bio-CCS concludes this part of the thesis.

7.1.2 A brief history of CCS in the UK

Although no full-chain projects yet exist, a UK CCS industry has been expanding steadily since the early 2000s with growing support from from politicians and technology developers. The following chronology details the development of UK CCS drawing heavily on the work of Watson et al. [2012] and technological advances that are mainly informed by presentations and reports of annual meetings of the Advanced Power Generation Technology Forum (APGTF). In policy terms, one of the earliest mentions of CCS appeared in relation to the UK commitment to working with Canada on a carbon sequestration project targeting coal bed methane extraction [DTI, 1999]. With no revenue stream apparent in the UK, a lack of domestic interest was perhaps the reason that early meetings of the APGTF did not mention CCS as a future technology, instead listing fuel cells and gasification as more likely issues to be taken through to commercialisation [APGTF, 2000]. However, support for the technology grew through the 2000s, both in policy and technology circles. By 2002 CCS (still monikered carbon sequestration) was beginning to gain traction with original equipment manufacturers (OEMs) and utility industry circles with mention of storage in the North Sea mooted in a presentation by King [2002] that referenced ongoing studies and suggested the following routes to technology development:

"R&D to improve capture efficiency and economics, costed design studies on capture and sequestration [and] demonstration of capture and sequestration from a coal-fired power plant". King [2002] also recognises *"Research and development alone [is] not sufficient"* and that demonstration and deployment programmes which involved industry and academia were needed. At the same meeting, McMullan [2002] stressed the need for a: "*commitment to long term strategic R,D&D, which should set out a strategy for a minimum of 10 years."*. Government interest in CCS began to show when it was noted that CCS would be key to many coal power stations continuing to operate from 2020 onwards by the 2003 White Paper [DTI, 2003] and reiterated in the Carbon Abatement Plan [DTI, 2005]. Responsible for 'keeping the lights on' as cheaply as possible, government interest in CCS was mainly economic noting that results from energy system modelling showed: "*Higher costs* [of emissions reductions] *were indicated if [...] carbon capture and storage* [was] *completely excluded in the longer term*" while also recognising that: "*CCS is currently constrained by a number of significant legal and technical issues.*" [DTI, 2003]

The UK CCS industry developed rapidly from 2005 onwards. Publication of IPCC Special Report on CCS and the establishment of the European Technology Platform for Zero Emission Fossil Fuel Power Plants (ZEP) began to create regional and international momentum for the development of CCS. In addition, the UK research councils (RCUK) began to rapidly increase funding for CCS projects as Figure 7.1 illustrates. Analysis of the data shows initially a small number of projects of relatively minor value were conducted in the period 2000 - 2003. However, from 2004 to 2010 the number of projects active in a given year increased from 4 to 86 at a fairly consistent rate of approximately 15 projects per year. Up until 2008, the majority of these projects were relatively small, valued under £250k, but from 2008 to 2013, the annual funding budget for CCS had grown from £2million to £20million with the number of projects valued $<$£250k remaining roughly constant despite substantial growth in larger projects. The lag between the number of projects and investment can be characterised as the initially small, typically individual, studies were steadily been replaced by work which had a larger brief, was more in depth and was typically conducted by a combination of researchers working in collaboration. As well as a growing focus in academic circles, building on the suggestions from early APGTF meetings, CCS received wider attention in government and following mentions by MPs a parliamentary note was even published [POST, 2005]. As well as domestic development, a number of international CCS demonstration programmes and technology

roadmaps spurred UK CCS on leading to the formation of the Office of Carbon Captures and Storage (OCCS) in the Department of Energy and Climate Change (DECC) and the lauch of the CCS Demonstration Competition (Demo1) in 2007. The competition was designed to provide £1bn in funding to the first operating post-combustion capture system on a coal-fired power plant with the provision of a CCS-Levy on electricity bills to support the development of several more demonstration projects. Even though the criteria was relatively narrow, nine applications were received and through two rounds of selection these were reduced to two finalists: E.ON's project at Kingsnorth and Scottish Power's project at Longannet. Despite the newly-elected coalition government's continued commitment guaranteeing £1bn in funding for the first project in the 2010 Comprehensive Spending Review, on the same day it was published E.ON pulled out of the competition. Following stakeholder engagement and recommendations from the Committee on Climate Change (CCC), DECC decided to broaden the competition for the remaining projects to include gas-fired plant and alternative methods of CO_2 capture while also changing the funding structure by removing the CCS levy and instead including CCS in the wider-focussed electricity market reform (EMR) [CCC, 2010, Watson et al., 2012].

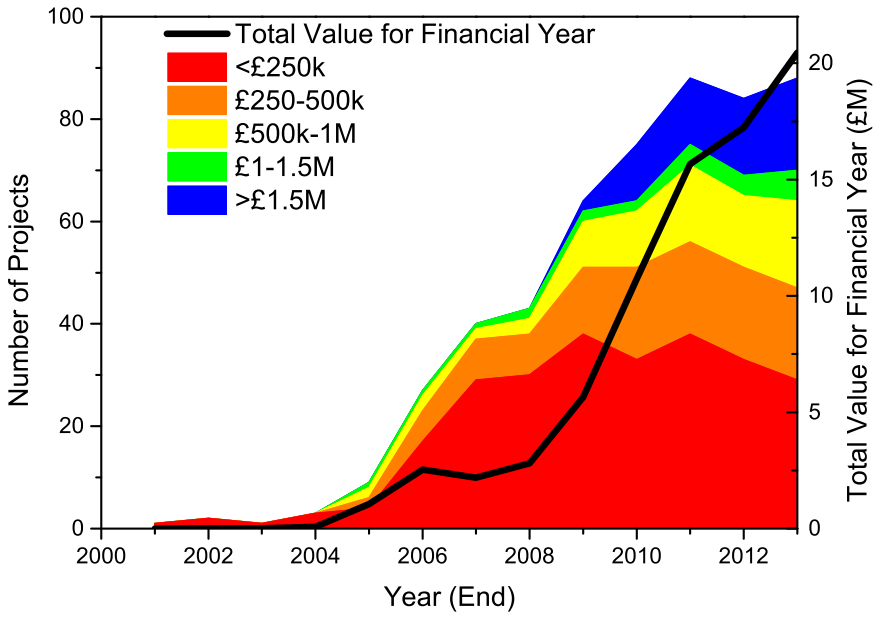

Figure 7.1: Research grants from RCUK between 2000 - 2013 which includes some CCS activity. Shaded areas show the number of projects financed in that year for five ranges of grant amounts. The solid line shows the total yearly spend with costs annualised for each project across their duration. Data from [UKERC, 2013]

Diversifying the technology options that qualified for funding put the UK more in line with

Europe where two other large-scale funding mechanisms that could apply to a range of CCS projects were in place. The European Energy Programme for Recovery (EEPR) was launched in 2009 with the intention of providing 4bn Euros for projects that were "*designed to make energy supplies more reliable and help reduce greenhouse emissions, while simultaneously boosting Europe's economic recovery.*"[EC, 2013] A proposed IGCC pre-combustion project at Hatfield won 180 million Euros of funding in 2009 and aimed to be operation by 2016/2017, even without initially entering the UK Demonstration Programme as it was based on pre-combustion capture technology. In late 2010, the European Union also announced the diversion of revenues from the sale of 300 million CO_2 allowances from the EU Emissions Trading Scheme (ETS) in order to fund the New Entrant Reserve (NER300) funding mechanism which aimed to support 8 CCS projects in the first round of funding [EC, 2010*a*]. By the end of 2010, technology-specific coalitions and several nations had publicly articulated their vision for the growth of CCS, both in terms of required levels of deployment [ACCAT, 2009, CSLF, 2010, IEA, 2009, ZEP, 2010] and in terms of knowledge gaps that needed to be filled in order for commercialisation to occur [APGTF, 2009, DOE-NETL, 2010]. In order to update the 2009 work by the Advisory Committee on Carbon Abatement Technologies (ACCAT) and further develop a national strategy DECC-OCCS also began work on the UK CCS Roadmap which was initially planned for publication in the Spring of 2011.

7.1.3 Involvement with the UK CCS Roadmap

During a presentation by Matthew Billson, head of technology development at OCCS, that outlined the plan for the R&D chapter it was apparent I could make a contribution to that section of the roadmap and benefit from experience working in a government department. I approached Matthew at the meeting and, with the support of my supervisors, during the period from November 2010 to March 2011 I worked with DECC-OCCS on developing the research and development (R&D) chapter of the UK CCS Roadmap.

Throughout the placement several meetings with an expert steering group were held with the goal of developing a view of the state of technological development and where R&D should be targeted across the entire CCS technology chain. I was responsible for creating the first draft of this matrix and completed this through an extensive literature search particularly focussing on the technology roadmaps mentioned above. After several iterations

with input from the expert steering group the research matrix was completed and, due to delay in publication of the UK CCS Roadmap, was published in a slightly modified form by the APGTF [2011]. The overview of future CCS research needs was subsequently included in the UK CCS Roadmap and is presented in Table 7.1. The meetings with the expert survey group and working alongside OCCS personnel strengthened the belief that although technical barriers to CCS development existed, a wide range of other factors were also important to the development of a UK CCS industry. The work that follows aims to fulfil the interdisciplinary aspect of my PhD and investigate the development of these factors and the UK CCS industry as a whole.

Table 7.1: Overview of future CCS research needs [DECC, 2012*a*]

R&D Theme	Short-term R&D needs (5–10 years)	Medium-term R&D needs (7–15 years)	Long-term R&D needs (10–20+ years)
Whole systems	• Investigate system operability and power plant interaction between CO_2 grid • Test flexibility to cope with change in demand • Develop CO_2 accounting	• Further investigation of complex interaction of CO_2 from multiple sources (capture technologies, industrial sources)	
Capture	• Learn from demonstration projects • Develop understanding of environmental impact • Identify requirements for retrofitting • Adapt technology for range of fuel types • Specify CO_2 standards • Establish common measures and monitoring	• Provide validation of demonstration capture technologies • Develop and demonstrate second generation capture agents and processes	• Develop commercially available systems with >85% capture rate for all fuel types • Develop capture systems with efficiency at least 45 percent including CO_2 capture
Industrial CCS	• Investigate extent to which CCS technologies could apply to industrial applications	• Identify sources with sufficient operational lifetime remaining to make retrofitting feasible	
Transport	• Understand potential hazards and risks to inform decisions on pipeline routes onshore • Develop techniques for leak mitigation and remediation • Develop ship-based transport	• Gather best practice data • Identify novel pipeline materials and sealing and joining technologies • Develop technologies to reduce power and cost of compression	• Develop performance database for CO_2 transport networks to enable grid optimisation
Storage	• Improve understanding of geological seal integrity and subsurface CO_2 behaviour/ flow • Estimate UK CO_2 storage capacity • Develop and demonstrate low-cost and sensitive CO_2 monitoring technologies	• Test injection at significant scale at multiple sites • Investigate water production • Develop techniques for rapid, detailed appraisal of formation capacity • Improve monitoring technologies	• Develop techniques for high efficiency use of formation capacity

7.1.4 Framing the research

Publications in the literature suggested the UK CCS industry could be analysed by considering it as a technical innovation system (TIS). Starting without a background in innovation studies predicated that for this research to be conducted in a successful manner, an accessible, proven technique of assessment needed to be found. While the initial literature search suggested investigation of industries based around technological innovation could be completed in a wide variety of ways depending on the discipline and focus of the analysis, modelling UK CCS as a TIS was quickly chosen as the most useful route of analysis for several reasons. Most notable among them were that a growing body of work focussing on using innovation systems to analyse the development of energy technologies was available in the literature (for example [Bergek et al., 2008, Foxon et al., 2005, Jacobsson and Bergek, 2011]) and the procedure had been used to analyse the industry in other nations developing CCS [van Alphen et al., 2009, 2010] and globally [Vergragt et al., 2011]. This meant that a peer-reviewed method of analysis was available and that any results from an analysis of the UK CCS industry could be compared to findings in other nations.

While the work of Vergragt et al. [2011] applies the TIS framework to CCS and Bio-CCS, the focus of that work was to compare the two technologies and to investigate the potential for fossil-fuel lock-in on a global scale. As a result of this, the application of TIS theory in the work of Vergragt et al. - while based on the same approach as van Alphen and colleagues - is only carried out by reviewing relevant published literature. Similarly, since the discussion of each of the system functions in that work relates to the global TIS it is very broad and difficult to highlight areas for recommendations (one of the key aspects of the functions of innovation approach). In this thesis it was thus decided to perform a similar expert survey to that reported by van Alphen et al. [2010] and complement this with an analysis of the wider aspects of the CCS industry. The following section presents background literature necessary to understand the development of the analysis method used during the expert survey and in the wider analysis.

7.2 Literature background

This is a targeted literature survey which is focussed on providing the background for analysing UK CCS as a TIS. A brief overview of innovation studies and the development

in this area includes examples of analysis of innovations by modelling them as TISs. This is then followed by selected complementary methods of analysis which are useful for the wider analysis of the UK CCS industry.

7.2.1 Innovation

Innovation is more than just technology development. In some cases it is useful to think of technical innovations in terms of their technology readiness levels (TRL), a concept developed by NASA in the 1970s and presented relative to developments in CCS in Table 7.2. However, the TRL method is somewhat linear in approach and does not capture many of the feedbacks present in the development of technology required for an in-depth analysis. Figure 7.2 shows a modification of the widely used innovation funnel to reflect the development stages of energy technologies that also can be considered to apply to CCS. Here it becomes clear that when talking about the development of innovation, feedbacks from different levels of the technology chain help to shape innovation at each stage of development. However, this too only addresses the ability of technology to fulfil a given criteria (in the case of CCS to significantly reduce the emissions to atmosphere of CO_2). To realise how innovation applies in actual markets a wider view of the process is necessary.

Table 7.2: Application of NASA technology readiness levels (TRLs) for CCS [GCCSi, 2011, Mankins, 1995]

TRL	Description
1	Basic principles observed
2	Application formulated
3	Analytical, 'proof of concept'
4	Laboratory component testing
5	Component validation in relevant environment
6	Process development unit (0.1-5 per cent of full-scale)
7	Pilot plant (>5 per cent commercial-scale)
8	Sub-scale commercial demonstration plant (>25 per cent commercial-scale)
9	Full-scale commercial development

In this work, the broad definition of innovation of "*covering the production, diffusion and use of new and economically useful knowledge*" described by Foxon et al. [2008] is used. This new knowledge of innovation can be discovered in a number of ways, and Lundvall [2010] "*insist upon the fact that not all important inputs to the process of innovation emanate from science and R & D efforts.*" Indeed as Lundvall then goes on to say "*learning by*

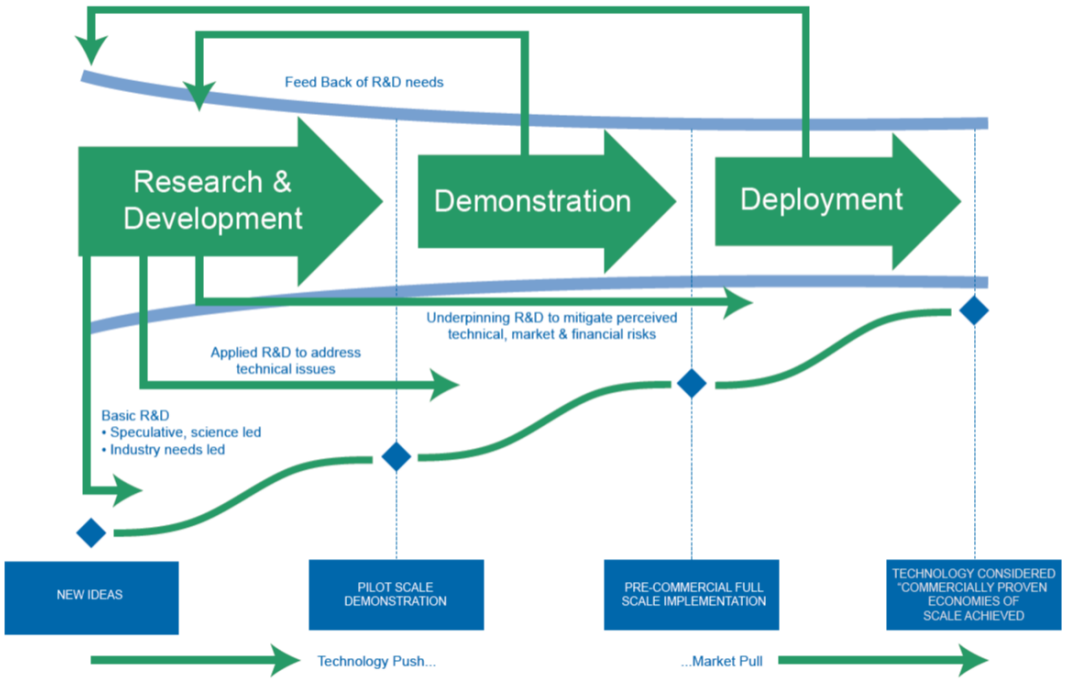

Figure 7.2: Innovation funnel adapted to UK energy technologies [ERP, 2006]

doing, increasing the efficiency of production operations [Arrow, 1962], learning-by-using, increasing the efficiency of the use of complex systems [Rosenberg, 1982], and learning-by-interacting, involving users and producers in an interaction resulting in product innovations [Lundvall, 1988]" all contribute to the development of new innovations. Innovation in these senses tends to build on the existing knowledge and therefore the addition to the knowledge pool is normally incremental where products are improved little-by-little over time through continued testing and development. Innovation may also occur in a radical fashion which may cause an innovation to occupy a niche that was previously unarticulated though this is intrinsically difficult to predict or analyse due to its unpredictable nature. Since innovation leads to quality improvements or cost reduction it is unsurprising that a large body of research focussing on how best to analyse (and promote it) exists in the literature.

While the development of innovations has historically been studied from distinct disciplinary viewpoints, more recently a collaborative atmosphere has developed allowing a better appreciation of the nature of innovations and their development in real world applications has become increasingly better understood. For example, it is now known that the development of a technological innovation is rarely the factor that is able to dictate the extent of market deployment of that technology. In fact the degree to which an innovation is able to penetrate a market is dependent on many factors which lie outside of the influence of

the technological developer. Rather than consideration of an innovation's development as a linear progression of discrete stages involving only technology-push and market-pull, more recent innovation thinking posits that an innovation exists within a system that is highly non-linear relying on feedbacks including R&D, market creation and learning-by-doing which all contribute to the state of development [Smits, 2002]. Moreover, as Hekkert et al. [2007] note "*the rate and direction of technological change is not so much determined by the simple competition between different technologies, but predominantly by the competition between various existing innovation systems, both fully developed and emerging ones.*"

7.2.1.1 Systems of innovation

Once it was recognised that innovations are part of a wider structure it becomes apparent that to understand the development of an innovation requires the system itself to be analysed. Innovation systems (IS) have been analysed in some form or another since at least the mid 1980s, and likely before that though not explicitly labelled as IS. For example, according to Johnson [2001], analysing large technological innovation systems was carried out by Hughes [1983] and analysis of innovation systems at a national level was reported by several others [Edquist and Johnson, 1997, Lundvall, 1992, Nelson, 1992]. However, Hekkert et al. [2007] point out that IS which are this broad include such a range of actors and institutions that their interactions are normally far too complex to analyse. Thus, it is argued that restricting the focus to a specific technology can greatly simplify the analysis. In formalising such a structure, Carlsson and Stankiewicz [1991] defined a Technical Innovation System (TIS) as "*a network of agents interacting in a specific economic/ industrial area under a particular institutional infrastructure or set of infrastructures and involved in the generation, diffusion, and utilization of technology*". Hekkert et al. [2007] argue that the complexity of large systems renders analysis must be static in nature and focus on past events which leads to criticism that they do not necessarily reflect what is actually happening in the innovation system and that through this they offer little guidance for policy. In their work Hekkert et al. [2007] instead suggest the "*activities that contribute to the goal of innovation systems (both positive and negative)*" should be analysed with such activities being named as "*functions of innovation systems*" by Johnson [2001].

System functions which aptly describe IS have been defined following several iterations of

analysis of empirical analyses. Having first defined system functions, Johnson [2001] goes on to describe two direct and eight indirect supporting functions of IS informed through assessing the methods used in relevant analyses in the literature. The work of Hekkert et al. [2007] updates this list, including work on national systems of innovations (NSIs) as well as TISs. Table 7.3 presents an overview of the functions from which Hekkert et al. [2007] conclude the seven system functions that best describe IS are (F1) entrepreneurial activity, (F2) knowledge creation, (F3) knowledge diffusion, (F4) guidance of the search, (F5) market creation, (F6) mobilisation of resources and (F7) creation of legitimacy. These system functions are adopted by van Alphen et al. [2010] in their work on CCS systems in which they provide an abridged description of each of these functions which is shown in Table 7.4

Although defining the system functions is important, it is only one stage of the process of analysing the TIS that Bergek et al. [2008] formalised, which is shown schematically in Figure 7.3. In their work, the authors suggest the TIS must first be identified along with the actors, institutions and networks existing within it. The system functions are then used to analyse the performance of the IS and the results of this interpreted to highlight factors which accelerate or block innovation and the development of the system. Highlighting strengths and weaknesses in the IS in this way provides a basis for policy recommendations.

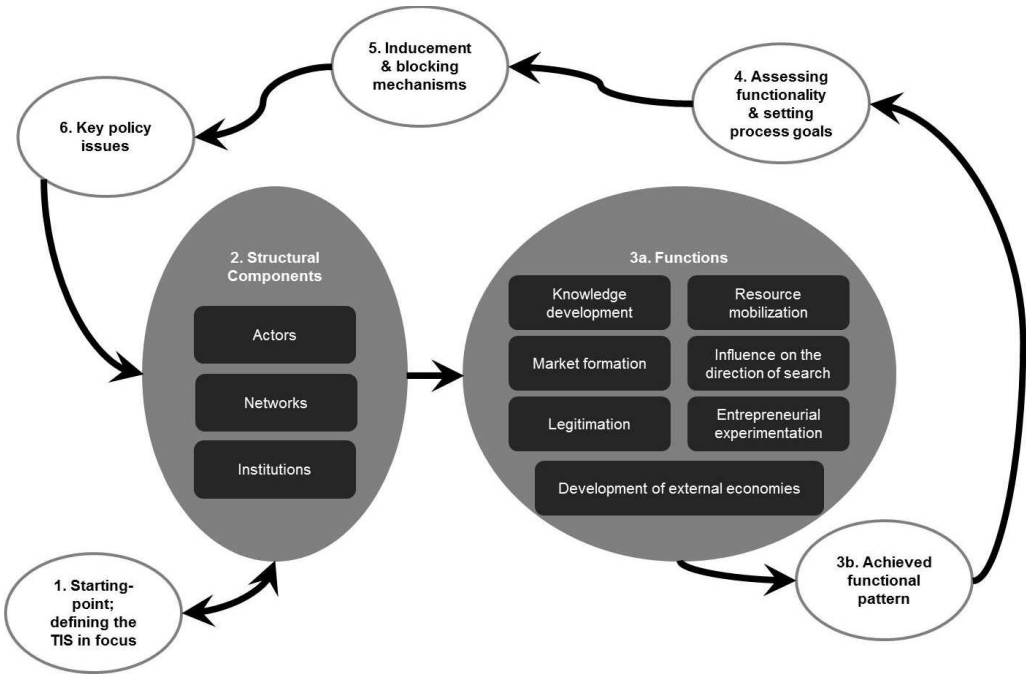

Figure 7.3: Scheme of analysis proposed by Bergek et al. [2008] for performing systems analysis of TIS

Table 7.3: A summary of the functions of innovation systems used by Hekkert et al. [2007] to formalise those shown in Table 7.4

Reference	Functions
McKelvey [1997]	• retention and transmission of information • generation of novelty leading to diversity • selection among alternatives
Galli and Teubal [1997]	*Hard functions* • R&D activities (public) • the supply of scientific and technical services to third parties *Soft functions* • diffusion of information, knowledge, and technology; • policy making; • design and implementation of institutions concerning patents, laws, standards, etc.; • diffusion of scientific culture, and • professional coordination.
Liu and White [2001]	• Research (basic, development, engineering) • Implementation (manufacturing) • End-use (customers of the product or process output) • Linkage (bringing together complementary knowledge) • Education
Johnson [2001]	Direct • Identification of the problem • creation of new knowledge Indirect • Supply incentives for companies to engage in innovative work • Supply resources (capital and competence) • Guide the direction of search (influence the direction in which actors deploy resources) • Recognize the potential for growth (identifying technological possibilities & economic viability) • Facilitate the exchange of information and knowledge • Stimulate/create markets • Reduce social uncertainty (i.e., uncertainty about how others will act and react) • Counteract the resistance to change that may arise in society when an innovation is introduced (provide legitimacy for the innovation)
Johnson and Jacobsson [2002]	• Create new knowledge • Guide the direction of search processes • Supply resources • Facilitate the creation of positive external economies (exchange of information, knowledge, and visions) • Facilitate the formation of markets
Smits and Kuhlmann [2004]	• Manage interfaces. • Build and organize (innovation) systems • Provide a platform for learning and experimenting • Provide an infrastructure for strategic intelligence • Stimulate demand articulation, strategy, and vision development • Stimulate and facilitate the search for possible applications

Table 7.4: Functions of the CCS innovation system presented by van Alphen et al. [2010] who abridged the work of Hekkert et al. [2007]

System Function	Description
Entrepreneurial activity	At the core of any innovation system are the entrepreneurs. These risk takers perform the innovative (pre-)commercial experiments, seeing and exploiting business opportunities
Knowledge development	Technology R&D are prerequisites for innovations, creating variety in technological options and breakthrough technologies
Knowledge diffusion	This is important in a strict R&D setting, but especially in a heterogeneous context where R&D meets government and market
Guidance of the search	This function represents the selection process that is necessary to facilitate a convergence in technology development, involving policy targets and expectations about technological options
Market creation	This function comprehends formation of new (niche) market by creating temporary competitive advantage through favourable tax regimes, consumption quotas, or other public policy activities
Resource mobilisation	Financial and human resources are necessary inputs for all innovative activities, and can be enacted through, e.g. investments by venture capitalists or through governmental support
Creation of legitimacy	The introduction of new technologies often leads to resistance from established actors, or society. Advocacy coalitions can counteract this inertia and lobby for compliance with legislation or institutions

7.2.2 Modelling CCS as a technical innovation system (TIS)

As noted in Section 7.1.4, a precedent exists for modelling national CCS industries as a TIS. In their work, van Alphen and his colleagues used the framework of analysis set our by Bergek et al. [2008] in combination with the functions defined by Hekkert et al. [2007] to analyse the CCS industries in a number of leading CCS nations in 2007/2008 [van Alphen et al., 2009, 2010]. These system functions were analysed by a series of semi-structured interviews with a variety of CCS experts, including academics, industrialists, policy makers and research funders. During the interviews, respondents were asked to rate their satisfaction with the fulfilment of each of the system functions on a 5-point Likert scale (where 1 = Very weak, 2 = Weak, 3 = Sufficient, 4 = Good and 5 = Very good). On the scale, a score of 3 rates a system function as sufficient with anything scoring below 3 being identified as potential blocking mechanism to the development of the IS. The work compares each of the system functions separately and also averages all scores to present a map of the aggregated innovation systems. Results from the work in other nations are discussed in detail alongside the results for the UK in section Section 7.3.2. The summary findings of van Alphen et al. [2010] are displayed in Table 7.5 where it is shown that some systems functions are better fulfilled than others. In Figure 7.12 the variation in the shape of the TIS in each nation in the [van Alphen et al., 2010] study is

Table 7.5: Results from an expert questionnaire on CCS in various countries [van Alphen et al., 2010]

Function	Netherlands	Norway	US	Canada	Australia	Average
Entrepreneurial Activities	2.5	2.7	3.2	3.1	3.3	2.9
Knowledge Development	3.7	3.8	3.9	3.9	3.7	3.8
Knowledge Diffusion	3.7	4	4	3.2	3.5	3.7
Guidance	3.3	3	3.2	2.6	3	3.0
Market Creation	2	2.9	2.2	2	2.1	2.2
Mobilization of Resources	2.5	2.7	3.0	3.1	2.9	2.8
Creation of Legitimacy	3	4	2.9	2.9	2.8	3.1

compared to that of the UK while variation between the views of expert groups in the UK is shown in Figure 7.13.

As noted in Section 7.1.4, Vergragt et al. [2011] also analysed CCS and Bio-CCS industries using the functions of innovation approach described by Bergek et al. [2008] and Hekkert et al. [2007]. However, unlike van Alphen and his colleagues who mainly focussed on semi-structured interviews, Vergragt et al. [2011] considered the TIS to function on a global scale and used a range of published literature to analyse how well each system function was performing. The focus of that work was more to provide a basis for arguing the possibility of technological lock-in to fossil fuels and lock out of Bio-CCS and as a result each of the system functions is only addressed in a cursory way in comparison to the analysis carried out in the work of van Alphen et al. [2010]. By focussing on the technologies at a global scale the work fails to capture many of the nuances that are highlighted between nations shown in Table 7.5. Similarly, the conclusions that all of the system functions can be rated as 'Strong' is markedly different to the expert views expressed in the questionnaires reported for individual nations where of the seven functions only knowledge development and diffusion are rated as significantly better than sufficient.

Although only making small references to the potential for Bio-CCS to develop on the back of a wider CCS industry - mainly focussing on the development of a dedicated biomass industry with CCS - the work also highlighted that many actors involved in CCS had little awareness of Bio-CCS and concluded that the TIS was currently very weak. This supports the decision of this work to analyse the wider CCS industry in the UK rather than specifically focus on Bio-CCS in the UK.

7.3 Expert survey

7.3.1 Methodology

According to the framework presented in Figure 7.3, the TIS in focus is defined as the CCS Industry in the UK. While it is recognised that actors, networks and influence from outside of the UK boundaries have potential to affect CCS in the UK, a number of circumstances mean the UK is relatively unique in the development of a domestic CCS industry. As noted by LCICG [2012]: "*There is no full-scale demonstration of a CCS technology chain directly replicable in the UK (Norway and North America have commercial scale CCS, but with major dissimilarities to CCS technology chains expected in the UK)*". This also means there is no perfect analogue to compare the state of development in the UK with which therefore introduces a degree of uncertainty which is noted.

The second stage of the framework suggested by Bergek et al. [2008] is to identify the actors, networks and institutions involved in the industry. In order for survey to well-represent the industry it was essential a range of actors involved in UK CCS were involved. Experts were identified as members of two groups: members of the steering group of the Research and Development chapter of the UK CCS Roadmap and speakers at UK CCS Community (UKCCSC) events. These groupings were chosen in an attempt to reduce bias since anyone in these groups had been identified as an expert by their peers in the organising committees (DECC-OCCS and the UKCCSC board respectively). At the time of the survey a total of 88 experts were identified as potential participants for the survey. Of this group contact was made by email with the 75 experts for whom addresses were known to the researcher or were publicly available.

On account of the research involving human participants it was necessary to ensure the research conformed with the University ethics policy. An application was submitted to the MaPS and Engineering joint Faculty Research Ethics Committee (MEEC FREC) under reference 10-024 and following the submission of further material and reasoning, clearance was granted for the project on 2 June, 2011.

In order to provide a basis for comparison with the expert findings for other nations surveyed by van Alphen et al. [2009] experts in the UK CCS Industry were asked to answer the same questions as those posed in the previous study. Through this decision, the third stage of the framework suggested by Bergek et al. [2008] - identification of development

of each of the system functions - was also performed. The questionnaire asked experts to rate on a 5-point Likert scale their level of satisfaction with the UK CCS industry in relation to questions covering the seven system functions shown in Table 7.4. In addition to numerically grading each of the aspects of the functions, participants were also given the opportunity to comment on the system functions and provide recommendations for improvement which may increase their level of satisfaction with that aspect of each system function. Although experts were drawn from a variety of backgrounds they were asked to answer the questions considering the entire CCS industry and not just their area of expertise. These questions, covering the seven system functions, were translated to create an online questionnaire using the Bristol Online Surveys, of which the University of Leeds is a paid subscriber.

7.3.2 Results and discussion

Of the 75 experts contacted, 34 completed the survey between July and September 2011 providing a snapshot of the industry at this time. Figure 7.4 shows the experts were drawn from all parts of the TIS and included representatives from academia (A), industry (I) and publicly-funded organizations (P).

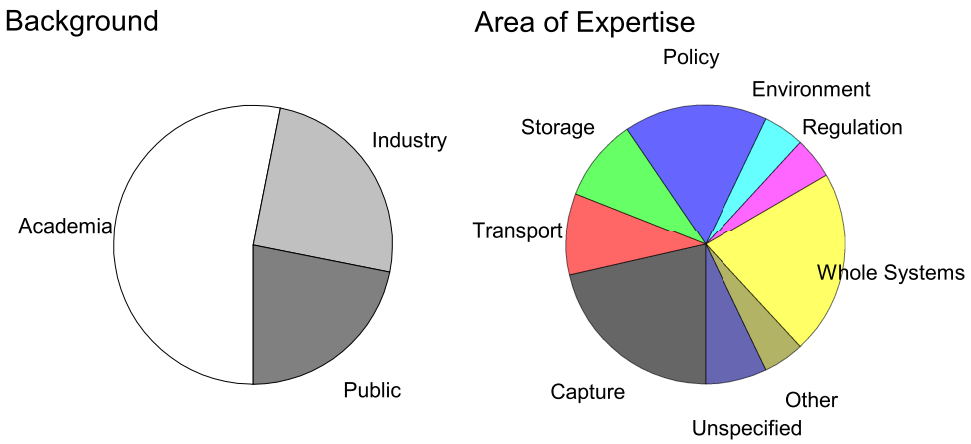

Figure 7.4: Background of the participants involved in the expert survey

In order to co-ordinate reminder emails, during the survey's operation it was useful to

maintain a register of experts who had completed the survey. However, once the survey period concluded the results were anonymised. For the numerical data generated by the Likert scale simple averages of values submitted for each question and for each system function were calculated. In this section, the results for each of the system functions are discussed separately with qualitative results used to add depth to the findings for each of the system functions. The results for each function are then aggregated for the UK with the functional pattern being mapped for each of the participant sectors in Figure 7.13 and compared to the patterns in other nations in Figure 7.12. An aggregated summary of qualitative responses is presented in Table 7.6.

7.3.2.1 Entrepreneurial activity

F1: Entrepreneurial activity		**A**	**I**	**P**	**Average**
a	The number and the degree of variety in entrepreneurial experiments?	2.31	2.50	2.13	2.31
b	The number of different types of applications?	2.47	3.00	2.38	2.58
c	The breadth of technologies used and the character of the complementary technologies employed?	2.50	2.75	2.63	2.59
d	The number of new entrants and diversifying established firms?	2.75	2.88	2.25	2.66
	Average:	2.51	2.78	2.34	2.54

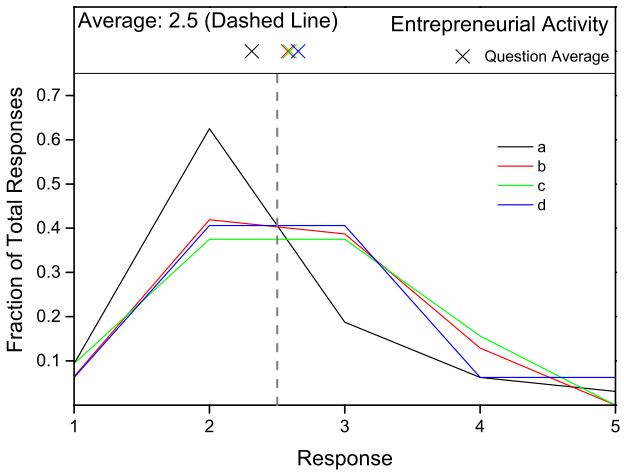

Figure 7.5: Questions and results of the expert survey - entrepreneurial activity

Figure 7.5 shows entrepreneurial activity in the UK is graded on average with a value of 2.54 indicating the average expert view is that more needs to be done to boost this system function. This value is equal to the Netherlands and lower than that reported for any of the other nations in the previous work which could suggest the UK is behind in this area.

However, more detailed analysis of the data suggests there is a marked split in the views of different sectors of experts.

In every question in this section, experts from industry scored their satisfaction the highest of all of the sectors. Publicly-funded experts rated their satisfaction the lowest in three of the questions (a, b and d) while experts from academic backgrounds viewed question c with the least satisfaction.

The number and degree of variety in entrepreneurial experiments was seen as least satisfactory aspect of this system function and was one of the lowest scoring results of the whole survey with an average value of 2.31, the lowest score for each sector within this system function. Over 70% of the experts were not satisfied with this aspect of CCS in the UK. The averaged scores for the other questions were all in the range 2.58–2.66 suggesting these areas may also require attention but with at least half of the respondents satisfied with these sub areas of entrepreneurial activity.

From the possible methods of strengthening this system function it appears that the main reason the experts felt entrepreneurial activity was lacking was due to commercial viability, with one expert noting "*there is no clear business model that is particularly appealing to entrepreneurs*". Strong scores for knowledge creation in the following section suggests that early-stage R&D is sufficient but it appears few companies, either SMEs or diversifying large companies, are willing to invest in capital-intensive projects that bridge the gap between laboratory or pilot-scale and full-scale demonstration. Many experts suggested an accessible national test centre that was available to industry could significantly strengthen this system function.

Although often described as being particularly cautious, the relative strength of the industrial view in this system function may represent the sentiment explained by van Alphen et al. [2009] of "*it is time to really start learning by doing, rather than 'learning by planning'* " while academics and policy makers may be keen to continue testing at small-scale to ensure picking the right technology option.

7.3.2.2 Knowledge creation

Knowledge creation was the second strongest function for CCS in the UK with an average score of 3.02. Within the sectors the average ranged from 2.88 for Industry to 3.19 for

F2: Knowledge creation		A	I	P	Average
a	The number and degree of variety in RD&D projects?	2.94	3.25	3.50	3.15
b	The type of knowledge (scientific, applied, patents) that is created and by whom?	3.06	3.00	3.38	3.12
c	The competitive edge of the knowledge base?	3.33	2.75	2.88	3.09
d	The (mis)match between the supply of technical knowledge by universities and demand by industry?	2.72	2.50	3.00	2.74
	Average:	3.01	2.88	3.19	3.02

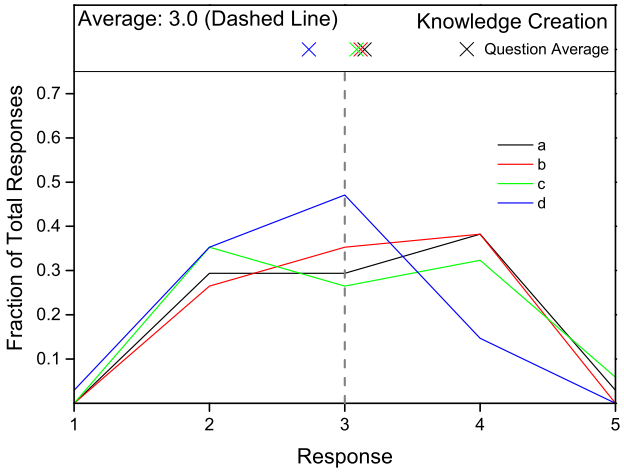

Figure 7.6: Questions and results of the expert survey - knowledge creation

publicly-funded experts and with academia scoring 3.01. In other nations this system function was on average the strongest with scores ranging from 3.5 for the Netherlands to 3.9 for the USA and Canada.

For all of the questions in this section, over half of the experts were at least satisfied with each subsection of the system function and approximately a third of experts awarded a 'Good' level of satisfaction for questions a,b and c.

Publicly-funded experts rated this system function the highest of the sectors in three of the questions (a, b and d) while industrial experts rated rated it lower than the other sectors in three of the questions (b, c, and d).

From the comments received, the experts appear to have slightly mixed views in terms of what is required to further develop this system function. In general, it appears to be felt that there is good research being conducted and good support from funding sources (particularly research councils and DECC). However, poor communication between industry and universities appears to hindering this system function with one industrial expert suggesting "*Universities may need more focus*" while an academic expert viewed it that "*there is*

still a lack of demand [for research] *by industry*". Contrastingly, other experts felt that the UK research portfolio may be too narrow and that a broader range of early-stage research should be carried out.

In response to whether the UK was at the leading edge of CCS research many respondents from all sectors noted that although "*Competition within the academic community is very high*" the "*UK is poor at commercialising*" new technology and that "*UK demonstration projects* [...are needed...] *to establish a UK lead in the technology.*"

7.3.2.3 Knowledge diffusion

F3: Knowledge diffusion		**A**	**I**	**P**	**Average**
a	The amount and type of (inter) national collaborating between actors in the innovation system?	3.50	3.13	3.25	3.35
b	The kind of knowledge that is shared within these existing partnerships?	3.28	2.75	3.25	3.15
c	The amount, type and 'weight' of official gatherings (e.g. conferences, platforms) organised?	3.83	3.00	3.50	3.56
d	Configuration of actor-networks (homo, or heterogeneous set of actors)?	3.33	3.00	3.25	3.23
	Average:	3.49	2.97	3.31	3.33

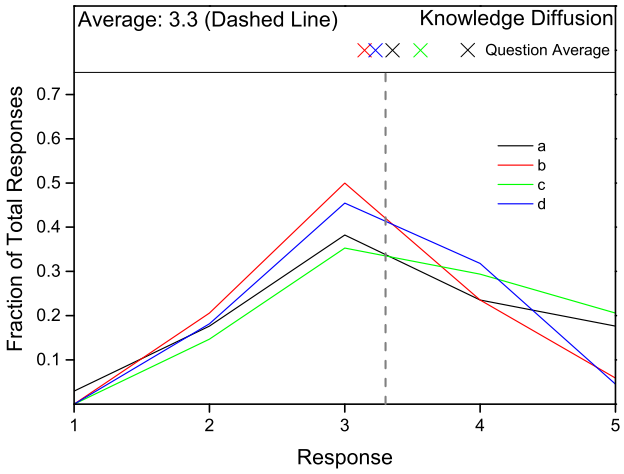

Figure 7.7: Questions and results of the expert survey - knowledge diffusion

Knowledge diffusion was seen as the strongest system function in the UK TIS scoring an average of 3.33. This was particularly strong in the academic community where experts scores were consistently the highest and averaged 3.49. Publicly-funded and industrial experts also rated this system function highly relative to the others. However, the diffusion of knowledge was consistently rated lower by industrial experts than those in publicly-

funded or academic roles.

High levels of satisfaction with this system function in the UK reflect similar findings for other nations where it was also found to be one of the strongest functions. The UK scored lower than the Netherlands, Norway and USA but this system function was seen as stronger than in Canada (3.2) and Australia (3.1).

For all questions in this function a sufficient level of satisfaction was the highest scoring response and over 70% rated each question as sufficient or better. Scores were particularly high for questions a and c with almost half of the experts suggesting the amount of collaborations and official gatherings were 'Good' or 'Very good'. In fact, when invited to comment several experts from a range of sectors suggested there were too many events and meetings and that these were often "*too diffuse*" indicating "*a need for more targeted interactions*" in the future. Interactions with European partners were seen to be strong and several references to benefits from European-funded projects were made though little collaboration outside of Europe was evident. Several industrial experts also drew attention to the commercial nature of knowledge noting "*confidentiality of commercially sensitive data may be an issue*" and one made the point that although knowledge sharing within collaborative groups may be effective that "*EU projects need to report more fully*" in order to share that knowledge with the wider community.

7.3.2.4 Guidance of the search

Guidance of the search was seen as performing relatively well for the UK scoring an average of 2.86. However, the variation between sectors was considerable. The view of publicly-funded experts was considerably more positive than the other sectors for three of the questions (a,b and d). Academic experts were most concerned about the amount and type of of expectations about the technology and the belief in its growth potential averaging 0.6-0.7 less than the score for the publicly-funded experts. Industrial experts believed the specific targets set by industry and government were of particular concern rating this factor at 1.75 - the lowest score for any sector to any question. Conversely, publicly-funded experts were on average satisfied with this sub-function illustrating significant variation between the groups of actors.

In comparison to other nations the UK scored was rated as slightly weaker than the average (3.0) but stronger than Canada (2.6). This may be explained by the postponement and

F4: Guidance of the search		A	I	P	Average
a	Amount and type of visions and expectations about the technology?	2.71	2.88	3.25	2.88
b	Belief in growth potential?	2.94	3.00	3.63	3.12
c	Clarity about the demands of leading users?	3.06	2.75	3.00	2.97
d	Specific targets or regulations set by the government or industry?	2.56	1.75	3.00	2.47
	Average:	2.82	2.59	3.22	2.86

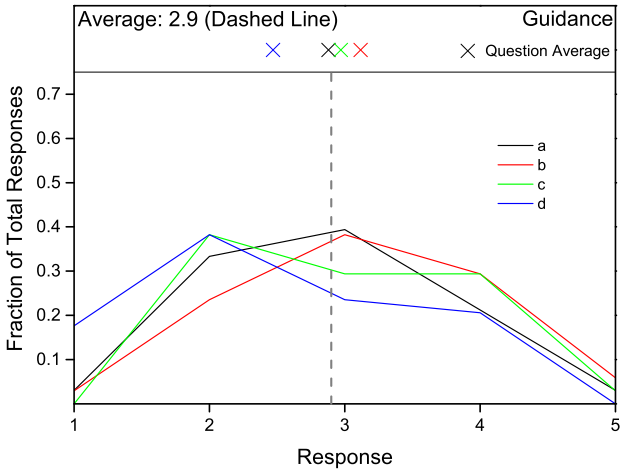

Figure 7.8: Questions and results of the expert survey - guidance of the search

cancellation of a large number of CCS projects around the world which could have caused UK respondents to be less inclined to trust the rhetoric of some governments. Indeed, one industrial expert noted: "*Vision is OK, but no government commitment*". However, this sharply contrasts with a public-funded expert's response of "*too much hyperbole from industry - expectations need to be realistic*". One expert summarised the feeling noting:"*There is a bit of a disconnect between aspiration and what is actually achievable and affordable in the real world.*" Many respondents suggested commitment to CCS in government policy was necessary to boost the belief in growth potential with the point made that there is "*no commitment beyond demonstration*" projects. In terms of clarity about the demands of leading users, many respondents pointed to the risks associated with the storage aspects of the CCS chain and that more information sharing was needed in this area. That the final question drew such a wide range of responses (with almost 20% rating this function as 'very poor' and also 20% rating it as 'good') suggests a complex set of issues here which is exemplified by the range of answers to suggested improvements. Some experts interpreted the question to mean targets for deployment of CCS at scale and either mentioned government policy was urgently needed to strengthen this or suggested industry needed

to catch up. Other respondents tended to focus on the regulation aspect and concluded more work was needed in this area in order actually get projects going noting "*pipeline and transport regulations could be improved*" and "*environmental regulations need specifying*". One respondent concluded with a mixed response noting: "*some targets are technically unrealistic...but others are technically achievable but politically big stretches*".

7.3.2.5 Market creation

F5: Market creation		A	I	P	Average
a	What phase is the market in and what is its (domestic & export) potential?	2.47	1.88	2.63	2.36
b	Who are the users of the technology how is their demand articulated?	2.80	3.00	2.71	2.83
c	Institutional stimuli for market formation?	2.38	2.38	2.75	2.48
d	Uncertainties faced by potential project developers?	1.88	1.88	2.25	1.97
	Average:	2.38	2.28	2.58	2.40

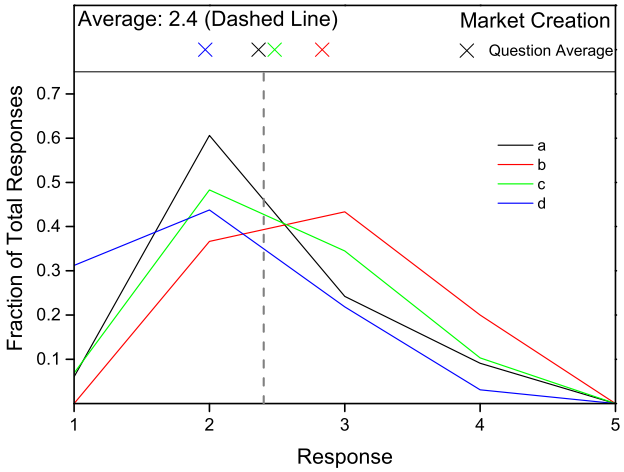

Figure 7.9: Questions and results of the expert survey - market creation

Market creation was viewed as the weakest of the system functions, scoring an average of 2.40. With the exception of industrial experts response to how well they believe they are articulating their demand, every sector averaged a score below 3 for each question. In all questions industry and publicly-funded experts are at the opposite ends of the range with publicly-funded experts being most satisfied on average with questions a, c and d and the least satisfied for question b. Industrial experts were particularly concerned with the phase that the market is in and the need for help to overcome uncertainties that developing new technologies presents. This worry regarding uncertainties is shared by

the other sectors too and with an average score of 1.97 this is the lowest scoring response to any question.

When compared to the results for other nations (average 2.2), the UK scores better than all except Norway (2.9) in this system function which may initially suggest, despite still being insufficient, the UK is performing relatively well in this area. However, the two-year time difference between the surveys is likely to be a contributing factor to this disparity and had experts in the UK been questioned two years previously it is believed they would have been less satisfied with the development of this system function. The low level of satisfaction notwithstanding, it is worth crediting the advances that have been made in recent years in moving towards creating a market that CCS can operate within while bearing in mind this still represents an area with much room for improvement.

Many experts from all three sectors tend to note that the market for the UK domestically and abroad could offer "*good potential for export*" but that at the moment because "*the market is in early stage of development*" more needs to be done to foster the growth of CCS in power generation and in capturing emissions of CO_2 from industrial sources. Potential users of CCS are seen to be reticent to commit to the market and knowledge sharing and instead tend "*to be developing 'in house' with little input from academics*". Institutional stimuli are widely seen to be needed in the form of price signals, specifically through Electricity Market Reform (EMR) for the power generation sector. Indeed it is noted that "*government will make the market*" and that "*DECC needs to maintain momentum*" in order to help the market mature. Uncertainty is the most common feature of comments from experts who identify a multitude of areas in which uncertainty must be addressed including funding, post-demonstration projects, long-term carbon pricing, storage liabilities and government intentions.

7.3.2.6 Resource mobilisation

The mobilisation of resources was viewed as one of the weaker system functions with an average score of 2.54. Again differences between the sectors were clear with publicly-funded experts more satisfied with this function than the other sectors for every question recording an average of 2.9. With the exception of the availability of human capital, industrial experts expressed the least satisfaction with all of the questions averaging a score of 2.34. Both academic and industrial experts were least satisfied with the availability of

F6: Resource mobilisation		A	I	P	Average
a	Availability of human capital (through education, entrepreneurship or management)?	2.67	3.13	3.25	2.91
b	Availability of financial capital (seed and venture capital, government funds for RD&D)?	2.17	1.88	3.00	2.29
c	Availability of complementary assets (complementary products, services, network infrastructure)?	2.59	2.25	2.71	2.53
d	Level of satisfaction with the amount of resources?	2.47	2.13	2.63	2.42
	Average:	2.47	2.34	2.90	2.54

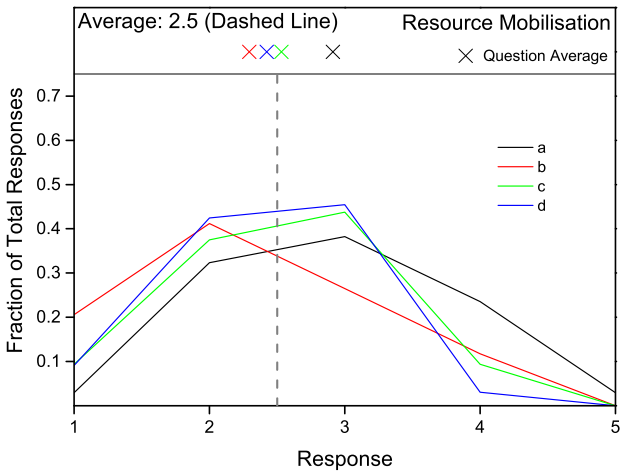

Figure 7.10: Questions and results of the expert survey - resource mobilisation

financial capital available to CCS projects while publicly-funded experts were most concerned with the amount of resources available to CCS more generally.

In comparison to other nations, which averaged a score of 2.8, satisfaction in the UK was, with the Netherlands (2.5), the joint worst amongst the nations. Experts from Norway (2.7) and Australia (2.9) were also dissatisfied with the development in this area while the USA and Canada were deemed to be making good progress scoring 3.0 and 3.1 respectively.

Although insufficient on average, the modal choice for experts for questions a, c and d was that they believed the development was sufficient. Most experts note that although human capital is currently sufficient because "*there are so few projects that this isn't yet a problem*", should the industry grow it is likely there will be a shortfall in capacity in when growth occurs and thus there is a need for "*capacity building*". Although some experts feel the government funding for research is sufficient, it appears there is "*little evidence that private sector will commit funding*" because "*technology is seen as unproven*" which as one expert commented it may be because "*the availability of capital for CCS implementation*

beyond 2020 is doubtful." Complementary assets to CCS are also thought to be being hampered by a lack of demonstration projects which could mean "*engineering skills and assets may be atrophying*".

7.3.2.7 Legitimisation

F7: Legitimisation		A	I	P	Average
a	Public opinion towards the technology and how is the technology depicted in the media?	2.24	2.63	2.75	2.45
b	How well articulated are the main arguments of actors pro or against the deployment of the technology?	2.83	2.88	3.00	2.88
c	Legitimacy to make investments in the technology?	2.65	2.43	3.14	2.71
d	Activity of lobby groups active in the innovation system (size and strength)?	3.06	2.88	3.00	3.00
	Average:	2.69	2.70	2.97	2.77

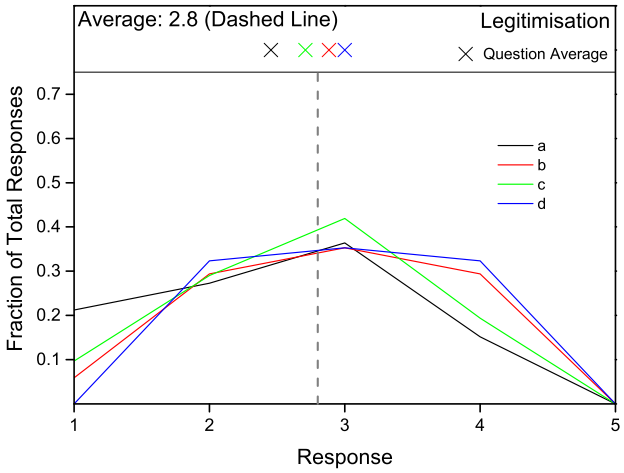

Figure 7.11: Questions and results of the expert survey - legitimisation

Legitimisation of the development of a UK CCS industry was rated on average to be insufficient with an average score of 2.77. Unlike other functions, there appeared to be relative agreement between the sectors. The publicly-funded researchers were generally more satisfied with this area scoring the highest in questions a, b and c. Academic experts were least satisfied with the general articulation of the need for CCS while industrial experts were least satisfied with legitimacy in order to make technological decisions and also at the activity of lobby groups.

The average score for the UK was similar to that reported for the lowest scoring of any of the other nations which averaged a satisfaction rating of 3.1 with scores ranging from 2.8 (Australia) to 4 (Norway).

Public opinion was clearly a worry for some experts with over 20% indicating they were very dissatisfied with public opinion to CCS and its depiction in the media. Some experts called for "*public education*" while others note that public opinion is relatively unknown since "*public interest is low*". This also led to some experts suggesting it may be better to "*ensure communications are well targeted*" and "*question exactly which publics actually need to be actively aware/ engaged with CCS*". Successful communication of risk to the public appears to be one area more energy is required with experts suggesting the research needs to mature before having more public conversations, while others suggest a lack of scientific understanding may be one reason those "*against* [CCS] *are very strong but pro* [CCS] *are very weak in getting the message across*"'. One expert suggested that the Climate Change Bill was "*a good start*" in creating legitimacy to make investments in the technology but another expert notes that "*long term investment needs*" are currently not met indicating more legitimacy is required before businesses can invest in long-term CCS assets.

7.3.2.8 Summary

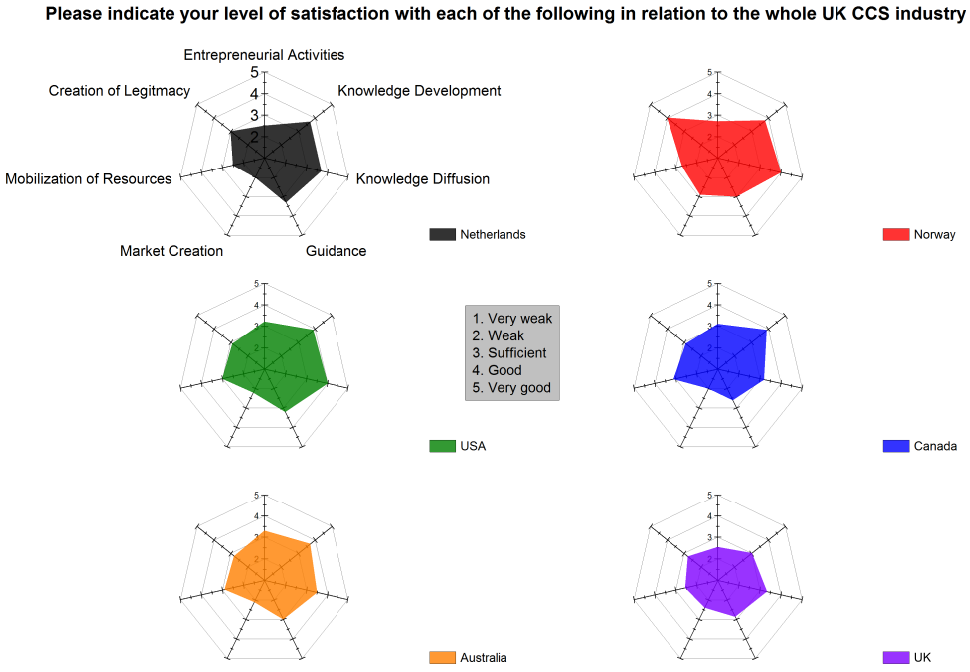

Figure 7.12: Quantitative results from the expert survey carried out in Autumn 2011 compared to other nations reported by van Alphen et al. [2010]

In the TISs of all of the nations analysed there is room for improvement if a CCS industry is to develop. The functional patterns of the TIS for the UK and the nations reported in van

Alphen et al. [2010] are shown in Figure 7.12 where it becomes clear that the innovation systems display somewhat different patterns for each of the nations. For example the functional pattern of Norway is distinctly different to the others presented where the tax on emissions of CO_2 initiated in 1991 has both had the effect of creating legitimacy for the development of CCS and also created a market for it to exist within. However, like the other nations analysed, the UK is weak in these two areas.

Although the UK TIS presents a considerably smaller footprint than the other nations, it appears to be the one developing in the most concomitant fashion. Although considering this analysis was conducted approximately two years after that for the other nations this suggests the UK is significantly behind in developing CCS as has been highlighted consistently throughout this section. The patterns for the Netherlands, USA, Canada and Australia clearly identify market creation as a potential blocking mechanism while in Norway entrepreneurial activity appears to be the most likely cause of delayed development as other functions are deemed as being fulfilled to at least a satisfactory level. As with many of the nations leading CCS development, the creation and diffusion of knowledge and the guidance of the search are relatively strong functions for the UK.

7.3.2.9 Variation in opinion between experts in the UK

A comparison of the averages from the different groups of respondents is presented in Figure 7.13 and highlights some striking disparities between sectors of the TIS. Experts from publicly-funded bodies are the most optimistic of the three expert groups scoring their level of satisfaction with fulfilment of system functions highest in five of the seven functions. Conversely, industry recorded the lowest level of satisfaction in all of the system functions except entrepreneurial activity which they viewed as the best fulfilled out of the three groups. Academics were generally less satisfied with how well system functions were being fulfilled than publicly-funded experts and marginally more optimistic than industry, except when asked about knowledge diffusion which they rated as by far the most well fulfilled function.

In analysing how the different sectors view the development of the industry, such variation in results between sectors across different functions indicates a significantly different view of the state of development of the UK CCS industry. On one hand the results suggest that each group of experts seems to have a higher opinion of their own role being satisfied

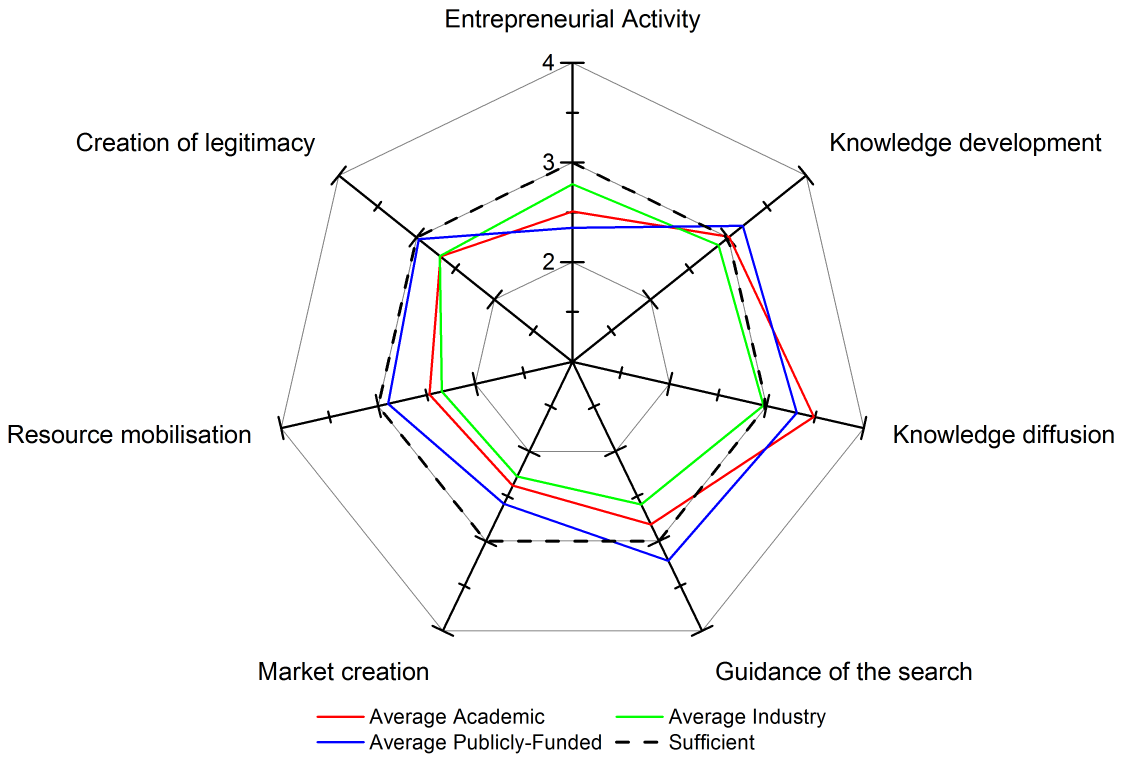

Figure 7.13: Quantitative results from the expert survey carried out in Autumn 2011 separated by the sector the respondents were drawn from

in the development of a UK CCS industry. For example, publicly-funded experts - including policy-makers and regulators - believe guidance of the search, resource mobilisation and the creation of legitimacy are considerably better fulfilled than their academic and industrial colleagues. When considering this it is useful to bear in mind two things. First, that at the time of the survey it is government policy (through the Climate Change Act and subsequent decarbonisation programmes) that mainly provides legitimacy for the development of CCS in the UK. Second at the time of the survey it was the Demonstration Programme that was most engaged with mobilising resources (including £1bn of Government funding) and, through its relatively strict criteria, guiding the search for future development. As well as having a higher opinion of their own role in UK CCS development, each of the three groups were generally less positive about the roles which are led by other sectors. For example, on average publicly-funded experts take the view that most needs to be done in entrepreneurial activity (which is largely the responsibility of industry who score it highly) while industry and academia think much is lacking in the three functions listed above that publicly-funded experts are most positive about.

When discussed in terms of self-reflection, it may not be so surprising that different groups believe that their own contribution to the development of the CCS industry is adequate

and that it is others who are responsible for its delayed development. However, such variation may in itself indicate that the TIS is not functioning effectively since it may create a complacency with groups of actors and fracture the need to develop with the other actor groups. Indeed, since all of these sectors need to act together and focus resources on areas that are currently preventing the UK moving forward, an inability to decide which areas are most pressing could in itself slow development of the industry.

7.3.2.10 Synthesis of qualitative results

Within each of the previous sections, a selection of the comments made were included to help explain some of the strengths and weaknesses reported in the scores given by the experts. A concise version of these comments and recommendations to strengthen system functions is presented in Table 7.6. In summary, research and the generation of new ideas is generally seen as performing well though how well the research generated aligns with industrial needs was questioned with shared facilities to bridge the gap between the laboratory and real-world suggested to foster more entrepreneurs and to connect the different groups responsible for developing CCS technology. While forecasts for the development of CCS in the UK were largely viewed favourably, a lack of detail on both the specifics of how the industry might operate and wider energy policy were seen as blocking the development of the market by restricting the mobilisation of resources and perhaps diminishing the legitimacy of the technology. Targeted campaigns to engender public support were highlighted on several occasions in attempt to overcome the potential blocking of projects due to poor awareness and opposed public sentiment.

7.3.2.11 Limitations of the results

Although the results and analysis provided in this section are believed to provide a robust snapshot of the state of development shaped by the view of some of the leading experts in the CCS field there are some limitations to how far the findings from the work can be extended. Indeed although the results in Figure 7.12 are useful, as noted by Bergek et al. [2008]: "*the functional pattern does not in itself tell us whether the TIS is well functioning or not; that a particular function is weak does not always constitute a problem, nor is a strong function always an important asset.*" Through extending the survey and incorporating the qualitative sections to augment and explain the scores provided by the experts

Table 7.6: Synthesis of the comments and recommendations for improvement from the expert survey

System Function	Synthesis of Issues and Recommendations
Entrepreneurial activity	• Lacking at-scale testing facilities for entrepreneurs and researchers • National test centre with accessible rates to all suggested • Government incentives to bring SMEs and diversifying incumbents into developing CCS technology
Knowledge development	• General satisfaction with research being completed and support provided • Breakdown of communication about research between industry and academia could stall development due to mis-matching ideas • Mixed view on whether UK research portfolio was optimal
Knowledge diffusion	• Generally felt that within UK and EU collaborations are strong • Knowledge transfer in academia more developed than in industry due to commercial sensitivity • Need for more focused meetings to continue to drive technology forward
Guidance of the search	• Long-term targets, guidance and policy are lacking • Visions and expectations for CCS satisfactory, but • Detailed demands of users and regulators need specifying
Market creation	• CCS has potential for UK domestically and as an exportable commodity • Protectionism and uncertainty is preventing market growth • Government needs to create long-term certainty for market and liabilities
Resource mobilisation	• Current human capital is sufficient • Investment in training needed now to ensure sufficient human capital for industry growth • Securing financing, particularly post-demonstration, widely seen as problem for developers
Creation of legitimacy	• Lack of public support is seen as a potential blocking mechanism • Targeted public awareness, education and media exposure of CCS all cited as necessary • Climate and energy policy helpful but need to go further. More lobbying suggested

helps provide a richer account of how the experts surveyed view the state of development. However, if the results were to be considered to give a complete picture of the state of development of CCS in the UK they would have to satisfy the following criteria:

- the questions would need to be accurate predictors of each of the system functions
- the system functions would have to cover all dimensions of development of the industry
- the input would need to be sought of all actors capable or engaged in affecting the development of the UK CCS industry.

Through adopting the system functions established by Hekkert et al. [2007] this work assumes the wider development landscape is well-represented by those system functions and that the questions posed by van Alphen et al. [2010] that are also employed here are good indicators of how each of those system functions relates to the UK CCS industry. It is beyond the scope of this thesis to analyse in detail how well the questions and system functions address the overall concept of development of CCS in the UK. However, the derivation of these system functions from a wide range of empirical studies (as noted in Table 7.3) and that the majority of comments received from experts aligned with one or several of the system functions suggested that as a framework this was a robust way of encompassing most of the facets of a developing CCS industry. Despite this, some notable areas are excluded from the system functions used in this work perhaps because to include them would require expanding the survey to include non-experts and people currently not engaged with the development of CCS. As the work of Poortinga et al. [2013] notes, the development of large infrastructure and energy projects may be completely derailed by relatively small pockets of local opposition. In this way, the system functions do not go far enough in including the public view into the discussion. Although creation of legitimacy broadly covers this, the pressing need for outreach, both as education and lobbying, for the CCS industry is strikingly clear in the comments received from the experts. To gauge how well the expert view on public support is reflective of the actual public view is difficult though the importance of calibrating this cannot be understated.

7.4 Developments in UK CCS

This section analyses how the CCS innovation system has changed since the survey was completed as, although the expert survey provided a snapshot of the industry during the period July–September 2011, the industry has since been in a fairly dynamic state. This is completed by conducting a review of relevant literature since published which is set alongside developments and setbacks to the industry. During the period of this research several useful documents have been published. Analysis of these documents strengthen the findings from the expert survey and being drawn from a variety of expert sectors continue to highlight differences in perspective between the various sectors of actors operating in the UK CCS Industry. The following list of reports is not exhaustive; the fact that there is such considerable interest in CCS indicates a large number of academic papers, government documents and other relevant literature has been published. However, in this analysis the focus is on the following publications which are judged to be particularly significant to the development of a UK CCS Industry. The analysis follows a chronological pattern based upon the publication of these reports and the announcements of milestones in CCS's development. The section concludes with a discussion of the findings and effects of the various publications on innovation in the UK CCS industry.

7.4.1 Cancellation of the CCS demonstration programme (Demo1)

Soon after the expert survey concluded in October 2011, the Demo1 was cancelled as DECC and the project partners failed to agree terms and costs for the Longannet plant. A subsequent report by the National Audit Office (NAO) found a number of areas in which the Government had failed to deliver best practice. In particular, a lack of flexibility in the original project specification and a failure to engage early enough with industrial stakeholders were highlighted as giving rise to the project's ultimate failure with the report noting: "*The Department engaged with the project costs but not the commercial costs until a later stage in negotiations with the final bidder. For its new programme, the Department needs to understand fully its commercial proposition to industry, fully investigate the costs and the technical, price and regulatory risks in individual projects and compare their value*"[NAO, 2012]. Since the project was a first-of-a-kind for the department it may be hoped that the failings in the first project will be learned from in the future. However, perhaps more worrying for the TIS in general was the "*Lack of clarity over government finance for the*

project" and, in particular, the "*evolving background of economic, policy and regulatory uncertainty*" [NAO, 2012]. That NAO note that the Government "*wanted industry to take up a commercial contract, for a large and potentially costly developmental project, with considerable uncertainty over its design and costs*" perhaps helps to illustrate the lack of guidance referred to by the industrial sector in the expert survey, a feature which was recognised by Scotland's First Minister Alex Salmond MSP who was quoted as saying the the cancellation was "*deeply disappointing* and attacking the Government's lack of "*courage and the vision to make the investment happen*" [BBC, 2011]. In an attempt to show continued support for CCS despite the cancellation of the demonstration project, the government announced that the £1bn in capital funding for CCS demonstration would continue to be available and a new competition would be launched for more projects.

7.4.2 Public and industrial support for CCS: late 2011–early 2012

The cancellation of the Longannet project in October 2011 further delayed the publication of DECC's CCS Roadmap though other Government and industrial reports aimed to buttress support in UK CCS. Although reasons for the postponement (to allow for the roadmap to include details of the second DECC-funded CCS support package) were broadly understood, this and the cancellation of the Longannet project were widely seen as a setback to UK CCS. Soon after the collapse of Demo1 the publication of the industrial-led CCSa strategy for UK CCS and DECC's Carbon plan in late 2011 were both designed to bolster support for CCS and underscored the need for rapid deployment over the coming decades [CCSa, 2011, HMG, 2011]. The CCSa report was published too soon to be able to include the cancellation of the Demonstration project and assumed the Longannet project was going ahead. This may explain why the projections for the industry's growth were considerably different to DECC's with the CCSa recommending 20 to 30 GW installed by 2030 and the Carbon Plan suggesting "*CCS contributed as much as 10 GW by 2030 in the scenarios modelled*". The CCSa report does not make recommendations for deployment past 2030. However, the Carbon Plan includes four modelling scenarios (one based on MARKAL modelling and the other three based on the DECC 2050 calculator), the cheapest of which include nearly 40 GW installed capacity by 2050 implying a tripling of the 2011–2030 CCS average build rate between 2030–2050 [HMG, 2011].

In early 2012 momentum for CCS development was dealt a further blow with the pub-

lication of more detail on Electricity Market Reform (EMR) and the Emissions Performance Standard (EPS). The DECC [2011] White Paper had previously set the standard at 450 gCO_2/kWh; essentially outlawing the building of any future coal-fired power plants that are not equipped with some degree of CCS though permitting the construction of unabated gas-fired plant operating below this threshold. Considered alone, EPS may be seen as creating legitimacy for CCS technology (a feature that was deemed lacking in the expert survey). However, the announcement of the decision to grandfather new gas-fired plant built under the EPS until 2045 [Davey, 2012] erodes confidence in investing in low-carbon technologies is required yet and questions whether gas-CCS would be necessary at all given the relatively low price of carbon in the EU-ETS and Carbon Floor Price[1].

7.4.3 UK CCS Roadmap

The delayed CCS Roadmap was published in April 2012 at the same time as the UK CCS Commercialisation Competition was launched [DECC, 2012*a*]. The second CCS competition took note of the findings of the NAO report and extended the options for funding to a wider range of CCS applications making the application process considerably more flexible. The criteria for projects included requiring offshore storage and power plant capture at a meaningful scale, being operational by 2016–2020 and may even include part-chain projects so long as they demonstrate ability to become full-chain at a later date. Outside of these specifications a range of fuels, technologies and storage sites were encouraged in the call demonstrating the government believes it is still too soon to pick winning technologies.

Alongside the relaunched Competition, the Roadmap sets out the Government's position for developing CCS and aims "*to enable industry to take investment decisions to build CCS equipped fossil fuel power stations in the early 2020s*" [DECC, 2012*a*]. The Roadmap takes the view that although technologically feasible, CCS will not proceed in the UK unless the costs of deploying it are reduced. This correlates with the outcome of the first Demonstration Programme and the findings of the expert survey that there are no insurmountable technological boundaries for initial deployment of CCS but it is largely a lack of a market

[1]For example consider the carbon floor price in 2030 is £70 per tonne of CO_2 and that CCGT emit 380 gCO_2 /kWh. The carbon tax on CCGT in 2030 would be £26.60 per MWh. Thus, so long as the levelised cost of generation from unabated gas is less than about £70 per MWh unabated gas would be cheaper and a less risky investment option than CCS and other low-carbon options which are targeting costs of £100 per MWh. CCGT projects beginning in 2012 are found to have LCOE of £61 per MWh without accounting for carbon costs [DECC, 2012*b*]

for CCS to operate in which is delaying deployment. In light of this, the main focus of the Roadmap and Competition is to reduce the costs of CCS to a point where the technology may compete with other low-carbon options. In acknowledging the NAO report the Roadmap lays what Watson et al. [2012] later call "*an adequate policy framework*".

The Roadmap states that the Government believes there are three key challenges that must be tackled in order to develop CCS: reducing the costs and risks associated with CCS; putting in place market frameworks; and removing key barriers to CCS. The report then lists five approaches the Government is taking to overcome these challenges as: the commercialisation competition; a £125m four-year coordinated research, development and innovation programme; electricity market reform; government interventions targeting specific barriers to CCS deployment; and international engagement.

Within the Roadmap specific reference is made to developing technological innovation by investing £125m in research. In March 2013 DECC published analysis of how this R&D funding had been allocated, of which £40m was for supporting fundamental research and increased understanding, £30m supporting component development and innovation and £55m supporting pilot-scale testing and projects [DECC, 2013*a*]. Analysis of this data produced the graph in Figure 7.14. This figure shows considerable government spending focussed on two areas of the technology development chain; a large number of early level research projects (TRL 2) and a large government spend on relatively few larger projects (TRL 5-6). Although it may appear Figure 7.14 illustrates a relative lack of funding made available by government for TRLs 3-4, it is perhaps better to view this figure as targeted funding at two stages of technological development. In their policy briefing paper, McGlashan et al. [2012] specifically highlight the need for government intervention in "*a very early stage of technology development and* [...] *when technologies are mature, but would be deployed as the first of a kind or demonstration projects*" to avoid two 'valleys of death' and to avoid obstructing the development process. The funding allocation also suggests approximately £50m of funding is being provided by industry over the same period.

The Roadmap also indicates the Government recognise that reducing the cost of CCS is only one aspect of driving it's deployment. In addition, the Roadmap notes efforts must be made to specify a regulatory framework and storage strategy, address potential skills shortages and develop large infrastructure networks. A lack of, or poor, public engagement was highlighted as a potential blocking mechanism during the expert survey and

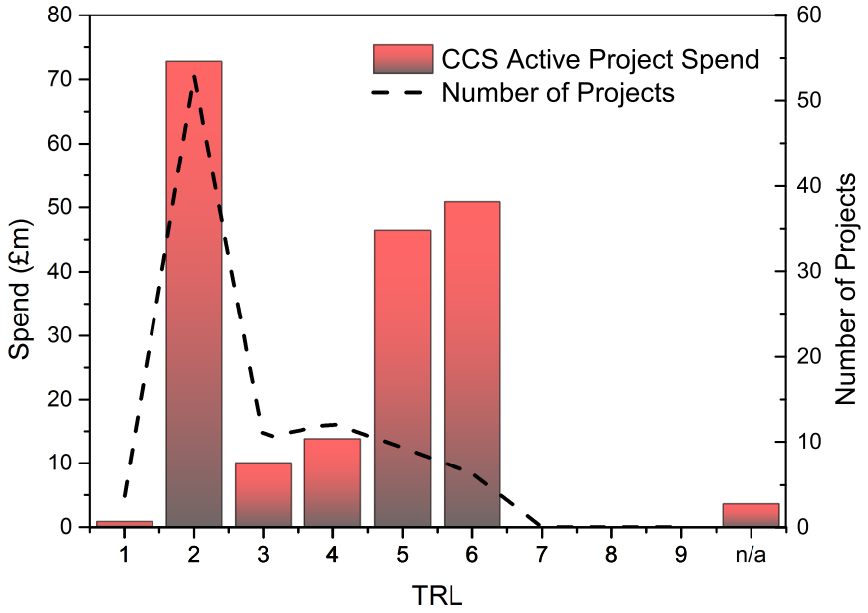

Figure 7.14: Analysis of DECC's £125m innovation spending project by TRL. Data from [DECC, 2013*a*]

in the Roadmap the Government appear to agree noting: "*experience to date* [..] *suggests that community engagement begins early and goes beyond the requirements under the regulatory regime*". There is also an underlying theme of attempting to distribute knowledge, skills and best-practice across the TIS. As well as formal dissemination of research being a pillar of the Commercialisation Programme, the Roadmap highlights the usefulness of sharing knowledge such as, for example, the SCCS published Regulatory Test Toolkit for developing projects. In terms of reducing the uncertainty levels across the CCS chain, long-term storage liabilities remain a problematic issue. With respect to this: "*The Government believes that more evidence is needed to help develop a more realistic estimate of these risks. We have therefore commissioned work to help develop a common understanding on the extent of these risks, we hope this will help to develop a consensus about the scale and most effective approach to managing these risks. We believe that such evidence will also be useful in helping the financial services sector develop third party risk mitigation products (such as insurance)*."

Perhaps recognising the variation in opinion between the different expert groups noted in the expert survey, more of the development of the CCS industry is hoped to be steered by a diverse group of actors from sectors across the TIS. The Roadmap details the formation of two what Bergek et al. [2008] label 'technology specific coalitions': the industry-led CCS

Cost Reduction Task Force (CCSCRTF) and the academia-led UK CCS Research Centre (UKCCSRC). Government is also "*consulting industry in advance of the European Commission's review of the CCS Directive in 2015 to ensure that UK experience is shared across the EU.*"

With regards to market creation, the Roadmap displays the Government's desire to support UK CCS in the near-term with subsidies through its innovation and R&D funding and the CCS commercialisation competition. In the longer term, reform of the electricity market is the driving force to providing an environment for CCS to develop within. No new information regarding EMR was published in this report.

7.4.4 UKERC Report

Published soon after the DECC's Roadmap, the UKERC report built on several academic publications ([Markusson et al., 2011, 2012, Russell et al., 2012] among others) that focussed on trying to analyse the state of the UK CCS system and provide insight as to how it could most effectively develop. Rather than mapping system functions to highlight blocking mechanisms, Watson et al. [2012] target uncertainties in the system as the reason for a lack of development of CCS in the UK. A suite of analyses are carried out comparing CCS in the UK to case studies of previous industrial developments in order to ascertain whether lessons from the past could be applied to these uncertainties. Drawing on these past experiences, four potential CCS deployment scenarios are then mapped with branching points along the way being described by reactions to specific uncertainties. The conclusions of the work argue two main points: that interactions between uncertainties are important, and that in order to develop not all of these uncertainties must be completely removed but that care is needed so that a critical mass of uncertainties is not created which could derail the entire system. The work highlights four uncertainties to be addressed and suggests routes for policy to allow UK CCS to develop. The report suggests:

- Variety in the technology developed for CCS should be preserved by Government for a period to allow more information before technology winners are chosen.
- Public financing is required for CCS demonstrations because the technology is not yet advanced enough for a regulatory approach to be successful in developing the industry.

- The costs of CCS will likely rise before economies of scale and technology learnings are realised, which should lead costs to eventually fall. Suitable incentives packages for developers to account for this should be provided to ensure technology development can occur.
- A clear balance on storage liabilities between attracting industry and not overburdening the taxpayer is yet to be established but must be put in place. The most likely route to achieve this may involve an independently managed fund for storage liabilities.

That technology choice is recognised as uncertain correlates with the relatively poor score for the guidance of the search and entrepreneurial activity system functions in the expert survey. The fact that the other three uncertainties highlighted by Watson et al. [2012] all relate to barriers to developing a commercial CCS industry strengthen the view of the expert survey that market creation is a poorly performing system function.

Although not highlighted directly as one of the key uncertainties, the potential for a poorly executed public awareness is mentioned as potential danger to the development of the UK CCS industry and the topic is presented with a case study in the report. The findings from the case study suggest successfully managing the public attitude to CCS is a complex topic citing the work of Reiner et al. [2011], which found in some cases more CCS-knowledge increased resistance to CCS, and noting that for poorly managed projects: "*delays, costs increases and even cancellations are all possible*"[Watson et al., 2012]. In short, the report concludes in terms of public acceptance: "*a wide range of local, national and international factors will shape public reactions – so each site needs to be considered on a case by case basis*."

The underlying theme of the report is perhaps best summarised by the following quote:

> "The key omission at present, then, is perhaps not so much an adequate policy framework, especially now that the CCS roadmap has finally been published. It is rather the confidence that this framework will be implemented with mechanisms that recognise the unique characteristics of CCS and within the timescales required . . . It remains to be seen whether the measures within the CCS roadmap, and the generous package of financial support that is now available, will be sufficient to significantly boost the confidence of investors."

7.4.5 TINA analysis

The Technology Innovation Needs Assessment (TINA) for CCS found that investments in technological research could lead to significant cost reductions in CCS. In order to assess where best to focus low-carbon innovation funding the Government formed the Low Carbon Innovation Co-ordination Group (LCICG) to carry out TINAs for a range of developing low-carbon technologies in 2010–2011. The summary report for the CCS TINA views innovation in a purely technical nature and was published in August 2012 finding "*Innovation across the CCS technology chain could reduce UK energy system costs by £10–45bn to 2050, and innovation to ensure the security of long-run CO_2 storage remains particularly critical to CCS viability.*"[LCICG, 2012] As well as identifying a number of areas in the CCS technology chain where investment in technology development would generate the best return on investment for the government, the report highlighted several barriers to further deployment of CCS. The report finds that demonstration of CCS at full-scale is critical to the development of the industry and as an enabler of the benefits brought about by technological innovations. LCICG report that:

> "Innovation has the potential to drive down the costs (ignoring fuel) of conversion with capture by 15% by 2025 and 40% by 2050. Innovation can further reduce the long-run costs of transport by $\sim$50% and of storage by >50%. Innovation in measuring, monitoring & verification (MMV) and mitigation & remediation (M&R) can ensure the security of sequestered CO_2, reducing the financing costs of CCS, as well as enabling its overall availability as an abatement option...
>
> "...Innovation areas with the biggest benefit to the UK are (i) deep sea storage, MMV and M&R; and (ii) advanced capture development (especially gas and biomass) and demonstration of integrated conversion-capture. In both, the UK should look to lead or join multi-national partnerships...
>
> "...Supporting all of the UK's priority innovation areas would require hundreds of millions of GBP over the next 5-10 years (leveraging 2-3 times that in private sector funding). The UK is addressing some of these innovation areas, but there remains considerable scope to expand this activity..."

However, the report also highlights uncertainties which could hinder or derail CCS deployment. As well as capacity to increase funding for innovation, uncertainties regarding long-term storage of CO_2 are still prevalent which "*constitutes a significant risk to the viability of CCS and its rapid roll-out in the near to mid term.*" The report also highlights that CCS exists within a much larger low-carbon system and that "*While innovation will play an important role in ensuring CCS is deployed cost effectively and in a timely manner, the overall capacity installed depends even more significantly on key 'exogenous' factors, especially the degree of public acceptability of onshore wind and nuclear, the availability of biomass for energy use, the overall energy/electricity demand, and the relative success of energy efficiency and demand reduction measures.*" This is in clear agreement with the findings of Hekkert et al. [2007] who state that :"*the rate and direction of technological change is not so much determined by the simple competition between different technologies, but predominantly by the competition between various existing innovation systems, both fully developed and emerging ones.*" Within UK CCS, LCICG highlight 5 market failures which are impeding the development of innovations in the UK CCS industry:

- policy dependent demand and uncertain support levels;
- barriers to developing novel or innovative concepts;
- key infrastructure dependency on uncertain public investment;
- long-term, global liabilities which are difficult to insure against; and
- uncertain environmental impacts and regulatory regime.

7.4.6 Cost Reduction Task Force (CRTF) report

The CRTF launched in the CCS Roadmap published an interim report in November 2012 on options for reducing CCS costs in order that CCS may compete with other low-carbon power generation technologies as the electricity moves towards decarbonisation. The key conclusion from the report was that "*UK gas and coal power stations equipped with carbon capture, transport and storage have clear potential to be cost competitive with other forms of low-carbon power generation, delivering electricity at a levelised cost approaching £100/MWh by the early 2020s, and at a cost significantly below £100/MWh soon thereafter.*" [UKCCSCRTF, 2012]. Figure 7.15 presents how the CRTF suggest these cost reductions may be made, emphasising improved economies of scale (both large projects and networks),

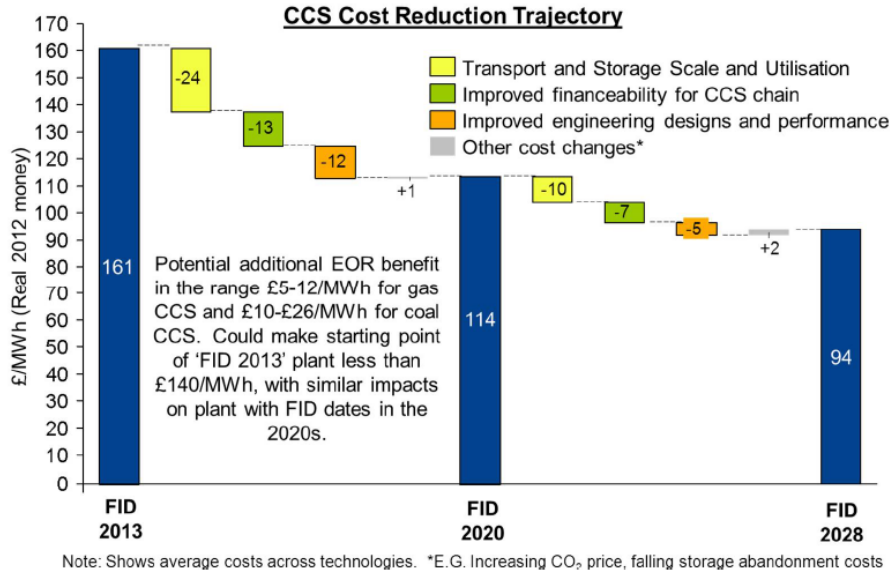

Figure 7.15: Projected cost reductions in CCS in the UK for final investment decisions (FID) in 2013, 2020 and 2028 [UKCCSCRTF, 2012]

de-risking capital expenditure (making borrowing cheaper) and combining early CCS projects with enhanced oil recovery (EOR) to offset the cost of storage with a revenue from oil production. The CRTF are optimistic about reducing costs as deployment occurs suggesting: "*The cost reductions available in the early 2020s will be based on technologies that are already widely used at large scale, and that can be invested in with confidence and manageable risk. Further benefits from 'learning curve' effects, technology innovation, improved construction techniques, supply chain competition and the like will reduce costs further in the later 2020s.*" Furthermore, "*The Task Force is reassured in this conclusion by similarities across capture technologies and the commercial development of analogous technologies such as Flue Gas Desulphurisation and Combined Cycle Gas Power Plant.*" However, unlike the UKERC report the Task Force do not comment on the fact that costs of technologies are likely to rise before they fall as highlighted by growth in FGD technologies.

Uncertainty is highlighted as a critical factor to be addressed if CCS is to deploy without further delays. In summarising how best to develop a UK CCS industry the Task Force recommend twelve actions. Four of these actions cover "*Multiple operating full-chain CCS projects*" and "*continued engagement with the financial sector*" with a further eight separate actions under the heading "*Credible long-term UK government policy commitment to CCS*".

7.4.7 Developments in the wider low-carbon sector

As noted previously, the development of CCS in the UK is highly dependent on events unfolding in the wider low-carbon environment. It is beyond the remit of this thesis to comment and analyse the breadth of factors affecting low-carbon technologies, yet some developments in the wider energy environment cannot be overlooked.

7.4.7.1 Unabated gas firing

The development of generating electricity from unabated gas plant strongly impacts upon UK CCS development. Unlike CCS this is an extremely mature technology option which is the current choice for developing new, large-scale, flexible power plant. This is because it is cheaper and quicker to build than a coal-fired power plant, provides considerably larger capacity than renewables of the same spatial footprint, and has very rapid response times to allow demand matching which is especially valuable in balancing variable electricity demand and supply on the grid. Despite domestic gas prices increasingly substantially over the last decade, the recent political interest in UK shale gas has also leant weight to the argument for developing more gas-fired power plant.

Although gas-fired plants produce about half of the emissions emissions per unit of electricity delivered than coal-fired plants (typically 380 gCO_2 /kWh) achieving the 80% reduction in 2050 requires almost no emissions at all from electricity generation. In fact, the CCC recommend that the average emissions from electricity generation should be around 50 gCO_2 /kWh by 2030, with early decarbonisation of the electricity sector allowing decarbonisation to proceed in other areas. The government publication of the Gas Generation Strategy in December 2012 [DECC, 2012*d*] which reinforced the central projection of 100 gCO_2 /kWh by 2030 as established by the Energy Bill [DECC, 2012*c*] was seen as weakening the legitimacy of low-carbon technologies in general. Moreover, the Government's refusal to commit to setting a target for carbon-intensity in 2030 increased uncertainty in the energy market for all low-carbon technologies. Despite wide criticism from experts [CCC, 2012] and an amendment being tabled by the Climate Change Select Committee the Energy Bill was passed without a 2030 decarbonisation target.

7.4.7.2 Gas-CCS

Both globally and domestically the capture of CO_2 has recently seen a shift towards capture from gas-fired power plant and away from solid-fuel combustion as illustrated for the UK by the recent UKCCSRC standalone Gas-CCS meeting. This change has largely been driven by the reduction in gas prices in the USA due to shale gas production, which may also contribute to future UK gas markets over the coming decades. However, the UK Commercialisation Competition is currently continuing to fund desk-studies to both the gas-fired Peterhead project and the coal and co-fired White Rose Project. Similarly, government funding for the UK Pilot-Scale Advanced Capture Technology (PACT) facilities includes a range of technology options firing coal, gas and biomass fuels.

7.4.7.3 Energy storage, demand management and interconnection

The legitimacy for CCS as a technology option is that it permits the continued use of fossil-fuelled power stations which are currently the only technology option available to provide sufficient flexibility of supply to accommodate changes in demand and variability of renewable energy sources. Although a small amount of energy storage is already present in the UK, the current technology option is in the form of pumped storage requiring two large storage reservoirs at significantly different heights. On account of these requirements, the capacity for extra pumped storage is widely considered to be small, though emerging technology options include energy storage as 'liquid air' which is compressed using excess energy and then expanded through a turbine to generate electricity when needed. Increasing interconnectivity with other electricity networks also allows variability in supply to be dampened, while in the decades to come developing technologies could offer a complementary service by reducing demand at times of low supply. Although undeveloped in the current UK energy system, these three technology options offer the potential to destroy some the legitimacy of fossil fuel plants (and therefore CCS too) by providing a degree of flexibility to the electricity grid and permitting a greater penetration of renewable technologies (particularly offshore wind).

7.4.8 UK Bio-CCS

As noted in Section 1.11, biomass-fired CCS plants are forecast to play a considerable part in the future of UK energy generation. Although Vergragt et al. [2011] found little evidence of a TIS prior to 2011 outside of academics, as well as gaining traction in Government and regional longer-term forecasts [DECC, 2010, POST, 2012, ZEP, 2012], some activity in Bio-CCS is beginning to appear in wider academic and industrial circles with the establishment of the EU Bio-CCS Joint Task Force the most prominent technology-specific coalition in the TIS. In late 2011 the Second International Workshop on Biomass and Carbon Capture and Storage was held in Cardiff which attracted both academics and industrialists as did a similar meeting of the Combustion Institute in May 2013. With input from industry and academia the Energy Technologies Institute ran a project in 2011–2012 focusing on a high-level engineering study of design of biomass-fuelled CCS plant and academic studies continue to provide legitimacy for Bio-CCS on account of its ability to actively reduce atmospheric CO_2 levels [Azar et al., 2013]. However, despite this relative growth in Bio-CCS, outside of early-research circles and long-range forecasting work the focus for CCS at the present time remains largely on abating the emissions from fossil fuel combustion.

As well as the technical and logistical challenges substituting biomass for fossil fuels brings, whcih are detailed in earlier chapters of this thesis, the regulatory and political landscape for the development of Bio-CCS is relatively sparse compared to CCS. Although the IPCC [2006] guidelines for reporting GHG emissions can include negative emissions, currently there is no financial incentive for companies to engage in Bio-CCS as no trading system which recognises the benefits of negative emissions process exists. Gough and Upham [2010] noted that "*significant incentives will be necessary to establish BECCS or CCS*" but the problem of accounting for negative emissions in Bio-CCS appears less well developed. As McGlashan et al. [2012] describe:

> "*the development of similar mechanisms* [to existing carbon trading systems] *for negative emissions technologies are still in their infancy. Considering that negative emissions technologies are relatively new concepts for policy makers, researchers and investors this is hardly surprising, as credible mechanisms to support development and deployment have not had the opportunity to emerge, but given the role negative emissions technologies can play in mitigating climate change, this*

state of affairs needs to change quickly albeit without impacting the investments in other low carbon technologies."

Recent academic work further advocates the need for a financial incentive to drive development of Bio-CCS [Ricci, 2012]. This is echoed by a recent policy briefing by the Institute of Mechanical Engineers which also suggests it is Government's role is to "*Support UK research, development and demonstration of CCS technology for use with biomass-based electricity generation while simultaneously pursuing the future inclusion of 'negative emissions' credits in international climate change mitigation agreements*" [IMechE, 2013]. Recently the awarding of funding to carry out the Front-End Engineering and Design (FEED) study to the White Rose Project could prove strategically important for Bio-CCS. The potential benefit is derived since as well as having the potential to cofire biomass, the project includes Drax which is also "*currently transforming the business into a predominantly biomass-fuelled generator*" [DECC, 2013*c*, Drax Group Plc, 2013]. The combination of developing CCS and significantly shifting the business to being fuelled by biomass represents a serious investment in building up expertise in the two components of Bio-CCS.

7.4.8.1 Biomass sustainability

Recent academic work [van Vuuren et al., 2013] and the most recent Emissions Gap report [UNEP, 2013] further highlights the need for more surety related to Bio-CCS, suggesting the assumption of the technology's ability to provide substantial emissions reductions is dependent on both: "*the technical and social feasibility of large-scale carbon capture and storage* [...] *and the technical and social feasibility of large-scale bio-energy production*". An additional concern for Bio-CCS is the sustainability and transparency of the production of biomass. A full analysis of the sustainability and life-cycle emissions of biomass used in power generation varies considerably between fuels and thus is beyond the scope of this thesis. In summary, if biomass is produced within an Annex-1 country (as denoted by the Kyoto Protocol) it is assumed that the direct emissions due to biomass processing and indirect emissions due to land use, land use change and forestry (LULUCF) are reported as part of the nation's reporting and strict sustainability criteria must be met. However, reporting in non-Annex 1 countries (which also includes the USA and Canada) is currently less demanding and thus indirect emissions may go unreported. Updates to the EU biomass sustainability strategy aim to avoid such a situation from being created by

requiring end-users to be able to demonstrate the carbon savings [IEA, 2011]. However, a recent report by the EU Joint Research Centre suggests that, particularly for energy derived from stem-cut forestry wood, the full life-cycle emissions of the process cannot be accurately measured without taking into account carbon pools, changes in land use and the time required for the emissions reduction to reach parity with a re-establishment of carbon stocks [Agostini et al., 2013]. As well as wider sustainability criteria - including, for example, ecosystem loss - most of the criticism of this type of biomass use relates to the long growth periods of the trees. This issue is largely negated when using fast-growing or short-rotation crops as tested in the experimental chapters of this thesis, though the change in land use in order to grow the plants in the first place remains important (for example if established forest is cleared to provide space for energy crop plantations). The Biomass Policies Project [2013] was set up to inform EU policy and aims to continue to address these criteria over the next three years.

7.5 Conclusions

This chapter has presented an analysis of the wider factors affecting the growth of Bio-CCS and CCS in the UK than just the level of technological development, which is the focus of Part 1 of this thesis. The findings of the analysis, which had previously not been investigated for the UK, suggest that the UK CCS TIS is developing but crucial areas of the system should be addressed quickly if the industry is to develop at a pace quick enough to help the UK reduce its GHG emissions in line with its emissions reduction commitments. As concluded in Section 7.3.2.8, the expert survey highlighted that in late 2011 the UK CCS TIS was viewed on average by experts as not satisfactorily fulfilling the system functions required for a UK CCS industry to develop. In particular, a lack of market creation, entrepreneurial activity and resource mobilisation were highlighted as potential blocking mechanisms for the development of the industry. In addition, a lack of public acceptance and uncertainties over long-term storage liabilities were highlighted as potential phenomena which could abort the development of the industry. Significant differences of opinion between expert groups were also observed during analysis of the results of the expert questionnaire with experts tending to perceive system functions they were engaged with were performing better than those that others were responsible for.

Analysis of relevant published literature suggested that the collapse of the first demon-

stration project in late 2011 further eroded stakeholder confidence in UK CCS despite the government reaffirming commitment both in redeploying the Commercialisation Programme and in projecting substantial CCS capacity in the coming decades. However, in the two years that have passed since the survey, considerable effort has been expended in attempt to further develop a UK CCS industry.

In the CCS Roadmap the Government recognise that in order to create a market CCS can operate in (as is one of the foci of EMR) the costs of deploying CCS must be able to compete with other technologies in the electricity market. The TINA analysis and Cost Reduction Task Force both highlight areas of the CCS technology chain which may offer substantial cost reductions which should help to make CCS cost-competitive with other low-carbon options. The decision to invite applications from a wide range of technologies to the Commercialisation Competition was welcomed by the UKERC report and represents clearer guidance to industry and academics as to which technologies should be employed. However, every document analysed in this section that was not authored by the Government insists that uncertainties created by the Government remain one of the largest mechanisms that is preventing the industry developing further.

At the storage side of the technology chain long-term storage liabilities are still considered to carry high levels of uncertainty which have impeded the ability of developers to develop strategies to deal with the regulations surrounding this. At the capture end CCS is dominated by capture from power plant and the development of CCS within the sphere of EMR has created an incredibly complex set of uncertainties where the development of CCS in the UK is ever less dependent on the CCS industry and ever more dependent on the wider electricity market.

Government's continuing refusal to commit to electricity decarbonisation targets that would provide industry the surety to invest in CCS and other low-carbon technologies has further delayed CCS development. This may in turn lock the UK into unabated fossil fuel use in the long term in order to maintain security of supply in the short-to-medium term. While uncertainty regarding EMR pervades, measures to bolster the development of the incumbent natural gas industry such as grandfathering of, and public commitments to, developing unconventional gas suggest CCS as once envisaged may find it particularly difficult to compete once the Commercialisation Competition concludes. Similarly, the emergence of other technology options able to contribute to a flexible electricity grid (such

as energy storage, interconnection and demand management) all present the possibility of eroding the legitimacy of fossil-fuels and therefore CCS. Although such an eventuality would be detrimental to CCS projects, it is essential to realise that CCS can only be conceived as a transitional technology that acts as a buffer in the move from fossil-based to renewable energy systems and that the development of a UK FF-CCS industry can only be conceived within this transition window.

Through offering the possibility of negative emissions, Bio-CCS potentially could be afforded a longer operating window in the transition to renewable energy systems than FF-CCS. However, although technological hurdles remain and are being tackled, the development of a Bio-CCS industry is almost entirely dependent on the wider development of the FF-CCS industry. As the previous section notes, uncertainties of FF-CCS are mainly dependent on exogenous factors and the impact of these factors is multiplied for Bio-CCS which must also contend with biomass sustainability issues and no current financial incentive mechanism for net negative emission processes.

Part III

Conclusions and Further Work

Chapter 8

Conclusions and Further Work

The focus of this thesis has been to investigate the technical feasibility of firing biomass in CCS applications and then to step back from these technical studies in attempt to understand the wider opportunities for, and barriers to, the development of this promising technology in the fight against climate change. With full conclusions for each of the research areas included at the end of the relevant chapters, this chapter aims to summarise the findings and draw together the research, providing a set of more generalised conclusions and to offer insight into potential areas of future work required to develop a Bio-CCS industry in the UK.

In the technically-focussed sections of the thesis, Part 1, the main goal of the research was to investigate the effects of burning types of biomass in CCS-relevant combustion atmospheres at a scale relevant to industrial practices, as was carried out in Chapter 6 according to research questions 3–6 detailed in Section 2.9. To explain the results found in Chapter 6 it was useful to study the decomposition of the fuels used at 20 kW scale using TGA, answering research question 2 in Section 2.9 in Chapter 5. However, providing useful comparisons between these TGA datasets required the development of a robust and accurate method of evaluating reactivity. This work was completed in Chapter 4 in response to the first research question. In Part II, the development of a CCS industry in the UK was analysed as a technical innovation system to understand how the wider system surrounding technological development could affect its ultimate level of deployment. This was carried out by enriching the results of an expert survey with an in-depth analysis of subsequently published relevant literature.

8.1 Summary of findings

8.1.1 Research Question 1: Develop, test and evaluate a methodology to rapidly and robustly analyse variation in the decomposition behaviour of biomass fuels in TGA experiments

To better understand and compare biomass decompositions, a novel and robust form of the Coats-Redfern procedure was developed in Chapter 4. The method was extensively tested using a theoretical idealised dataset to understand the effects of data treatment - such as data smoothing, the temperature range for the fit of the Coats-Redfern plot and a technique to overcome the compensation effect - and identification of reactions on the reactivity of the mixture of fuel and combustion atmosphere. The ability of the method to estimate reactivity parameters was judged based on the correlation between the original data and data recreated by substituting the predicted parameters in a multicomponent Arrhenius decomposition. The results suggested that data smoothing reduces the ability of the method to estimate reactivity parameters. Testing with mildly-overlapping parallel reactions illustrated that a fit of the Coats-Redfern plot to the leading edge of the reaction on the DTG plot was able to accurately predict the reactivity parameters of the total decomposition. Testing of the method with real experimental data resulted in it being shown to be adept at identifying changes in reactivity between the biomass samples, as was the focus of this work. However, the method was found to be less applicable to decompositions where clear distinctions of separate pseudo-reactions could not be made, as in the case of types of biomass with high-lignin content and coals.

As well as being essential for the development of understanding in the following chapters, this work is expected to interest researchers working with TGA experiments for fuel and combustion atmosphere screening applications. The method described is rapid and traceable and, noting that the comparison of TGA data with full scale is only qualitative in nature, does not require the extra effort that multiple heating rate methods or advanced computer solver techniques employ in order to ascertain ostensibly more precise reactivity parameters.

8.1.2 Research Question 2: Use the above methodology to investigate the variation in reactivity and decomposition behaviour of three UK-relevant energy resource biomasses in OEC and oxyfuel atmospheres

The method developed in Chapter 4 was used to compare the reactivity of three energy crop biomass samples - short-rotation willow coppice, miscanthus and reed canary grass - decomposing at bench-scale in combustion atmospheres that were enriched in O_2 and CO_2 in Chapter 5. Analysis of the decomposition of shea meal (a high-lignin biomass) and Williamson coal were also performed using traditional methods. In these experiments, enrichment of O_2 in the combustion atmosphere was found to have the largest effect by significantly increasing the reactivity of combustion, causing the decompositions to begin at lower temperatures and complete over narrower temperature ranges. These effects were especially noted during the breakdown of cellulosic material and during the oxidation of char. At the temperatures investigated in the analysis, little difference in reactivity was observed for atmospheres enriched in CO_2 compared to those that were N_2-based. A final finding was that the relative reactivity was observed to change due to heating rate in some cases: the apparent reactivity of the char oxidation stage was lower at higher heating rates while the devolatilisation reactions were less affected.

The results presented in Chapter 5 are useful in understanding the changes observed in Chapter 6 when answering research questions 3–6. It is also expected the results will be of interest to the wider academic and industrial community where currently little data exists for the combustion of biomass in CCS-relevant atmospheres.

8.1.3 Research Question 3: Investigate the impact of the biomass blending ratio on pollutant emissions and combustion characteristics for cofiring with coal in OEC conditions through cofiring UK-relevant energy resource biomasses, including brownfield-derived biomass, at 20 kW scale

Three energy crop samples, including one brownfield-derived biomass, were fired with coal in a 20 kW furnace as described in the experimental methodology in Chapter 3. The first experiment for each of the biomass samples was an investigation into the effect of increasing the biomass blending ratio (BBR, thermal basis) during combustion in air and air enriched to 30% O_2 (En-Air). In air, cofiring tended to delay combustion due to the

changes in fuel composition and particle size compared to coal. However, although reducing temperatures in the early stage of the furnace, increasing BBR up to 15% tended to increase the carbon burnout of the fuel blends. Although further increase of BBR past 15% tended to decrease the value of carbon burnout, carbon burnout at 20% BBR remained greater than that for coal-firing. Particle size was highlighted as a key difference between the fuel samples with the average particle size of the willow sample being twice and three times as great as the other types of biomass and coal respectively. The large particle size was assumed to exaggerate temperature and species concentration gradients in fuel particles leading to delayed devolatilisation and ultimate combustion of the larger fuel particles during firing in air. Increasing BBR in En-Air produced broadly similar trends to those observed in air firing. However, combustion in En-Air increased furnace temperatures, carbon burnout of the fuel, the concentration of CO_2 in the flue gas and emissions of NO for all fuels compared to firing in air. In En-Air, the increased concentration of O_2 overcame the delay in combustion observed during cofiring in air due to higher devolatilisation rates and a reduced amount of thermal diluent. Emissions of SO_2 were found to decrease almost linearly with increasing BBR in both air and En-Air atmospheres. Analysis of the ash produced from the experiments suggested the higher concentration of alkali metals and alkaline earth metals in the biomass ash were responsible for increasing the amount of sulphur captured by ash particles but that at 15% BBR the Alkali Index of the ashes suggested they were likely to be tolerable to plant operators. The increase in furnace temperature and carbon burnout observed for oxygen-enriched combustion resulted in a larger number of smaller, more uniformly spherical particles in the ash.

8.1.4 Research Question 4: Investigate the impact of oxidant staging on pollutant emissions and combustion characteristics for cofiring with coal in OEC conditions through cofiring UK-relevant energy resource biomasses, including brownfield-derived biomass, at 20 kW scale

The second experiment at 20 kW scale investigated the effect of oxidant-staged combustion on cofired fuel mixtures reacting in air and En-Air. The results showed that reducing the burner stoichiometric ratio (BSR) of oxidant to fuel was able to effect large reductions in NO emissions. Cofiring in air while staging was able to reduce NO emissions by up to 70% compared to unstaged coal-firing. However, this tended to result in lower

carbon burnout values, though the reduction was slightly mitigated by cofiring of biomass. Oxygen-enrichment of the combustion atmosphere was able to negate this reduction in carbon burnout which remained above 95.5% and reduce NO emissions faster than in air-firing achieving reductions on NO emissions of up to 80% compared to coal-firing in air. Thus, cofiring under oxidant-staged, oxygen-enriched conditions was able to produce higher furnace temperatures and improved burnout results while effecting significant reductions in NO emissions. Combustion in En-Air was also able to provide a flue gas with a higher concentration of CO_2, which is useful as it reduces the energy penalty of CO_2 capture. However, the ability of cofired fuel mixtures to reduce SO_2 emissions observed in unstaged condition was reduced by oxidant staging compared to during unstaged-firing.

8.1.5 Research Question 5: Investigate the impact of CO_2-enrichment of the combustion atmosphere on pollutant emissions and combustion characteristics for cofiring with coal in OEC conditions through cofiring UK-relevant energy resource biomasses, including brownfield-derived biomass, at 20 kW scale

The third experimental regime in Chapter 6 investigated substitution of a portion of the N_2 in the combustion atmosphere with CO_2, creating a partial oxyfuel combustion system with a significantly higher concentration of CO_2 in the flue gas. Results showed that this change tended to decrease combustion temperatures, NO emissions and carbon burnout compared to N_2-based environments. With only CO_2-enrichment, cofiring of biomass at 15% was found to accelerate combustion compared to firing coal alone, though furnace temperatures were still significantly lower than when firing in air which may have been responsible for the larger ash particles collected, indicating less complete combustion. However, compared to air-firing of coal, combustion of all fuels in an environment enriched with CO_2 and O_2 produced better carbon burnout results, higher furnace temperatures, slightly reduced NO emissions and significantly lower SO_2 emissions.

8.1.6 Research Question 6: Investigate the impact of dedicated biomass firing in OEC and CO_2-enriched combustion on pollutant emissions and combustion characteristics, at 20 kW scale

A final series of tests investigated the effects on combustion of dedicated biomass firing in air and partial-oxyfuel atmospheres. Results firing 100% willow indicated delays to the combustion process, which was also observed to be considerably less stable than when firing coal or cofiring. Such results suggest it would likely be necessary to reduce the size of the biomass particles compared to those used in the current study and that optimisation of the burner would likely be required if more stable combustion is to be achieved. Emissions of both NO and SO_2 were greatly reduced compared to coal-firing in all atmospheres.

In summary, the combustion experiments showed that, although dedicated biomass firing would likely require modifications to combustion practices, cofiring of three types of biomass at up to 20% of the energy input present no significant technological hurdles when considering biomass for CCS applications, and the combination of cofiring and oxidant-staged, O_2- and CO_2-enriched combustion could provide a useful technology option for reducing GHG emissions from power generation.

The results and discussion presented in Chapter 6 and summarised here are expected to interest academics and industrialists working in the fields of biomass and oxyfuel combustion. Even though several years has passed since this research began, very little data from cofiring biomass in CCS-relevant atmospheres at a meaningful scale has been published. Thus, it is hoped the work here, which represents a considerable amount of experimental data will be of interest to experimentalists and computer modellers working in Bio-CCS (both cofiring and dedicated biomass firing).

8.1.7 Analysing the UK CCS industry as a TIS

Noting that industrial development is dependent on a wide range of factors, of which the level of technology readiness is only one, the work in Part II of the thesis includes analysis of the wider environment for the development of Bio-CCS. Here, understanding that the development of Bio-CCS is dependent on the development of a fossil-fuelled CCS industry, the development of a UK CCS industry was investigated by modelling it as a

technical innovation system (TIS). Evaluation of the state of development was carried out through charting the development in relevant government, industry and academic literature and conducting a survey of CCS experts in 2011. Comparison of these results with data for other nations showed on most criteria that in 2011 the UK CCS industry was less developed than in other leading CCS nations. The survey revealed differing points of view between expert groups in the UK, with each tending to overestimate the impact of their own role in the development of the wider CCS industry. However, from the averaged results a lack of market creation, entrepreneurial activity and resource mobilisation were highlighted as potential blocking mechanisms for the development of the industry. In addition, a lack of public acceptance and uncertainties over long-term storage liabilities were explicitly noted as potential phenomena which could abort the development of the industry.

Following the results of the survey, a critical analysis of relevant industry, academic and government policy documents provided a richer account of the development of the CCS industry over the period 2011–2013. The analysis suggested that although stakeholder confidence in UK CCS fell when the first Demonstration project was cancelled, much effort has since been expended by Government, industry and academia to develop the industry. However, despite commitments to the development of CCS, an often-changing policy landscape has tended to erode trust in projections for CCS's growth. Some notable technical uncertainties remain (not least those related to storage liabilities) but the absence of clear policy for decarbonisation of the electricity market is the main factor that has delayed commercial development of CCS in the UK. The recent announcement to fund the Front-End Engineering and Design study for the White Rose and Peterhead CCS projects is a positive step in developing the UK CCS industry. However, the increasing articulation of desire for development of unconventional gas production and support for new unabated gas-fired power plant reduce the economic viability of CCS. Alongside this, novel technologies like energy storage and increased interconnectivity offer a credible possibility of eroding the legitimacy of a CCS industry in the UK. That the White-Rose project includes a major biomass user and a co-firing component is a strong suggestion that Bio-CCS could develop very quickly into a wider CCS environment. However, this cannot occur until agreements on rewards for negative emissions and universally-agreed sustainability criteria are implemented.

8.2 Areas for potential further research

While this research provides an insight into some of the aspects that relate to developing a Bio-CCS industry in the UK and globally, the current lack of published research in the area means a large amount of work is still required to further develop this technology. Further technical research is required to understand the myriad of technological options for Bio-CCS. Similarly, effort is required to better understand the framework that governs the development of a niche, emerging industry such as CCS.

On the technical side, considerably more data is required to understand the reactions of types of biomass in the novel combustion atmospheres expected in CCS applications. Many biomass fuels are yet to be tested in relevant combustion atmospheres and the variation between and within biomass samples suggests a considerably larger databank should be built up, as has occurred with fossil fuel firing in air over previous decades. Initial analysis of the devolatilisation, char oxidation and overall combustion of novel, promising fuels should be carried out using bench-scale techniques. However, to fully understand the technical potential for biomass and Bio-CCS to reduce GHG emissions, testing at a meaningful scale is required. Firing at small laboratory scales (similar to the 20 kW work presented in this thesis) highlights many issues and allows testing of traditional combustion practices such as oxidant staging. However, in order to validate computer modelling studies and even better understand the combustion of biomass fuels, larger-scale, more highly-instrument experiments should be conducted. Measurement techniques such as particle tracing and profiling of species and heat flux would allow characterisation of how fuel particles actually react in the novel combustion atmospheres expected in CCS applications, while integration of combustion with the other sections of the CCS chain will be required to demonstrate the utility of the full process. More work that investigates the technical potential for Bio-CCS in industry could be carried out which may, in turn, provide attractive areas for further development.

As well as extending the experimental work as detailed above, there are several areas that have been highlighted as lacking information during the research conducted in this thesis. These include:

- Investigate the usefulness of fitting more than three pseudo-reactions to the decompositions of lignin-rich biomass fuels to methods that aim to evaluate the reactivity

of the fuel-combustion atmosphere mixture without expending unjustified effort;

- Investigate the effect of particle size and heating rate on decomposition reactivity of biomass fuels in oxidising atmospheres;
- Measure all known sulphur species during cofiring in O_2 - and CO_2-enriched oxidant staged combustion in order to complete the sulphur balance and definitively detail the fate of sulphur species in the fuel;
- Investigate the impact of using oxygenated recycled flue gas as the primary oxidant in furnace combustion tests on combustion characteristics and emissions of NO;
- Investigate the impact of steam at TGA and 20 kW scale in order to understand issues related to high moisture content biomasses and wet recycling of flue gas.

In terms of understanding the wider development of the CCS and Bio-CCS industries, a continual updating of literature, stakeholder views and the impact of lobbying and information groups is needed in this rapidly changing environment. While this work has focussed on analysing CCS in the UK as a TIS, there are many other methods of analysis that may be considered which could highlight other factors affecting the industry's development or help to confirm the findings presented here. The potential for targeted effort and policy at domestic and regional level should be investigated more fully to understand whether duplication of effort in developing the industries may be avoided in the coming decades, while an analysis of whether different viewpoints between actor groups pervade and deter the development of a unified CCS industry also merits study.

8.3 Concluding thoughts

Bio-CCS is one of a few negative emissions processes that could effect significant emissions reductions and help to stabilise the climate. However, set alongside the potential benefit of Bio-CCS is the worry that negative emissions technologies continue to provide space for unsustainable practices to occur, locking us in to fossil fuel consumption. Fossil fuels will continue to play an important role in our energy systems but a transition to a system where behavioural change and renewable energy technologies create a sustainable energy system is still the final aspiration of most forecasts. Thus, in order to avoid legitimising the continued use of fossil fuels where their implementation may delay the deployment

of renewable energy technologies, it may be useful to recall that CCS and Bio-CCS should only be viewed as transition technologies.

Despite this temporary nature, the sooner the development of Bio-CCS occurs, the sooner it can reduce emissions in the short term. In light of this urgency the body of work in this thesis offers several contributions to developing a necessary understanding of the technical and non-technical issues relevant to the implementation of Bio-CCS in the UK. Combustion tests at bench and laboratory scale suggest cofiring of biomass and coal in CCS-relevant atmospheres could effectively produce energy required for power combustion with retrofitted equipment. However, dedicated biomass firing may require some technical modifications. Analysis of the development of CCS in the UK shows that over the last decade the industry has been hampered by a range of factors. Government has worked hard to develop a CCS strategy and most factors have been addressed, though some important uncertainties remain, including electricity market reform, public engagement and storage liabilities. In Bio-CCS, issues of sustainability and monetisation of negative emissions provide extra areas that require further effort, though work to address both of these issues is ongoing.

Bibliography

ABB [2009], Advance Optima Continuous Gas Analysers AO2000 Series Software Version 5.0 Operating Manual, Technical report, ABB.

Abraham, B., Asbury, J., Lynch, E. and Teotia, A. [1982], 'Coal-oxygen process provides CO2 for enhanced recovery', *Oil and Gas Journal* **80**(11), 68–70.

ACCAT [2009], Accelerating the deployment of carbon abatement technologies - with special focus on Carbon Capture and Storage, Technical Report February, Advisory Committee on Carbon Abatement Technologies.

Adams, J. M. M., Ross, A. B., Anastasakis, K., Hodgson, E. M., Gallagher, J. A., Jones, J. M. and Donnison, I. S. [2011], 'Seasonal variation in the chemical composition of the bioenergy feedstock Laminaria digitata for thermochemical conversion.', *Bioresource Technology* **102**(1), 226–234.
URL: *http://dx.doi.org/10.1016/j.biortech.2010.06.152*

Agostini, A., Giuntoli, J. and Boulamanti, A. [2013], Carbon accounting of forest bioenergy critical literature review, Technical report, EU Joint Research Centre, Ispra, Italy.
URL: *http://tinyurl.com/EUJRC2013*

Akahira, T. and Sunose, T. [1971], 'Method of determining activation deterioration constant of electrical insulating materials', *Research Report, Chiba Inst Technol* **16**, 22–23.

Al-Mansour, F. and Zuwala, J. [2010], 'An evaluation of biomass co-firing in Europe', *Biomass and Bioenergy* **34**, 620–629.
URL: *http://linkinghub.elsevier.com/retrieve/pii/S096195341000005X*

Andersson, K. [2005], Fundamental oxy-fuel combustion research carried out within the ENCAP project, *in* 'International Oxy-combustion Network for CO2 Capture. Inaugural (1st) workshop', Cottbus, Germany.
URL: *http://www.ieaghg.org/docs/oxyfuel/w1/08W1Andersson.pdf*

Anthony, E. J. and Preto, F. [1995], Pressurized combustion in FBC systems, *in* M. Cuenca and E. J. Anthony, eds, 'Pressurized Fluidized Bed Combustion SE - 3', Springer Netherlands, pp. 80–120.
URL: *http://dx.doi.org/10.1007/978-94-011-0617-7_3*

APGTF [2000], Summary of Reports from Breakout Groups - Q1 Response, *in* '1st APGTF Workshop', London.
URL: *http://tinyurl.com/APGTF2000*

APGTF [2009], Cleaner Fossil Power Generation in the 21st Century: a technology strategy for carbon capture and storage, Technical Report April, Advanced Power Generation Technology Forum.
URL: *http://tinyurl.com/APGTF2009*

APGTF [2011], Cleaner Fossil Power Generation in the 21st Century – Maintaining a Lead-

ing Role, Technical Report August, Advanced Power Generation Technology Forum.
URL: *http://tinyurl.com/APGTF2011*

Arias, B., Pevida, C., Rubiera, F. and Pis, J. [2008], 'Effect of biomass blending on coal ignition and burnout during oxy-fuel combustion', *Fuel* **87**(12), 2753–2759.
URL: *http://linkinghub.elsevier.com/retrieve/pii/S0016236108000331*

Arrow, K. J. [1962], 'The Economic Implications of Learning by Doing', *The Review of Economic Studies* **29**(3), 155–173.

ASTM [2007], 'E1641 - 07: Standart Test Method for Decomposition Kinetics by Thermogravimetry'.

ASTM [2008], 'D7348 - 08: Standard Test Methods for Loss on Ignition (LOI) of Solid Combustion Residues'.

Azar, C., Johansson, D. J. a. and Mattsson, N. [2013], 'Meeting global temperature targets—the role of bioenergy with carbon capture and storage', *Environmental Research Letters* **8**(3), 034004.
URL: *http://iopscience.iop.org/1748-9326/8/3/034004/*

Babcock and Wilcox [2005], Fuel Ash Effects on Boiler Design and Operation, *in* 'Steam: It's Generation and Use', Babcock and Wilcox, chapter 21, pp. 1–28.

Bartolomé, C. and Gil, A. [2013], 'Emissions during co-firing of two energy crops in a PF pilot plant: Cynara and poplar', *Fuel Processing Technology* **113**, 75–83.
URL: *http://linkinghub.elsevier.com/retrieve/pii/S037838201300115X*

Bashir, M. S., Jensen, P. A., Frandsen, F., Wedel, S., Dam-Johansen, K. and Wadenback, J. [2012], 'Suspension-Firing of Biomass. Part 2: Boiler Measurements of Ash Deposit Shedding', *Energy & Fuels* **26**, 5241–5255.

BBC [2011], 'Longannet carbon capture scheme scrapped'.
URL: *http://www.bbc.co.uk/news/uk-scotland-north-east-orkney-shetland-15371258*

Bedi, S. [2013], NOx Control & Technology for an Equipment, *in* 'The Coal Research Forum 24th Annual Meeting and Meeting of the Environmental Division', Cranfield, UK.
URL: *http://tinyurl.com/BEDI2013*

Bergek, A., Jacobsson, S., Carlsson, B., Lindmark, S. and Rickne, A. [2008], 'Analyzing the functional dynamics of technological innovation systems: A scheme of analysis', *Research Policy* **37**, 407–429.
URL: *http://linkinghub.elsevier.com/retrieve/pii/S004873330700248X*

Bernstein, L., Bosch, P., Canziani, O., Chen, Z., Christ, R., Davidson, O., Hare, W., Huq, S., Karoly, D., Kattsov, V., Kundzewicz, Z., Liu, J., Lohmann, U., Manning, M., Matsuno, T., Menne, B., Metz, B., Mirza, M., Nicholls, N., Nurse, L., Pachauri, R., Palutikof, J., Parry, M., Qin, D., Ravindranath, N., Reisinger, A., Ren, J., Riahi, K., Rosenzweig, C., Rusticucci, M., Schneider, S., Sokona, Y., Solomon, S., Stott, P., Stouffer, R., Sugiyama, T., Swart, R., Tirpak, D., Vogel, C. and Yohe, G. [2007], Climate Change 2007: Synthesis Report, Technical Report November, Intergovernmental Panel on Climate Change, Valencia, Spain.
URL: *http://www.ipcc.ch/pdf/assessment-report/ar4/syr/ar4_syr.pdf*

Biomass Policies Project [2013], 'Biomass Policies Project'.
URL: *http://www.biomasspolicies.eu/*

Biorecro and GCCSi [2010], Global Status of BECCS Projects 2010, Technical report, Biorecro and the Global Carbon Capture and Storage Institute.
URL: *http://www.globalccsinstitute.com/publications/global-status-beccs-projects-2010*

Boardman, R. and Smoot, L. D. [1993], Pollutant Formation and Control, *in* L. D. Smoot, ed., 'Fundamentals of Coal Combustion for clean and efficient use', Elsevier, chapter 6.

Borrego, A. and Alvarez, D. [2007], 'Comparison of chars obtained under oxy-fuel and conventional pulverized coal combustion atmospheres', *Energy & Fuels* (9), 3171–3179.
URL: *http://pubs.acs.org/doi/abs/10.1021/ef700353n*

Borrego, A., Garavaglia, L. and Kalkreuth, W. [2009], 'Characteristics of high heating rate biomass chars prepared under N2 and CO2 atmospheres', *International Journal of Coal Geology* **77**(3-4), 409–415.
URL: *http://linkinghub.elsevier.com/retrieve/pii/S016651620800116X*

BP [2013], Statistical Review of World Energy 2013, Technical report, British Petroleum, London.
URL: *http://www.bp.com/statisticalreview*

Bridgeman, T., Darvell, L., Jones, J., Williams, P., Fahmi, R., Bridgwater, a., Barraclough, T., Shield, I., Yates, N. and Thain, S. [2007], 'Influence of particle size on the analytical and chemical properties of two energy crops', *Fuel* **86**(1-2), 60–72.
URL: *http://linkinghub.elsevier.com/retrieve/pii/S0016236106002249*

Bridgeman, T., Jones, J. and Williams, A. [2010], Overview of Solid Fuels, Characteristics and Origin, *in* M. Lackner, F. Winter and A. K. Agarwal, eds, 'Handbook of Combustion - Volume 4: Solid Fuels'.

Bryers, R. W. [1996], 'Fireside slagging, fouling, and high-temperature corrosion of heat-transfer surface due to impurities in steam-raising fuels', *Progress in Energy and Combustion Science* **22**, 29–120.
URL: *http://dx.doi.org/10.1016/0360-1285(95)00012-7*

B&W [2013], Radiant Boilers for Reliable Subcritical Steam Applications, Technical report, Babcock & Wilcox Power Generating Group.
URL: *http://www.babcock.com/library/pdf/E1013193.pdf*

Carlsson, B. and Stankiewicz, R. [1991], 'On the nature, function and composition of technological systems', *Journal of evolutionary economics* **1**, 93–118.
URL: *http://www.springerlink.com/index/n6452q03224r33m0.pdf*

Carpenter, A. M., Niksa, S., SRI International, Scott, D. H. and Wu, Z. [2007], Fundamentals Of Coal Combustion, Technical report, IEA Clean Coal Centre.
URL: *http://tinyurl.com/carpenter2007*

Carrier, M., Loppinet-Serani, A., Denux, D., Lasnier, J.-M., Ham-Pichavant, F., Cansell, F. and Aymonier, C. [2011], 'Thermogravimetric analysis as a new method to determine the lignocellulosic composition of biomass', *Biomass and Bioenergy* **35**(1), 298–307.
URL: *http://dx.doi.org/10.1016/j.biombioe.2010.08.067*

CCC [2010], Building a low-carbon economy – the UK's innovation challenge, Technical report, The Committee on Climate Change, London.
URL: *http://archive.theccc.org.uk/aws/CCC_Low-Carbon_web_August 2010.pdf*

CCC [2012], Letter to Rt Hon Edward Davey MP: The need for a carbon intensity target in the power sector, Technical Report September, The Committee on Climate Change, London.
URL: *http://www.theccc.org.uk/wp-content/uploads/2013/02/EMR-letter-September-12.pdf*

CCC [2013], Meeting Carbon Budgets – 2013 Progress Report to Parliament, Technical Report June, The Committee on Climate Change, London.
URL: *http://www.theccc.org.uk/publication/2013-progress-report/*

CCSa [2011], A strategy for CCS in the UK and Beyond, Technical report, Carbon Capture and Storage Association, London.
URL: *http://tinyurl.com/ccsa2011*

Chen, C., Ma, X. and Liu, K. [2011], 'Thermogravimetric analysis of microalgae combustion under different oxygen supply concentrations', *Applied Energy* **88**(9), 3189–3196.
URL: *http://linkinghub.elsevier.com/retrieve/pii/S0306261911001589*

Coats, A. and Redfern, J. [1964], 'Kinetic parameters from thermogravimetric data', *Nature* **201**(4914), 68–69.
URL: *http://www.nature.com/nature/journal/v201/n4914/abs/201068a0.html*

Coats, A. and Redfern, J. [1965], 'Kinetic Parameters from Thermogravimetric Data. II.', *Journal of Polymer Science Part B: Polymer Letters* **3**(11), 917–920.
URL: *http://onlinelibrary.wiley.com/doi/10.1002/pol.1965.110031106/abstract*

COP15 [2009], 'Report of the Conference of the Parties on its fifteenth session, held in Copenhagen from 7 to 19 December 2009. Part Two: Action taken by the Conference of the Parties at its fifteenth session'.
URL: *http://unfccc.int/resource/docs/2009/cop15/eng/11a01.pdf*

Corlett, R. C., Monteith, L. E., Halgren, C. a. and Malte, P. C. [1979], 'Molecular Nitrogen Yields from Fuel-Nitrogen in Backmixed Combustion', *Combustion Science and Technology* **19**(3-4), 95–106.
URL: *http://www.tandfonline.com/doi/abs/10.1080/00102207908946871*

Costa, M. and Azevedo, J. L. T. [2007], 'Experimental Characterization of an Industrial Pulverized Coal-Fired Furnace Under Deep Staging Conditions', *Combustion Science and Technology* **179**(9), 1923–1935.
URL: *http://www.tandfonline.com/doi/abs/10.1080/00102200701385042*

CSLF [2010], CSLF Technology Roadmap: A global response to the challenge of climate change, Technical report, Carbon Sequestration Leadership Forum.
URL: *http://tinyurl.com/cslf2010*

Daood, S., Nimmo, W., Edge, P. and Gibbs, B. [2011], 'Deep-staged, oxygen enriched combustion of coal', *Fuel* (February), 2–11.
URL: *http://linkinghub.elsevier.com/retrieve/pii/S0016236111000652*

Daood, S. S. [2011], 'Private Communication'.

Darvell, L., Jones, J., Gudka, B., Baxter, X., Saddawi, a., Williams, a. and Malmgren, a. [2010], 'Combustion properties of some power station biomass fuels', *Fuel* **89**(10), 2881–2890.
URL: *http://linkinghub.elsevier.com/retrieve/pii/S0016236110000955*

Davey, E. [2012], 'Press notice 2012/025'.
URL: *http://tinyurl.com/Davey2012*

Davidson, R. and Santos, S. [2010], Oxyfuel Combustion of Pulverised Coal, Technical Report August, IEAGHG, Cheltenham.
URL: *http://tinyurl.com/davidson2010*

Davini, P., Ghetti, P. and Michele, D. [1996], 'Investigation of the combustion of particles of coal', *Fuel* **75**(9), 1083–1088.

De Jong, W., Dinola, G., Venneker, B., Spliethoff, H. and Wojtowicz, M. [2007], 'TG-FTIR pyrolysis of coal and secondary biomass fuels: Determination of pyrolysis kinetic parameters for main species and NOx precursors', *Fuel* **86**(15), 2367–2376.
URL: *http://linkinghub.elsevier.com/retrieve/pii/S0016236107000634*

De Soete, G. [1975], 'Overall Reaction Rates of NO and N2 Formation from Fuel Nitrogen', *Symposium (International) on Combustion* **15**(1), 1093–1102.
URL: *http://linkinghub.elsevier.com/retrieve/pii/S0082078475803742*

DECC [2010], 2050 Pathways Analysis, Technical Report July, UK Department of Energy and Climate Change, London.
URL: *https://www.gov.uk/2050-pathways-analysis*

DECC [2011], Planning our electric future: a White Paper for secure, affordable and low-carbon electricity, Technical report, Department of Energy & Climate Change, London.
URL: *http://tinyurl.com/DECCEMR2011*

DECC [2012*a*], 'CCS Roadmap: Supporting deployment of Carbon Capture and Storage in the UK'.
URL: *http://tinyurl.com/DECC2012a*

DECC [2012*b*], Electricity Generation Costs, Technical Report October, Department of Energy & Climate Change, London.
URL: *http://tinyurl.com/DECC2012b*

DECC [2012*c*], 'Energy Bill'.
URL: *https://www.gov.uk/government/collections/energy-bill*

DECC [2012*d*], Gas Generation Strategy, Technical Report December, Department of Energy and Climate Change, London.
URL: *http://tinyurl.com/DECC2012*

DECC [2013*a*], Cross-Government Carbon Capture and Storage R&D Programme 2011-2015: list of projects spreadsheet, Technical report, Department of Energy and Climate Change, London.
URL: *http://tinyurl.com/DECC2013*

DECC [2013*b*], Official statistics: Provisional UK greenhouse gas emissions, Technical report, Department of Energy and Climate Change, London.
URL: *https://www.gov.uk/government/publications/provisional-uk-emissions-estimates*

DECC [2013*c*], 'Press release: Cleaner, greener future for British coal plants'.
URL: *http://tinyurl.com/DECC2013c*

DEFRA and ONS [2012], Statistical Release: 18 December 2012: Emissions of Air Pollutants in the UK, 1970 to 2011, Technical report, Department for Environment Food and Rural Affairs & Office of National Statistics, London.

DfT, DECC and DEFRA [2012], UK Bioenergy Strategy, Technical report, Department for Transport, Department of Energy and Climate Change, Department for Environment Food and Rural Affairs, London.
URL: *https://www.gov.uk/government/publications/uk-bioenergy-strategy*

Di Blasi, C. [2008], 'Modeling chemical and physical processes of wood and biomass pyrolysis', *Progress in Energy and Combustion Science* **34**(1), 47–90.
URL: *http://linkinghub.elsevier.com/retrieve/pii/S0360128507000214*

DOE-NETL [2010], Carbon Dioxide Capture and Storage RD&D Roadmap, Technical report, Department of Energy/ National Energy Technology Laboratories.
URL: *http://tinyurl.com/DOE2010*

Dong, N. [2010], Profiles: Reducing carbon-in-ash, Technical Report July, IEA Clean Coal Centre.
URL: *http://tinyurl.com/Dong2010*

Doyle, C. D. [1961], 'Kinetic analysis of thermogravimetric data', *Journal of Applied Polymer Science* **5**(15), 285–292.
URL: *http://doi.wiley.com/10.1002/app.1961.070051506*

Doyle, C. D. [1962], 'Estimating isothermal life from thermogravimetric data', *Journal of Applied Polymer Science* **6**(24), 639–642.
URL: *http://doi.wiley.com/10.1002/app.1962.070062406*

Drax Group Plc [2010], Biomass : the fourth energy source, Technical report.
URL: *http://tinyurl.com/Drax2010*

Drax Group Plc [2013], 'About Us - Drax'.
URL: *http://www.drax.com/aboutus/*

DTI [1999], Cleaner coal technologies, Technical report, Department for Trade and Industry, London.
URL: *http://www.berr.gov.uk/files/file22078.pdf*

DTI [2003], Our energy future - creating a low carbon economy, Technical report, Department for Trade and Industry, London.
URL: *http://www.berr.gov.uk/files/file10719.pdf*

DTI [2005], A strategy for developing carbon abatement technologies for fossil fuel use, Technical report, Department for Trade and Industry, London.
URL: */http://www.dti.gov.uk/energy/coal/cfft/cct/pub/catreportlinked.pdf*

EA [2011], Best availlable techniques (BAT) for NOx for existing baseload UK coal units >300MW, Technical report, Environment Agency, Technical Working Group 13.
URL: *http://tinyurl.com/pu5dqrm*

EC [2006], Integrated Pollution Prevention and Control Reference Documnet on Best Available Techniques for Large Combustion Plants, Technical report, European Commission.
URL: *http://ec.europa.eu/environment/ippc/brefs/lcp_bref_0706.pdf*

EC [2010*a*], 'Decisions: C(2010) 7499', *Official Journal of the European Union* **290**(2009), 39–48.
URL: *http://tinyurl.com/28tqds5*

EC [2010*b*], 'Directive 2010/75/EU of the European Parliament and of the Council', *Official Journal of the European Union* .
URL: *http://tinyurl.com/EC2010b*

EC [2011], A Roadmap for moving to a competitive low carbon economy in 2050, Technical report, European Commission, Brussels.
URL: *http://ec.europa.eu/clima/policies/roadmap/*

EC [2013], 'Energy: European Energy Programme for Recovery'.
URL: *http://ec.europa.eu/energy/eepr/*

EC-JRC [2013], 'Emissions Database for Global Atmospheric Research'.
URL: *http://edgar.jrc.ec.europa.eu/*

Edquist, C. and Johnson, B. [1997], Institutions and Organizations, *in* 'Systems of Innovation: Technologies, Institutions and Organizations', Pinter Publishers, London, pp. 41–63.

ERP [2006], UK Energy Innovation, Technical report, Energy Research Partnership.
URL: *http://www.energyresearchpartnership.org.uk/tiki-download_file.php?fileId=16*

Farrow, T. S. and Snape, C. E. [2010], Devolatilisation behaviour and combustion reactivity of biomass fuel under oxy-fuel conditions, *in* 'Third International Symposium on Energy from Biomass and Waste', number November, CISA, Venice, Italy.

Fenimore, C. [1976], 'Reactions of fuel-nitrogen in rich flame gases', *Combustion and Flame* **26**, 249–256.
URL: *http://www.sciencedirect.com/science/article/pii/0010218076900754*

Flynn, J. [1997], 'The 'Temperature Integral' — Its use and abuse', *Thermochimica Acta* **300**(1-2), 83–92.
URL: *http://linkinghub.elsevier.com/retrieve/pii/S0040603197000464*

Flynn, J. and Wall, L. [1966], 'A quick, direct method for the determination of activation energy from thermogravimetric data', *Journal of Polymer Science Part B: Polymer Letters* **4**(5), 323–328.
URL: *http://onlinelibrary.wiley.com/doi/10.1002/pol.1966.110040504/abstract*

Font, O., Córdoba, P., Leiva, C., Romeo, L., Bolea, I., Guedea, I., Moreno, N., Querol, X., Fernandez, C. and Díez, L. [2012], 'Fate and abatement of mercury and other trace elements in a coal fluidised bed oxy combustion pilot plant', *Fuel* **95**, 272–281.
URL: *http://linkinghub.elsevier.com/retrieve/pii/S001623611100771X*

Forster, P., Ramaswamy, V., Artaxo, P., Berntsen, T., Betts, R., Fahey, D., Haywood, J., Lean, J., Lowe, D., Myhre, G., Nganga, J., Prinn, R., Raga, G., Schulz, M. and Dorland, R. V. [2007], Changes in Atmospheric Constituents and in Radiative Forcing, *in* M. Solomon, S., D. Qin, M. Manning, Z. Chen, M. Marquis, K.B. Averyt and H. Miller, eds, 'Climate Change 2007: The Physical Science Basis. Contribution of Working Group I to the Fourth Assessment Report of the Intergovernmental Panel on Climate Change', Cambridge University Press, chapter 2.

Foxon, T., Gross, R., Chase, a., Howes, J., Arnall, a. and Anderson, D. [2005], 'UK innovation systems for new and renewable energy technologies: drivers, barriers and systems failures', *Energy Policy* **33**(16), 2123–2137.
URL: *http://linkinghub.elsevier.com/retrieve/pii/S030142150400120X*

Foxon, T., Kohler, J. and Neuhoff, K. [2008], Innovation for a low carbon economy: economic, institutional and management approaches, *in* T. Foxon, J. Kohler and K. Neuhoff, eds, 'Innovation for A Low Carbon Economy', Edward Elgar, chapter 1.

Friedman, H. [1964], 'Kinetics of thermal degradation of char-forming plastics from thermogravimetry. Application to a phenolic plastic', *Journal of Polymer Science Part C: Polymer* **6**(1), 183–195.
URL: *http://doi.wiley.com/10.1002/polc.5070060121*

Fryda, L., Sobrino, C., Cieplik, M. and van de Kamp, W. [2010], 'Study on ash deposition under oxyfuel combustion of coal/biomass blends', *Fuel* **89**(8), 1889–1902.
URL: *http://linkinghub.elsevier.com/retrieve/pii/S0016236109005316*

Fujimori, T. and Yamada, T. [2013], 'Realization of oxyfuel combustion for near zero emission power generation', *Proceedings of the Combustion Institute* **34**(2), 2111–2130.
URL: *http://linkinghub.elsevier.com/retrieve/pii/S1540748912004002*

Galli, R. and Teubal, M. [1997], Paradigmatic Shifts in National Innovation Systems, *in* C. Edquist, ed., 'Systems of Innovation: Technologies, Institutions and Organisations', Pinter Publishers, chapter 15, pp. 342–370.

GCCSi [2011], The Global Status of CCS: 2011, Technical report, Global CCS Institute.
URL: *http://tinyurl.com/GCCSi2011*

Gibbins, J. and Chalmers, H. [2008*a*], 'Carbon capture and storage', *Energy Policy* **36**, 4317–4322.
URL: *http://dx.doi.org/10.1016/j.enpol.2008.09.058*

Gibbins, J. and Chalmers, H. [2008*b*], 'Preparing for global rollout: A 'developed country first' demonstration programme for rapid CCS deployment', *Energy Policy* **36**(2), 501–507.
URL: *http://dx.doi.org/10.1016/j.enpol.2007.10.021*

Gil, M., Riaza, J., Álvarez, L., Pevida, C., Pis, J. and Rubiera, F. [2012*a*], 'Kinetic models for the oxy-fuel combustion of coal and coal/biomass blend chars obtained in N2 and CO2 atmospheres', *Energy* **48**(1), 510–518.
URL: *http://linkinghub.elsevier.com/retrieve/pii/S0360544212007955*

Gil, M., Riaza, J., Álvarez, L., Pevida, C., Pis, J. and Rubiera, F. [2012*b*], 'Oxy-fuel combustion kinetics and morphology of coal chars obtained in N2 and CO2 atmospheres in an entrained flow reactor', *Applied Energy* **91**(1), 67–74.
URL: *http://linkinghub.elsevier.com/retrieve/pii/S0306261911005885*

Gil, M. V., Riaza, J., Álvarez, L., Pevida, C., Pis, J. J. and Rubiera, F. [2012*c*], 'A study of oxy-coal combustion with steam addition and biomass blending by thermogravimetric analysis', *Journal of Thermal Analysis and Calorimetry* **109**(1), 49–55.
URL: *http://www.springerlink.com/index/10.1007/s10973-011-1342-y*

Glarborg, P. [2003], 'Fuel nitrogen conversion in solid fuel fired systems', *Progress in Energy and Combustion Science* **29**(2), 89–113.
URL: *http://linkinghub.elsevier.com/retrieve/pii/S036012850200031X*

Glassman, I. [1996], *Combustion*, 3rd edn, Academic Press Inc., San Diego.

Gough, C. and Upham, P. [2010], 'Biomass energy with carbon capture and storage (BECCS): a review', *Working Paper* .
URL: *http://www.tyndall.ac.uk/sites/default/files/twp147.pdf*

Grønli, M., Varhegyi, G. and Di Blasi, C. [2002], 'Thermogravimetric analysis and devolatilization kinetics of wood', *Industrial & Engineering Chemistry Research* **41**, 4201–4208.
URL: *http://pubs.acs.org/doi/abs/10.1021/ie0201157*

Han, L., Wang, Q., Ma, Q., Yu, C., Luo, Z. and Cen, K. [2010], 'Influence of CaO additives on wheat-straw pyrolysis as determined by TG-FTIR analysis', *Journal of Analytical and Applied Pyrolysis* **88**(2), 199–206.
URL: *http://linkinghub.elsevier.com/retrieve/pii/S0165237010000586*

Hayhurst, A. N. [2013], 'The kinetics of the pyrolysis or devolatilisation of sewage sludge and other solid fuels', *Combustion and Flame* **160**(1), 138 – 144.
URL: *http://dx.doi.org/10.1016/j.combustflame.2012.09.003*

Haykiri-Acma, H., a.Z. Turan, Yaman, S. and Kucukbayrak, S. [2010], 'Controlling the excess heat from oxy-combustion of coal by blending with biomass', *Fuel Processing Technology* **91**(11), 1569–1575.
URL: *http://linkinghub.elsevier.com/retrieve/pii/S0378382010002006*

Haykiri-Acma, H., Yaman, S. and Kucukbayrak, S. [2013], 'Co-combustion of low rank coal/waste biomass blends using dry air or oxygen', *Applied Thermal Engineering* **50**(1), 251–259.
URL: *http://linkinghub.elsevier.com/retrieve/pii/S1359431112004498*

Hecht, E. S., Shaddix, C. R., Molina, A. and Haynes, B. S. [2011], 'Effect of CO2 gasification reaction on oxy-combustion of pulverized coal char', *Proceedings of the Combustion*

Institute **33**(2), 1699–1706.
URL: *http://linkinghub.elsevier.com/retrieve/pii/S1540748910003718*

Hegerl, G., Zwiers, F. W., Braconnot, P., Gillett, N., Luo, Y., Orsini, J. M., Nicholls, N., Penner, J. and Stott, P. [2007], Understanding and Attributing Climate Change, *in* S. Solomon, D. Qin, M. Manning, Z. Chen, M. Marquis, K. Averyt, M. Tignor and H. Miller, eds, 'Climate Change 2007: The Physical Science Basis. Contribution of Working Group I to the Fourth Assessment Report of the Intergovernmental Panel on Climate Change', Cambridge University Press, Cambridge, UK, chapter 9.

Hein, K. and Bemtgen, J. [1998], 'EU clean coal technology—co-combustion of coal and biomass', *Fuel Processing Technology* **54**(1-3), 159–169.
URL: *http://linkinghub.elsevier.com/retrieve/pii/S0378382097000672*

Hekkert, M., Suurs, R., Negro, S., Kuhlmann, S. and Smits, R. [2007], 'Functions of innovation systems: A new approach for analysing technological change', *Technological Forecasting and Social Change* **74**(4), 413–432.
URL: *http://linkinghub.elsevier.com/retrieve/pii/S0040162506000564*

Hill, S. and Smoot, L. D. [2000], 'Modeling of nitrogen oxides formation and destruction in combustion systems', *Progress in Energy and Combustion Science* **26**(4-6), 417–458.
URL: *http://linkinghub.elsevier.com/retrieve/pii/S0360128500000113*

Hillier, J., Bezzant, T. and Fletcher, T. H. [2010], 'Improved Method for the Determination of Kinetic Parameters from Non-isothermal Thermogravimetric Analysis (TGA) Data', *Energy & Fuels* **24**(5), 2841–2847.
URL: *http://pubs.acs.org/doi/abs/10.1021/ef1001265*

HMG [2008], 'Climate Change Act 2008'.
URL: *http://www.legislation.gov.uk/ukpga/2008/27/contents*

HMG [2011], The Carbon Plan: Delivering our low carbon future, Technical report, UK Government, London.
URL: *http://tinyurl.com/cx6y9zd*

Holtmeyer, M. L., Kumfer, B. M. and Axelbaum, R. L. [2012], 'Effects of biomass particle size during cofiring under air-fired and oxyfuel conditions', *Applied Energy* **93**, 606–613.
URL: *http://linkinghub.elsevier.com/retrieve/pii/S0306261911007392*

Hughes, T. P. [1983], *Networks of Power: Electrification in Western Society, 1880- 1930*, The Johns Hopkins University Press, Baltimore.

Huhne, C. [2011], 'Fourth Carbon Budget: oral ministerial statement by The Rt Hon Chris Huhne MP - 17 May 2011'.
URL: *http://tinyurl.com/Huhne2011*

Hussain, T., Khodier, A. and Simms, N. [2013], 'Co-combustion of cereal co-product (CCP) with a UK coal (Daw Mill): Combustion gas composition and deposition', *Fuel* **112**, 572–583.
URL: *http://linkinghub.elsevier.com/retrieve/pii/S0016236113000082*

IEA [2009], Technology Roadmap: Carbon Capture and Storage, Technical report, International Energy Agency (IEA).
URL: *http://tinyurl.com/oj8o6kf*

IEA [2010], 'Energy Technology Perspectives', *Energy* .
URL: *http://www.iea.org/etp/publications/*

IEA [2011], Combining Bioenergy with CCS, Technical report, International Energy Association, Paris, France.

IEA [2012], Energy Technology Perspectives 2012, Technical report, International Energy Agency, Paris, France.
URL: *http://www.oecd-ilibrary.org/content/book/energy_tech-2012-en*

IMechE [2013], 'BECCS for electricity: Land-use tensions'.
URL: *http://tinyurl.com/IMechE2013*

IPCC [2006], Carbon Dioxide Transport, Injection and Geological Storage, *in* H. Eggleston, L. Buendia, K. Miwa, T. Ngara and K. Tanabe, eds, 'IPCC Guidelines for National Greenhouse Gas Inventories. Volume 2: Energy', IGES, Japan, chapter 5.
URL: *http://tinyurl.com/IPCC2006*

IPCC WG III [2000], IPCC Special Report: Emissions Scenarios - Summary for Policymakers, Technical report, Intergovernmental Panel on Climate Change.
URL: *https://www.ipcc.ch/pdf/special-reports/spm/sres-en.pdf*

Irfan, M. F., Arami-Niya, A., Chakrabarti, M. H., Wan Daud, W. M. A., Usman, M. R. and Dauda, W. M. A. W. [2012], 'Kinetics of gasification of coal, biomass and their blends in air (N2 /O2) and different oxy-fuel (O2 /CO2) atmospheres', *Energy* **37**(1), 665–672.
URL: *http://dx.doi.org/10.1016/j.energy.2011.10.032*

Jacobsson, S. and Bergek, A. [2011], 'Innovation system analyses and sustainability transitions : Contributions and suggestions for research', *Environmental Innovation and Societal Transitions* **1**(1), 41–57.
URL: *http://dx.doi.org/10.1016/j.eist.2011.04.006*

Jappe Frandsen, F. [2005], 'Utilizing biomass and waste for power production—a decade of contributing to the understanding, interpretation and analysis of deposits and corrosion products', *Fuel* **84**(10), 1277–1294.
URL: *http://linkinghub.elsevier.com/retrieve/pii/S0016236104003230*

Jenkins, B. M., Baxter, L. L., Miles, T. R. J. and Miles, T. R. [1998], 'Combustion properties of biomass', *Fuel Processing Technology* **54**, 17–46.
URL: *http://www.sciencedirect.com/science/article/pii/S0378382097000593*

Johnson, A. [2001], Functions in Innovation System Approaches, *in* 'DRUID Nelson and Winter Conference', Aaborg, Sweden.
URL: *http://www.druid.dk/conferences/nw/paper1/a_johnson.pdf*

Johnson, A. and Jacobsson, S. [2002], The Emergence of a Growth Industry: A Comparative Analysis of the German , Dutch and Swedish Wind Turbine Industries, *in* 'DRUID Academy Winter 2002 PhD Conference', Aaborg, Sweden.
URL: *www.druid.dk/conferences/winter2002/gallery/jacobsson.pdf*

Jones, J., Bridgeman, T., Darvell, L., Gudka, B., Saddawi, a. and Williams, a. [2012], 'Combustion properties of torrefied willow compared with bituminous coals', *Fuel Processing Technology* **101**, 1–9.
URL: *http://linkinghub.elsevier.com/retrieve/pii/S0378382012001038*

Kazagic, A. and Smajevic, I. [2009], 'Synergy effects of co-firing wooden biomass with Bosnian coal', *Energy* **34**(5), 699–707.
URL: *http://linkinghub.elsevier.com/retrieve/pii/S0360544208002892*

Khare, S., Wall, T., Farida, A., Liu, Y., Moghtaderi, B. and Gupta, R. [2008], 'Factors influencing the ignition of flames from air-fired swirl pf burners retrofitted to oxy-fuel', *Fuel* **87**(7), 1042–1049.
URL: *http://linkinghub.elsevier.com/retrieve/pii/S0016236107003213*

Khatami, R., Stivers, C., Joshi, K., Levendis, Y. a. and Sarofim, A. F. [2012], 'Combustion behavior of single particles from three different coal ranks and from sugar cane bagasse

in O2/N2 and O2/CO2 atmospheres', *Combustion and Flame* **159**(3), 1253–1271.
URL: *http://linkinghub.elsevier.com/retrieve/pii/S001021801100294X*

Khodier, A., Hussain, T., Simms, N., Oakey, J. and Kilgallon, P. [2012], 'Deposit formation and emissions from co-firing miscanthus with Daw Mill coal: Pilot plant experiments', *Fuel* **101**, 53–61.
URL: *http://linkinghub.elsevier.com/retrieve/pii/S0016236111005898*

Kiga, T., Takano, S., Kimura, N., Omata, K., Okawa, M., Mori, T. and Kato, M. [1997], 'Characteristics of pulverized-coal combustion in the system of oxygen/recycled flue gas combustion', *Energy Conversion and Management* **38**(Suppl.), S129–S134.
URL: *http://dx.doi.org/10.1016/S0196-8904(96)00258-0*

Kim, A. G., Kazonich, G. and Dahlberg, M. [2003], 'Relative solubility of cations in Class F fly ash.', *Environmental science & technology* **37**(19), 4507–11.
URL: *http://www.ncbi.nlm.nih.gov/pubmed/14572108*

King, L. [2002], Coal Issues, *in* '3rd APGTF Workshop', London.
URL: *http://tinyurl.com/King2002*

Kissinger, H. [1957], 'Reaction kinetics in differential thermal analysis', *Analytical chemistry* **29**(11), 1702–1706.
URL: *http://pubs.acs.org/doi/abs/10.1021/ac60131a045*

Lai, Z., Ma, X., Tang, Y., Lin, H. and Chen, Y. [2012], 'Thermogravimetric analyses of combustion of lignocellulosic materials in N2/O2 and CO2/O2 atmospheres.', *Bioresource technology* **107**, 444–50.
URL: *http://www.ncbi.nlm.nih.gov/pubmed/22209440*

LCICG [2012], Carbon Innovation Coordination Group Technology Innovation Needs Assessment (TINA) Carbon Capture & Storage in the Power Sector Summary report, Technical report, Low Carbon Innovation Coordination Group.
URL: *http://tinyurl.com/LCICG2012*

Li, Z., Zhao, W., Meng, B., Liu, C., Zhu, Q. and Zhao, G. [2008], 'Kinetic study of corn straw pyrolysis: comparison of two different three-pseudocomponent models.', *Bioresource technology* **99**(16), 7616–22.
URL: *http://www.ncbi.nlm.nih.gov/pubmed/18343656*

Lin, W., Jensen, P. A. and Jensen, A. D. [2009], 'Biomass Suspension Combustion: Effect of Two-Stage Combustion on NOx Emissions in a Laboratory-Scale Swirl Burner', *Energy & Fuels* **23**, 1398–1405.
URL: *http://pubs.acs.org/doi/abs/10.1021/ef8004866*

Liu, H. [2009], 'Combustion of Coal Chars in O2 /CO2 and O2 /N2 Mixtures: A Comparative Study with Non-isothermal Thermogravimetric Analyzer (TGA) Tests', *Energy & Fuels* **23**(9), 4278–4285.
URL: *http://pubs.acs.org/doi/abs/10.1021/ef9002928*

Liu, H., Zailani, R. and Gibbs, B. [2005], 'Comparisons of pulverized coal combustion in air and in mixtures of O2/CO2', *Fuel* **84**(7-8), 833–840.
URL: *http://linkinghub.elsevier.com/retrieve/pii/S001623610400362X*

Liu, K., Ma, X. Q. and Xiao, H. M. [2010], 'Experimental and kinetic modeling of oxygen-enriched air combustion of paper mill sludge.', *Waste Management* **30**(7), 1206–11.
URL: *http://www.ncbi.nlm.nih.gov/pubmed/20392627*

Liu, X., Chen, M. and Yu, D. [2013], 'Oxygen enriched co-combustion characteristics of herbaceous biomass and bituminous coal', *Thermochimica Acta* **569**, 17–24.
URL: *http://linkinghub.elsevier.com/retrieve/pii/S0040603113003560*

Liu, X. and White, S. [2001], 'Comparing innovation systems : a framework and application to China' s transitional context', *Research Policy* **30**, 1091–1114.
URL: *http://dx.doi.org/10.1016/S0048-7333(00)00132-3*

Lord, R. [2011], Biomass grown on brownfield land - a sustainable fuel source without food displacement?, Technical report, (TFI Research Day) Contaminated Land and Water Centre, University of Teeside.

Lu, H., Ip, E., Scott, J., Foster, P., Vickers, M. and Baxter, L. L. [2010], 'Effects of particle shape and size on devolatilization of biomass particle', *Fuel* **89**(5), 1156–1168.
URL: *http://linkinghub.elsevier.com/retrieve/pii/S0016236108004031*

Lundvall, B. A. [1988], Innovation as an interactive process: from user-producer interaction to the national system of innovation, *in* G. Dosi, C. Freeman, R. Nelson, G. Silverberg and L. Soete, eds, 'Technical Change and Economic Theory', Pinter Publishers, London, chapter 17, pp. 349–369.

Lundvall, B. A. [1992], *National Systems of Innovation: Towards a Theory of Innovation and Interactive Learning*, Pinter Publishers, London.

Lundvall, B. A. [2010], *National Systems of Innovation: Toward a Theory of Innovation and Interactive Learning*, Anthem Other Canon Economics Series, Anthem Press.
URL: *http://books.google.co.uk/books?id=iDXGwacw-4oC*

Luo, S., Xiao, B., Hu, Z., Liu, S. and Guan, Y. [2009], 'Experimental study on oxygen-enriched combustion of biomass micro fuel', *Energy* **34**(11), 1880–1884.
URL: *http://linkinghub.elsevier.com/retrieve/pii/S0360544209003259*

Ma, L., Jones, J., Pourkashanian, M. and Williams, A. [2007], 'Modelling the combustion of pulverized biomass in an industrial combustion test furnace', *Fuel* **86**(12-13), 1959–1965.
URL: *http://linkinghub.elsevier.com/retrieve/pii/S0016236106005199*

Mackrory, A. J. and Tree, D. R. [2009], 'Predictions of NOx in a Laboratory Pulverized Coal Combustor Operating under Air and Oxy-Fuel Conditions', *Combustion Science and Technology* **181**(11), 1413–1430.
URL: *http://www.tandfonline.com/doi/abs/10.1080/00102200903373457*

Makino, K. [2005], Overview of the oxy-fuel combustion studies in Japan, *in* 'International Oxy-combustion Network for CO2 Capture. Inaugural (1st) workshop', Cottbus, Germany.
URL: *http://www.ieaghg.org/docs/oxyfuel/w1/02W1Makino.pdf*

Man, C. K. and Gibbins, J. R. [2011], 'Factors affecting coal particle ignition under oxyfuel combustion atmospheres', *Fuel* **90**(1), 294–304.
URL: *http://dx.doi.org/10.1016/j.fuel.2010.09.006*

Mankins, J. [1995], HRST Technology Assessments: Technology Readiness Levels, Technical report, NASA Office of Space Access and Technology, Advanced Concepts Office.
URL: *http://www.hq.nasa.gov/office/codeq/trl/trlchrt.pdf*

Markusson, N., Ishii, A. and Stephens, J. C. [2011], 'The social and political complexities of learning in carbon capture and storage demonstration projects', *Global Environmental Change* **21**(2), 293–302.
URL: *http://linkinghub.elsevier.com/retrieve/pii/S0959378011000112*

Markusson, N., Kern, F., Watson, J., Arapostathis, S., Chalmers, H., Ghaleigh, N., Heptonstall, P., Pearson, P., Rossati, D. and Russell, S. [2012], 'A socio-technical framework for assessing the viability of carbon capture and storage technology', *Technological Forecast-*

ing and Social Change **79**(5), 903–918.
URL: *http://linkinghub.elsevier.com/retrieve/pii/S0040162511002769*

McGlashan, N., Workman, M. W., Caldecott, B. and Shah, N. [2012], Negative Emissions Technologies, Technical Report 8, Imperial College London, Grantham Institute for Climate Change, London.
URL: *http://tinyurl.com/McGlashan2012*

McKelvey, M. [1997], Using Evolutionary Theory to Define Systems of Innovation, *in* C. Edquist, ed., 'Systems of Innovation: Technologies, Institutions and Organisations', 1st in pap edn, Routledge, chapter 9, pp. 200–222.

McKendry, P. [2002], 'Energy production from biomass (Part 1): Overview of biomass.', *Bioresource technology* **83**(1), 37–46.
URL: *http://www.ncbi.nlm.nih.gov/pubmed/12058829*

McLennan, A. R., Bryant, G. W., Stanmore, B. R. and Wall, T. F. [2000], 'Ash Formation Mechanisms during pf Combustion in Reducing Conditions', *Energy & Fuels* **14**(1), 150–159.
URL: *http://pubs.acs.org/doi/abs/10.1021/ef990095u*

McMullan, J. [2002], Innovation and Institutional, *in* '3rd APGTF Workshop', London.
URL: *http://tinyurl.com/McMullan2002*

Mekaroonreung, M. and Johnson, A. L. [2012], 'Estimating the shadow prices of SO2 and NOx for U.S. coal power plants: A convex nonparametric least squares approach', *Energy Economics* **34**(3), 723–732.
URL: *http://linkinghub.elsevier.com/retrieve/pii/S0140988312000035*

Meng, F., Yu, J., Tahmasebi, A. and Han, Y. [2013], 'Pyrolysis and Combustion Behavior of Coal Gangue in O2/CO2 and O2/N2 Mixtures Using Thermogravimetric Analysis and a Drop Tube Furnace', *Energy & Fuels* **27**, 2923–2932.

Miles, T. R., Miles, T. R. J., Baxter, L. L. and Bryers, R. W. [1996], 'Deposits from firing biomass fuels', *Biomass and Bioenergy* **10**(2-3), 125–138.
URL: *http://dx.doi.org/10.1016/0961-9534(95)00067-4*

Miller, B. G. and Tillman, D. A. [2008], Coal Characteristi, *in* 'Combustion Engineering Issues for Solid Fuels', Academic Press Inc., chapter 2.

Molina, A. and Shaddix, C. R. [2007], 'Ignition and devolatilization of pulverized bituminous coal particles during oxygen/carbon dioxide coal combustion', *Proceedings of the Combustion Institute* **31**(2), 1905–1912.
URL: *http://linkinghub.elsevier.com/retrieve/pii/S1540748906003658*

Moukhina, E. [2012], 'Determination of kinetic mechanisms for reactions measured with thermoanalytical instruments', *Journal of Thermal Analysis and Calorimetry* **109**(3), 1203–1214.
URL: *http://www.springerlink.com/index/10.1007/s10973-012-2406-3*

Munir, S., Daood, S. S., Nimmo, W., Cunliffe, A. M. and Gibbs, B. M. [2009], 'Thermal analysis and devolatilization kinetics of cotton stalk, sugar cane bagasse and shea meal under nitrogen and air atmospheres.', *Bioresource technology* **100**(3), 1413–8.
URL: *http://dx.doi.org/10.1016/j.biortech.2008.07.065*

Munir, S., Nimmo, W. and Gibbs, B. [2010], 'Shea meal and cotton stalk as potential fuels for co-combustion with coal.', *Bioresource technology* **101**(19), 7614–23.
URL: *http://dx.doi.org/10.1016/j.biortech.2010.04.055*

Munir, S., Nimmo, W. and Gibbs, B. M. [2011], 'The effect of air staged, co-combustion of

pulverised coal and biomass blends on NOx emissions and combustion efficiency', *Fuel* **90**(1), 126–135.
URL: *http://dx.doi.org/10.1016/j.fuel.2010.07.052*

Murphy, J. and Shaddix, C. [2006], 'Combustion kinetics of coal chars in oxygen-enriched environments', *Combustion and Flame* **144**(4), 710–729.
URL: *http://linkinghub.elsevier.com/retrieve/pii/S0010218005002658*

Nalbandian, H. [2009], Profiles: NOx control for coal-fired plant, Technical report, IEA Clean Coal Centre.
URL: *http://www.iea-coal.org/documents/82237/7266/NOx-control-for-coal-fired-plant*

NAO [2012], Carbon capture and storage : lessons from the competition for the first UK demonstration, Technical Report March, National Audit Office, London.
URL: *http://www.nao.org.uk/wp-content/uploads/2012/03/10121829.pdf*

Nelson, R. R. [1992], 'National Innovation Systems: A Retrospective on a Study', *Industrial and Corporate Change* **2**, 347–374.
URL: *http://icc.oxfordjournals.org/content/1/2/347*

Nester, S., Bryan, B., Wohadlo, S. and Rabovitser, J. [2003], Current Status of Coal Preheating Technology for NOX Reduction from Pulverized Coal-Fired Boilers, *in* '2003 Conference on Selective Catalytic Reduction and Non-Catalytic Reduction for NOx Control', Pittsburgh.
URL: *http://tinyurl.com/Nester2003*

Nimmo, W., Daood, S. S. and Gibbs, B. M. [2010], 'The effect of O2 enrichment on NOx formation in biomass co-fired pulverised coal combustion', *Fuel* **89**(10), 2945–2952.
URL: *http://dx.doi.org/10.1016/j.fuel.2009.12.004*

Nordgren, D., Hedman, H., Padban, N., Boström, D. and Öhman, M. [2013], 'Ash transformations in pulverised fuel co-combustion of straw and woody biomass', *Fuel Processing Technology* **105**, 52–58.
URL: *http://linkinghub.elsevier.com/retrieve/pii/S0378382011002268*

Nordstrand, D., Duong, D. N. and Miller, B. G. [2008], Post-Combustion Emissions Control, *in* B. G. Miller and D. A. Tillman, eds, 'Combustion Engineering Issues for Solid Fuels', Academic Press Inc., chapter 9.

Normann, F., Andersson, K., Leckner, B. and Johnsson, F. [2009], 'Emission control of nitrogen oxides in the oxy-fuel process', *Progress in Energy and Combustion Science* **35**(5), 385–397.
URL: *http://linkinghub.elsevier.com/retrieve/pii/S0360128509000185*

OECD [2011], Climate Change, *in* 'OECD Environmental Outlook to 2050', number November, chapter 3.
URL: *http://tinyurl.com/kxhmx5x*

Omega [2013], 'Thermocouple Color Codes'.
URL: *http://www.omega.com/techref/colorcodes.html*

Ozawa, T. [1965], 'A new method of analyzing thermogravimetric data', *Bull Chem Soc Jpn* **38**(11), 1881–1886.
URL: *http://d.wanfangdata.com.cn/NSTLQK_10.1246-bcsj.38.1881.aspx*

Ozawa, T. [1992], 'Estimation of activation energy by isoconversion methods', *Thermochimica acta* **203**, 159–165.
URL: *http://www.sciencedirect.com/science/article/pii/004060319285192X*

Pedersen, L., Nielsen, H., Kiil, S., Hansen, L., Dam-Johansen, K., Kildsig, F., Christensen,

J. and Jespersen, P. [1996], 'Full-scale co-firing of straw and coal', *Fuel* **75**(13), 1584–1590.
URL: *http://www.sciencedirect.com/science/article/pii/0016236196826421*

Pérez-Maqueda, L., Sánchez-Jiménez, P. and Criado, J. [2005], 'Evaluation of the integral methods for the kinetic study of thermally stimulated processes in polymer science', *Polymer* **46**(9), 2950–2954.
URL: *http://linkinghub.elsevier.com/retrieve/pii/S0032386105001527*

Pershing, D. and Wendt, J. [1979], 'Relative contributions of volatile nitrogen and char nitrogen to NOx emissions from pulverized coal flames', *Industrial & Engineering Chemistry Process Design and Development* **18**(1), 60–67.
URL: *http://pubs.acs.org/doi/abs/10.1021/i260069a008*

Poortinga, W., Pidgeon, N. F., Capstick, S. and Aoyagi, M. [2013], 'Public Attitudes to Nuclear Power and Climate Change in Britain Two Years after the Fukushima Accident', *Working Paper* (UKERC/WP/ES/2013/006), 1–54.
URL: *http://tinyurl.com/Poortinger2013*

POST [2005], POST Note: Carbon Capture and Storage (CCS), Technical Report 238, Parliamentary Office of Science and Technology, London.
URL: *http://www.parliament.uk/documents/post/postpn335.pdf*

POST [2012], POST Note: Bioenergy, Technical Report 410, Parliamentary Office of Science and Technology, London.
URL: *http://www.parliament.uk/briefing-papers/POST-PN-410/bioenergy*

Pratt, D. and Lord, R. [2010], LIFE05 ENV/UK/00128 Final Report: Biomass , Remediation , re-Generation (BioReGen): Re-using brownfield sites for renewable energy crops, Technical report, European Union.

Praxair [2004], 'Praxair's Oxygen-enhanced Low NOx Technology'.
URL: *http://tinyurl.com/Praxair2004*

Prins, M., Ptasinski, K. and Janssen, F. [2007], 'From coal to biomass gasification: Comparison of thermodynamic efficiency', *Energy* **32**(7), 1248–1259.
URL: *http://linkinghub.elsevier.com/retrieve/pii/S0360544206002106*

Rathnam, R. K., Elliott, L. K., Wall, T. F., Liu, Y. and Moghtaderi, B. [2009], 'Differences in reactivity of pulverised coal in air (O2/N2) and oxy-fuel (O2/CO2) conditions', *Fuel Processing Technology* **90**(6), 797–802.
URL: *http://dx.doi.org/10.1016/j.fuproc.2009.02.009*

Reiner, D., Riesch, H., Chyong, C. K., Brunsting, S., de Best-Waldhober, M., Duetschke, E., Oltra, C., Lis, A., Desbarats, J., Pol, M., Breukers, S., Upham, P. and Mander, S. [2011], NearCO2 WP 2: Opinion shaping factors towards CCS and local CCS projects: Public and stakeholder survey and focus groups, Technical report, Judge Business School, Cambridge University, Cambridge, UK.
URL: *http://tinyurl.com/Reiner2011*

Riaza, J., Gil, M., Álvarez, L., Pevida, C., Pis, J. and Rubiera, F. [2012], 'Oxy-fuel combustion of coal and biomass blends', *Energy* **41**(1), 429–435.
URL: *http://linkinghub.elsevier.com/retrieve/pii/S0360544212001715*

Ribeirete, A. and Costa, M. [2009], 'Impact of the air staging on the performance of a pulverized coal fired furnace', *Proceedings of the Combustion Institute* **32**, 2667–2673.
URL: *http://linkinghub.elsevier.com/retrieve/pii/S1540748908001223*

Ricci, O. [2012], 'Providing adequate economic incentives for bioenergies with CO2 cap-

ture and geological storage', *Energy Policy* **44**, 362–373.
URL: *http://linkinghub.elsevier.com/retrieve/pii/S0301421512000948*

Riley, G., Sakellaropoulos, G., Kaldis, S., Gimeno, J. A., Fryda, L., Houkema, M., Grammelis, P., Klimantos, P., Kakaras, E., Pourkashanian, M., Nimmo, W., Gibbs, B., Papapavlou, C., Liese, T. and Schmidt, S. [2013], Enhanced capture with oxygen scrubbing of CO2 (ECO-Scrub), Technical report, EU Directorate-General for Research and Innovation, Luxembourg.
URL: *http://tinyurl.com/Riley2013*

Robbins, M. P., Evans, G., Valentine, J., Donnison, I. S. and Allison, G. G. [2012], 'New opportunities for the exploitation of energy crops by thermochemical conversion in Northern Europe and the UK', *Progress in Energy and Combustion Science* **38**(2), 138–155.
URL: *http://linkinghub.elsevier.com/retrieve/pii/S0360128511000414*

Rosenberg, N. [1982], *Inside the black box: technology and economics*, Cambridge University Press.

Russell, S., Markusson, N. and Scott, V. [2012], 'What will CCS demonstrations demonstrate ?', *Mitigation and Adaptation Strategies for Global Change* **17**, 651–668.
URL: *http://link.springer.com/article/10.1007%2Fs11027-011-9313-y*

Saddawi, A., Jones, J. M., Williams, A. and Wojtowicz, M. A. [2010], 'Kinetics of the Thermal Decomposition of Biomass', *Energy & Fuels* **24**(2), 1274–1282.
URL: *http://pubs.acs.org/doi/abs/10.1021/ef900933k*

Saloojee, F. [2011], Kinetics of Pyrolysis and Combustion of A South Afrcan Coal Using the The Distributed Activation Energy Model, PhD thesis, University of the Witwatersand.
URL: *http://wiredspace.wits.ac.za//handle/10539/11217*

Salour, D., Jenkins, B. M., Vafaei, M. and Kayhanian, M. [1993], 'Control of In-Bed Agglomeration by Fuel Blending in a Pilot Scale Straw and Wood Fuelled AFBC', *Biomass and Bioenergy* **4**(2), 117–133.
URL: *http://www.sciencedirect.com/science/article/pii/096195349390033Z*

Sami, M., Annamalai, K. and Wooldridge, M. [2001], 'Co-firing of coal and biomass fuel blends', *Progress in Energy and Combustion Science* **27**(2), 171–214.
URL: *http://linkinghub.elsevier.com/retrieve/pii/S0360128500000204*

Sarofim, A. F. [1987], Pollutant Formation and Destruction, *in* J. Lahaye and G. Prado, eds, 'Fundamentals of the Physical-Chemistry of Pulverised Coal Combustion', Martinus Nijhoff Publishers, chapter 10.

Sarofim, A. F. [2007], Oxy-fuel Combustion:Progress and Remaining Issues, *in* '2nd meeting of the oxy-fuel network', number January, Windsor, CT.
URL: *http://tinyurl.com/oxlwtyd*

Sathaye, J., Lucon, O., Rahman, A., Christensen, J., Denton, F., Fujino, J., Heath, G., Kadner, S., Mirza, M., Schlaepfer, A., Shmakin, A., Change, C., Sokona, Y., Seyboth, K., Matschoss, P., Eickemeier, P. and Hansen, G. [2011], Renewable Energy in the Context of Sustainable Development, *in* C. v. S. O. Edenhofer, R. Pichs-Madruga, Y. Sokona, K. Seyboth, P. Matschoss, S. Kadner, T. Zwickel, P. Eickemeier, G. Hansen, S. Schlömer, ed., 'IPCC Special Report on Renewable Energy Sources and Climate Change Mitigation', Cambridge University Press, Cambridge, UK, chapter Chapter 9, pp. 707–790.

SCCS [2013], 'CCS Full Chain'.
URL: *http://www.sccs.org.uk/education/downloads/ccs-fullchain.jpg*

Scheffknecht, G., Al-makhadmeh, L., Schnell, U. and Maier, J. [2011], 'Oxy-fuel coal combustion — A review of the current state-of-the-art', *International Journal of Greenhouse*

Gas Control **5**, 1–20.
URL: *http://linkinghub.elsevier.com/retrieve/pii/S1750583611000806*

Scott, V., Gilfillan, S., Markusson, N., Chalmers, H. and Haszeldine, R. S. [2012], 'Last chance for carbon capture and storage', *Nature Climate Change* **3**(2), 105–111.
URL: *http://www.nature.com/doifinder/10.1038/nclimate1695*

Senum, G. I. and Yang, R. T. [1977], 'Rational Approximations of the Integral of the Arrhenius Function', *Journal of Thermal Analysis* **11**(1), 445–447.
URL: *http://link.springer.com/article/10.1007%2FBF01903696*

Shaddix, C. R. and Molina, A. [2009], 'Particle imaging of ignition and devolatilization of pulverized coal during oxy-fuel combustion', *Proceedings of the Combustion Institute* **32**(2), 2091–2098.
URL: *http://linkinghub.elsevier.com/retrieve/pii/S1540748908002770*

Sharp, G. [2013], NOx Control Issues for a Power Generator, *in* 'The Coal Research Forum 24th Annual Meeting and Meeting of the Environmental Division', Cranfield, UK.
URL: *http://www.coalresearchforum.org/crfagm2013/G Sharpe, SSE, Cranfield, 10-04-13.pdf*

Shen, D. K., Gu, S., Jin, B. and Fang, M. X. [2011], 'Thermal degradation mechanisms of wood under inert and oxidative environments using DAEM methods.', *Bioresource technology* **102**(2), 2047–52.
URL: *http://www.ncbi.nlm.nih.gov/pubmed/20951030*

Siemens [2012], 'News Release: Drax cements position as the cleanest, most efficient power station in the UK as £100m turbine upgrade nears completion'.
URL: *http://tinyurl.com/p3nlmbb*

Signal [2010], Chemiluminescence NOx Analyser Model 448, Technical report, Signal Group.

Singh, S., Wu, C. and Williams, P. T. [2012], 'Pyrolysis of waste materials using TGA-MS and TGA-FTIR as complementary characterisation techniques', *Journal of Analytical and Applied Pyrolysis* **94**, 99–107.
URL: *http://linkinghub.elsevier.com/retrieve/pii/S0165237011001975*

Skalska, K., Miller, J. S. and Ledakowicz, S. [2010], 'Trends in NO(x) abatement: a review.', *The Science of the total environment* **408**(19), 3976–89.
URL: *http://www.ncbi.nlm.nih.gov/pubmed/20580060*

Skeen, S. a., Kumfer, B. M. and Axelbaum, R. L. [2010], 'Nitric Oxide Emissions during Coal and Coal/Biomass Combustion under Air-Fired and Oxy-fuel Conditions', *Energy & Fuels* **24**(8), 4144–4152.
URL: *http://pubs.acs.org/doi/abs/10.1021/ef100299n*

Skreiberg, A., Skreiberg, O., Sandquist, J. and Sø rum, L. [2011], 'TGA and macro-TGA characterisation of biomass fuels and fuel mixtures', *Fuel* **90**(6), 2182–2197.
URL: *http://linkinghub.elsevier.com/retrieve/pii/S0016236111000706*

Skrifvars, B.-J., Laurén, T., Hupa, M., Korbee, R. and Ljung, P. [2004], 'Ash behaviour in a pulverized wood fired boiler—a case study', *Fuel* **83**(10), 1371–1379.
URL: *http://linkinghub.elsevier.com/retrieve/pii/S0016236104000092*

Smart, J., O'Nions, P. and Riley, G. [2010], 'Radiation and convective heat transfer, and burnout in oxy-coal combustion', *Fuel* **89**(9), 2468–2476.
URL: *http://linkinghub.elsevier.com/retrieve/pii/S0016236110001547*

Smart, J. P., Patel, R. and Riley, G. S. [2010], 'Oxy-fuel combustion of coal and biomass,

the effect on radiative and convective heat transfer and burnout', *Combustion and Flame* **157**(12), 2230–2240.
URL: *http://linkinghub.elsevier.com/retrieve/pii/S0010218010002014*

Smart, J. P. and Riley, G. S. [2012], 'Use of oxygen enriched air combustion to enhance combined effectiveness of oxyfuel combustion and post-combustion flue gas cleanup Part 1 - combustion', *Journal of the Energy Institute* **85**(3), 123–130.
URL: *http://dx.doi.org/10.1179/1743967112Z.00000000026*

Smith, G., Cameron, A. and Bustin, R. [1994], Coal Resources of the Western Canada Sedimentary Basin, *in* 'Geological Atlas of the Western Canada Sedimentary Basin', Canadian Society of Petroleum Geologists and Alberta Research Council, chapter 33.
URL: *http://www.ags.gov.ab.ca/publications/wcsb_atlas/atlas.html*

Smits, R. [2002], 'Innovation studies in the 21st century; Questions from a user's perspective', *Technological Forecasting and Social Change* **69**(9), 861–883.
URL: *http://linkinghub.elsevier.com/retrieve/pii/S0040162501001810*

Smits, R. and Kuhlmann, S. [2004], 'The rise of systemic instruments in innovation policy', *Int. J. of Foresight and Innovation Policy* **1**(1/2), 4–32.
URL: *http://www.inderscience.com/info/inarticle.php?artid=4621*

Spliethoff, H. and Hein, K. [1998], 'Effect of co-combustion of biomass on emissions in pulverized fuel furnaces', *Fuel Processing Technology* **54**, 189–205.
URL: *http://linkinghub.elsevier.com/retrieve/pii/S0378382097000696*

Srivastava, R. K., Hall, R. E., Khan, S., Culligan, K. and Lani, B. W. [2005], 'Nitrogen oxides emission control options for coal-fired electric utility boilers.', *Journal of the Air & Waste Management Association* **55**(9), 1367–88.
URL: *http://www.ncbi.nlm.nih.gov/pubmed/16259432*

Starink, M. [2003], 'The determination of activation energy from linear heating rate experiments: a comparison of the accuracy of isoconversion methods', *Thermochimica Acta* **404**(1-2), 163–176.
URL: *http://linkinghub.elsevier.com/retrieve/pii/S0040603103001448*

Stern, N., Peters, S., Bakhshi, V., Bowen, A., Cameron, C., Catovsky, S. and Crane, D. [2006], Stern Review: The economics of climate change, Technical report.
URL: *http://en.scientificcommons.org/51856700*

Syed, A., Simms, N. and Oakey, J. [2011], 'Fireside corrosion of superheaters: Effects of air and oxy-firing of coal and biomass', *Fuel* **101**, 62–73.
URL: *http://dx.doi.org/10.1016/j.fuel.2011.03.010*

Tan, Y., Croiset, E., Douglas, M. and Thambimuthu, K. [2006], 'Combustion characteristics of coal in a mixture of oxygen and recycled flue gas', *Fuel* **85**(4), 507–512.
URL: *http://linkinghub.elsevier.com/retrieve/pii/S0016236105002668*

Tang, Y., Ma, X. and Lai, Z. [2011], 'Thermogravimetric analysis of the combustion of microalgae and microalgae blended with waste in N(2)/O(2) and CO(2)/O(2) atmospheres.', *Bioresource technology* **102**(2), 1879–85.
URL: *http://www.ncbi.nlm.nih.gov/pubmed/20817514*

Tanger, P., Field, J. L., Jahn, C. E., Defoort, M. W. and Leach, J. E. [2013], 'Biomass for thermochemical conversion: targets and challenges.', *Frontiers in plant science* **4**(July), 218.
URL: *http://dx.doi.org/10.3389%2Ffpls.2013.00218*

Tans, P. and Keeling, R. [2013], Atmospheric CO2 at Mauna Loa Observatory, Technical report, Scripps Institution of Oceanography & NOAA Earth System Research Laboratory,

Mauna Loa, Hawaii.
URL: *http://www.esrl.noaa.gov/gmd/ccgg/trends/*

Tappe, S. and Krautz, H. J. [2009], Experimental investigations of combustion behaviour in various O2/CO2 atmospheres, *in* 'Fourth International Conference on Clean Coal Technologies (CCT)', IEA Clean Coal Centre, Dresden, Germany.
URL: *http://tinyurl.com/Tappe2009*

Tees Valley Joint Strategy Unit, Valley, T. and Region, C. [2006], Tees Valley City Region: A Business Case for Delivery, Technical report, Tees Valley Joint Strategy Unit.

Thompson, D. R., Bool, L. E. and Chen, J. C. [2004], Oxygen enhanced combustion for NOx control, Technical report, Praxair & US Department of Energy, Pittsburgh.
URL: *http://tinyurl.com/Thompson2004*

Tillman, D. A. [1991], *The Combustion of Solid Fuels and Wastes*, 1st edn, Academic Press Inc.

Tillman, D. A. [2008], Introduction, *in* B. G. Miller and D. A. Tillman, eds, 'Combustion Engineering Issues for Solid Fuels', Elsevier, chapter 1.

Tobiasen, L., Skytte, R., Pedersen, L. S., Pedersen, S. r. T. and Lindberg, M. a. [2007], 'Deposit characteristic after injection of additives to a Danish straw-fired suspension boiler', *Fuel Processing Technology* **88**(11-12), 1108–1117.
URL: *http://linkinghub.elsevier.com/retrieve/pii/S037838200700152X*

Toftegaard, M. B., Brix, J., Jensen, P. A., Glarborg, P. and Jensen, A. D. [2010], 'Oxy-fuel combustion of solid fuels', *Progress in Energy and Combustion Science* **36**(5), 581–625.
URL: *http://linkinghub.elsevier.com/retrieve/pii/S0360128510000201*

UKCCSCRTF [2012], The potential for reducing the costs of CCS in the UK: Interim Report, Technical Report November, UK CCS Cost Reduction Task Force, London.
URL: *http://tinyurl.com/CRTF2012*

UKERC [2013], 'UKERC Energy Research Atlas'.
URL: *http://ukerc.rl.ac.uk/*

UN [1998], 'Kyoto Protocol to the United Nations Framework Convention on Climate Change'.
URL: *http://unfccc.int/resource/docs/convkp/kpeng.pdf*

UN [2012], 'Doha Amendment to the Kyoto Protocol'.
URL: *http://tinyurl.com/pb7otc8*

UNECE [2012], Guidance document on control techniques for emissions of sulphur, NOx, VOC, dust (including PM 10, PM 2.5 and black carbon) from stationary sources for the implementation of the 1999 Protocol to Abate Acidification, Eutrophication and Ground-level Ozone (, Technical report, United Nations Economic Commission for Europe.

UNEP [2012], The Emissions Gap Report 2012, Technical report, United Nations Environment Programme, Nairobi, Kenya.
URL: *www.unep.org/pdf/2012gapreport.pdf*

UNEP [2013], The Emissions Gap Report 2013, Technical report, United Nations Environment Programme, Nairobi, Kenya.
URL: *http://www.unep.org/pdf/UNEPEmissionsGapReport2013.pdf*

UNFCCC [2012], Report of the Conference of the Parties on its seventeenth session. Part Two : Action taken by the Conference of the Parties at its seventeenth session Contents Decision 1 / CP . 17, Technical Report March, United Nations Framework Convention

on Climate Change, Durban, South Africa.
URL: *http://unfccc.int/resource/docs/2011/cop17/eng/09a01.pdf*

University of Leeds [2013], 'Thermal Analysis'.
URL: *http://www.engineering.leeds.ac.uk/eri/facilities/thermal-analysis.shtml*

van Alphen, K., Hekkert, M. P. and Turkenburg, W. C. [2009], 'Comparing the development and deployment of carbon capture and storage technologies in Norway, the Netherlands, Australia, Canada and the United States – An innovation system perspective', *Energy Procedia* **1**(1), 4591–4599.
URL: *http://dx.doi.org/10.1016/j.egypro.2009.02.279*

van Alphen, K., Hekkert, M. P. and Turkenburg, W. C. [2010], 'Accelerating the deployment of carbon capture and storage technologies by strengthening the innovation system', *International Journal of Greenhouse Gas Control* **4**(2), 396–409.
URL: *http://dx.doi.org/10.1016/j.ijggc.2009.09.019*

van Vuuren, D. P., Deetman, S., Vliet, J., Berg, M., Ruijven, B. J. and Koelbl, B. [2013], 'The role of negative CO2 emissions for reaching 2 °C—insights from integrated assessment modelling', *Climatic Change* **118**(1), 15–27.
URL: *http://link.springer.com/10.1007/s10584-012-0680-5*

Várhegyi, G., Czégény, Z., Jakab, E., McAdam, K. and Liu, C. [2009], 'Tobacco pyrolysis. Kinetic evaluation of thermogravimetric–mass spectrometric experiments', *Journal of Analytical and Applied Pyrolysis* **86**(2), 310–322.
URL: *http://linkinghub.elsevier.com/retrieve/pii/S0165237009001235*

Varhegyi, G., Sebestyen, Z., Czegeny, Z., Lezsovits, F. and Konczol, S. [2012], 'Combustion Kinetics of Biomass Materials in the Kinetic Regime', *Energy & Fuels* **26**, 1323–1335.
URL: *http://pubs.acs.org/doi/abs/10.1021/ef201497k*

Vassilev, S. V., Baxter, D., Andersen, L. K. and Vassileva, C. G. [2010], 'An overview of the chemical composition of biomass', *Fuel* **89**(5), 913–933.
URL: *http://linkinghub.elsevier.com/retrieve/pii/S0016236109004967*

Vergragt, P. J., Markusson, N. and Karlsson, H. [2011], 'Carbon capture and storage, bio-energy with carbon capture and storage, and the escape from the fossil-fuel lock-in', *Global Environmental Change* **21**(2), 282–292.
URL: *http://linkinghub.elsevier.com/retrieve/pii/S0959378011000215*

Vyazovkin, S., Burnham, A. K., Criado, J. M., Pérez-Maqueda, L. a., Popescu, C. and Sbirrazzuoli, N. [2011], 'ICTAC Kinetics Committee recommendations for performing kinetic computations on thermal analysis data', *Thermochimica Acta* **520**(1-2), 1–19.
URL: *http://linkinghub.elsevier.com/retrieve/pii/S0040603111002152*

Vyazovkin, S. and Dollimore, D. [1996], 'Linear and Nonlinear Procedures in Isoconversional Computations of the Activation Energy of Nonisothermal Reactions in Solids', *Journal of Chemical Information and Modeling* **36**(1), 42–45.
URL: *http://pubs.acs.org/cgi-bin/doilookup/?10.1021/ci950062m*

Wall, T., Liu, Y., Spero, C., Elliott, L., Khare, S., Rathnam, R., Zeenathal, F., Moghtaderi, B., Buhre, B., Sheng, C., Gupta, R., Yamada, T., Makino, K. and Yu, J. [2009], 'An overview on oxyfuel coal combustion—State of the art research and technology development', *Chemical Engineering Research and Design* **87**(8), 1003–1016.
URL: *http://linkinghub.elsevier.com/retrieve/pii/S0263876209000598*

Wang, C., Zhang, X., Liu, Y. and Che, D. [2012], 'Pyrolysis and combustion characteristics of coals in oxyfuel combustion', *Applied Energy* **97**, 264–273.
URL: *http://linkinghub.elsevier.com/retrieve/pii/S0306261912001055*

Wang, X., Tan, H., Niu, Y., Pourkashanian, M., Ma, L., Chen, E., Liu, Y., Liu, Z. and Xu, T. [2011], 'Experimental investigation on biomass co-firing in a 300MW pulverized coal-fired utility furnace in China', *Proceedings of the Combustion Institute* **33**(2), 2725–2733.
URL: *http://linkinghub.elsevier.com/retrieve/pii/S1540748910000933*

Watson, J., Kern, F., Gross, M., Gross, R., Heptonstall, P., Jones, F., Haszeldine, S., Ascui, F., Chalmers, H., Ghaleigh, N., Gibbins, J., Markusson, N., Marsden, W., Rossati, D., Russell, S., Winskel, M., Pearson, P. and Arapostathis, S. [2012], Carbon Capture and Storage: Realising the potential ?, Technical report, UK Energy Research Centre.
URL: *http://www.ukerc.ac.uk/support/tiki-download_file.php?fileId=2421*

White, J. E., Catallo, W. J. and Legendre, B. L. [2011], 'Biomass pyrolysis kinetics: A comparative critical review with relevant agricultural residue case studies', *Journal of Analytical and Applied Pyrolysis* **91**(1), 1–33.
URL: *http://dx.doi.org/10.1016/j.jaap.2011.01.004*

Williams, A., Jones, J., Ma, L. and Pourkashanian, M. [2012], 'Pollutants from the combustion of solid biomass fuels', *Progress in Energy and Combustion Science* **38**(2), 113–137.
URL: *http://linkinghub.elsevier.com/retrieve/pii/S0360128511000530*

WRI [2013], 'CAIT 2.0 WRI's Climate Data Explorer'.
URL: *http://cait2.wri.org/wri/*

Wu, H., Bashir, M. S., Jensen, P. A., Sander, B. and Glarborg, P. [2013], 'Impact of coal fly ash addition on ash transformation and deposition in a full-scale wood suspension-firing boiler', *Fuel* **113**, 632–643.
URL: *http://linkinghub.elsevier.com/retrieve/pii/S0016236113005450*

Yang, H., Yan, R., Chen, H., Lee, D. H. and Zheng, C. [2007], 'Characteristics of hemicellulose, cellulose and lignin pyrolysis', *Fuel* **86**(12-13), 1781–1788.
URL: *http://linkinghub.elsevier.com/retrieve/pii/S001623610600490X*

Yüzbaşı, N. and Selçuk, N. [2012], 'Pyrolysis and Combustion Behavior of Ternary Fuel Blends in Air and Oxy-Fuel Conditions by Using TGA-FTIR', *Combustion Science and Technology* **184**(7-8), 1152–1163.
URL: *http://www.tandfonline.com/doi/abs/10.1080/00102202.2012.664005*

Yuzbasi, N. S. and Selçuk, N. [2011], 'Air and oxy-fuel combustion characteristics of biomass/lignite blends in TGA-FTIR', *Fuel Processing Technology* **92**(5), 1101–1108.
URL: *http://linkinghub.elsevier.com/retrieve/pii/S0378382011000233*

Zanganeh, K. and Shafeen, a. [2007], 'A novel process integration, optimization and design approach for large-scale implementation of oxy-fired coal power plants with CO2 capture', *International Journal of Greenhouse Gas Control* **1**(1), 47–54.
URL: *http://linkinghub.elsevier.com/retrieve/pii/S1750583607000357*

Zeldovich, J. [1946], 'The oxidation of nitrogen in combustion and explosions', *European Physical Journal A - Hadrons and Nuclei* **21**, 577–628.

ZEP [2010], Recommendations for research to support the deployment of CCS in Europe beyond 2020, Technical report, European Technology Platform for Zero Emission Fossil Fuel Power Plants.
URL: *http://tinyurl.com/ZEP2010*

ZEP [2012], Biomass with CO2 Capture and Storage (Bio-CCS) The way forward for Europe, Technical report, European Technology Platform for Zero Emission Fossil Fuel Power Plants.
URL: *http://www.zeroemissionsplatform.eu/downloads/1131.html*

Zhang, X., Jong, W. D. and Preto, F. [2009], 'Estimating kinetic parameters in TGA using B-spline smoothing and the Friedman method', *Biomass and Bioenergy* **33**(10), 1435–1441.
URL: *http://dx.doi.org/10.1016/j.biombioe.2009.06.009*